

BIOACTIVE COMPOUNDS FROM LICHEN *Usnea aciculifera* Vain AND USNIC ACID  
CONJUGATES



A Dissertation Submitted in Partial Fulfillment of the Requirements  
for the Degree of Doctor of Philosophy in Chemistry

Department of Chemistry

FACULTY OF SCIENCE

Chulalongkorn University

Academic Year 2019

Copyright of Chulalongkorn University

สารออกฤทธิ์ทางชีวภาพจากไลเคน *Usnea aciculifera* Vain และคอนจูเกตของกรดอูสุนิก



วิทยานิพนธ์นี้เป็นส่วนหนึ่งของการศึกษาตามหลักสูตรปริญญาวิทยาศาสตรดุษฎีบัณฑิต

สาขาวิชาเคมี ภาควิชาเคมี

คณะวิทยาศาสตร์ จุฬาลงกรณ์มหาวิทยาลัย

ปีการศึกษา 2562

ลิขสิทธิ์ของจุฬาลงกรณ์มหาวิทยาลัย

Thesis Title                      BIOACTIVE COMPOUNDS FROM LICHEN *Usnea aciculifera* Vain AND USNIC ACID CONJUGATES

By                                      Mr. Truong Tuong Lam

Field of Study                      Chemistry

Thesis Advisor                      Assistant Professor Dr. WARINTHORN CHAVASIRI

---

Accepted by the FACULTY OF SCIENCE, Chulalongkorn University in Partial Fulfillment of the Requirement for the Doctor of Philosophy

..... Dean of the FACULTY OF SCIENCE  
(Professor Dr. POLKIT SANGVANICH)

DISSERTATION COMMITTEE

..... Chairman  
(Associate Professor Dr. VUDHICHAJ PARASUK)

..... Thesis Advisor  
(Assistant Professor Dr. WARINTHORN CHAVASIRI)

..... Examiner  
(Associate Professor Dr. SURACHAI PORNPAKAKUL)

..... Examiner  
(Assistant Professor Dr. NUMPON INSIN)

..... External Examiner  
(Assistant Professor Dr. Potjane Srimanote)

ตรัง ดวง ลัม : สารออกฤทธิ์ทางชีวภาพจากไลเคน *Usnea aciculifera* Vain และคอนจูเกตของกรดอูสนิก. ( BIOACTIVE COMPOUNDS FROM LICHEN *Usnea aciculifera* Vain AND USNIC ACID CONJUGATES) อ.ที่ปรึกษาหลัก : ผศ. ดร.วรินทร ขวศิริ

การศึกษาองค์ประกอบทางเคมีของไลเคน *Usnea aciculifera* Vain นำไปสู่การค้นพบไดเมอริกแซนโทน ชนิดใหม่ 9 สาร usneaxanthones A-I (36–44) และสารที่เคยมีรายงานแล้วอีก 36 สาร ได้วิเคราะห์โครงสร้างเคมีของสารที่แยกได้ด้วยวิธีการผสมผสานของข้อมูลสเปกโทรสโกปี (1D, 2D NMR, HRESIMS ECD และ single-crystal X-ray crystallographic analyses) รวมถึงการเปรียบเทียบกับข้อมูล NMR ของสารที่เคยมีรายงานแล้ว ได้ทดสอบฤทธิ์ทางชีวภาพของสารที่แยกได้ ได้แก่ การยับยั้งแบคทีเรีย ยับยั้งไวรัสไข้เลือดออก และความเป็นพิษต่อเซลล์ พบว่าเดปไซด์บางชนิด มีโอกาสนำไปสู่การพัฒนาเป็นสารยับยั้งแบคทีเรีย และยับยั้งไวรัสไข้เลือดออกได้ ยังพบอีกว่าไดเมอริกแซนโทนมีความเป็นพิษต่อเซลล์มะเร็งชนิด HT-29, HCT116, MCF-7 และ A549 มีค่า  $IC_{50}$  ในช่วง 2.41 ถึง 9.86  $\mu M$

จากการแยกสารทั้งหมดพบว่า กรดอูสนิกเป็นองค์ประกอบหลัก จึงสังเคราะห์อนุพันธ์ของกรดอูสนิก 25 ชนิด (UA01–UA25) เมื่อทดสอบฤทธิ์  $\alpha$ -glucosidase พบว่า UA01, UA03–UA04, UA06, UA11–UA13 และ UA17–UA18 สามารถยับยั้ง  $\alpha$ -glucosidase ด้วยค่า  $IC_{50}$  ระหว่าง 14.51–99.04  $\mu M$  โดยใช้ acarbose ( $IC_{50}$  93.6  $\mu M$ ) เป็นสารมาตรฐาน

จุฬาลงกรณ์มหาวิทยาลัย  
CHULALONGKORN UNIVERSITY

สาขาวิชา เคมี  
ปีการศึกษา 2562

ลายมือชื่อนิสิต .....  
ลายมือชื่อ อ.ที่ปรึกษาหลัก .....

# # 6072804823 : MAJOR CHEMISTRY

KEYWORD: Lichen, *Usnea aciculifera*, dimeric xanthone, cytotoxic activity, usnic acid, alpha-glucosidase

Truong Tuong Lam : BIOACTIVE COMPOUNDS FROM LICHEN *Usnea aciculifera* Vain AND USNIC ACID CONJUGATES. Advisor: Asst. Prof. Dr. WARINTHORN CHAVASIRI

Phytochemical investigation of lichen *Usnea aciculifera* Vain led to the isolation of nine new dimeric xanthenes, usneaxanthenes A-I (36–44), along with 36 known compounds (1–35, 45). The chemical structures of the isolated compounds were elucidated by a combination spectroscopic data (1D, 2D NMR, HRESIMS), ECD experiments, and single-crystal X-ray as well as comparison of their NMR data with those in the literature. The biological activities of isolated compounds were evaluated for antibacterial, anti-dengue and cytotoxic activities. The results revealed that depsides may have potential as lead compounds for the development of new antibacterial and anti-dengue agents. Furthermore, dimeric xanthenes exhibited highly potent cytotoxicity against HT-29, HCT116, MCF-7 and A549 cancer cell lines with  $IC_{50}$  values ranging from 2.41 to 9.86  $\mu$ M. Among isolated compounds, usnic acid was obtained as a major compound. Twenty-five usnic acid derivatives (UA01–UA25) were synthesized and evaluated on  $\alpha$ -glucosidase activity. UA02, UA06, UA08, UA11–UA14, UA16–UA17 and UA24–UA25 were identified as new semisynthetic compounds. For  $\alpha$ -glucosidase activity, UA01, UA03–UA04, UA06, UA11–UA13 and UA17–UA18 exhibited potential activity with  $IC_{50}$  from 14.51–99.04  $\mu$ M compared with acarbose ( $IC_{50}$  93.6  $\mu$ M) as a positive control.

Field of Study: Chemistry

Student's Signature .....

Academic Year: 2019

Advisor's Signature .....

## ACKNOWLEDGEMENTS

There are many individuals without whom the work described in this thesis might not have been possible, and to whom I am greatly indebted.

First and foremost, I offer my sincerest gratitude to my advisor, Assistant Professor Dr. Warinthorn Chavasiri, who has supported me throughout my thesis with his patience, kindness, invaluable advice, guidance, encouragement and correction throughout in the most challenging times and in this thesis. I also thank the Center of Excellent in Natural Products Chemistry and all members of WC-lab for their kind help in my research.

I also gratefully acknowledge the members of my thesis committee, Associate Professor Dr. Vudhichai, Associate Professor Dr. Surachai Pornpakakul, Assistant Professor Dr. Numpon Insin and Assistant Professor Dr. Potjane Srimanote for their best guidance and advise.

Specially, I would like to say an deeply thank to Dr. Lien Do Thi My, who was then postdoc of Department Chemistry, Faculty of Science, Chulalongkorn University but is now a lecturer in Saigon University, Vietnam, the one has helped me since the beginning of application, and for her physical and mental supporting, encouragement and recommendation during the time I did my thesis. Without these things, the author could not be strong enough to get over difficulties last three years.

In addition, I would like to thank Prof. Phung Nguyen Kim Phi, Associate Professor Dr. Santi Ty-pyang, Dr. Dung Nguyen Thi My, Dr. Kittichai Chaiseeda, Dr. Sutin Khaenakham, Dr. Kieu Van Nguyen, Mrs Huong Ng Thi My for their recommendation, many insightful discussions and suggestions throught this research.

Moreover, I am also thankful for the helping from Prof. Thammarat Aree for X-ray analysis. I would also like to thank Dr. Piyanuch Wonganan from Department of Pharmacology, Faculty of Medicine, Chulalongkorn University for performing the cytotoxic activity assay against HCT116, MCF-7, A549, OVCAR-3 and HT-29 human cancer cell lines. Futhermore, I also thank Mr Ade Danova, PhD student of Department Chemistry, Faculty of Science, Chulalongkorn University for testing anti-bacterial and

alpha glucosidase activities.

I acknowledge my gratitude to the Graduate School of Chulalongkorn University for ASEAN Scholarship and the 90th Anniversary Chulalongkorn University Fund (Ratchadaphiseksomphot Endowment Fund). All kind support and opportunities supplied me to achieve my research goals.

Finally, I would like to thank my family in Vietnam for believing in me and for being proud of me. Their unconditional love and support has given me the strength and courage while I am away from home. I am also grateful my wife for her love, support and encouragement.

Truong Tuong Lam



## TABLE OF CONTENTS

	Page
ABSTRACT (THAI).....	iii
ABSTRACT (ENGLISH).....	iv
ACKNOWLEDGEMENTS.....	v
TABLE OF CONTENTS.....	vii
LIST OF SCHEMES.....	x
LIST OF TABLES.....	x
LIST OF FIGURES.....	xi
LIST OF ABBREVIATIONS.....	xiii
CHAPTER 1.....	1
INTRODUCTION.....	1
1.1 The lichen.....	2
1.2 Biosynthetic pathways to lichen secondary metabolites.....	4
1.3 The medicinal uses and useage of lichens.....	5
1.4 Biological activities of lichen substances.....	9
1.5 The objectives of this research.....	17
CHAPTER 2.....	18
CHEMICAL CONSTITUENTS OF <i>Usnea aciculifera</i> VAIN (PARMELIACEAE).....	18
2.1 General description of <i>Usnea</i> genus and <i>Usnea aciculifera</i> Vain (Parmeliaceae) .....	18
2.2 Experimental.....	26
2.2.1 Instruments and chemicals.....	26



2.2.2 Lichen material <i>U. aciculifera</i> .....	27
2.2.3 Extraction and isolation procedures .....	28
2.2.4 Biological activities.....	29
2.2.4.1 Antibacterial activity .....	29
2.2.4.2 Anti-Dengue activity .....	30
2.2.4.3 Cytotoxic activity .....	33
2.3 RESULTS AND DISCUSSION .....	33
2.3.1 Extraction and fractionation of lichen <i>Usnea aciculifera</i> .....	33
2.3.2 Separation of hexane extract.....	33
2.3.3 Separation of dichloromethane extract.....	34
2.3.4 Structural elucidation of compounds from lichen <i>Usnea aciculifera</i> .....	38
2.3.4.1 Monocyclic phenolic compounds .....	39
2.3.4.4 Dibenzofuran Compound .....	60
2.3.4.5 Steroid and triterpenoid compounds.....	61
2.3.4.6 Dimeric xanthone compounds .....	65
2.4 Biological activities.....	99
2.4.1 Antibacteria activity .....	99
2.4.2 Anti-dengue activity.....	102
2.4.2 Cytotoxic activity.....	103
2.4.2.1 HT-29 human colorectal cancer cell evaluation .....	104
2.4.2.2 Cytotoxic activity against other four cancer cell lines.....	105
2.5 Conclusion .....	106
CHAPTER 3.....	110
USNIC ACID CONJUGATES AND THEIR $\alpha$ -GLUCOSIDASE INHIBITORY .....	110

3.1 Introduction .....	110
3.1.1 Usnic acid derivatives and biological activities .....	112
3.1.2 Objectives .....	116
3.2 Experimental .....	116
3.2.1 Instrument and equipment .....	116
3.2.2 Chemicals .....	117
3.2.3 General procedure .....	117
3.3 Results and discussion .....	118
3.3.1 Synthesis of usnic acid enamine-conjugated 1–22 .....	119
3.3.2 Synthesis of usnic acid conjugates UA23–25 .....	122
3.4 $\alpha$ -glucosidase inhibitory activity of usnic acid conjugates .....	122
3.5 Conclusion .....	124
Chapter 4 .....	126
CONCLUSIONS .....	126
4.1 Chemical constituents of lichen <i>Usnea aciculifera</i> .....	126
4.2 Synthesis of usnic acid conjugates .....	127
APPENDIX .....	128
CONTENT OF SUPPORTING INFORMATION .....	129
REFERENCES .....	205
VITA .....	217

## LIST OF SCHEMES

Scheme 2.1. The extraction scheme of the extracts of <i>U. aciculifera</i> .....	29
Scheme 2.2: Isolation of compounds from different fractions of <i>Usnea aciculifera</i> Vain (Parmeliaceae).....	37
Scheme 3.1. Synthesis of usnic acid derivatives .....	118
Scheme 3.2 Synthesis of UA01–UA22 .....	119
Scheme 3.3 Synthesis of compounds.....	122

## LIST OF TABLES

Table 1.1 Pharmacological properties of extracts obtained from <i>Usnea spp.</i> .....	11
Table 1.2 Pharmacological properties of chemical constituents isolated from <i>Usnea</i> <i>spp.</i> .....	13
Table 1.3 Antibiotic and antifungal activities of some lichen compounds. ....	15
Table 1.4 Antiviral activities of some lichen compounds.....	16
Table 1.5 Antitumour and antimutagenic activities of some lichen compounds. ....	16
Table 2.1 <sup>1</sup> H Spectroscopic Data of 33–35.....	70
Table 2.2: <sup>13</sup> C NMR spectroscopic data of 33–35 (100 MHz, CDCl <sub>3</sub> , $\delta$ ppm).....	71
Table 2.3 <sup>1</sup> H Spectroscopic Data of 36–38.....	78
Table 2.4: <sup>13</sup> C NMR spectroscopic data of 36–38 (100 MHz, CDCl <sub>3</sub> , $\delta$ ppm).....	79
Table 2.5 <sup>1</sup> H Spectroscopic Data of 39–41.....	86
Table 2.6. <sup>13</sup> C NMR spectroscopic data of 39–41 (100 MHz, CDCl <sub>3</sub> , $\delta$ ppm).....	87
Table 2.7. <sup>1</sup> H NMR spectroscopic data of 42–44.....	95
Table 2.8 <sup>13</sup> C NMR spectroscopic data of 42–44 (100 MHz, CDCl <sub>3</sub> , $\delta$ ppm).....	96
Table 2.9 <sup>1</sup> H and <sup>13</sup> C NMR spectroscopic data of 45 .....	98
Table 2.10 Antibacterial activity of isolated compounds .....	101

Table 2.1 Anti-dengue results of isolated compounds .....	102
Table 2.12 IC <sub>50</sub> value of 33-45 and 5-fluorouracil on HT-29 cells <sup>a</sup> .....	104
Table 2.13 IC <sub>50</sub> values of 41–44 and cisplatin on human cancer cells <sup>a</sup> .....	106
Table 3.1 Biological activities of usnic acid.....	111
Table 3.2 The yields and characteristics of usnic acid derivatives UA01-22.....	121
Table 3.3 The yields and characteristics of usnic acid derivatives UA23–25 .....	122
Table 3.4 $\alpha$ -Glucosidase inhibitory assay of usnic acid conjugates .....	123

## LIST OF FIGURES

Fig 1.1 Selected natural products derived from plants.....	2
Fig 1.2 Types of lichens.....	4
Fig 1.3 Biosynthetic pathways of lichen secondary metabolites [12].....	1
Fig 2.1 The lichen <i>Usnea aciculifera</i> .....	28
Fig 2.2 Chemical structures of monocyclic phenolic compounds.....	39
Fig. 2.3 The structures of isolated depsides .....	47
Fig. 2.4 The structures of isolated depsidones.....	53
Fig. 2.5 The structures of isolated steroid and terpenoids.....	61
Fig. 2.6 The structures of isolated dimeric xanthenes.....	67
Fig. 2.7 The key COSY, HMBC correlations of 33 and 34.....	68
Fig. 2.8 ORTEP diagram for the single crystals X-ray geometry of 33 & 35 .....	72
Fig. 2.9 The key COSY, HMBC correlations of 35 and 36.....	75
Fig. 2.10 Experimental ECD spectra of 36–40 .....	76
Fig. 2.11 ORTEP diagram for the single crystal X-ray geometry of 36 & 38.....	77
Fig. 2.12 Structure and key COSY, HMBC correlations of 37.....	80

Fig. 2.113 Structure and the key COSY, HMBC correlations of 38 .....	82
Fig. 2.14 The key COSY, HMBC correlations of 39 and 40.....	84
Fig. 2.15 ORTEP diagram for the single crystals X-ray geometry of 39–41 .....	88
Fig. 2.16 Structure and the key COSY, HMBC correlations of 41 .....	89
Fig. 2.17 Experimental ECD spectra of 41–44 .....	90
Fig. 2.18 The key COSY, HMBC correlations of 42–44 .....	92
Fig. 2.19 Conformations and key NOESY correlations of 42 and 43 .....	93
Fig. 2.20 Structure and key COSY, HMBC, NOESY correlations of 45 .....	97
Fig. 2.21 Chemical structures of 1–32 .....	108
Fig. 2.22 Chemical structures of 33–45 .....	109
Fig. 3.1 Reported of usnic acid derivatives .....	114
Fig.3.2 Chemical structures of UA01-25 .....	120

## LIST OF ABBREVIATIONS

EC <sub>50</sub>	the molar concentration of an agonist that produces 50% of the maximal possible effect of that agonist
CC <sub>50</sub>	cytotoxic concentrations, the concentration of compound required for the reduction of 50% cell viability
IC <sub>50</sub>	the molar concentration of an antagonist that reduces the response to an agonist by 50%
kg	kilogram
$\mu$ g	microgram
mg	milligram
h	hour(s)
mmol	millimole
$\mu$ M	micromolar
L	liter
mL	milliliter
<i>m/z</i>	mass per charge number of ions (Mass Spectroscopy)
$\delta$	chemical shift (NMR)
$\delta_{\text{H}}$	chemical shift of proton (NMR)
$\delta_{\text{C}}$	chemical shift of carbon (NMR)
<i>J</i>	coupling constant (NMR)
s	singlet (NMR)
d	doublet (NMR)
dd	doublet of doublet (NMR)
t	triplet (NMR)

brs	broad singlet (NMR)
Hz	hertz
MHz	megahertz
DMSO-d <sub>6</sub>	deuterated dimethyl sulfoxide
CDCl <sub>3</sub>	deuterated chloroform
HR-ESI-MS	high resolution electrospray ionization mass spectroscopy
<sup>1</sup> H NMR	proton nuclear magnetic resonance
<sup>13</sup> C NMR	carbon-13 nuclear magnetic resonance
1D-NMR	one dimensional nuclear magnetic resonance
2D-NMR	two dimensional nuclear magnetic resonance
COSY	correlation spectroscopy
HSQC	heteronuclear single quantum correlation
HMBC	heteronuclear multiple bond correlation
ECD	electronic circular dichroism
calcd.	calculated
TLC	thin layer chromatography
EtOAc	Ethyl acetate
MeOH	Methanol
DCM	Dichloromethane

## CHAPTER 1

### INTRODUCTION

Natural products have played an important role in medicine since the 1940s (e.g. penicillin) and continually served as an important source and inspiration for new drugs [1]. Continuous searches for novel chemical entities, by expanding the natural products search, are essential to combat the adaptability of infectious bacteria and to keep pace of the ever-increasing need for new drugs to cure various diseases. The diverse structures of natural products have been selected over millions of years of chemical evolution and interacted with various biological molecules.

Medicinal plants have a long history of use by humans, and originally were employed as crude drugs in forms such as teas, tinctures, poultices, and powders [2]. Beginning with the purification of morphine from the opium poppy at the beginning of the nineteenth century, a number of important plant-derived drugs have been obtained in pure form in the intervening period, including artemisinin, atropine, colchicine, cocaine, digoxin, galantamine, quinine, paclitaxel, and vinblastine [2-6]. Selected examples are presented in Fig 1.1. There are a large number of secondary metabolites known already from plants, with about 170,000 unique compounds of this type having been characterized [7], of which the largest groups are isoprenoids, phenolics, and terpenoids [4]. Given that a high proportion of the estimated 270,000 species of plants in existence has not yet been subjected to any phytochemical or biological activity investigation and there is a good chance that additional new lead



compounds for use in drug discovery programs will continue to be elucidated for the foreseeable future. The screening of chemically complex natural product extracts for the discovery of new drugs in a timely manner presents a number of logistical challenges, but various modern technological approaches may be applied to enhance this process [7-10]. It is considered that when innovative methods of discovery are applied, natural products will continue to offer a vast resource to yield structurally novel compounds with promising biological activities [7-11].

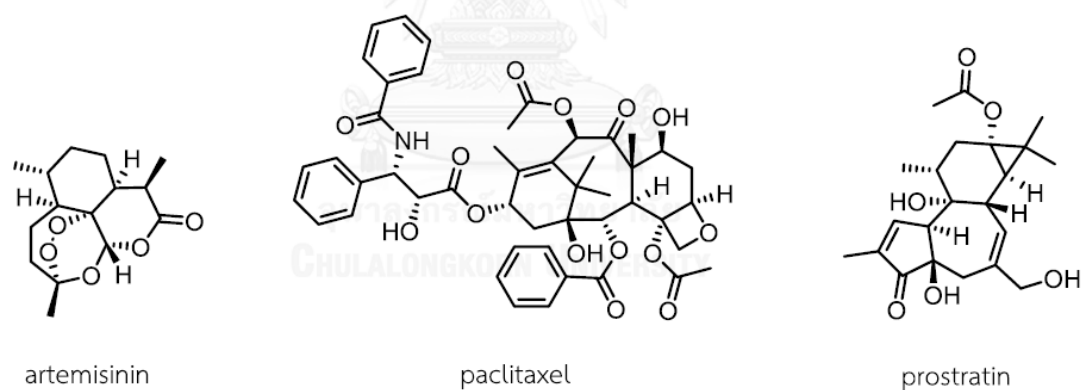


Fig 1.1 Selected natural products derived from plants

### 1.1 The lichen

Lichens are association between fungi (mycobiont) and photoautotrophic, algal partners (photobionts) [12]. In lichen associations both partners have benefit. The mycobiont has two principal roles in the lichen symbiosis: to protect the photobiont from exposure to intense sunlight and desiccation and to absorb mineral nutrients from the underlying surface or from minute traces of atmospheric contaminants. The photobiont also has two roles: to synthesize organic nutrients from carbon dioxide and, in the case of cyanobacteria, to produce ammonium (and

then organic nitrogen compounds) from  $N_2$  gas, by nitrogen fixation. Through the lichen partnership, the photobionts are protected and able to grow in conditions in which they could not grow alone; they also benefit from the highly efficient uptake of mineral nutrients by the lichen fungi. The fungi, in turn, obtain sugars and in some cases organic nitrogen from the photosynthetic partner, enabling them to grow in environments deficient in organic nutrients [13]. In nature, lichens grow very slowly. Their radial growth is measured in millimeters per year. The generalization about growth rates of lichens: most foliose species grow 0.5–4 mm per year, fruticose species 1.5–5 mm per year, and crustose species 0.5–2 mm per year [13]. Lichens grow practically everywhere - on and within rocks, on soil and tree bark, and on almost any inanimate object, in harsh environmental living from temperate zones to tropics. They grow in deserts and in tropical rainforests, where they occur on living leaves of plants and ferns. The sensitivity of lichens to atmospheric pollutants such as sulfur dioxide, ozone, and fluorides has made them valuable indicators of pollution in cities and industrial regions [14].

Based on this association, lichens can grow in soil, stone, bark and leaf in harsh environmental living from temperate zones to tropics. Lichens are divided into three main types of thalli: crustose, foliose and fruticose (Fig. 1.2). [12]



*Candellariella sp*  
(Crustose)

*Lobaria\_pulmonaria*  
(Foliose )

*Usnea sp*  
(Fruticose)

**Fig 1.2 Types of lichens**

+ Crustose lichens: The lichen thallus is closely attached to the substratum without leaving any free margin. The thallus usually lacks lower cortex and rhizine (root - like structure). Such lichens have to be collected along with their substratum for the study.

+ Foliose lichens are also known as leafy lichens. The thallus in this case is loosely attached at least at the margin. Such lichens can be collected by scraping them from the substratum.

+ Fruticose lichens: The lichen thallus is attached to the substratum at one point and remaining major portion is either growing erect or hanging. The lichen usually appears as small shrub or bush.

### 1.2 Biosynthetic pathways to lichen secondary metabolites

Specific conditions in which lichens live are the reason of production of many metabolites that they provide good protection against various negative physical and biological influences. There are two main groups of lichen compounds: primary

metabolites (intracellular) and secondary metabolites (extracellular). Common intracellular products occurring in lichens include proteins, amino acids, polyols, carotenoids, polysaccharides, and vitamins. They are generally soluble in water and can be easily isolated from the lichens by boiling water. The majority of organic compounds found in lichens are secondary metabolites of the fungal component, which are deposited on the surface of the hyphae rather than within the cells. These products are usually insoluble in water and can only be extracted with organic solvents. Lichen secondary metabolites are derived from three chemical pathways: acetate-polymalonate pathway, shikimic acid pathway and mevalonic acid pathway (Fig 1.3). [15]

### 1.3 The medicinal uses and useage of lichens

Lichens are used in traditional medicine by cultures across the world, particularly in temperate and arctic regions. Lichens in traditional medicine are most commonly used for treating wounds, skin disorders, respiratory and digestive issues, and obstetric and gynecological concerns. They have been used for both their secondary metabolites and their storage carbohydrates [12].

There are records of medicinal uses of lichens by cultures in Africa, Europe, Asia, Oceania, North America, and South America. The majority of these uses are in North America, Europe, India, and China, but this is most likely because that is where the majority of the ethnographic work has been done. . Lichens are often drunk as a decoction to treat ailments relating to either the lungs or the digestive system. This is

particularly common in Europe, but is also found across the world. Many other uses of lichens are related to obstetrics or treating gynecological issues. This may be related to the common use of lichens for treating sexually transmitted infections and ailments of the urinary system.

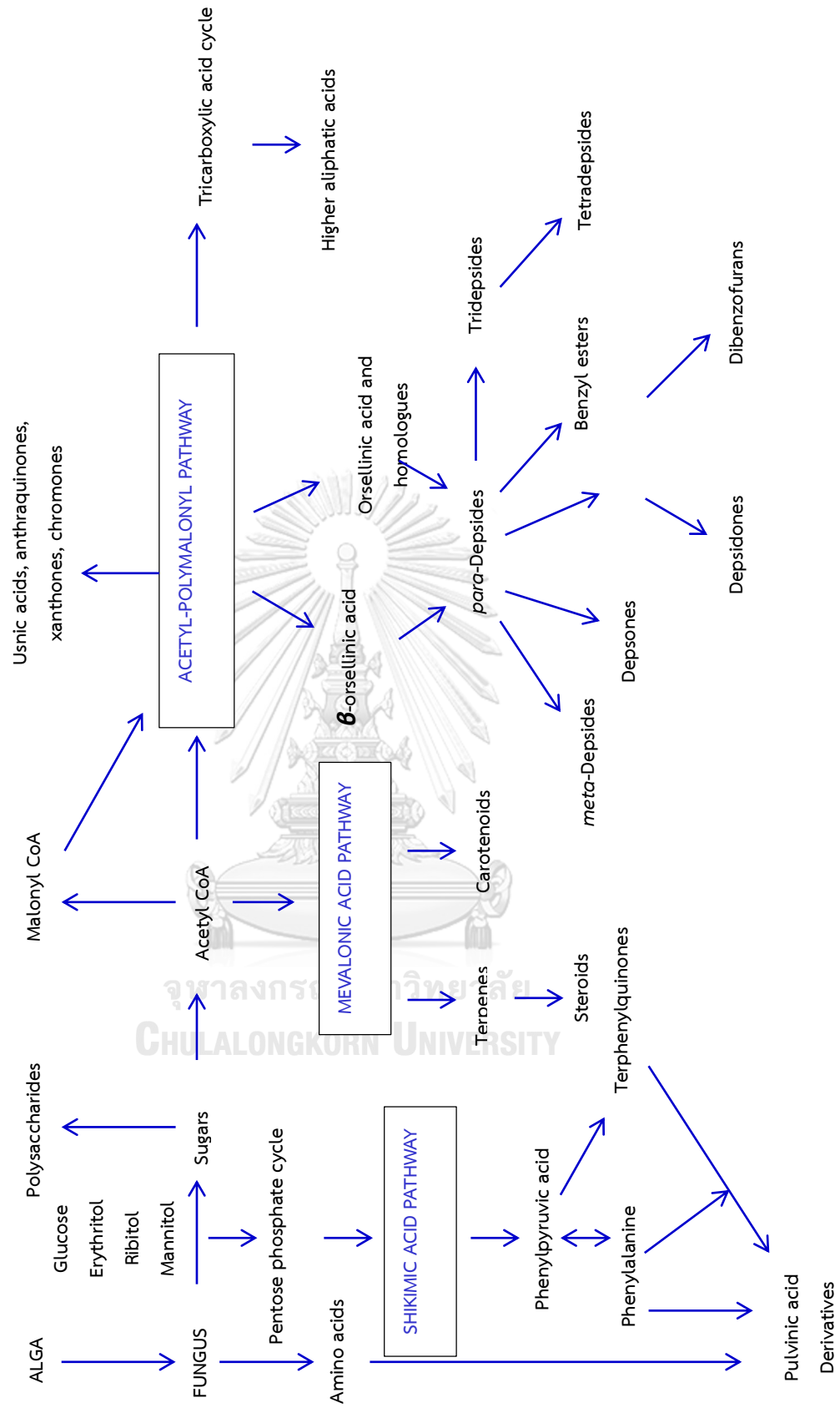
Three other uses of lichens that are less common, but reoccur in several different cultures, are for treating eye afflictions, treating issues with feet, and for use in smoking mixtures [12]. Examples, lichen *Cladonia stellaris* was used to expel intestinal worms and treat wounds or some infections in Canada and Russia. *Letharia vulpine* (L.) was used for treating stomach diseases in Northern California [15]. *Evernia furfuracea* (L.) Mann was used as drug [15]. *Cladonia amaurocraea* was used for headaches and dizziness in China [12]. In Estonia, *Cetraria islandica* (L.) Ach was used as tea for cancer [16], cough, colds, bronchitis, lung diseases, respiratory problems, and fever [17]. *Usnea* genus, a fructicose lichen, generally grows by hanging from tree branches, resembling grey and greenish hair [15]. *Usnea sp.* was used in traditional medicines around the world. *Usnea spp.* Dill. ex Adans was used for stomachache, heartburn, malaria, backache, fever, loss of appetite, and typhoid in Kenya [18]. Lichen *Usnea sp* used for stomachache, heartburn, malaria, backache, fever in Kenya, or used in a bath for women following childbirth, to aid parturition and prevent infection in Doi Inthanon (Chiang Mai, Thailand) [12]. *Usnea* sect. *Neuropogon* spp. used for coughs gastrointestinal, respiratory, cardiovascular, obstetric-gynecological,

and genitourinary afflictions, as well as cultural syndromes in Argentina and Chile [19].

Lichens also used as basic material for perfume produces [20]. More than 9,000 tons of two lichens: *Pseudevernia furfuracea* (L.) Zopf. and *Evernia prunastri* (L.) Ach. have been processed in France. Nowadays, there are many products of cosmetics make from lichen also. In the cosmetics industry, usnic acid is used as preservative in cosmetic creams [21]. Many lichen compounds are also photoprotectants that absorb UV light [22] making them suitable for use as UV protectant in sunscreens. Atranorin, pannarin, gyophoric acid and usnic acid are applied in suntan preparations [23]. Atranorin was proven to be an effective elastase inhibitor [24]. Skin elastase is responsible for the sagging and wrinkling of skin and so atranorin might be useful as an anti-wrinkle agent in cosmetic products. Divarinol and bis-(2,4-dihydroxy-6-*n*-propyl-phenyl)-methane are effective tyrosinase inhibitors that could potentially be used as skinwhitening agents in creams [25-27].

Moreover, lichens were used as basic material for dyes, for examples *Roccella* species and other lichens were published by Kok [20].

Fig 1.3 Biosynthetic pathways of lichen secondary metabolites [12]



#### 1.4 Biological activities of lichen substances

To date, there are many lichens have proved to be a source of important secondary metabolites for pharmaceutical industries and still hold a considerable interest as alternative treatments in various parts of the world [20]. A wide spectrum of biological potential is shown by the lichens, but they have been long neglected by mycologists and overlooked by pharmaceutical industry because of their slow growing nature and difficulties in their artificial cultivation and have scarcely been studied from a biochemical perspective [28].

Lichen secondary metabolites exhibit antimicrobial, antioxidant, antiinflammatory, cytotoxic, analgesic, antipyretic, and antiviral properties and could be potential sources of pharmaceutically useful chemicals. Some of the possible biological functions of lichen metabolites, as summarized by Huneck, S. [20] are as below:

- Antibiotic activities – provide protection against microorganisms.
- Photoprotective activities – aromatic substances absorb UV light to protect algae (photobionts) against intensive irradiation.
- Promote symbiotic equilibrium by affecting the cell wall permeability of photobionts.
- Chelating agents – capture and supply important minerals from the substrate.



- Antifeedant/ antiherbivory activities – protect the lichens from insect and animal feedings.
- Hydrophobic properties – prevent saturation of the medulla with water and allow continuous gas exchange.
- Stress metabolites – metabolites secreted under extreme conditions.

Several examples are described below. (Tables [1.1-1.2](#))



Table 1.1 Pharmacological properties of extracts obtained from *Usnea spp.*

Extract	Source	Bioactivity	Target/system	Dose
<b>a) In vitro study</b>				
Methanol extract	<i>U. filipendula</i>	Antipopulation [29]	Human lung cancer (A549, PC3), liver cancer (Hep3B) and rat glioma (C6) cells	1.5 -100 µg/mL
Methanol, acetone extracts	<i>U. arctica</i> , <i>U. aurantiocetra</i>	Antioxidant [30]	In vitro system	IC <sub>50</sub> 1mg/mL
Acetone extract	<i>U. barbata</i>	Anti-cancer, anti-oxidant [31]	FemX (human melanoma) and LS174 (human colon carcinoma)	IC <sub>50</sub> 102 and 130 µg/mL
Acetone extract	<i>U. complanta</i>	Anti-viral [32]	Herpes simplex viruses (HSV)	IC <sub>50</sub> 100 µg/mL
Methanol extract	<i>U. longissima</i>	Melanogenesis Inhibition [33]	Human melanoma cells	0.1 %
Acetone, methanol extracts	<i>U. lapponica</i>	Anti-bacterial [34]	<i>S. aureus</i> , <i>E. coli</i> , <i>P. aureginosa</i> and <i>Methicillin resistant S.</i>	MIC: 15.6 µg /mL

Acetone extract	<i>U. barbata</i>	Antimycobacterial [31]	<i>aureus</i>	MIC: 32 and 62 µg/mL
Acetone extract	<i>U. rubicunda</i>	Antitumor [35]	<i>Mycobacterium tuberculosis</i> , <i>M. kansasii</i> and <i>M. avium</i>	-
<b>b) In vivo study</b>			<i>In vitro</i> system	-
Aqueous extract	<i>U. longissima</i>	Anti-ulcer [36]	Rats	100 mg /Kg
Methanol extract	<i>U. longissima</i>	Anti-platelet, Antithrombotic [37]	Mice	100 – 200 mg /Kg
Methanol extract	<i>U. articulate</i> , <i>U. filipendula</i>	Anti-oxidative, anti-genotoxic [38]	Rats	5–20 µg/ mL
Methanol extract	<i>U. ghattensis</i>	Hepatoprotective [39]	Rats	20 µg/ mL

Table 1.2 Pharmacological properties of chemical constituents isolated from

*Usnea spp.*

Compound	Bioactivity	Target/system	Dose
<b>a) <i>In vitro</i> study</b>			
Usnic acid [40]	Anti-bacterial	<i>E. aerogenes</i> , <i>B. brevis</i> , <i>M. luteus</i> , <i>E.coli</i> , <i>B. megaterium</i> , <i>P.</i> <i>aeruginosa</i> , <i>E. cloacae</i> , <i>S. aureus</i> , <i>C. albicans</i> and <i>S. cerevisiae</i>	0.25–2 mg/mL
Usnic diffractaic acids [41]	Anti- proliferative	UACC-62 and B16-F10 melanoma cells	IC <sub>50</sub> : 24.7– 36.6 mg/mL (UACC-62) and 25.4 mg/mL (B16-F10)
Heptaketides, corynesporol, 1- hydroxydehydro herbarin [42]	Anti-cancer	Human metastatic breast and prostate cancer cell lines including MDA-MB-231 and PC-3M MDAMB- 231 and PC-3M	5.0 μM   5.0 μM
Eumitrin A1 [43]	Cytotoxic	P388 cells	4.5 μg /mL
Diffractaic, usnic, norstictic, psoromic	Cytotoxic	UACC-62 and B16-F10 melanoma cells and 3T3 normal cells	24.7 to 36.6 μg/mL

acids [41]

Table 1.2

(Continue)

Gautinol [44]		Antiinflammatory, cytotoxic	Spectroscopic model system			200 µg/mL
Norstictic acid [45]		Antimicrobial	<i>B. cereus</i> , <i>B. subtilis</i> , <i>S. epidermidis</i>			31–62.5 µg/mL
Methyl orsellinate [45]	β-	Antibacterial	<i>B. cereus</i> , <i>B. subtilis</i> , <i>S. epidermidis</i>			31–62.5 µg/mL
<b>b) In vivo studies</b>						
Diffractaic acid [46]		Pro-apoptotic	Rabbits			30 mg/kg
Usnic acid [47]		Anti-genotoxicity	Mice			60–120 µg/mL
Diffractaic acid [48]		Hepatoprotective	Mice			50 mg/kg
Diffractaic usnic acid [49]	acid,	Analgesic, antipyretic	Mice			500–1 g/kg

Table 1.3 Antibiotic and antifungal activities of some lichen compounds.

Compounds	Organisms	References
Usnic acids and derivatives	Gram (+) bacteria	[50]
	<i>Bacteroides</i> spp.; <i>Clostridium perfringens</i> <i>Bacillus subtilis</i> ; <i>Staphylococcus aureus</i> <i>Staphylococcus</i> spp.; <i>Enterococcus</i> spp. <i>Mycobacterium aurum</i>	[51-54] [55]
Protolichesterinic acid	<i>Helicobacter pylori</i>	[56]
Methylorsellinate	<i>Epidermophyton floccosum</i> ; <i>Microsporium</i>	[57, 58]
Ethylorsellinate	<i>canis</i>	
Methyl $\beta$ -orsellinate	<i>M. gypseum</i> ; <i>Trichophyton rubrum</i>	
Methylhematommate	<i>T. mentagrophytes</i> ; <i>Verticillium achliae</i> <i>Bacillus subtilis</i> ; <i>Staphylococcus aureus</i> <i>Pseudomonas aeruginosa</i> ; <i>Escherichia coli</i> <i>Candida albicans</i>	
Pulvinic acid and derivatives	<i>Drechslera rostrata</i>	[51]
	<i>Alternaria alternata</i> Aerobic and anaerobic bacteria	[59]
Emodin	<i>Bacillus brevis</i>	[60]
Physcion		
Leprapinic acid and derivatives	Gram (+) and (-) bacteria	[59]
Alectosarmentin	<i>Staphylococcus aureus</i> <i>Mycobacterium smegmatitis</i>	[61]

Table 1.4 Antiviral activities of some lichen compounds.

Compounds	Viruses or viral enzymes	References
Depsidones Virensic acid and derivatives	Human immunodeficiency virus (HIV) integrase	[62]
Butyrolactone protolichesterinic acid	HIV reverse transcriptase	[63]
(+)-Usnic acid and four other depsides	Epstein-Barr virus (EBV)	[35]
Emodin, 7-Chloroemodin 7-Chloro-1-Omethylemodin 5,7-Dichloroemodin Hypericin	HIV, cytomegalovirus and other viruses	[64-66]

Table 1.5 Antitumour and antimutagenic activities of some lichen compounds.

Compounds	Activities/cell types	References
(-)-Usnic acids	Antitumoral effect against Lewis lung carcinoma	[67] [68]
	P388 leukaemia	[69]
	Mitotic inhibition	
	Apoptotic induction	
Protolichesterinic acid	Antiproliferative effect against leukaemia cell K-562 and Ehrlich solid tumour	[70]
	Cytotoxic effect against cell cultures of lymphocytes	[71]
Pannarin, 1'- Chloropannarin Sphaerophorin		
Naphthazarin	Cytotoxic effect against human epidermal carcinoma cells Antiproliferative effects	[72]

Scabrosin esters and derivatives	against human keratinocyte cell line Cytotoxic effect against murine P815 mastocytoma and other cell lines	[73]
Euplectin Hydrocarpone		
Salazinic acid Stitic acid Psoromic acid	Apoptotic effect against primary culture of rat hepatocytes	[38]
Chrysophanol and emodin derivatives	Antiproliferative effect against leukemia cells	[74]

**Table 1.5 (Continue)**

### 1.5 The objectives of this research

The major aim of this thesis is to:

1. Investigate the chemical constituents of the lichen *Usnea aciculifera* Vain (Parmeliaceae)
2. Evaluate the cytotoxic activity of isolated metabolites on cancer cell lines.



## CHAPTER 2

CHEMICAL CONSTITUENTS OF *Usnea aciculifera* VAIN (PARMELIACEAE)2.1 General description of *Usnea* genus and *Usnea aciculifera* Vain (Parmeliaceae)

The genus *Usnea* (Parmeliaceae) one of the lichen genera has a world wide distribution and reproduces *via* vegetative or through fragmentation [75-77]. Specific conditions in which *Usnea* lichens live are the reason of production of many metabolites that they provide good protection against various negative physical and biological influences. Most of the *Usnea* lichen substances are phenolic compounds and are reported to have wide variety of biological actions: antioxidant, antimicrobial, antiviral, anti-inflammatory, analgesic, antipyretic, antiproliferative and cytotoxic effects. Over 600 species of *Usnea* have been reported [12], however, there is only one paper reported for *U. aciculifera*. Therefore, the literature review of *Usnea* genus was described. The secondary metabolites of *Usnea* genus mainly consisted of monocyclic phenolic compounds, depsides, depsidones, dibenzofurans, xanthones, triterpenoids, steroids, quinones and aliphatic acid.

From *U. diffracta*, Qui [78] and co-workers reported the presence of atranol (1), orsellinic acid (2), methyl orsellinate (3), ethyl orsellinate (4), lecanorin (16), diffractone A (31), and excelsione (32).

From *U. longissima*, several compounds were isolated, including longissiminone A (**8**), longissiminone B (**9**), glutinol (**43**) [79], (+)-usnic acid (**36**), barbatinic acid (**12**), diffractaic acid (**11**), 4-*O*-demethylbarbatic acid (**13**), evernic acid (**17**) [35]. (±) 4-*O*-demethylbarbatic acid (**13**), squamatic acid (**18**), atranorin (**21**), ergosterol-5 $\beta$ ,8 $\beta$ -peroxide (**47**) and (-)-placodiolic acid (**39**).

From *U. alata*, Keeton [80] and co-workers isolated usnic acid (**37**), norstictic acid (**19**), stictic acid (**20**) and caperatic acid (**55**).

From *U. aliphatica* [81], (+)-usnic acid (**37**) and norstictic acid (**19**) were isolated.

From *U. annulata* (Mull Argo) [82], (+)-usnic acid (**37**), 5 $\alpha$ ,8 $\alpha$ -epidioxy-5 $\alpha$ -ergosta-6,22-diene-3 $\beta$ -ol (**45**) were isolated.

From *U. articulata* (L.) Hoffm [83], fifteen compounds were isolated, including hypoprotocetraric acid (**36**), cryptostictinolide (**31b**), stictic acid (**20**), norstictic acid (**19**), fumarprotocetraric acid (**37b**), peristictic acid (**29**), cryptostictic acid (**30**), constictic acid (**23**), menegazziaic acid (**26**), barbatinic acid (**12**), atranorin (**21**), methyl  $\beta$ -orcinolcarboxylate (**7**), usnic acid (**37**) and ergosterol peroxide (**46**).

From *U. baileyi* (Stirt.) Zahlbr, since 1973 to 2018, several metabolites were isolated. In 1973, Yang and Shibata isolated eumitrin A<sub>1</sub> (**40**), eumitrin A<sub>2</sub> (**42**) and eumitrin B (**41**) from yellow pigment of lichen *U. baileyi* (Stirt.) Zahlbr collected at Yuriagehama [84]. In 2010, Din and Elix [85] reported the presence of usnic acid (**37**),

salazinic acid (22), norstictic acid (19), atranorin (14) and protocetraric acid (33) as major compounds from lichen *U. baileyi* collected in Bukit Larut, Taiping, Malaysia. In 2018, Nguyen [86] and co-workers reported twenty seven metabolites from acetone extract of *U. baileyi* thalli collected on tree barks at Lam Dong province, Vietnam, elucidated as bailexanthone (43), bailesidone (28), stictic acid (20), constictic acid (23), cryptostictic acid (30), hypoconstictic acid (24), menegazziaic acid (26), 8'-*O*-methylconstictic acid (25), methylstictic acid (21), 8'-*O*-methylmenegazziaic acid (27), virensic acid (35), 9'-*O*-methylprotocetraric acid (34), protocetraric acid (33), barbatic acid (10), diffractaic acid (11), 4-*O*-demethylbarbatic acid (13), atranorin (14), (20*R*, 24*R*)-ocotillone (48), (20*S*, 24*R*)-ocotillone (49), betulonic acid (50), usnic acid (37), dasypogalactone (51), 7-hydroxy-5-methoxy-6-methylphthalide (54), methyl 4-*O*-methylhaematomate (6), methyl orcinolcarboxylate (7), atranol (1), and eumitrin A<sub>2</sub> (42).

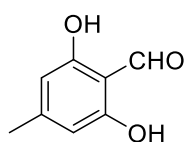
From *U. cavernosa*, Paranagama and Gunatilaka (2007) [42] isolated heptaketides 1-hydroxydehydroherbarin (53), along with herbarin (52).

From *U. meridensis*, a new fatty acid was isolated, methyl 3,4-dicarboxy-3-hydroxy-19-oxoeicosanoate (56) [87].

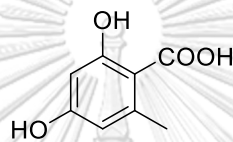
Up to now, although there have been many reports on *Usnea* genus, but there is only one paper reported for chemical constituents of *U. aciculifera*. This lichen was collected on pine tree barks at Lam Dong province, Vietnam. Tuong [88] and co-

workers reported twelve metabolites from a detailed chromatographic fractionation of its methanol extract, elucidated as aciculiferin A (**15**), (+)-(12*R*)-usnic acid (**37**), methyl haematommate (**5**), methyl **β**-orsellinate (**7**), methyl orsellinate (**3**), atranol (**1**), 7-hydroxy-5-methoxy-6-methylphthalide (**54**), norstictic acid (**19**), stictic acid (**29**), atranorin (**14**), barbatinic acid (**12**), and diffractaic acid (**11**).

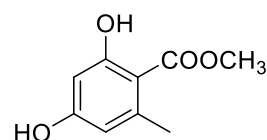
### Mononuclear phenolic compounds



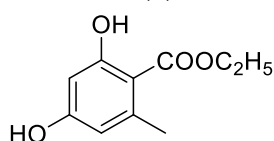
Atranol (**1**)



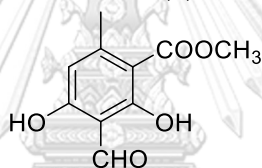
Orsellinic acid (**2**)



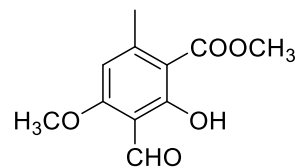
Methyl orsellinate (**3**)



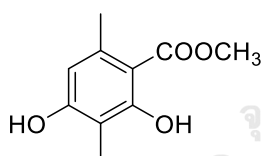
Ethyl orsellinate (**4**)



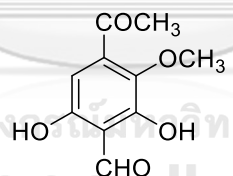
Methylhaematommate (**5**)



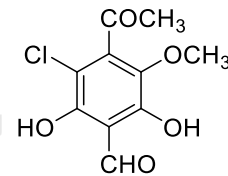
Methyl 4-O-methylhaematommate (**6**)



Methyl orcinolcarboxylate (**7**)

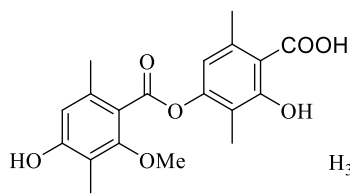


Longissiminone A (**8**)

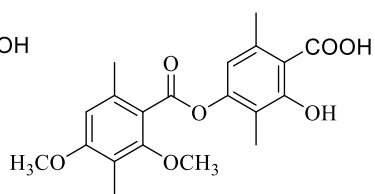


Longissiminone B (**9**)

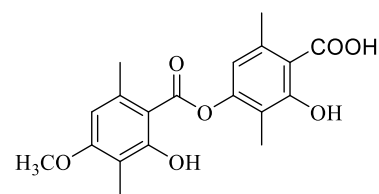
### Depsides



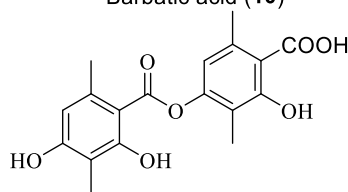
Barbatic acid (10)



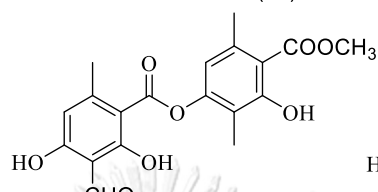
Diffractaic acid (11)



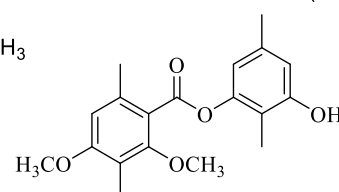
Barbatinic acid (12)



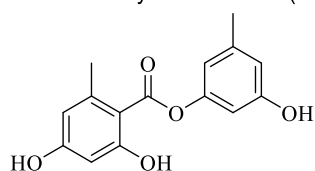
Demethylbarbatic acid (13)



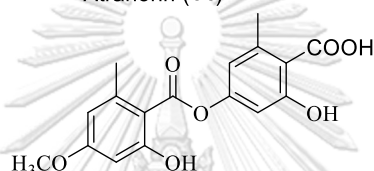
Atranorin (14)



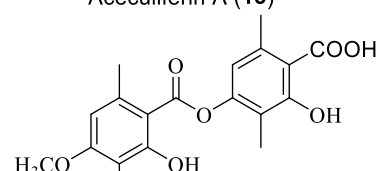
Aceculiferin A (15)



Lecanorin (16)

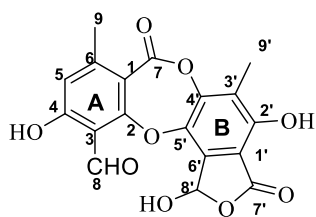


Evernic acid (17)

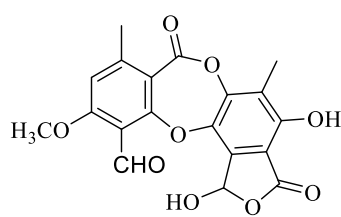


Squamatic acid (18)

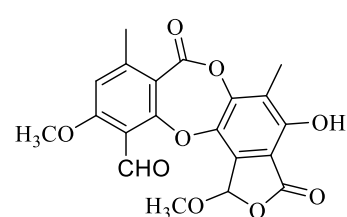
### Depsidones



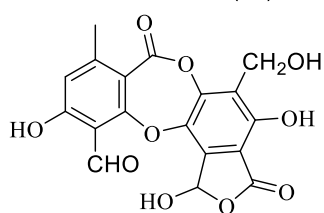
Norstictic acid (19)



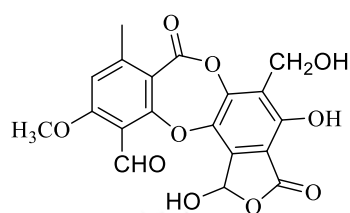
Stictic acid (20)



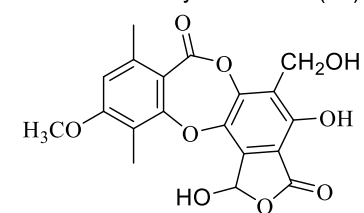
Methylstictic acid (21)



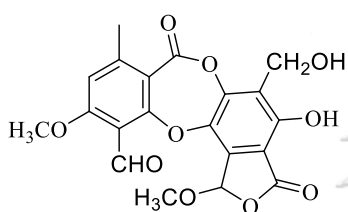
Salazinic acid (22)



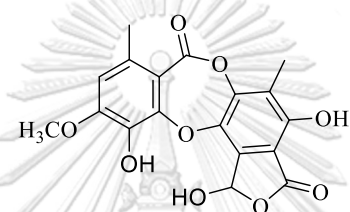
Constictic acid (23)



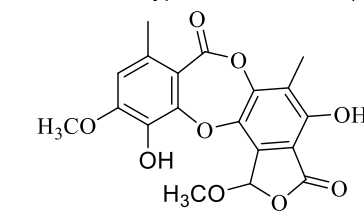
Hypoconstictic acid (24)



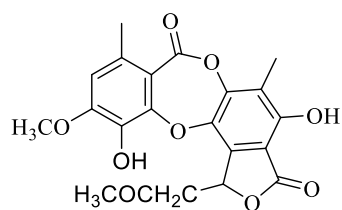
8'-O-methylconstictic acid (25)



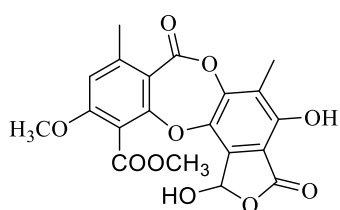
Menegazziaic acid (26)



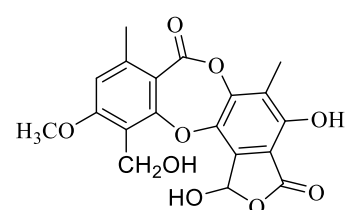
8'-O-methylmenegazziaic acid (27)



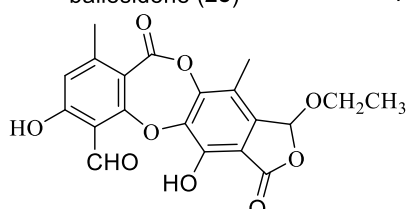
baileisidone (28)



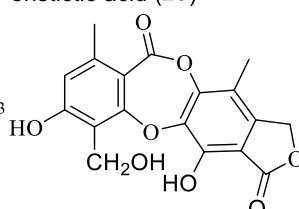
Peristic acid (29)



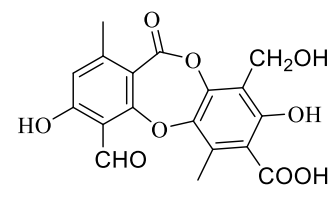
Cryptostictic acid (30)



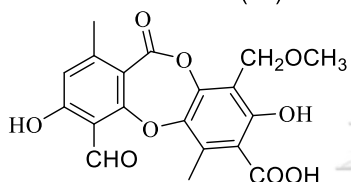
Diffraction A (31)



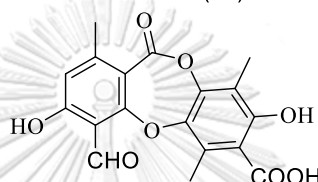
Excelsione (32)



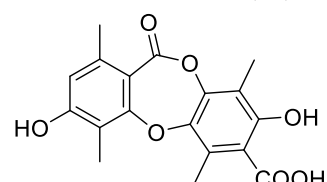
Protocetraric acid (33)



9'-O-methylprotocetraric acid (34)

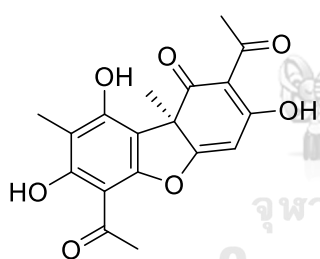


Virensic acid (35)

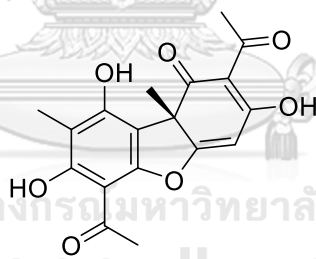


Hyporotocetraric acid (36)

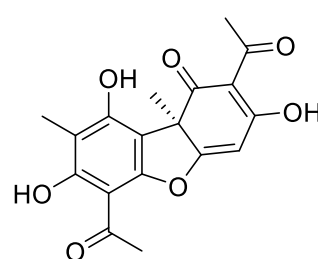
### Dibenzofurans



(+) -Usnic acid (37)

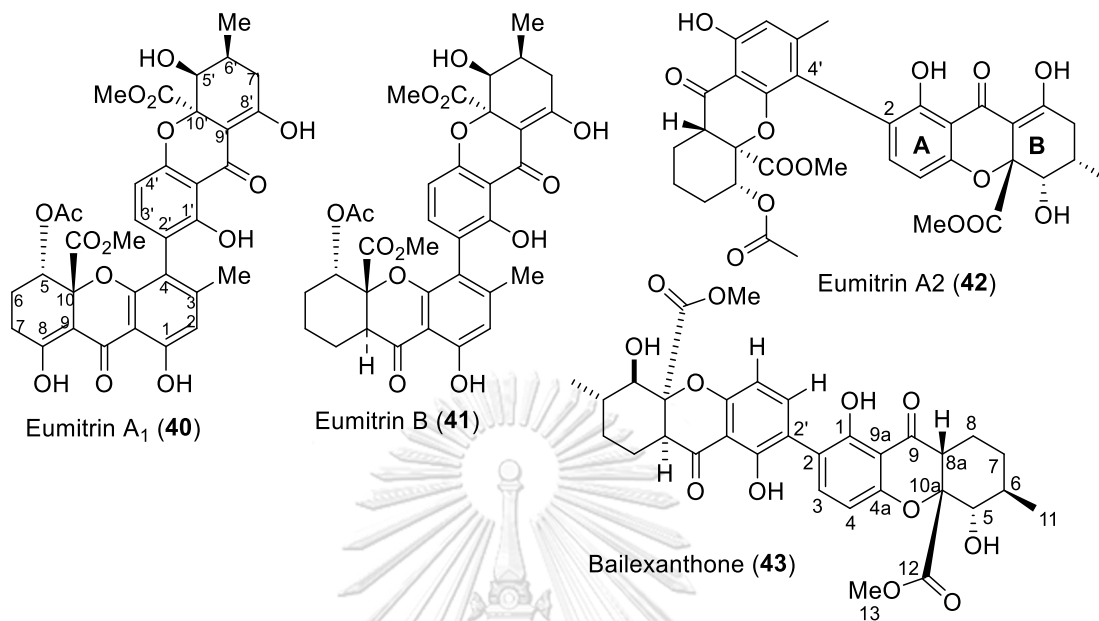


(-) -Usnic acid (38)

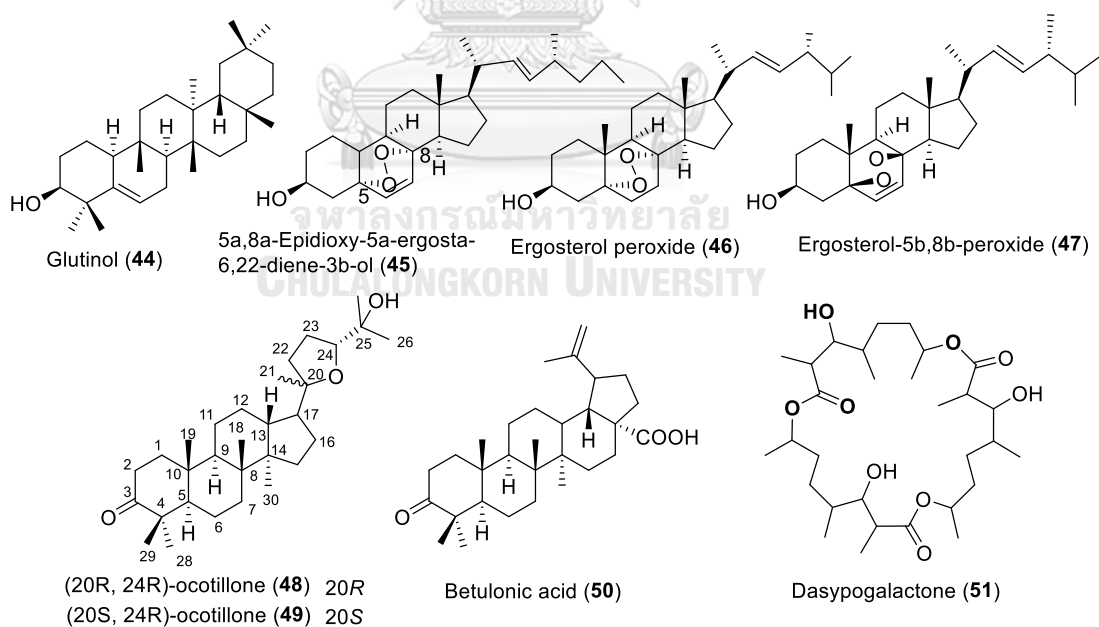


(-) -Placodiolic acid (39)

### Xanthenes

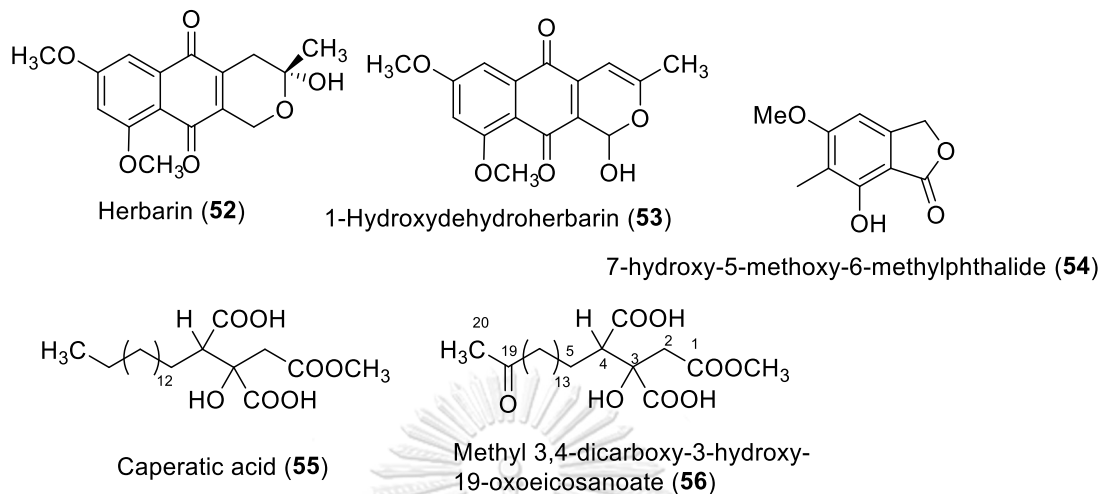


### Triterpenoids – Steroids - Macrolactone





## Quinones – Aliphatic acids – Phthalides



## 2.2 Experimental

### 2.2.1 Instruments and chemicals

- TLC was carried out on precoated silica gel 60 F<sub>254</sub> (Merck) and precoated 60 RP-18 F<sub>254</sub>S (Merck).
- Gravity column chromatography was performed with silica gel 60 (Merck) and silica gel 60 (0.040–0.063 mm, Silicycle).
- TLC spots were detected under ultraviolet (UV<sub>254</sub>) irradiation or visualized by spraying with a solution of 5% vanillin in ethanol, followed by heating at 100 °C.
- Solvents: *n*-hexane (95%), chloroform (95%), ethyl acetate (95%), acetone (95%), methanol (90%), acetic acid (90%), and distilled water.
- The NMR experiments using residual solvent signal as internal reference: acetone-*d*<sub>6</sub>  $\delta_H$  2.05, 2.84,  $\delta_C$  29.84, 206.26, chloroform-*d*  $\delta_H$  7.26,  $\delta_C$  77.23 and dimethyl sulfoxide-*d*<sub>6</sub>  $\delta_H$  2.50, 3.33,  $\delta_C$  39.52 were performed with:

- JEOL 500 (500 MHz for  $^1\text{H}$  and 125 MHz for  $^{13}\text{C}$ -NMR)
- Bruker 400 Avance spectrometer (400 MHz for  $^1\text{H}$  and 100 MHz for  $^{13}\text{C}$ )
- The HR ESI MS were recorded on
  - Bruker microTOF Q-II mass spectrometer.
- The UV spectra were analyzed using
  - UV-2550 UV-vis spectrometer (Shimadzu, Kyoto, Japan)
- The IR spectra were obtained with
  - Shimadzu FTIR-8200 infrared spectrophotometer (Shimadzu, Kyoto, Japan).
- Optical rotations were measured on
  - Kruss (German) digital polarimeter.
- Absorption and ECD spectra were measured on
  - UV-2550 UV-Vis spectrophotometer (Shimadzu, Kyoto, Japan).
  - Jasco J-815 circular dichroism (CD) spectrometer (JASCO Inc., Tokyo, Japan).

### 2.2.2 Lichen material *U. aciculifera*

The thalli of the lichen were separated from the bark of various old trees at 2,100–2,200 m altitude in Dalat City, Lam Dong province, Vietnam in July – August 2015 (Fig. 2.1). The species was authenticated as *Usnea aciculifera* Vain by Dr. Harrie Sipman (Botanic Garden and Boany Museum Berlin – Dahlem, Freie University of Berlin, Germany). A voucher specimen (No US–B029) was deposited at the Herbarium

of the Department of Organic Chemistry, University of Science, National University – Ho Chi Minh City – Vietnam.

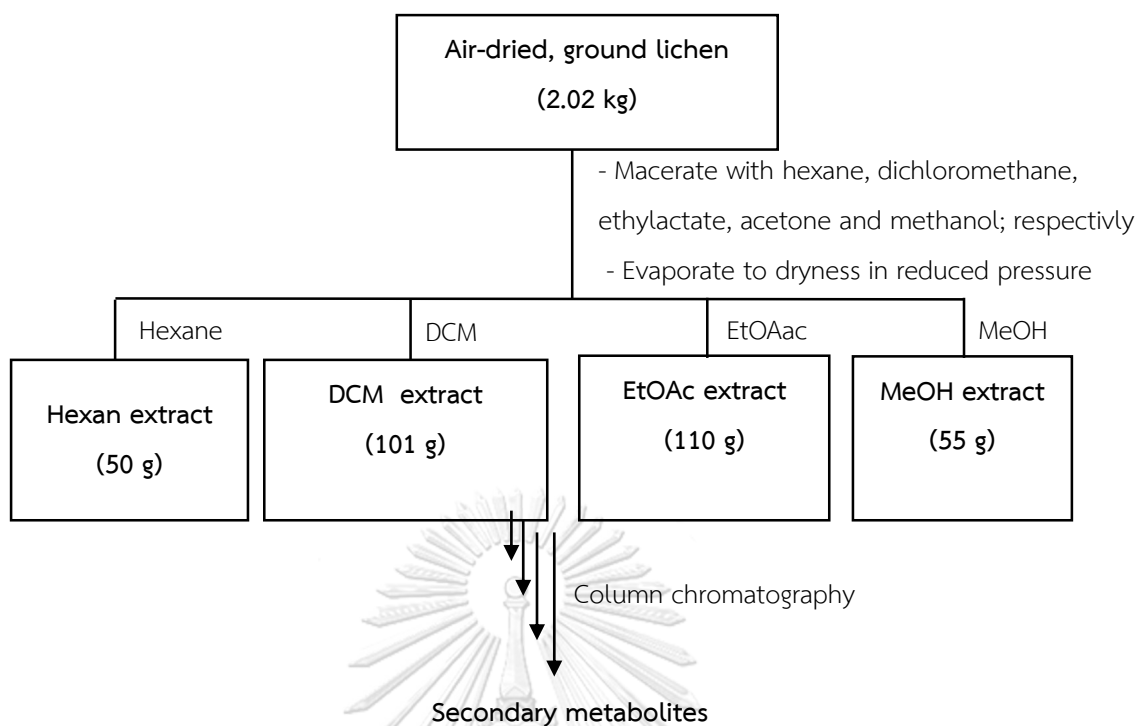


Fig 2.1 The lichen *Usnea aciculifera*

### 2.2.3 Extraction and isolation procedures

Before extraction, the lichen was carefully inspected for contaminants. Air-dried parts of *U. aciculifera* (2.02 kg) were ground and extracted with *n*-hexane, dichloromethane (DCM,  $\text{CH}_2\text{Cl}_2$ ), ethyl acetate (EtOAc), and methanol (MeOH) (4 x 10 L), respectively, by the maceration method at ambient temperature, and the filtered solution was evaporated under reduced pressure to afford the extracts.

Isolation and purification of secondary metabolites from the extracts of lichen *U. aciculifera* were conducted by various methods such as column chromatography on each fraction as shown in Scheme 2.1.



Scheme 2.1. The extraction scheme of the extracts of *U. aciculifera*

## 2.2.4 Biological activities

### 2.2.4.1 Antibacterial activity

The antibacterial activity towards bacteria were determined with modified agar well diffusion method described by Karupiah and Mustafa [89] against tooth decay bacteria *Streptococcus mutans* ATCC 25175 and *Streptococcus sobrinus* KCCM 11898. Bacteria causing skin disease such as *Staphylococcus aureus* ATCC 25923 and *Propionibacterium acnes* KCCM 4147. Extracts, fractions and compounds were also tested with Gram-negative bacteria caused typhi fever *Salmonella typhi* ATCC 422.

Microorganisms were inoculated in nutrient broth and left overnight. The density of each microbial suspension was equal to that of  $1-1.5 \times 10^8$  cells/mL

(standardized by 0.5 McFarland). About 25 mL of nutrient agar was transferred into 9 cm sterilized petri dish. The plates were left at room temperature to let medium solidify. 100  $\mu$ L of bacteria sub-culture then swabbed over the agar media and allow to dry. Wells were made by using a sterile corked borer (6 mm). 30  $\mu$ L of compounds and antibiotics were placed into the wells. Negative control used solvent for dissolving the sample. Clear zone inhibition was measured after incubation overnight at 37 °C. All experiments were done in triplicates and the results were expressed as means values.

Diameter of inhibition zone including diameter of well (6 mm) was observed with range of activity as described here where 6.0 mm means no activity, 6.1 – 8.0 mm means compounds show weak activity, 8.1 – 10.0 mm means moderate activity, 10.1 – 13.0 mm means good activity, 13.1 – 15.0 mm means very good activity and more than 15 mm means excellent activity.

#### 2.2.4.2 Anti-Dengue activity

The experiments were conducted under the collaboration with Department of Microbiology, Faculty of Medicine, Chulalongkorn University.

##### 2.2.4.2.1 Preliminary screening

LLC/MK2 cells (ATCC® CCL-7™) and DENV2 NGC were maintained as previously described.[90] LLC-MK2 ( $5 \times 10^4$  cells) were seeded into each well of 24-well plate and incubated overnight at 37°C under 5% CO<sub>2</sub>. DENV2 was added to the

cells at a multiplicity of infection (M.O.I.) of 0.1 and the plate was incubated at 37°C under 5% CO<sub>2</sub> with gentle rocking every 15 min. The plate was washed with phosphate buffer saline and incubated in maintenance media.[90] Each compound was prepared in DMSO and was introduced into each well to the final concentration of 10 μM during and after infection. One percent DMSO was used as a no-inhibition control and the maintenance media alone was used as a no-virus control. Supernatants were collected at day 3 of incubation and the virus titers were determined by plaque titration. The active compounds were determined by the ability of the compound to inhibit greater than 1-log or 90% of viral titer (plaque forming unit/mL).

#### 2.2.4.2.2 Cytotoxicity of compounds with cell lines

The compound toxicity was determined at 10 μM final concentration. LLC/MK2 (1x10<sup>4</sup> cells/well) were seeded into each well of 96-well plates and incubated overnight at 37°C 5% CO<sub>2</sub>. Compounds were prepared and added to the cells to the final concentration of 10 μM. 1% DMSO was used as a 100% cell viability control. Cells were incubated for 48 h before analyzing their viability by CellTiter 96® AQueous One Solution Cell Proliferation Assay kit (Promega) according to manufacturer's protocol. The plate was read by spectrophotometry at A<sub>450</sub> and data were calculated to percent cell viability proportioned to DMSO control.

#### 2.2.4.2.3 Effective concentration (EC<sub>50</sub>)

Effective concentration ( $EC_{50}$ ) was also studied using LLC/MK2  $5 \times 10^4$  cells, which were seeded and infected with DENV2 (M.O.I. of 0.1). Compounds were serially diluted in DMSO to the final concentrations as follows: 0, 0.1, 0.25, 0.5, 1, 2, 2.5, 5, 7.5, 10, and 25  $\mu\text{M}$ . DMSO at the concentration of 1% was used as a mock treatment referring to 100% infection. Infected cells were treated with the designated compounds during and post infection. Supernatants were collected at 3 days after infection for analysis of virion production by plaque titration. Non-linear regression analysis was used to determine the effective concentrations. Three independent experiments were performed and results were reported as means and standard error of the means (SEM). The therapeutic index (TI) was a ratio of  $CC_{50}/EC_{50}$  of the compound.

#### 2.2.4.2.4 Cytotoxic concentration ( $CC_{50}$ )

Cytotoxic concentrations ( $CC_{50}$ ) were also studied using LLC/MK2 cells. Briefly, the  $10^4$  cells were seeded into each well of 96-well plates. After an overnight incubation, compounds were serially diluted in DMSO to the final concentrations as follows: 1, 5, 7.5, 10, 25, 50, 100, and 250  $\mu\text{M}$ . Each concentration was performed in triplicates. DMSO at 1% was used as a mock treatment referring to 100% cell viability. Cells were incubated for 48 h before cell viability was accessed using CellTiter 96® Aqueous One Solution Cell Proliferation Assay kit (Promega, Wisconsin, USA). Non-linear regression analysis was used to determine cytotoxic concentrations

(CC<sub>50</sub>) of each experiment. Results were derived from three independent experiments and reported as means and standard error of the means (SEM).

#### 2.2.4.3 Cytotoxic activity

This activity was carried out Department of Pharmacology, Faculty of Medicine, Chulalongkorn University. The compound cytotoxicity was evaluated against a panel of 5 representative cell lines, namely HT-29 (human colorectal cancer cell), HCT116 (colorectal cancer), MCF-7 (breast cancer), A549 (lung cancer), and OVCAR-3 (ovarian cancer). 5-Fluorouracil and cisplatin were used as positive control.

### 2.3 RESULTS AND DISCUSSION

#### 2.3.1 Extraction and fractionation of lichen *Usnea aciculifera*

Air-dried parts of *U. aciculifera* (2.02 kg) were ground and extracted with *n*-hexane, dichloromethane (DCM, CH<sub>2</sub>Cl<sub>2</sub>), ethyl acetate (EtOAc), and methanol (MeOH) (4 x 10 L), respectively, by the maceration method at ambient temperature, and the filtered solution was evaporated under reduced pressure to afford a *n*-hexane extract (50.0 g), CH<sub>2</sub>Cl<sub>2</sub> extract (101.0 g), EtOAc extract (110.0 g) and MeOH extract (55.0 g).

#### 2.3.2 Separation of hexane extract

This extract (50.0 g) was separated by silica gel column chromatography using gradient elution with *n*-hexane–EtOAc (stepwise 95:5–0:100) and EtOAc–MeOH (stepwise 10:0–0:100) to give seven fractions, Hex.1–Hex.7.



Fraction Hex.3 (10.9 g) was applied to silica gel column chromatography, eluted with *n*-hexane–EtOAc (97:3) and then with EtOAc to give 4 sub-fractions (Hex3.1 to Hex3.4). Sub-fraction EA3.1 (12.3 g) was separated by silica gel column chromatography, eluted with *n*-hexane–CHCl<sub>3</sub> (8:2) to give nine compounds **1** (7.5 mg), **2** (5.2 mg), **3** (8.1 mg), **4** (4.5 mg), **5** (12.2 mg), **6** (10.4 mg), **7** (5.6 mg), **9** (4.1 mg) and **28** (5501.0 mg).

### 2.3.3 Separation of dichloromethane extract

The DCM extract (101.0 g) was separated by quick column chromatography using gradient elution with (stepwise 80:20–0:10) and EtOAc–MeOH (stepwise 10:0–0:10) to give thirteen fractions, DCM.1–DCM.13.

Fraction DCM.1 (28.0 g) was subjected to silica gel column eluted with *n*-hexane–EtOAc (85:15) to give seven sub-fractions 1.1–1.7. Sub-fraction 1.1 (4.95 g) was chromatographed with sephadex LH-20 column (100 g) with MeOH – CH<sub>2</sub>Cl<sub>2</sub> (60:40) followed by chromatographed with normal silica gel eluted with hexane–DCM (60:40) to yield **8** (8.0 mg), **15** (8.6 mg), **16** (4.5 mg), **27** (8.1 mg), **35** (11.9 mg), **33** (45 mg), and **34** (101 mg). Sub-fraction 1.2 (1.8 g) was chromatographed with sephadex LH-20 column (100 g) with MeOH – CH<sub>2</sub>Cl<sub>2</sub> (60:40) followed by chromatographed with RP–C<sub>18</sub> silica gel eluted with H<sub>2</sub>O–MeOH (60:40) to yield **19** (28 mg), **41** (12.6 mg), **43** (6.8 mg), **44** (4.4 mg), and **42** (4.5 mg). Sub-fraction 1.3 (7.9 g) was subjected to silica gel column using gradient elution with *n*-hexane–EtOAc (85:15 – 0:100) to give **12**

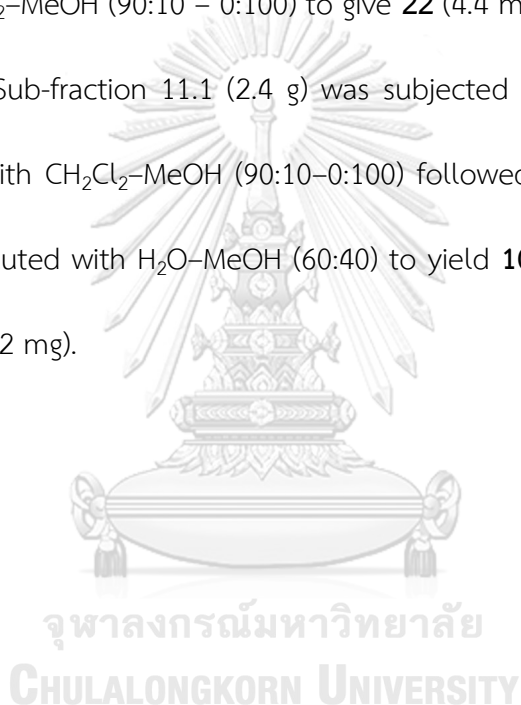
(2025.0 mg), **13** (2560.0 mg), **30** (5.6 mg), and **45** (4.5 mg). Sub-fraction 1.4 (2.3 g) was purified by Sephadex LH-20 column (100 g) with MeOH - CH<sub>2</sub>Cl<sub>2</sub> (60:40) followed by chromatography with silica gel eluted with *n*-hexane-CH<sub>2</sub>Cl<sub>2</sub> (70:30) to yield **21** (26.8 mg) and also separated again **12** and **13**.

Fraction DCM.2 (10.8 g) was subjected to silica gel column chromatography eluted with *n*-hexane-EtOAc (8:2) to give five sub-fractions 2.1-2.5. Sub-fraction 2.2 (0.8 g) was chromatographed with RP-C<sub>18</sub> silica gel eluted with H<sub>2</sub>O-MeOH (60:40) to give **39** (4.1 mg), and **40** (3.4 mg). Sub-fraction 2.3 (3.3 g) was purified by a Sephadex LH-20 column (100 g) with MeOH followed by chromatography with RP-C<sub>18</sub> silica gel eluted with H<sub>2</sub>O-MeOH (60:40) to yield **38** (10.8 mg). Sub-fraction 2.4 (4.1 g) was subjected to silica gel column chromatography using gradient elution with *n*-hexane-CH<sub>2</sub>Cl<sub>2</sub> (70:30-0:100) to give **36** (5.5 mg) and **37** (5.0 mg).

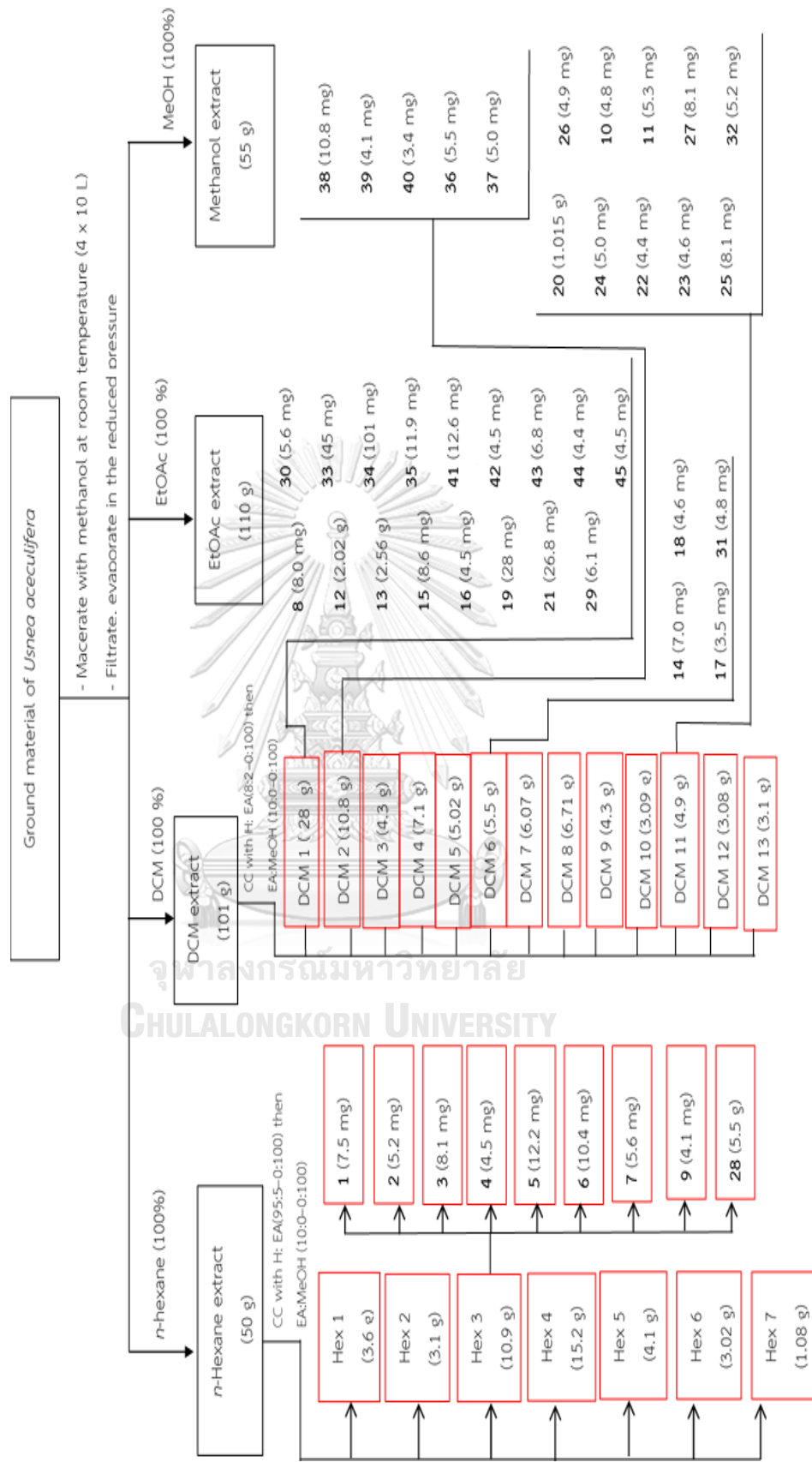
Fraction DCM.6 (6.8 g) was subjected to silica gel column chromatography eluted with *n*-hexane-EtOAc (7:3) to give six sub-fractions 2.1-2.6. Sub-fraction 6.1 (0.8 g) was chromatographed with sephadex LH-20 column (100 g) with MeOH - CH<sub>2</sub>Cl<sub>2</sub> (60:40) followed by chromatographed with silica gel eluted with *n*-hexane-CH<sub>2</sub>Cl<sub>2</sub>-EtOAc (4:4:2) to yield **14** (7.0 mg). Sub-fraction 6.3 (0.4 g) was subjected to silica gel column using gradient elution with CH<sub>2</sub>Cl<sub>2</sub>-MeOH (98:2 - 0:100) to give **17** (3.5 mg), **18** (4.6 mg) and **31** (4.8 mg).

Fraction DCM.11 (18.7 g) was subjected to silica gel column eluted with *n*-hexane–EtOAc (65:35) to give 5 sub-fractions 1.1–1.5. Sub-fraction 11.1 (2.4 g) was subjected to silica gel column using gradient elution with *n*-hexane–EtOAc (75:15 – 0:100) to give **20** (1015.0 mg) and **24** (5.0 mg).

Sub-fraction 11.3 (2.04 g) was subjected to silica gel column using gradient elution with CH<sub>2</sub>Cl<sub>2</sub>–MeOH (90:10 – 0:100) to give **22** (4.4 mg), **23** (4.6 mg), **25** (8.1 mg) and **26** (4.9 mg). Sub-fraction 11.1 (2.4 g) was subjected to silica gel column using gradient elution with CH<sub>2</sub>Cl<sub>2</sub>–MeOH (90:10–0:100) followed by chromatography with RP–C<sub>18</sub> silica gel eluted with H<sub>2</sub>O–MeOH (60:40) to yield **10** (4.8 mg), **11** (5.3 mg), **29** (6.1 mg) and **32** (5.2 mg).



Scheme 2.2: Isolation of compounds from different fractions of *Usnea aciculifera* Vain (Parmeliaceae)



#### 2.3.4 Structural elucidation of compounds from lichen *Usnea aciculifera*

From lichen *U. aciculifera* collected in Lam Dong province of Vietnam, 45 lichen substances were isolated, including 9 new secondary metabolites (**36-44**) and 36 known ones (**1-33, 45**).

The chemical structures of the isolated compounds were elucidated by a combination spectroscopic data (1D, 2D NMR, HRESIMS), electronic circular dichroism (ECD) experiments, and single-crystal X-ray crystallographic analyses as well as comparison of their NMR data with those in the literature.

For better interpretation of the chemical structures of the isolated compounds, they were classified into six groups:



<b>Group 1:</b> Monocyclic compounds	11 compounds
<b>Group 2:</b> Depsides	7 compounds
<b>Group 3:</b> Depsidones	9 compounds
<b>Group 4:</b> Dibenzofurans	1 compounds
<b>Group 5:</b> Steroids - Triterpenoids	4 compounds
<b>Group 6:</b> Dimeric xanthones	13 compounds

### 2.3.4.1 Monocyclic phenolic compounds

Eleven monocyclic phenolic compounds (**1–11**) were isolated from *n*-hexane and CH<sub>2</sub>Cl<sub>2</sub> extracts. (Fig. 2.2)

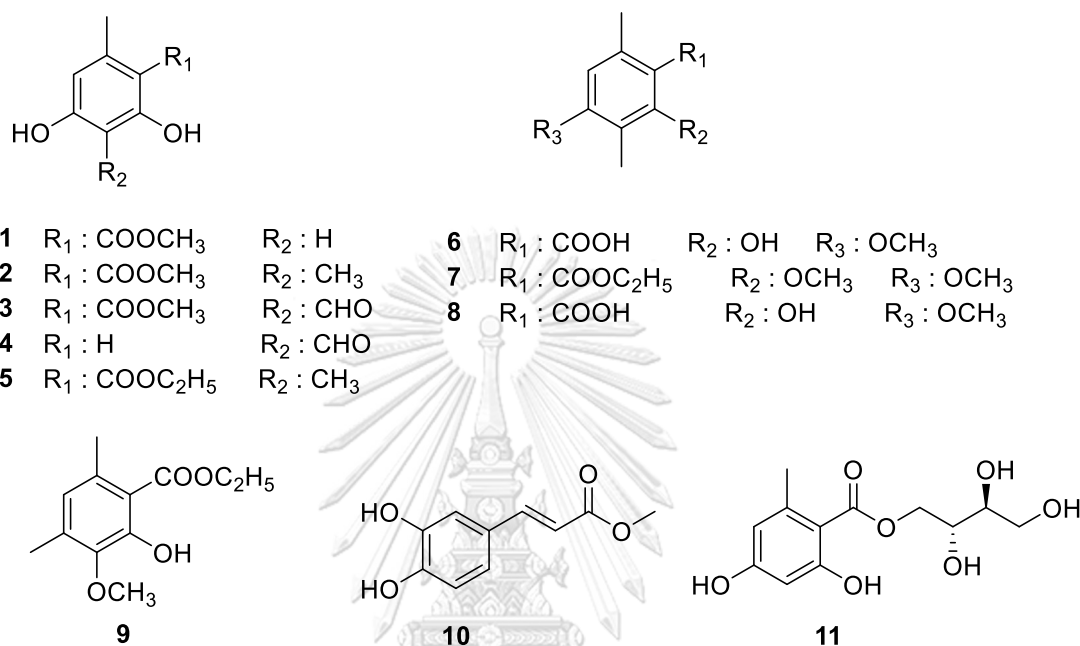
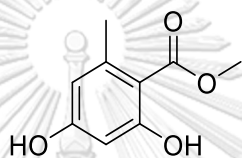


Fig 2.2 Chemical structures of monocyclic phenolic compounds

#### Methyl orsellinate (**1**)

Compound **1** was isolated as a colorless crystalline solid. TLC: red spot with  $R_f = 0.65$ , when eluted with solvent system of CH<sub>2</sub>Cl<sub>2</sub> : MeOH (98: 2) and visualized by a 5% vanillin/H<sub>2</sub>SO<sub>4</sub> solution. The <sup>1</sup>H-NMR spectral features indicated the presence of a pair of meta-coupled aromatic protons at  $\delta$  6.24 (1H, *d*, *J* = 2.0 Hz, H-3) and  $\delta$  6.29 (1H, *d*, *J* = 2.0 Hz, H-5), a methoxy group at  $\delta$  3.92 (3H, *s*, -OCOCH<sub>3</sub>) and a methyl group at  $\delta$  2.46 (3H, *s*), and a chelated phenolic hydroxyl group at  $\delta$  11.59 (1H, *s*, 2-OH)].

The  $^{13}\text{C}$  NMR spectrum showed the resonances of 9 carbons including of one aromatic methyl group ( $\delta$  24.4), one methyl ester ( $\delta$  173.2 (C=O), 52.4 (OCH<sub>3</sub>)), two methine carbons ( $\delta$  101.5, 111.5) and four substituted aromatic carbons, two of which were oxygenated ( $\delta$  166.6, 163.6, 144.6, 105.8). These spectroscopic data were compatible with the data of methyl orsellinate in the literature.[20] Therefore, **1** was methyl orsellinate.



Methyl 2,4-dihydroxy-6-methylbenzoate  
or methyl orsellinate (**1**)

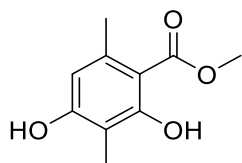
### Methyl $\beta$ -orsellinate (**2**)

Compound **2** was isolated as colorless needles (recrystallized in chloroform).

The NMR spectral features of **2** were similar to those of **1** except for the presence of an additional methyl group ( $\delta_{\text{H}}$  2.10,  $\delta_{\text{C}}$  7.8) and the absence of an aromatic proton.

These spectroscopic data were suitable with the data of methyl  $\beta$ -orsellinate.[20]

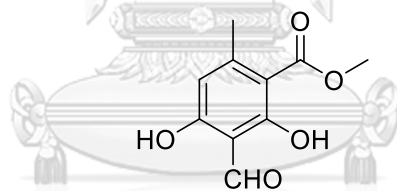
Therefore, **2** was methyl  $\beta$ -orsellinate.



Methyl 2,4-dihydroxy-3,6-dimethylbenzoate  
or methyl  $\beta$ -orsellinate (**2**).

### Methyl haematommate (3)

The  $^1\text{H-NMR}$  spectrum of **3** showed six singlets of two chelated hydrogen-bonded phenolic hydroxyl groups at  $\delta_{\text{H}}$  12.87 and 12.41, a formyl proton at  $\delta_{\text{H}}$  10.34, an aromatic proton at  $\delta_{\text{H}}$  6.29, a methoxyl and methyl group at  $\delta_{\text{H}}$  3.96 and 2.53. The  $^{13}\text{C}$  NMR spectrum showed the resonances of 10 carbon signals including a methyl group ( $\delta_{\text{C}}$  25.1), a methyl ester [ $\delta_{\text{C}}$  171.9 (C=O)], a methoxyl ( $\delta_{\text{C}}$  52.2), a formyl group ( $\delta_{\text{C}}$  193.9) and five quaternary carbon signals. These spectral features resembled those of **2**, except for the presence of the formyl group at C-3 position instead of a methyl group. The NMR data of **3** were suitable to the published ones.[91] Therefore **3** was elucidated as methyl haematommate.



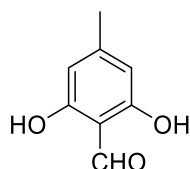
จุฬาลงกรณ์มหาวิทยาลัย  
CHULALONGKORN UNIVERSITY  
Methyl haematommate (**3**).

### Atranol (4)

The  $^1\text{H-NMR}$  spectrum displayed signals of one methyl group at  $\delta_{\text{H}}$  2.23, two aromatic methine protons appeared with the same chemical shift at  $\delta_{\text{H}}$  6.25 (2H, s), and one formyl group at  $\delta_{\text{H}}$  10.26. The  $^{13}\text{C-NMR}$  spectrum showed the resonances of 6 carbons including of one aromatic methyl groups ( $\delta_{\text{C}}$  22.4), two methine carbons ( $\delta_{\text{C}}$  108.5) one formyl group ( $\delta_{\text{C}}$  194.2) and two oxygenated aromatic carbons ( $\delta_{\text{C}}$



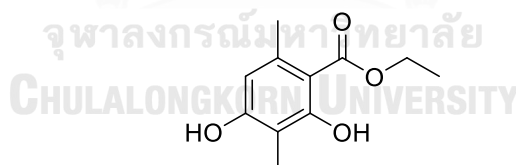
163.1). These spectroscopic data were suitable to the published ones.[91] Therefore **4** was elucidated as atranol.



Atranol (**4**).

### Ethyl $\beta$ -orsellinate (**5**)

The NMR spectral features of **5** were similar to those of **2** except for the presence of an additional ethyl ester group [92] instead of a methyl ester group. These spectroscopic data were suitable with the data of ethyl  $\beta$ -orsellinate.[20] Therefore, **5** was ethyl  $\beta$ -orsellinate.



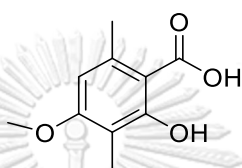
Ethyl 2,4-dihydroxy-3,6-dimethylbenzoate

Ethyl  $\beta$ -orsellinate (**5**).

### 4-hydroxy-2-methoxy-3,6-dimethylbenzoic acid (**6**)

The  $^1\text{H-NMR}$  spectrum of **6** displayed signals of two methyl groups, an aromatic methine proton, a chelated phenolic hydroxyl group, and a methoxyl

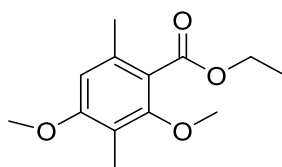
group. The  $^{13}\text{C}$ -NMR spectrum showed the resonances of 10 carbons including of two aromatic methyl groups, a methine carbon, a methoxy carbon, a carboxylic acid group, two quaternary carbon signals and two oxygenated aromatic carbons. These spectroscopic data were suitable to the published ones.[91] Therefore **6** was elucidated as 4-hydroxy-2-methoxy-3,6-dimethylbenzoic acid.



4-hydroxy-2-methoxy-3,6-dimethylbenzoic acid (**6**).

#### **Ethyl 2,4-dimethoxy-3,6-dimethylbenzoate (7)**

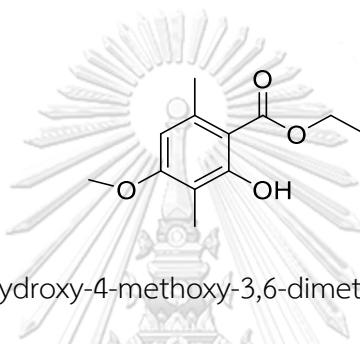
The NMR spectral features of **7** were similar to those of **5** except for the presence of two additional methoxyl groups ( $\delta_{\text{H}}$  3.75 and 3.80) instead of two hydroxyl groups. These spectroscopic data were suitable with the data of ethyl 2,4-dimethoxy-3,6-dimethylbenzoate.[20] Therefore, **7** was elucidated as ethyl 2,4-dimethoxy-3,6-dimethylbenzoate.



Ethyl 2,4-dimethoxy-3,6-dimethylbenzoate (**7**).

### Ethyl 2,4-dimethoxy-3,6-dimethylbenzoate (8)

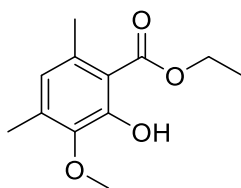
The NMR spectral features of **8** were similar to those of **5** except for the presence of an additional methoxyl group ( $\delta_H$  3.83) instead of a hydroxyl group at position C-2. These spectroscopic data were suitable with the data of ethyl 2-hydroxy-4-methoxy-3,6-dimethylbenzoate.[20] Therefore, **8** was elucidated as ethyl 2-hydroxy-4-methoxy-3,6-dimethylbenzoate.



Ethyl 2-hydroxy-4-methoxy-3,6-dimethylbenzoate (**8**).

### Ethyl 2-hydroxy-3-methoxy-4,6-dimethylbenzoate (9).

The  $^1\text{H-NMR}$  spectrum of **9** displayed signals of two aromatic methyl groups, an aromatic methine proton, a methoxyl group, and an oxygenated methylene group connected with methyl group. The  $^{13}\text{C-NMR}$  spectrum showed the resonances of 12 carbons including of two aromatic methyl groups, a methine carbon, a methoxy carbon, a methylene group, a saturated methyl group, three quaternary carbon signals, two oxygenated aromatic carbons and a carbonyl group. These spectroscopic data were suitable to the published ones,[91] therefore **9** was elucidated as ethyl 2-hydroxy-3-methoxy-4,6-dimethylbenzoate.

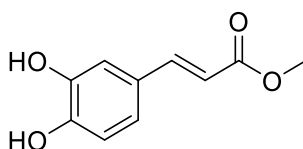


Ethyl 2-hydroxy-3-methoxy-4,6-dimethylbenzoate (**9**).

### Methyl (*E*)-3-(3,4-dihydroxyphenyl)acrylate (**10**)

Compound **10** was obtained as orange oil. The molecular formula of **9** was established as  $C_{10}H_{10}O_4$  by HR-EIMS. The  $^1H$  NMR spectrum displayed signals for one methoxy group at  $\delta_H$  3.68 (3H, s), three aromatic protons at  $\delta_H$  7.05 (1H, *d*,  $J = 1.6$  Hz, H-2), 6.99 (1H, *dd*,  $J = 1.6$  and 8.0 Hz, H-6), and 6.76 (1H, *d*,  $J = 8.0$  Hz, H-5), and two protons of a double bond with the *E* configuration at  $\delta_H$  7.48 (1H, *d*, 16.0 Hz, H-7), and 6.27 (1H, *d*, 16.0 Hz, H-8).

The  $^{13}C$  NMR spectrum of **10** also showed a methyl ester group at  $\delta_C$  51.3 (COOCH<sub>3</sub>), 167.1 (COOCH<sub>3</sub>), three aromatic methine carbons at  $\delta_C$  121.5 (C-6), 115.8 (C-5), 114.8 (C-2) and two olefinic carbons at  $\delta_C$  145.2 (C-7) and 113.8 (C-8). These spectroscopic data were compatible with the published one.[93] Therefore, **10** was proposed as methyl (*E*)-caffeate.

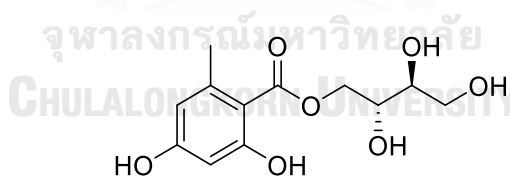


Methyl (*E*)-3-(3,4-dihydroxyphenyl)acrylate or methyl (*E*)-caffeate (**10**)

**(+)-D-Montagnetol (11)**

Compound **11** was obtained as yellow oil. Its  $^1\text{H}$  NMR spectra showed two oxygenated methylenes and two oxygenated methines in the zone of 3.0–4.5 ppm. Additionally, **11** contained one orcinol unit, including one aromatic methyl at  $\delta_{\text{H}}$  2.08 and two *meta*-coupled protons at  $\delta_{\text{H}}$  6.14 and 6.18.

The  $^{13}\text{C}$  NMR spectrum of **11** revealed two oxygenated methines ( $\delta_{\text{C}}$  72.5 and 69.7), two oxygenated methylenes ( $\delta_{\text{C}}$  66.7 and 63.0), two aromatic methines ( $\delta_{\text{C}}$  100.5 and 110.6), two quaternary aromatic carbons ( $\delta_{\text{C}}$  106.7 and 141.9), two oxygenated aromatic carbons ( $\delta_{\text{C}}$  161.4 and 161.9), one carboxyl carbon at  $\delta_{\text{C}}$  170.0, and one methyl group at  $\delta_{\text{C}}$  22.6. The combination of the compatibility of the spectral data of **11** with the published one,[20] as well as the positive optical rotation, **11** was elucidated as (+)-*D*-montagnetol.



(+)-*D*-Montagnetol (**11**)

### 2.3.4.2 Depsides Compounds

Seven depsides were isolated from *U. aciculifera* including **12** – **18**. (Fig. 2.3)

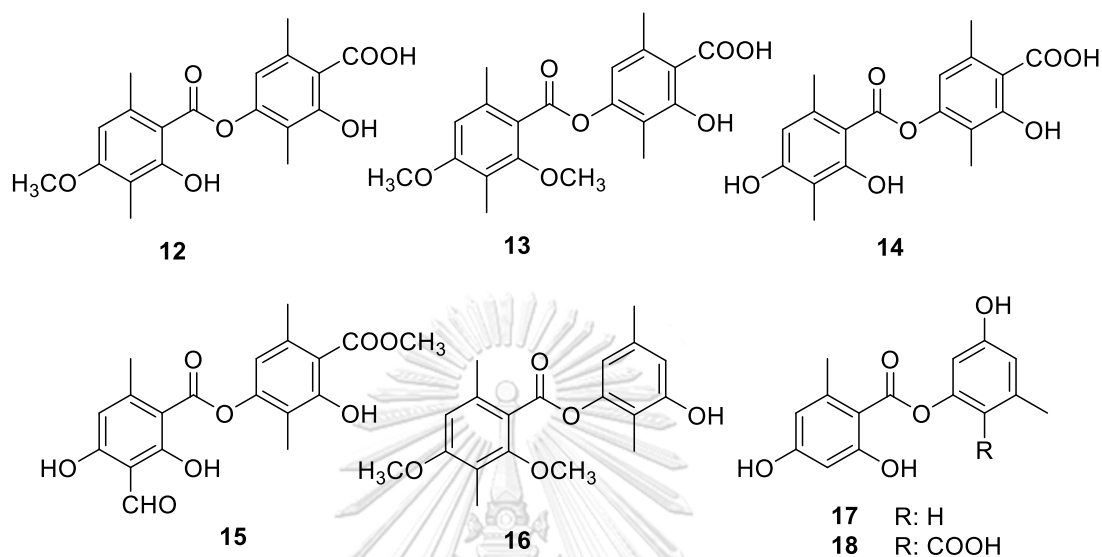


Fig. 2.3 The structures of isolated depsides.

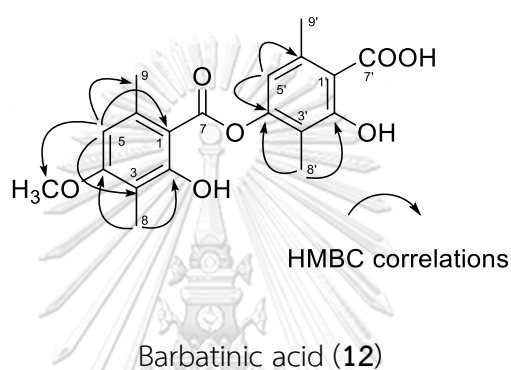
#### Barbaticinic acid (**12**)

Compound **12** was obtained as colorless needles (recrystallized in acetone).

The  $^1\text{H-NMR}$  spectrum exhibited signals for one chelated hydroxyl group ( $\delta_{\text{H}}$  11.43, 2-OH), four methyl groups at  $\delta_{\text{H}}$  2.03 (3H, s, 3- $\text{CH}_3$ ), 2.05 (3H, s, 3'- $\text{CH}_3$ ), 2.60 (3H, s, 6- $\text{CH}_3$ ) and 2.70 (3H, s, 6'- $\text{CH}_3$ ), respectively], two aromatic methine protons at  $\delta_{\text{H}}$  6.70 (1H, s, H-5') and 6.61 (1H, s, H-5) and one methoxy at  $\delta_{\text{H}}$  3.93 (3H, s, 4- $\text{OCH}_3$ ).

The  $^{13}\text{C-NMR}$  spectra revealed 19 carbons: two carbonyl groups ( $\delta_{\text{C}}$  174.3 (C-7') and 170.8 (C-7)), four oxygenated carbons ( $\delta_{\text{C}}$  163.4 (C-4), 164.0 (C-2), 163.2 (C-2'), 153.5 (C-4')), two aromatic methine carbons ( $\delta_{\text{C}}$  117.1 (C-5'), 107.5 (C-5)), four aromatic methyl groups ( $\delta_{\text{C}}$  24.8 (6- $\text{CH}_3$ ), 23.7 (6'- $\text{CH}_3$ ), 9.3 (3'- $\text{CH}_3$ ) and 7.9 (3- $\text{CH}_3$ )), one methoxy group

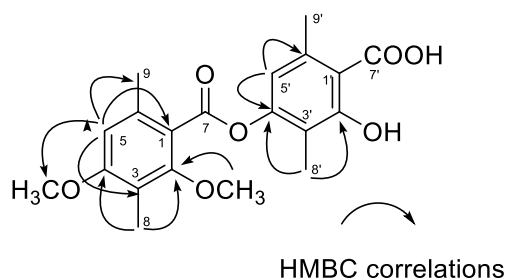
at  $\delta_C$  56.1 (4-OCH<sub>3</sub>), one carboxylic group at  $\delta_C$  174.3 (C-7'). The last six carbons were C-1 ( $\delta_C$  111.3), C-1' (110.6), C-3 (105.3), C-3' (117.1), C-6 (141.8) and C-6' (141.0). These findings implied that **12** was composed of two mono-aromatic units. The substitution pattern was confirmed by HMBC correlations. Thus, **12** was elucidated as a typical depside, barbatinic acid.[15, 45]



### Diffractaic acid (**13**)

Compound **13** was obtained as colorless needles (recrystallized in acetone).

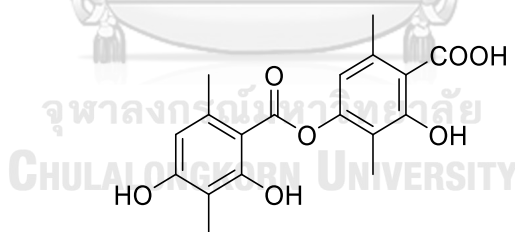
The molecular formula of **13** was identified as C<sub>20</sub>H<sub>22</sub>O<sub>7</sub> by HR-EIMS. The NMR spectral features of **13** resembled to those of barbatinic acid (**12**) except for the presence of a methoxyl group at C-2 position instead of hydroxyl group. This was confirmed by the HMBC correlation from methoxyl protons at  $\delta_H$  3.84 to carbon C-2 at  $\delta_C$  157.8. Therefore, the structure of **13** was determined to be diffractaic acid.[25]



Diffractaic acid (**13**)

#### Demethylbarbatinic acid (**14**)

Compound **14** was obtained as light needles. The NMR spectral features of **14** resembled to those of barbatinic acid (**12**) except for the disappearance of a methoxyl group at C-4, indicating the presence of hydroxyl group at this position. These spectroscopic data were compatible with the data of demethylbarbatinic acid in the literature.[26] Therefore, the structure of **14** was determined.



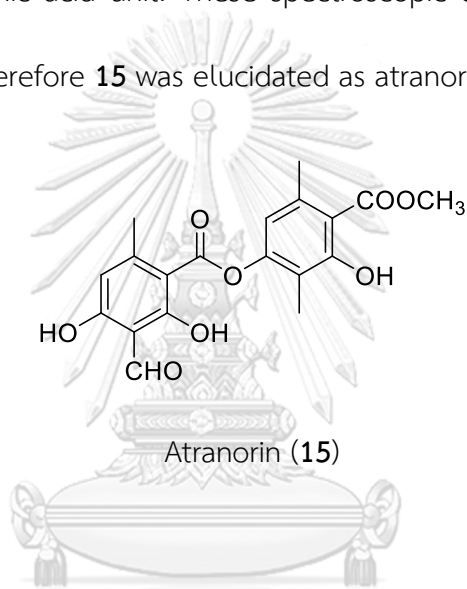
Demethylbarbatinic acid (**14**)

#### Atranorin (**15**)

Compound **15** was isolated as light yellow crystal, mp 195-197°C. The  $^1\text{H-NMR}$  spectrum indicated the presence of two aromatic siglets at  $\delta_{\text{H}}$  6.40 and 6.52, three methyls at  $\delta_{\text{H}}$  2.09, 2.55 and 2.69, one methoxy at  $\delta_{\text{H}}$  3.99, three hydroxyls at  $\delta_{\text{H}}$



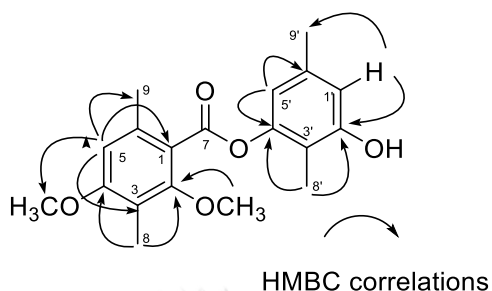
11.94, 12.49 and 12.54, and a formyl group at  $\delta_{\text{H}}$  10.35. The  $^{13}\text{C}$ -NMR spectrum of **15** showed, besides signals due to three methyl and one methoxyl groups, two aromatic CH carbons and thirteen quaternary carbons including a formyl carbon at  $\delta_{\text{C}}$  193.8, two ester carbonyl carbons at  $\delta_{\text{C}}$  169.7 and 172, and four oxygenated carbons. These findings implied that **15** was composed of two mono-aromatic units, haematommic acid unit and  $\beta$ -orsellinic acid unit. These spectroscopic data were suitable to the published ones.[91] Therefore **15** was elucidated as atranorin.



#### Aceculiferin A (**16**)

Compound **16** was obtained as colorless needles (recrystallized in acetone). Its HR-EIMS established the molecular formula of  $\text{C}_{19}\text{H}_{22}\text{O}_5$ , that is, 44 mass units less than that of **13**. The UV, IR and NMR spectral features of **16** resembled those of **13**. The difference between two compounds was that the NMR spectral of **16** showed the signal of an additional aromatic methine proton ( $\delta_{\text{H}}$  6.53 s) and the quaternary carbon in **13** was replaced by an aromatic methine carbon in **16**. The HMBC correlations from aromatic proton H-1' ( $\delta_{\text{H}}$  6.53) to oxygenate C-2' ( $\delta_{\text{C}}$  151.5) and aromatic methyl group C-7' ( $\delta_{\text{C}}$  21.1) suggested the carboxylic group in **13** was

replaced by an aromatic proton at C-1'. Accordingly, the structure of **16** was established as aciculiferin A.[88]

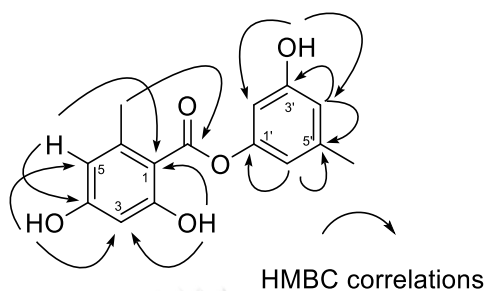


Aciculiferin A (**16**)

### Lecanorin (**17**)

Compound **17** was isolated as a yellow amorphous powder. The  $^1\text{H-NMR}$  spectrum displayed signals of two methyl groups at  $\delta_{\text{H}}$  2.29 (3H, s, 6'-CH<sub>3</sub>) and 2.59 (3H, s, 6-CH<sub>3</sub>), two aromatic methine protons at  $\delta_{\text{H}}$  6.29 (1H, d,  $J = 2.5$  Hz, H-3), 6.38 (1H, d,  $J = 2.5$  Hz, H-5), three aromatic methine protons at  $\delta$  6.58 (2H, s, H-3' and H-5'), 6.63 (1H, s, H-1'), and three hydroxyl protons at  $\delta_{\text{H}}$  8.60 (1H, s, 2'-OH), 9.33 (1H, s, 4-OH), 11.31 (1H, s, 2-OH). The  $^{13}\text{C-NMR}$  and HSQC spectra showed the resonances of 15 carbons, namely two aromatic methyl groups at  $\delta_{\text{C}}$  21.4 (C-7), 24.4 (C-8), five aromatic methine carbons at  $\delta_{\text{C}}$  101.8 (C-3), 107.4 (C-3'), 112.8 (C-5), 114.4 (C-5'), 114.7 (C-1'), seven substituted aromatic carbons, three of which were oxygenated at  $\delta_{\text{C}}$  105.1 (C-1), 141.1 (C-6'), 144.7 (C-6), 151.9 (C-4'), 159.1 (C-2'), 164.0 (C-4), 166.8 (C-2), and one carbonyl carbon at  $\delta_{\text{C}}$  171.1 (C-7). These findings implied that compound **17** was composed of two mono-aromatic units, orsellinic acid unit and orcinol unit. The

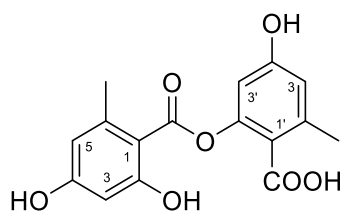
substitution pattern was confirmed by HMBC correlations. Thus, compound **17** was elucidated as lecanorin.[94]



Lecanorin (**17**)

#### Isolecanoric acid (**18**)

Compound **18** was isolated as yellow amorphous powder. The NMR spectral features of **18** resembled to those of lecanorin (**17**). The only difference was that the disappearance of one signal for an aromatic methine proton in **17** and the signal for the aromatic carbon in **17** was replaced by a quaternary carbon in **18** together with one more carboxylic group showed in **18**. These spectroscopic data were compatible with the published ones in the literature.[95] Therefore **18** was isolecanoric acid.



Isolecanoric acid (**18**)

### 2.3.4.3 Depsidones Compounds

Nine depsidones were isolated from *U. aciculifera*, including **19–27**. (Fig. 2.4)

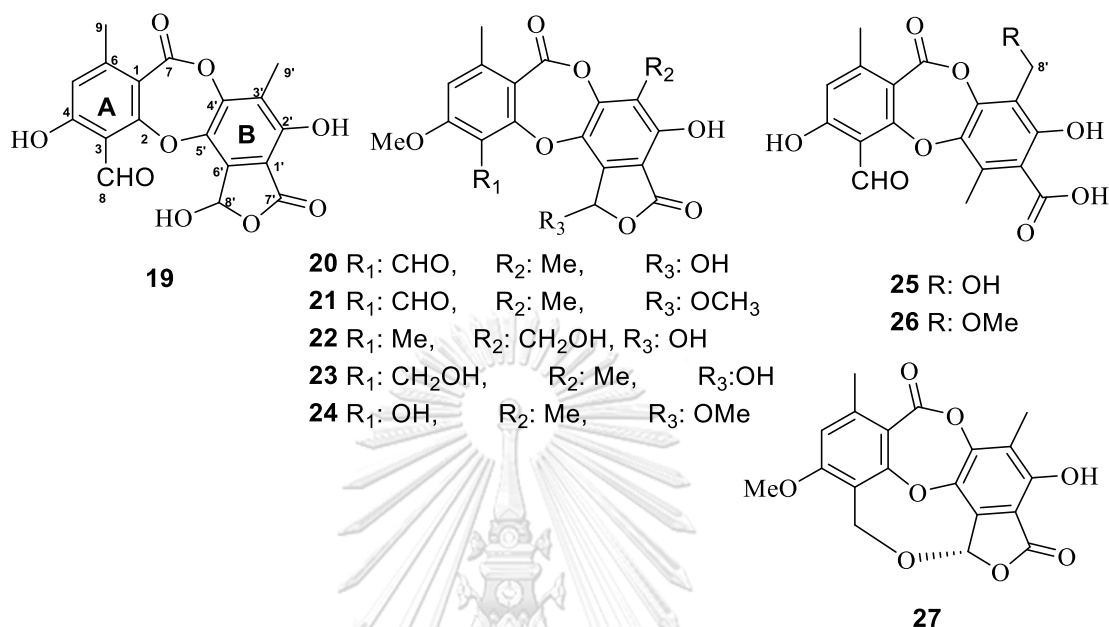
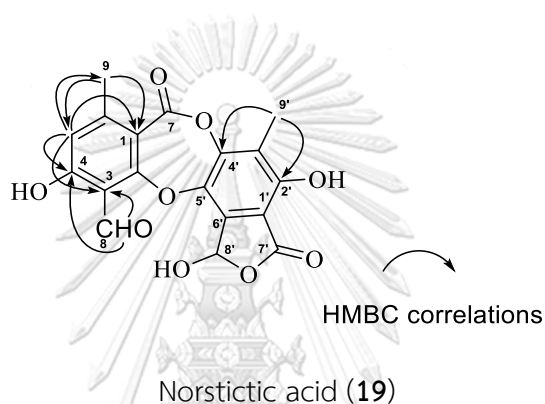


Fig. 2.4 The structures of isolated depsidones.

#### Norstictic acid (**19**)

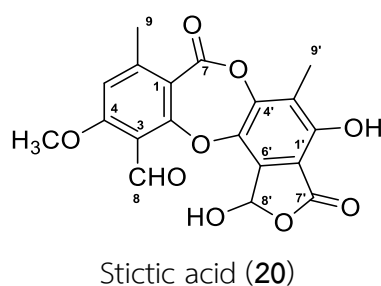
Compound **19** was isolated as a white powder. The <sup>1</sup>H NMR spectrum of **19** contained eight proton signals including two aromatic methyl groups at  $\delta_H$  2.20 (H-8') and 2.44 (H-9), one aromatic proton at  $\delta_H$  6.84 (H-5), one hemiacetal proton at  $\delta_H$  6.78 (H-9'), one CHO group at  $\delta_H$  10.45 (3-CHO), one chelated hydroxyl group to a neighboring carboxyl groups at  $\delta_H$  12.04 (2'-OH) and two hydroxyl groups at  $\delta_H$  10.16 (4-OH) and 8.26 (9'-OH). The presence of only one aromatic proton at  $\delta_H$  6.84 (H-5) was supportive of the ether bridge between C-2 and C-5' leading to a depsidone

skeleton.[96] The  $^{13}\text{C}$ -NMR spectrum showed 18 carbons including two carboxyl group signals at  $\delta_{\text{C}}$  163.6, 160.3 and one hemiacetal carbon at  $\delta_{\text{C}}$  95.0 . It showed two methyl signals at  $\delta_{\text{C}}$  9.6 ( $3'\text{-CH}_3$ ), 21.4 ( $6\text{-CH}_3$ ) and one CHO group at  $\delta_{\text{C}}$  192.8. The positions of substituted functional groups were confirmed by HMBC correlations. Accordingly, the structure of **19** was determined as a typical depsidone, norstictic acid. [82]



### Stictic acid (**20**)

Compound **20** was isolated as a white powder. The NMR spectral features of **20** resembled to those of norstictic acid (**19**) except for the presence of a signal of methoxyl group at C-4 instead of hydroxyl group. This was confirmed by the HMBC correlation from methoxyl protons at  $\delta_{\text{H}}$  3.94 to carbon C-4 at  $\delta_{\text{C}}$  163.0. Therefore, the structure of **20** was determined to be stictic acid.[97]

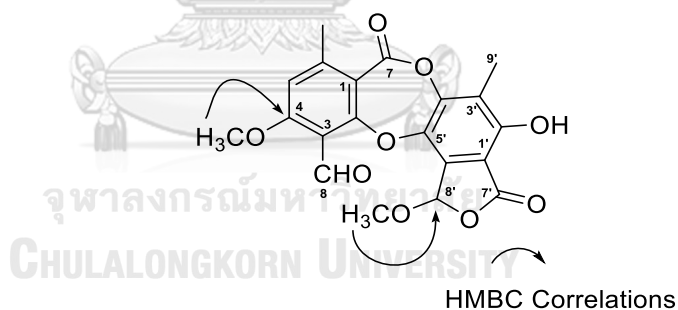


### 8'-O- Methylstictic acid (21)

The NMR spectral features of **21** resembled to those of stictic acid (**20**) except for the presence of one more signal of methoxyl group at C-8' instead of hydroxyl group.

This was confirmed by the HMBC correlation from methoxyl protons at  $\delta_{\text{H}}$  3.44 to carbon C-8' at  $\delta_{\text{C}}$  100.0. Therefore, the structure of **21** was determined to be 8'-O-methylstictic acid.[97]

9

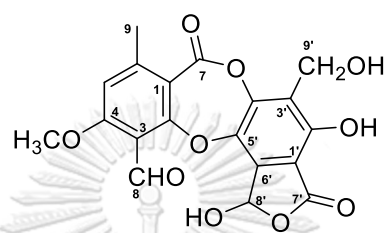


8'-O-methylstictic acid (**21**)

### Hypoconstictic acid (22)

The NMR spectral features of compound **22** resembled those of stictic acid (**20**). The only difference was that the presence of one oxygenated methylene group at C-3' instead the signal for an aromatic methyl group at C-3' in **20**. This was

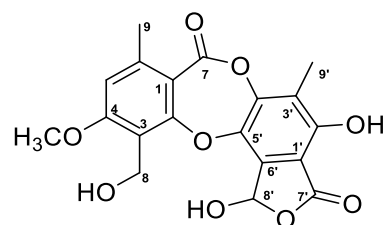
confirmed by the HMBC correlation from methylene protons at  $\delta_{\text{H}}$  4.63 to carbon C-3' at  $\delta_{\text{C}}$  125.1. Therefore, the structure of **22** was determined to be hypoconstictic acid.[97]



Hypoconstictic acid (**22**)

### Cryptostictic acid (**23**)

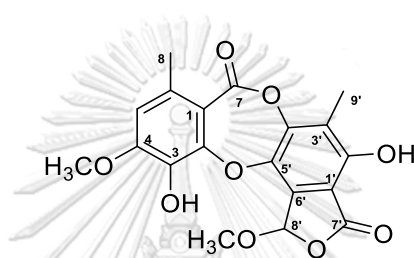
Compound **23** was isolated as a white powder. The NMR spectral features of **23** resembled to those of stictic acid (**20**) except for the presence of a signal of oxygenated methylene group  $\delta_{\text{H}}$  4.71 at C-3 instead of formyl group  $\delta_{\text{H}}$  10.49. This was confirmed by the HMBC correlation from methylene protons to carbon C-3 at  $\delta_{\text{C}}$  112.7. Therefore, the structure of **23** was determined to be cryptostictic acid.[97]



Cryptostictic acid (**23**)

### 8'-O-methylmenegazziaic acid (**24**)

Compound **24** was obtained as white amorphous powder. The comparison NMR spectral data of **24** with those of 8'-O-methylsalazinic acid [98] showed that they were identical. Thus, **24** was elucidated as 8'-O-methylsalazinic acid.



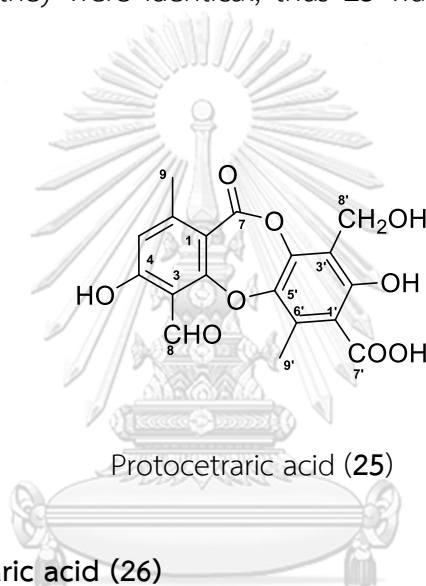
8'-O-methylmenegazziaic acid (**24**)

### Protocetraric acid (**25**)

Compound **25** was obtained as white amorphous powder. The  $^1\text{H}$  NMR and HSQC spectra of **25** showed the presence of one formyl ( $\delta_{\text{H}}$  10.55, 1H, s), one aromatic proton ( $\delta_{\text{H}}$  6.78, 1H, s), one oxygenated methylene proton ( $\delta_{\text{H}}$  4.43, 2H, s), one methoxy group ( $\delta_{\text{H}}$  3.19, 3H, s), two methyl groups ( $\delta_{\text{H}}$  2.45, 3H, s and 2.35, 3H, s). The  $^{13}\text{C}$  NMR spectrum in accordance with HSQC spectrum confirmed the presence of nineteen carbons comprising one aldehyde carbon ( $\delta_{\text{C}}$  191.8), two carboxyl carbons ( $\delta_{\text{C}}$  170.4 and 161.3), twelve aromatic carbons ( $\delta_{\text{C}}$  164.4, 163.8, 158.2, 151.8, 145.1, 141.2, 131.2, 116.9, 115.5, 115.1, 112.3, and 111.8), one oxygenated methylene carbon ( $\delta_{\text{C}}$  62.4), one methoxy group ( $\delta_{\text{C}}$  57.3), and two methyls ( $\delta_{\text{C}}$  21.3 and 14.4).

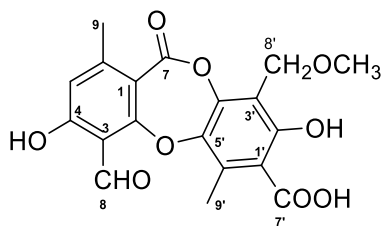


HMBC cross peaks of H<sub>3</sub>-9 ( $\delta_{\text{H}}$  2.35) to C-1 ( $\delta_{\text{C}}$  111.8), C-5 ( $\delta_{\text{C}}$  116.9) and C-6 ( $\delta_{\text{C}}$  151.8), H-5 to C-9 ( $\delta_{\text{C}}$  21.3), and both H-5 ( $\delta_{\text{H}}$  6.78) and 3-CHO ( $\delta_{\text{H}}$  10.55) to C-3 ( $\delta_{\text{C}}$  112.3) defined the connectivity through C-1–C-6–C-5–C-4–C-3 in A-ring. In addition, the cross peaks of H<sub>3</sub>-9' ( $\delta_{\text{H}}$  2.34) to C-6' ( $\delta_{\text{C}}$  131.2), C-5' ( $\delta_{\text{C}}$  141.2), and C-1' ( $\delta_{\text{C}}$  115.5) confirmed its position in B-ring. The comparison of NMR data of **25** and those of protocetraric acid,[98] showed that they were identical, thus **25** was elucidated as protocetraric acid.



#### 8'-O-methylprotocetraric acid (26)

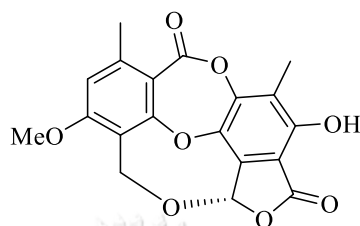
The NMR spectral features of **26** resembled to those of stictic acid (**25**) except for the presence of a signal of methoxyl group  $\delta_{\text{H}}$  3.19 at C-8' instead of hydroxyl group. the HMBC cross peaks of methoxy group (3.19, s, 3H) to C-8' ( $\delta_{\text{C}}$  62.4), H<sub>2</sub>-8' to C-2' ( $\delta_{\text{C}}$  158.2), C-3' ( $\delta_{\text{C}}$  115.1), and C-4' ( $\delta_{\text{C}}$  145.1) determined the linkage of –CH<sub>2</sub>OCH<sub>3</sub> at C-3'. The comparison of NMR data of **26** and those of 8'-O-methylprotocetraric acid [98] showed that they were identical, thus **26** was elucidated as 8'-O-methylprotocetraric acid.

8'-O-methylprotocetraric acid (**26**)

### Lobarientalone B (**27**)

Compound **27** was obtained as white amorphous powder. The molecular formula of **27** was identified as  $C_{19}H_{14}O_8$  by HR-EIMS. A comparison of the NMR spectroscopic data of **27** and **21** showed similarities, particularly in the A- and B-rings, but the former lacked the signals of methoxyl and formyl groups. The formyl group in **21** ( $\delta_H$  10.50;  $\delta_C$  187.0) was replaced by an oxymethylene carbon ( $\delta_H$  4.80, 4.99;  $\delta_C$  54.0) and lacked a signal of one methoxy group in **27**. The chemical shift values of the oxymethylene carbon C-8 ( $\delta_C$  51.4) of the A ring the carboxyl carbon C-7' ( $\delta_C$  166.6) and the acetal carbon C-9' ( $\delta_C$  95.4) of the  $\Psi$ -butyrolactone moiety in **27** were shielded comparing to the corresponding ones of **21** ( $\delta_C$  54.0, 169.8 and 103.0, respectively). The high-field shifted values of these carbons suggested that the oxymethylene group of the A ring did not link to a hydrogen atom as in **21** but to the  $\Psi$ -butyrolactone moiety through an oxygen bridge formed between C-8 and C-9'. This was also supported by the HRESIMS data of **27**. The ECD spectrum in MeOH of **27** contained negative Cotton Effects (CEs) at ( $\Delta\epsilon$ ) 293 (−16.3), compared with those of lobarientalone B, possessing (S) absolute configuration of the stereogenic acetal

center of the  $\alpha,\beta$ -unsaturated- $\gamma$ -lactone moiety. Finally, the comparison of NMR data of **27** and those of lobarientalone B [99] showed that they were identical, thus **27** was elucidated as lobarientalone B.



lobarientalone B (**27**)

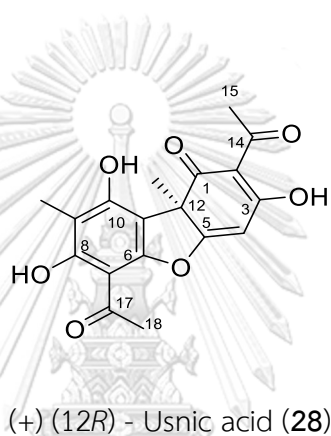
#### 2.3.4.4 Dibenzofuran Compound

A dibenzofuran compound (**28**) was isolated as a major component in lichen *U. aceculifera*.

#### (+)(12*R*)-Usnic acid (**28**)

Compound **28** was isolated as yellow prisms,  $[\alpha]_D^{25} +74$  (EtOH, C 0.001), as a major compound in this lichen. The proton spectrum for **28** was very similar to that of atranorin (**15**), in that all of the proton resonances are singlets, and all of the hydroxyl protons are present as sharp singlet resonances indicating that they formed H-bonds with the oxygen of neighboring keto groups. The  $^1\text{H-NMR}$  spectrum exhibited signals for two chelated hydroxyl groups [ $\delta_H$  13.29 and 11.01 (1H each, s, 8-OH and 10-OH)], two methoxyl groups [ $\delta_H$  2.68 and 2.66 (3H each, s, 18-H and 15-H), two methyl groups [ $\delta_H$  2.11 and 1.76 (3H each, s, 16-H and 13-H), and an aromatic methine proton at  $\delta_H$  5.97 (s, 4-H). The  $^{13}\text{C}$  NMR spectrum showed signals for three

carbonyl carbons [ $\delta_c$  201.7 (C-14), 200.3 (C-17) and 198.1 (C-1)], four methyl groups [ $\delta_c$  32.1 (C-13), 31.2 (C-18), 27.8 (C-15) and 7.5 (C-16)]. Comparison of these spectroscopic data with the ones of usnic acid [100] confirmed that the NMR data of usnic acid is in agreement with the present data. Furthermore, **28** was dextrorotary [ $\alpha$ ] $^{25}$  +74 (EtOH, C 0.001). The structure of **28** was therefore determined to be (+)-(12*R*)-usnic acid.



#### 2.3.4.5 Steroid and triterpenoid compounds

Three terpenoid and one steroid compounds were isolated from lichen *U. aciculifera* including **29–32**. (Fig. 2.5)

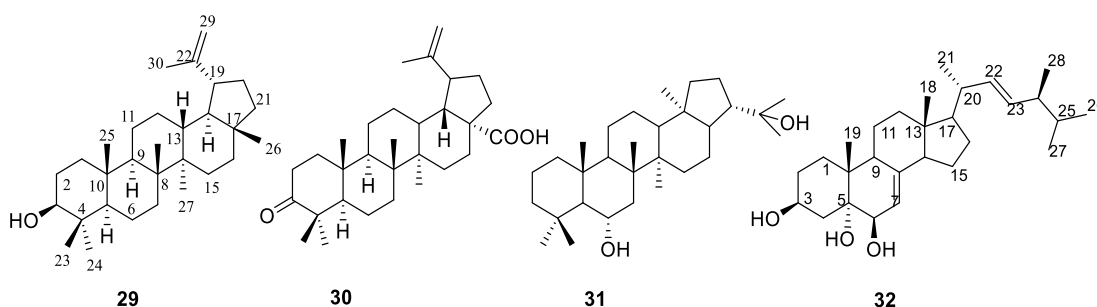


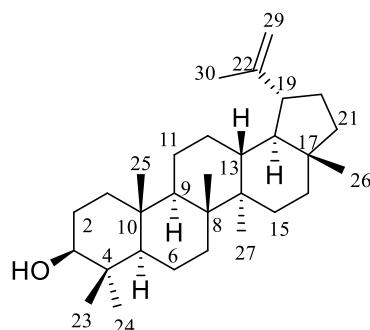
Fig. 2.5 The structures of isolated steroid and terpenoids

Lupeol (**29**)

Compound **29** was obtained as white powder. The  $^1\text{H}$  NMR spectrum showed a pair of signals of two olefinic protons at  $\delta_{\text{H}}$  4.68 (1H, *d*,  $J = 2.0$  Hz, H-29a) and 4.56 (1H, *dd*,  $J = 2.5, 1.5$  Hz, H-29b) along with a singlet signal at  $\delta_{\text{H}}$  1.68 (3H, *s*, H-30) suggested the presence of an isopropenyl side chain. Besides, there were a double of doublet signal of a methine proton at  $\delta_{\text{H}}$  3.18 (1H, *dd*,  $J = 11.0, 5.0$  Hz, H-3), a double of triplet at  $\delta_{\text{H}}$  2.37 (1H, *dt*, 11.0, 5.5 Hz) for the methine proton at C-19 and six singlet methyl signals at  $\delta_{\text{H}}$  0.76 (3H, *s*, H-24), 0.79 (3H, *s*, H-28), 0.83 (3H, *s*, H-25), 0.94 (3H, *s*, H-27), 0.96 (3H, *s*, H-23), 1.03 (3H, *s*, H-26).

The  $^{13}\text{C}$  NMR spectrum displayed thirty carbon signals, among them, there were two olefinic carbon signals at  $\delta_{\text{C}}$  150.9 (C-20) and  $\delta_{\text{C}}$  109.3 (C-29) as well as an oxygenated methine signal at  $\delta_{\text{C}}$  79.0 (C-3).

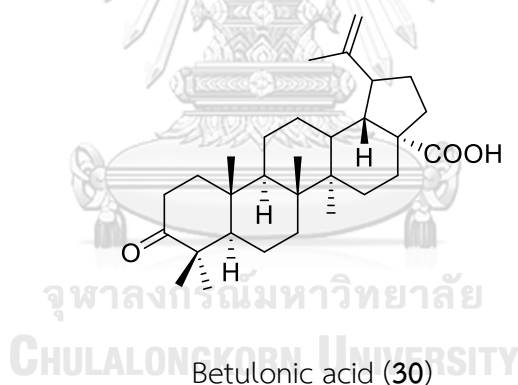
The above information supported the lupane skeleton of **29**. The chemical structure of **29** was identified as lupeol by the comparison of its NMR data with the published ones.[101]



Lupeol (**29**)

### Betulonic acid (30)

The molecular formula of **30** was suggested to be  $C_{30}H_{46}O_3$  by the HR-EIMS. The  $^1H$  and  $^{13}C$  NMR of **29** showed the presence of characteristic signal of lupane – type triterpenes, such as those of five tertiary methyl groups ( $\delta_H$  0.91, 0.96, 0.98, 1.00, 1.06), an isopropenyl group [ $\delta_H$  1.68 (3H, s, vinyl methyl), 4.60 and 4.73 (each H, br s, exomethylene), and  $\delta_C$  109.7, and 150.3], a carbonyl group ( $\delta_C$  218.2) and a carboxyl group ( $\delta_C$  182.4). These results indicated that **30** is lupane – type triterpene, having a 3-keto group. A comparison of the  $^{13}C$  NMR spectrum of **30** with that of betulonic acid [102] indicated that **30** is betulonic acid.

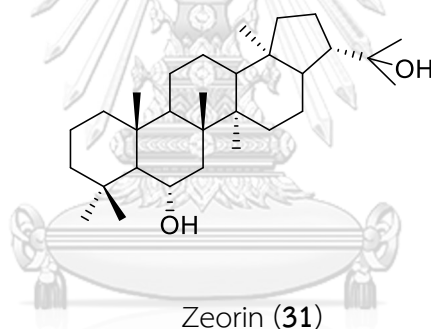


### Zeorin (31)

Compound **31** was isolated as white amorphous powder. The  $^1H$  NMR spectrum revealed signals of eight methyl singlets at  $\delta_H$  0.71 (3H, s, H-28), 0.81 (3H, s, H-25), 0.92 (3H, s, H-27), 0.94 (3H, s, H-24), 0.98 (3H, s, H-26), 1.03 (3H, s, H-29), 1.07 (3H, s, H-30), and 1.12 (3H, s, H-23), one methine proton at  $\delta_H$  2.10 (1H, dd,  $J = 9.0, 20.0$  Hz, H-21).

Detailed analysis of the coupling constants of the *triplet of doublet* proton signal at  $\delta_H$  3.74 (1H, *ddd*,  $J = 4.0; 9.5; 13.5$  Hz, H-6 $\beta$ ) indicated that this proton was coupled to two axial protons at  $\delta_H$  0.72 (*d*,  $J_{aa} = 13.0$  Hz, H-5 $\alpha$ ) and 1.93 (*d*,  $J_{aa} = 13.0$  Hz, H-7 $\alpha$ ) and one equatorial proton at  $\delta_H$  1.37 (*d*,  $J_{ae} = 3.6$  Hz, H-7 $\beta$ ).

The  $^{13}\text{C}$  NMR spectrum showed two signals at  $\delta_C$  50.3 and 71.5 specialized for C-21 and C-22 of 22-hydroxyhopane skeleton. The comparison of these spectroscopic data of **31** with those of zeirin in the literature [103] showed good compatibility. Therefore, **31** was hopane-6 $\alpha$ ,22-diol or zeirin.

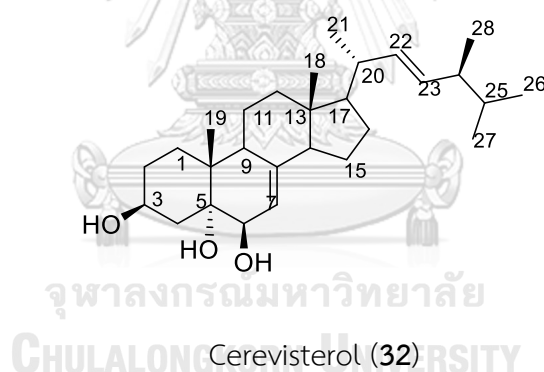


#### Cerevisterol (**32**)

Compound **32** was isolated as white amorphous powder. The  $^1\text{H}$  NMR spectrum contained four doublets for secondary methyl groups at  $\delta_H$  0.99 (3H, *d*,  $J = 6.5$  Hz, H-21), 0.81 (3H, *d*,  $J = 6.5$  Hz, H-26), 0.80 (3H, *d*,  $J = 6.5$  Hz, H-27), 0.89 (3H, *d*,  $J = 7.0$  Hz) and two singlets of two tertiary methyl groups at  $\delta_H$  0.54 and 0.91. The signal at  $\delta_H$  3.76 (1H, *ddd*,  $J = 11.0$  & 5.5 Hz) was assigned to the proton on carbon bearing a hydroxyl group. Moreover, signals of two olefinic proton at  $\delta_H$

5.17 (1H, *dd*,  $J = 8.0, 15.0$  Hz, H-22) and 5.24 (1H, *dd*,  $J = 7.0, 15.0$  Hz, H-23), an oxymethine protons at  $\delta_H$  3.37 (s, H-6), a methine proton at 5.08 (1H, *dd*,  $J = 5.5$  & 3.0 Hz, H-7) and three signal of hydroxyl group at 3.58 (s, 5-OH). 4.22 (d,  $J = 5.5$  Hz), 4.49 (d,  $J = 5.5$  Hz) of a cholestane skeleton were also observed.

The  $^{13}\text{C}$  NMR spectrum showed the presence of 28 carbon signals including four olefinic carbon signals at  $\delta_C$  119.4 (C-7), 139.6 (C-8), 135.4 (C-22), 131.4 (C-23) and three oxygenated carbons at  $\delta_C$  74.4 (C-5), 72.1 (C-6) and 65.9 (C-3). Analysis of the spectral data of **32** and the comparison with cerevisterol in the literature [104] suggested that **32** was cerevisterol.



#### 2.3.4.6 Dimeric xanthone compounds

Thirteen dimeric xanthones compounds were isolated from *U. aciculifera* including nine new dimeric xanthones **36–44** together with four knowns (**33–35**, **45**).

(Fig. 2.6)

#### Eumitrin B (**33**)



Compound **33** was obtained as light yellow needles. The HR-ESIMS of **33** exhibited a peak at  $m/z$  689.1901  $[M+Na]^+$  (calcd for  $C_{34}H_{34}O_{14}Na$ , 689.1847), indicating a molecular formula of  $C_{34}H_{34}O_{14}$ . It showed UV maxima at 251, 272, 293 and 335 nm, and IR bands at 3523, 1755, 1614, 1582 and  $1563\text{ cm}^{-1}$ , suggesting the presence of hydroxyl group(s), carbonyl group and substituted aromatic system.

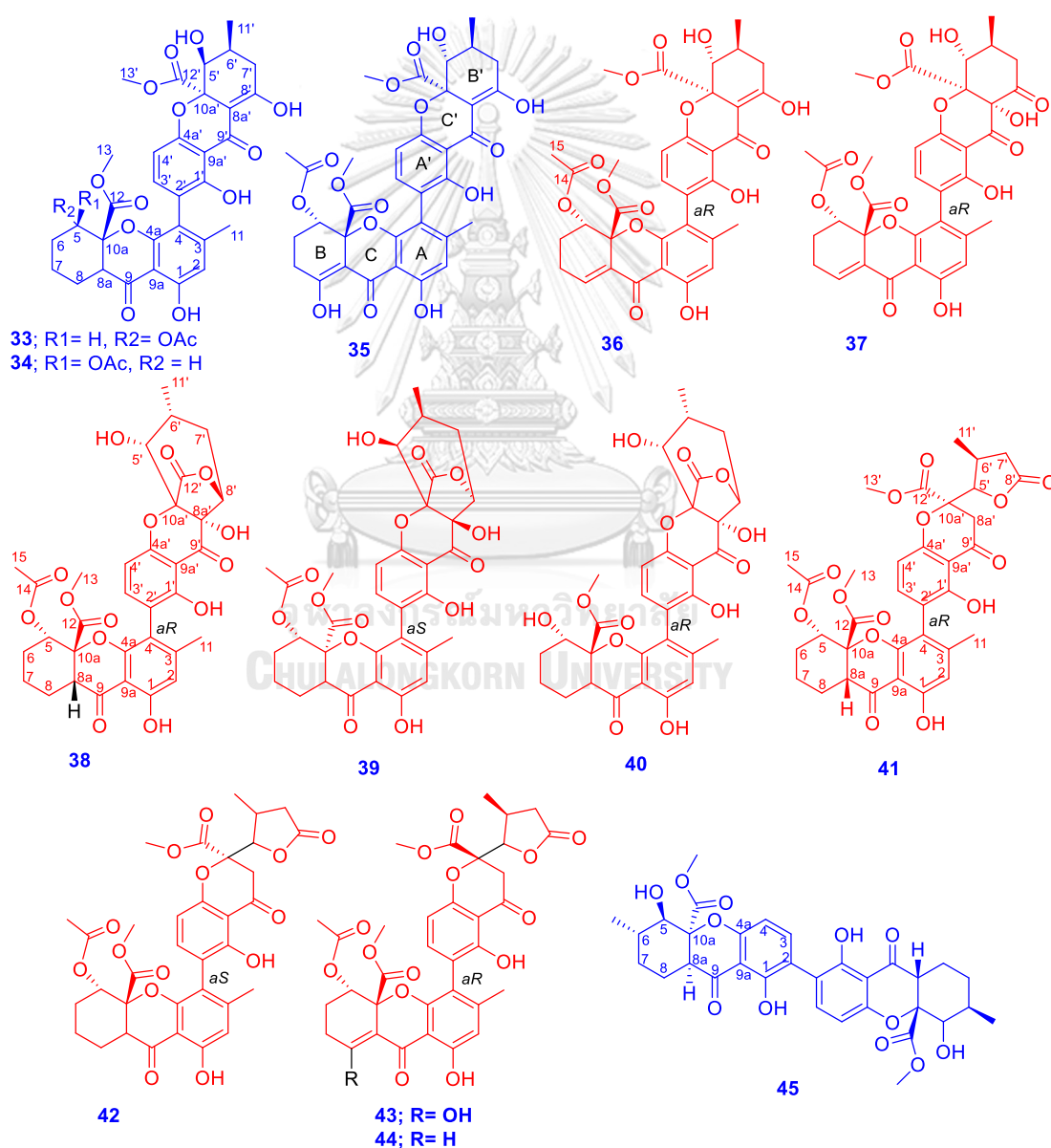


**Fig. 2.6** The structures of isolated dimeric xanthenes.

The  $^1\text{H}$  NMR spectrum of **33** showed the presence of three hydrogen-bonded hydroxyl groups at  $\delta_{\text{H}}$  13.90 (1H, s, OH-8'), 11.71 (1H, s, OH-1') and 11.44 (1H, s, OH-1); two *ortho* aromatic protons at  $\delta_{\text{H}}$  7.07 and 6.56 with the coupling constant of 8.4 Hz, one singlet aromatic proton at  $\delta_{\text{H}}$  6.43 (1H, s, H-2), two oxymethines at  $\delta_{\text{H}}$  5.41 (1H, d, 1.6 Hz, H-5) and 4.14 (1H, d, 0.8 Hz, H-5'), two methine protons at  $\delta_{\text{H}}$  3.24 (1H, dd, 11.6 & 4.0 Hz, H-8a) and 2.09 (1H, d,  $J = 5.6$  Hz, H-6'), two methoxy groups at  $\delta_{\text{H}}$  3.66 (3H, s, H-13) and 3.76 (3H, s, H-13'), one *doublet* methyl ( $\delta_{\text{H}}$  1.14, 3H, d,  $J = 6.8$  Hz, H<sub>3</sub>-11'), one singlet aromatic methyl ( $\delta_{\text{H}}$  1.96, 1H, s, H-11') and one methyl of acetoxy group at  $\delta_{\text{H}}$  1.86 (3H, s, H-15) and eight protons in the high-field range of 1.42–2.32 ppm. The  $^{13}\text{C}$  NMR in accordance with the HSQC spectra of **33** revealed the existence of 34 carbon signals, comprising of two conjugated ketone carbon ( $\delta_{\text{C}}$  197.9, 187.9), two ester carbonyl carbon ( $\delta_{\text{C}}$  168.7, 171.2), one acetoxy carbonyl carbon ( $\delta_{\text{C}}$  168.7), three aromatic methines ( $\delta_{\text{C}}$  139.8, 111.1 and 107.9), two methoxy groups ( $\delta_{\text{C}}$  53.6 and 53.0), four methines ( $\delta_{\text{C}}$  28.5, 45.4, 68.0 and 71.3), four methylene groups ( $\delta_{\text{C}}$  20.7, 18.4, 27.2 and 32.6), three methyl groups ( $\delta_{\text{C}}$  17.5, 20.7, 20.9), and thirteen quaternary carbons ( $\delta_{\text{C}}$  179.7, 160.4, 159.4, 157.4, 155.2, 149.2, 115.5, 117.4, 107.0, 105.3, 100.3, 84.9 and 84.4). Based on comparison of physical properties and spectroscopic data (UV, IR, 2D NMR, and MS) with the consideration of the chemical profile of the genus *Usnea*, along with 34 carbons resonances in the  $^{13}\text{C}$  NMR spectrum of **33** leading to

infer that it might correspond to a dimeric xanthone. This is homologous compound structurally related to secalonic A which is coupled through the 2–2' positions, while the two monomeric units of **33** dimerized through a 4–2' linkage with an asymmetrical structure.

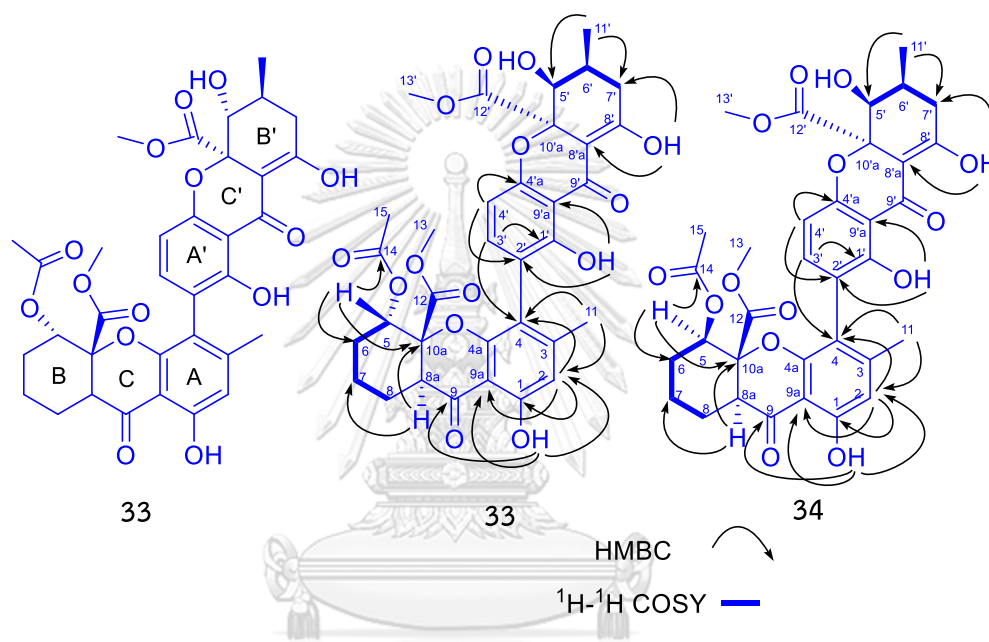


Fig. 2.7 The key COSY, HMBC correlations of **33** and **34**

The first subunit was determined as a hexahydroxanthone based on the 2D NMR spectrum. In the ring A of monomer I, H-2 exhibited  $^3J$  HMBC correlations to C-4 and C-9a. Peri to a carbonyl group, chelated hydroxyl proton 1-OH correlated to C-1, C-2, C-9 and C-9a. The methyl group at  $\delta_{\text{H}}$  2.03 (H<sub>3</sub>-11) showed HMBC correlations to C-2, C-4 and C-4a. Therefore, the ring A was determined as a 2,4,5,6-tetrasubstituted phenol (1,3,4,4a-tetrasubstituted phenol). Since, 1-OH was chelated and C-4a was oxygenated, it could be deduced that ring A joined ring C to form a 4-chromanone.

The remaining parts of the first subunit to be determined are ring B. The oxygenated methine at  $\delta_H$  5.01 (H-5) exhibited correlations to C-10a, C-8a, C-6, 5-O $\underline{C}$ OCH<sub>3</sub> ( $\delta_C$  168.7) and 10a-COOCH<sub>3</sub> ( $\delta_C$  168.7). The methine proton at  $\delta_H$  3.24 (H-8a) correlated to C-7, C-8 and C-9 ( $\delta_C$  197.9). Therefore, this ring was determined to be methyl 2-acetoxycyclohexane-1-carboxylate, with the other two substituents at the 1,6-positions of this fragment, which could be ring B.

The second monomer, subunit II, was also determined as a hexahydroxanthone base on the 2D NMR spectrum. In the ring A' of monomer II, H-4' showed the  $^3J$  HMBC correlations to C-2', C-4'a and C-9'a. The chelated 1'-OH group correlated to C-1', C-2' and C-9'a. H-3' was ortho coupled with H-4' and showed  $^3J$  HMBC correlations to C-1', C-4'a and C-4. Therefore, ring A' was determined as a 2,3,6-trisubstituted phenol (2',4'a,9'a-trisubstituted phenol), and rings A and A' were connected through the C-4-C-2' bond. The chemical shift of chelated 1'-OH and C-4'a was oxygenated, it could be confirmed that ring A' joined C' to form a 4-chromanone. Similarly, the last ring of monomer II to be ring B' which was determined to be 4-hydroxyl-3-(methoxycarbonyl)-5-methyl cyclohexanol based on the HMBC correlations of methyl group at  $\delta_H$  1.14 (H<sub>3</sub>-11'), oxygenated methine at  $\delta_H$  4.14 (H-5') and hydroxyl group at  $\delta_H$  13.90 (8'-OH). With the other two substituents at 2,3-positions of this fragment, which could be ring B'. The tentative  $^1H$  and  $^{13}C$  NMR chemical shift assignments of **33-35** are presented in Table 2.1-2.2.

Table 2.1 <sup>1</sup>H Spectroscopic Data of 33–35

No.	33	34	35
	$\delta_{\text{H}}$ , mult, ( <i>J</i> in Hz)	$\delta_{\text{H}}$ , mult, ( <i>J</i> in Hz)	$\delta_{\text{H}}$ , mult, ( <i>J</i> in Hz)
2	6.43, 1H, s	6.48, 1H, s	6.48, 1H, s
5	5.41, 1H, d, 1.6	5.01, 1H, dd, 5.2, 10.8	5.42, 1H, d, 3.2
6	1.81, 1H, m	1.68, 2H, m	1.91, 2H, m
	1.42, 1H, m		
7	1.63, 2H, m	1.50, 1H, m	1.40, 1H, m
		1.86, 1H, m	1.51, 1H, m
8	1.77, 1H, m	1.50, 1H, m	
	2.32, 1H, m	1.86, 1H, m	
8a	3.24, 1H, dd, 4.0, 11.6	2.96, 1H, dd, 3.6, 11.6	
11	2.03, 3H, s	1.96, 3H, s	2.06, 3H, s
13	3.66, 3H, s	3.65, 3H, s	3.69, 3H, s
15	1.86, 3H, s	2.14, 3H, s	1.80, 3H, s
1-OH	11.44 s	11.44 s	11.24, 1H, s
8-OH			13.85, 1H, s
3'	7.07, 1H, d, 8.4	7.66, d, 8.4	7.26, 1H d, 8.4
4'	6.56, 1H, d, 8.4	6.56, 1H, d, 8.4	6.60, 1H, d 8.4
5'	4.14, 1H, d, 0.8	4.13, 1H, s	4.162, 1H, s
6'	2.09, 1H, d, 5.6	2.11, 1H, d, 5.6	2.10, 1H, d 4.8
7'	2.09, 1H, m	2.41, 1H, m	2.40, 1H, m
	2.09-2.21, 1H, m	2.54, 1H, m	2.49, 1H, m
11'	1.14, 3H, d, 6.8	1.17, 3H, d, 5.6	1.17, 3H, d 6.8
13'	3.76, 3H, s	3.64, 3H, s	3.76, 3H, s
1'-OH	11.71, 1H, s	11.61, 1H, s	11.58, 1H, s
8'-OH	13.90, 1H, s	13.95, 1H, s	13.93, 1H, s

Table 2.2:  $^{13}\text{C}$  NMR spectroscopic data of **33**–**35** (100 MHz,  $\text{CDCl}_3$ ,  $\delta$  ppm)

No.	<b>33</b>	<b>34</b>	<b>35</b>	No.	<b>33</b>	<b>34</b>	<b>35</b>
	$\delta_{\text{C}}$	$\delta_{\text{C}}$	$\delta_{\text{C}}$		$\delta_{\text{C}}$	$\delta_{\text{C}}$	$\delta_{\text{C}}$
1	160.4	161.6	161.3	1'	159.4	159.4	159.5
2	111.1	111.3	111.3	2'	117.4	117.8	117.7
3	115.5	151.1	150.5	3'	139.8	141.4	140.2
4	155.2	115.8	115.8	4'	107.9	107.5	108.0
4a	155.2	156.4	156.2	4a'	157.4	157.3	157.5
5	68.0	72.6	66.2	5'	71.4	71.4	71.5
6	27.2	26.1	23.5	6'	28.5	28.7	28.6
7	18.4	25.2	21.9	7'	32.6	32.7	36.7
8	20.7	22.3	177.5	8'	179.7	179.8	179.7
8a	45.4	48.6	100.7	8a'	100.3	100.2	100.3
9	197.9	197.5	184.8	9'	187.9	187.9	188.0
9a	105.3	104.8	105.7	9a'	107.0	107.0	107.1
10a	84.4	83.3	81.0	10a'	84.9	85.0	85.0
11	20.9	20.8	21.2	11'	17.5	17.6	17.6
12	168.7	170.0	171.3	12'	171.2	171.3	171.4
13	53.0	53.1	53.6	13'	53.6	53.3	53.7
14	168.7	169.7	169.2				
15	20.7	21.2	20.4				

According to the 2D NMR spectrum of **33**, the planar structure of **33** was assigned as shown in Figure 2.7. The key COSY, HMBC correlations of **33** are summarized as in Figure 2.7.

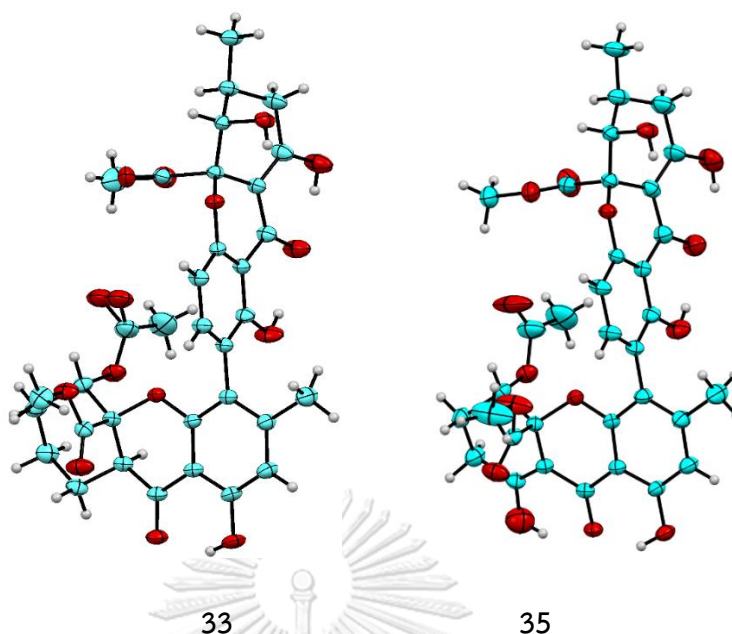


Fig. 2.8 ORTEP diagram for the single crystals X-ray geometry of **33** & **35**.

The relative configurations of **33** were determined by analysis of 1D and 2D NMR data, especially by coupling constants and experimental ECD spectrum of **33**.

Accordingly, the magnitude of the vicinal coupling constant value of the oxymethine proton at H-5' bisects the dihedral angle of the adjacent proton(s). The elevated small coupling constant of H-5' ( $^3J_{\text{H-5'-H-6'}} = 0.8$  Hz) implied a pseudoaxial/pseudoequatorial *cis* orientation of H-5'/H-6' in **33**. The large coupling constants between H-8a and H-8 ( $^3J_{\text{8a-8ax}} = 11.6$  Hz;  $^3J_{\text{8a-8eq}} = 4.0$  Hz) and small coupling constants between H-5 and H-6 ( $^3J_{\text{8a-8ax}} = 1.6$  Hz) suggested the pseudoequatorial *trans* orientation for acetoxy group at C-5 and methoxycarbonyl at C-10a. Finally, the assigned structure of **33** was unambiguously determined by using single-crystal X-ray diffraction analysis (CCDC 1854037, Fig. 2.8) with a Flack

parameter of 0.09. This analysis also enabled unambiguous assignment of the absolute configurations of the stereocenters in **33** as (5*S*,8*aS*,10*aS*,5'*S*,6'*S*,10'*aS*). The structure of **33** was elucidated as eumitrin B, a dimeric xanthone was previously isolated from lichen *Usnea baileyi*. [84]

#### Eumitrin A2 (**34**)

Compound **34** was obtained as light yellow needles. **34** and **33** shared the same molecular formula of  $C_{34}H_{34}O_{14}$  based on the HR-ESIMS of **34** exhibited a peak at  $m/z$  667.2022  $[M+H]^+$  (calcd for  $C_{34}H_{34}O_{14}H$ , 667.2027). The mass spectra and 2D NMR data of **33** and **34** suggested that they could be stereoisomers. The NMR spectral patterns of **34** and **33** resemble with each other, except for the coupling pattern of the proton attached to the carbon bearing the acetoxy group. These protons in **34** and **33** were assigned to the signals at  $\delta_H$  5.01 (*dd*,  $J = 5.2, 10.8$  Hz) and 5.41 (*d*,  $J = 1.6$  Hz), respectively. It can be concluded that **34** and **33** were epimers at the second acetoxy group connected to C-5. The relative configurations of the tetrahydroxanthone monomeric units in **34** were found to be (5*R*,8*aS*,10*aS*,5'*S*,6'*S*,10'*aS*), deduced from NMR data, especially of the coupling constants (Table 2.1), as well as the ECD data. Finally, the structure of **34** was elucidated as eumitrin A2, a dimeric xanthone was previously isolated from lichen *Usnea baileyi*. [84]

#### Eumitrin A1 (**35**)



Compound **35** was obtained as light yellow needles. Its molecular formula was deduced to be  $C_{34}H_{32}O_{15}$  (19 DBEs) by HRESIMS 681.1809  $[M + H]^+$  (calcd for  $C_{34}H_{32}O_{15}H$ , 681.1819). The NMR spectral features of **35** were similar to those of **33** and **34** except for the presence of an additional hydrogen-bonded hydroxy signal detected at  $\delta_H$  13.85 instead of a methylene group at position C-8, which was further supported by correlations of signal at  $\delta_H$  13.85 with C-7 ( $\delta_C$  21.9), C-8 ( $\delta_C$  177.5) and C-8a ( $\delta_C$  100.7) in the HMBC spectrum of **35** (Fig. 2.9).

The relative configurations of **35** were found to be the same as those of **33**, as indicated by similar NMR data (Table 2.1), and coupling constants. Furthermore, the absolute configuration of **35** was unambiguously determined by using single-crystal X-ray diffraction analysis with Cu K $\alpha$  radiation as (5*S*,10*aS*,5'*S*,6'*S*,10*a'S*), (Fig. 2.8). Finally, the structure of **35** was elucidated as eumitrin A1. [84]

The known compounds were identified as eumitrin B (**33**), eumitrin A2 (**34**) and eumitrin A1 (**35**), which were previously isolated from lichen *Usnea baileyi* [84]. However, their structure elucidation has not yet been accomplished.

#### New dimeric xanthone Usneaxanthone D (**36**)

Usneaxanthone D (**36**) was obtained as yellow crystals. Its molecular formula was deduced to be  $C_{34}H_{32}O_{14}$  (19 DBEs) by HRESIMS ( $m/z$  687.1733  $[M + Na]^+$ , calcd 687.1690). The NMR spectroscopic data (Table 2.3-2.4) of **36** was similar to those of eumitrin A1 (**35**), except for the replacement of the hydroxyl group at C-8 in eumitrin

A1 by an olefinic proton ( $\delta_{\text{H}}$  7.30, H-8) in **36**, which was further supported by correlations of signal at  $\delta_{\text{H}}$  7.30 with C-9 ( $\delta_{\text{C}}$  184.7), and C-10a ( $\delta_{\text{C}}$  80.9) in the HMBC spectrum of **36** (Fig. 2.9). The configurations of **36** were identical to those of eumitrin A1 by detailed analysis of 1D and 2D NMR spectra, especially of the coupling constants (Table 2.2), as well as ECD data (Figure 2.10) of **36**. The axial chiralities were deduced on the basis of an ECD exciton chirality method [110]. The anticlockwise manner of the two benzoyl chromophores in **36** resulted in positive exciton couplings near 218 nm, allowing assignment of axial chirality as *aR* (Fig. 2.10).

[105]

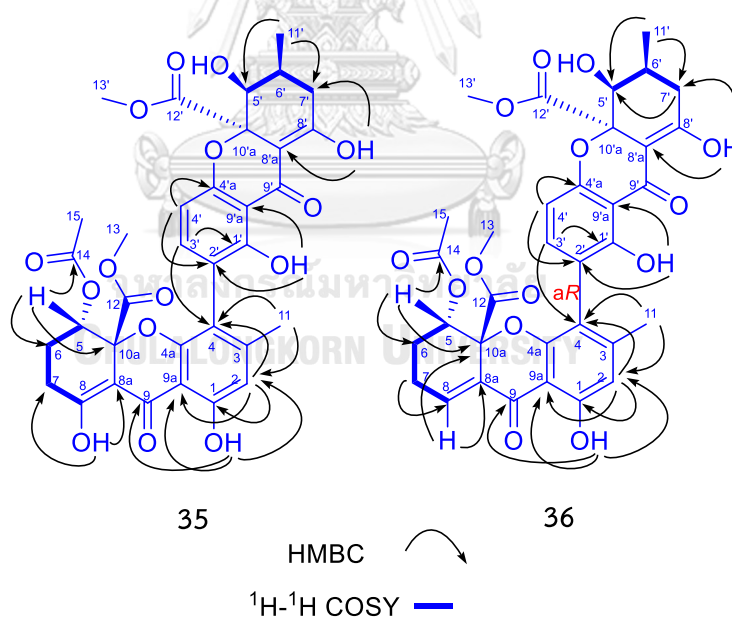


Fig. 2.9 The key COSY, HMBC correlations of **35** and **36**

Furthermore, when a biaryl natural product contains both axial and central chirality elements, the ECD method can afford only the assignment of the axial

chirality, as the ECD curves of axially chiral biaryl dimers generally dominated by the exciton coupled interaction of the two aryl moieties, which is governed by the sign and value of the biaryl torsional angle [106]. It is usually impracticable to determine the absolute configurations of the chirality centers by using the ECD method [107]. Therefore, with the aid of the single crystals, the absolute configurations of **36** were directly determined as (5*S*,10*aR*,5'*S*,6'*S*,10'*aR*) by X-ray diffraction analysis with Cu  $K\alpha$  radiation [Flack parameter = 0.03 (Fig. 2.11)]. Finally, **36** was a dimeric tetrahydroxanthone as shown in Fig. 2.6 and was named usneaxanthone D.

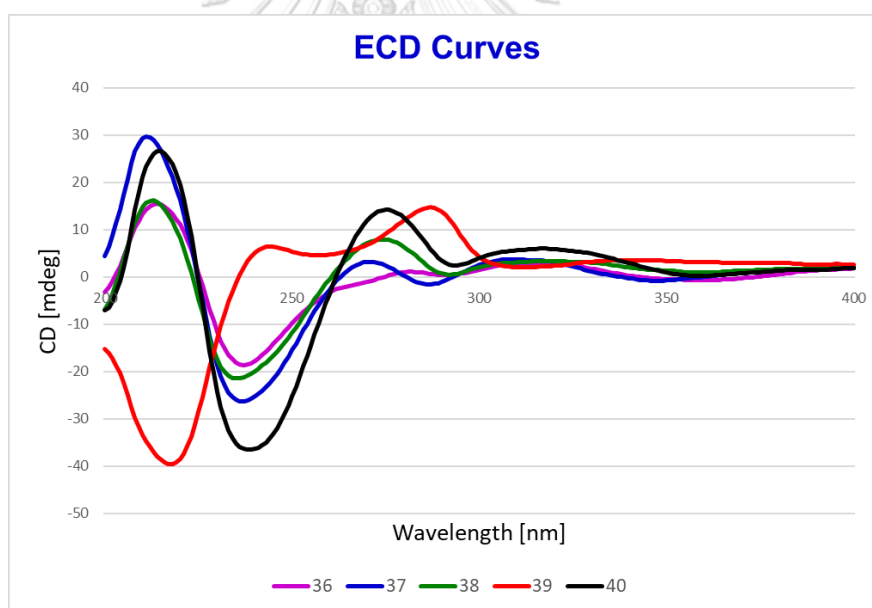


Fig. 2.10 Experimental ECD spectra of 36–40

#### New dimeric xanthone Usneaxanthone I (37)

Usneaxanthone D (**37**) was obtained as yellow crystals. The molecular formula of **37** was assigned as  $C_{34}H_{32}O_{15}$  by positive HRESIMS analysis ( $[M+Na]^+$   $m/z$

703.1669, calcd 703.1639), which was 16 units more than those of **36**. The NMR spectral features of **37** were similar to those of **36** except for the presence of an additional singlet hydroxy signal detected at  $\delta_H$  6.42 (1H, s) instead of a hydrogen-bonded hydroxyl at  $\delta_H$  13.93 (1H, s) in **36**, which was further supported by correlations of signal at  $\delta_H$  6.42 with C-8'a ( $\delta_C$  72.6), C-10'a ( $\delta_C$  86.1) and C-9' ( $\delta_C$  190.5) in the HMBC spectrum of **37** (Fig. 2.12) and the intense chemical shift of carbon at C-8' and C-8'a in **37** compared to their carbons in **36** (with respective  $\delta_C$  values of 198.4 and 72.6 in **37** & 179.6 and 100.2 in **36**) that indicated the singlet hydroxyl group connected to C-8'a and C-8' changed to carbonyl carbon. The tentative chemical shift assignments of **37** are tabulated in Tables 2.3 and 2.4.

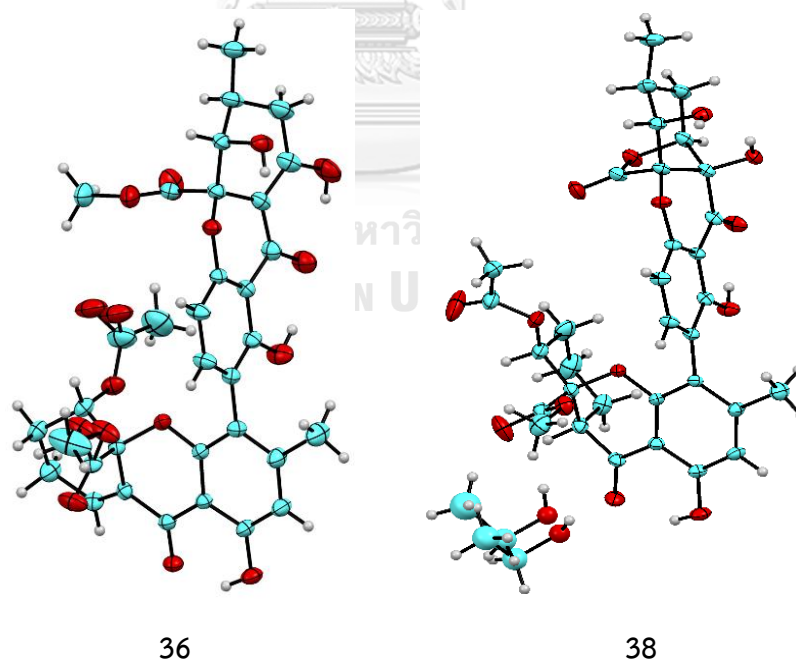


Fig. 2.11 ORTEP diagram for the single crystal X-ray geometry of **36** & **38**.

Table 2.3  $^1\text{H}$  Spectroscopic Data of 36–38

No.	36	37	38
	$\delta_{\text{H}}$ , mult, ( $J$ in Hz)	$\delta_{\text{H}}$ , mult, ( $J$ in Hz)	$\delta_{\text{H}}$ , mult, ( $J$ in Hz)
2	6.49, 1H, s	6.48, 1H, s	6.46, 1H, s
5	5.43, 1H, dd, 2.8, 4.4	5.41, 1H, d, 3.2	4.97, 1H, dd, 4.8, 11.2
6	1.91, 1H, m	1.89, 1H, m	1.74, 2H, m
	2.00, 1H, m	1.98, 1H, m	
7	2.40, 1H, m	2.41, 1H, m	1.47, 1H, m
	2.50, 1H, m	2.50, 1H, m	1.84, 1H, m
8	7.30, 1H, m	7.31, 1H, m	1.47, 1H, m
	-	-	1.84, 1H, m
8a	-	-	2.94, 1H, dd, 4.0, 11.6
11	2.08, 3H, s	2.04, 3H, s	2.10, 3H, s
13	3.70, 3H, s	3.79, 3H, s	3.62, 3H, s
15	1.81, 3H, s	1.81, 3H, s	1.90, 3H, s
1-OH	12.01 s	12.03 s	11.45, 1H, s
3'	7.26, 1H, d, 8.0	7.31, 1H, d, 8.0	7.72, 1H d, 8.4
4'	6.61, 1H, d, 8.0	6.66, 1H, d, 8.4	6.66, 1H, d 8.4
5'	4.17, 1H, br,	4.47, 1H, d, 1.2	5.25, 1H, d, 3.6
6'	2.12, 1H, m	2.08, 1H, m	2.14, 1H, m
7'	2.40, 1H, m	3.17, 1H, m	2.13, 1H, m
	2.50, 1H, m	2.37, 1H, m	2.15, 1H, m
8'	-	-	4.31, 1H, d, 3.6
11'	1.18, 3H, d, 6.8	1.23, 3H, d, 6.4	1.15, 3H, d, 6.0
13'	3.77, 3H, s	3.70, 3H, s	-
1'-OH	11.59, 1H, s	11.67, 1H, s	11.74, 1H, s
8'-OH	13.93, 1H, s	-	-
8'a-OH	-	6.42, 1H, s	-

Table 2.4:  $^{13}\text{C}$  NMR spectroscopic data of **36**–**38** (100 MHz,  $\text{CDCl}_3$ ,  $\delta$  ppm)

No.	<b>36</b>	<b>37</b>	<b>38</b>	No.	<b>36</b>	<b>37</b>	<b>38</b>
	$\delta_{\text{C}}$	$\delta_{\text{C}}$	$\delta_{\text{C}}$		$\delta_{\text{C}}$	$\delta_{\text{C}}$	$\delta_{\text{C}}$
1	162.1	162.4	161.5	1'	159.4	161.0	160.6
2	111.2	111.4	111.2	2'	117.6	118.5	117.6
3	150.4	150.7	150.8	3'	140.1	140.8	143.6
4	115.7	115.6	115.4	4'	107.9	107.3	107.0
4a	156.1	156.1	156.6	4a'	157.3	156.8	158.1
5	66.1	66.2	72.6	5'	71.4	75.5	77.0
6	23.3	23.4	26.1	6'	28.5	31.2	29.5
7	21.8	21.9	25.4	7'	32.6	39.8	27.5
8	141.6	141.9	22.2	8'	179.6	198.4	74.3
8a	128.9	128.8	48.6	8a'	100.2	72.6	76.0
9	184.7	184.8	197.7	9'	187.9	190.5	191.9
9a	105.6	105.7	104.7	9a'	107.0	106.4	106.6
10a	80.9	81.2	83.3	10a'	84.9	86.1	82.5
11	21.1	21.3	21.2	11'	17.5	17.2	15.3
12	169.0	168.5	169.7	12'	171.2	169.8	169.8
13	53.5	54.3	53.3	13'	53.6	53.6	-
14	169.7	169.5	170.7				
15	20.3	20.6	20.6				

The comparison ECD method was used to assign axial chirality of **37**. The ECD curves of **37** were almost identical to those of **36**, particularly the similar patterns of positive exciton coupling near 215 nm indicated an *aR* axial configuration for **37** (Fig. 2.10), which is in agreement with **36**. The absolute configurations in two monomeric units of **37** were proposed to be the same as those in **36**, as indicated by similar NMR data (Table 2.3 & 2.5), and the coupling constants. Thus, the absolute

configurations of **37** were deduced as (5*S*,10*aR*,5'*S*,6'*S*,8'*aS*,10'*aR*). Therefore, **37** was a new dimeric tetrahydroxanthone and was named usneaxanthone I.

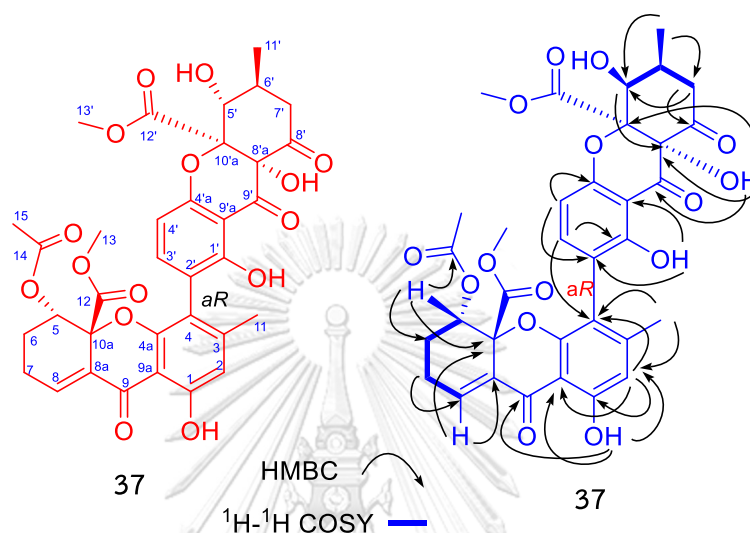


Fig. 2.12 Structure and key COSY, HMBC correlations of **37**

#### New dimeric xanthone Usneaxanthone A (**38**)

Usneaxanthone A (**38**), light yellow crystals, had a molecular formula of  $C_{33}H_{32}O_{14}$  as determined by the HRESIMS through the protonated molecular ion at  $m/z$  653.1862  $[M + H]^+$  (calcd for  $C_{33}H_{33}O_{14}$  653.1870) and the sodium adduct ion at  $m/z$  675.1681 ( $[M+Na]^+$ , calcd 675.1645).

The <sup>1</sup>H NMR spectrum of **38** showed the presence of two phenolic hydroxyl protons at  $\delta_H$  11.45 (1H, s) and 11.74 (1H, s), three aromatic protons at  $\delta_H$  6.46 (1H, s), 6.66 (1H, d,  $J = 8.4$  Hz), and 7.72 (1H, d,  $J = 8.4$  Hz) (Table 2.3).

A careful analysis of its 1D and 2D NMR indicated that two subunits **38a** and **38b** existed in **38** (Fig. 2.12) highly resembled that of eumitrin B (**33**). However,

detailed analysis revealed that the methoxycarbonyl group in the partial subunit II in **33** was replaced by a  $\gamma$ -butyrolactone ring in **38** and the double bond conjugating to the ketone group in **33** was transformed into a single bond with a hydroxyl group bonded to C-8'a in **38** instead of C-8' in **33**. The  $^1\text{H}$ - $^1\text{H}$  COSY correlations of H-5'/H-6'/H-7'/H-8' and H-11' ( Fig. 2.12), along with the network of HMBC cross – peaks (Fig. 2.12) of H-5'/C-6', C-10'a, C-12'; H-8'/C-9', C-7'; H-11'/C-6', C-7', and C-8', indicated the presence of a  $\gamma$ -butyrolactone ring, consisting of C-8'–C-8'a–C-10'a in **38** with a methyl (C-11'), and two hydroxyl groups at C-5' and C-8'a, respectively. Thus, the planar structure of **38** was determined.

The comparison ECD method was used to assign axial chirality of **38**. The ECD curves of **38** were almost identical to those of **36**, particularly the similar patterns of positive exciton coupling near 213 nm indicated an *aR* axial configuration for **38** (Fig. 2.10), which is in agreement with **36**.



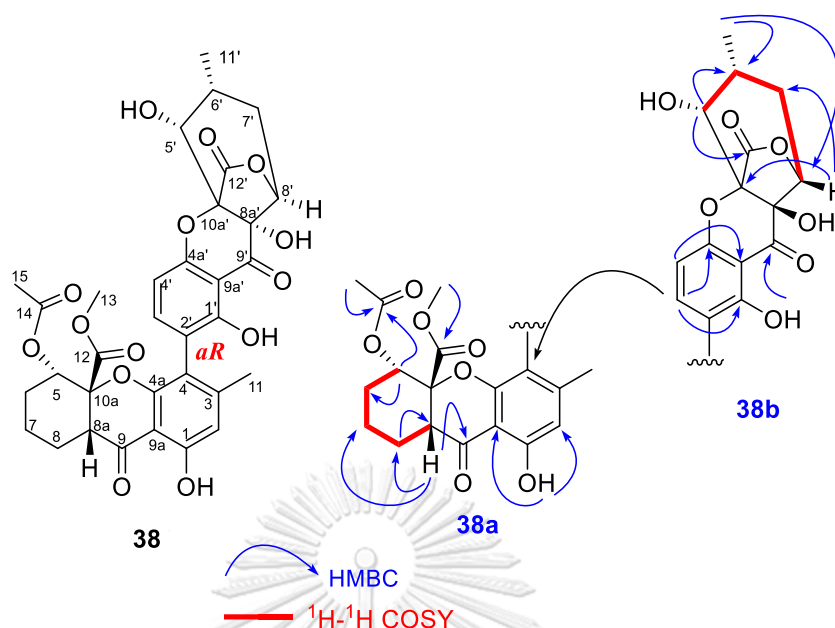


Fig. 2.113 Structure and the key COSY, HMBC correlations of **38**

The relative configurations of **38** were determined by analysis of 1D and 2D NMR data, especially by coupling constants and experimental ECD spectrum of **38**. In the partial **38a**, the large coupling constants between proton H-5 and H-6 ( $^3J_{5-6ax} = 11.2$  Hz;  $^3J_{5-6eq} = 4.8$  Hz) and between H-8a and H-8 ( $^3J_{8a-8ax} = 11.6$  Hz;  $^3J_{8a-8eq} = 4.0$  Hz) suggested H-5 and H-8a be in the axial positions and the equatorial orientation for acetoxy group at C-5 and methoxycarbonyl at C-10a. For the partial **38b**, the small coupling constants between H-5' and H-6' ( $^3J_{H-5'-H-6'} = 3.6$  Hz), and H-8' and H-7' ( $^3J_{H-8'-H-7'} = 3.6$  Hz) suggested H-5' and H-8' must have a *cis*-equatorial position. Finally, the assigned structure of **38** was unambiguously determined by using single-crystal X-ray diffraction analysis with Cu K $\alpha$  radiation (Fig. 2.11) to assign of the absolute configurations of the stereocenters in **38** as (5*S*,8*aR*,10*aS*,5'*R*,

6'*R*,8'*S*,8'*aS*,10'*aR*). Thus, the structure of **38** was elucidated and named usneaxanthone A.

#### New dimeric xanthone Usneaxanthone B (**39**)

Usneaxanthone B (**39**), light yellow crystals. The molecular formula  $C_{33}H_{32}O_{14}$  of **39** was determined to be identical to that of **38** by HRESIMS with  $m/z$  675.1711 [ $M + Na$ ]<sup>+</sup> (calcd for  $C_{33}H_{32}O_{14}Na$ , 675.1690) but showed different rotation value ( $[\alpha]_D^{25} = -232$  for **38** and  $+286$  for **39**).

The similarity of the  $^1H$  and  $^{13}C$  NMR resonances for **39** with those of **38** indicated that **38** has the same planar structure with those of **38**. The relative configurations in the monomeric unit **39a** of **39** was proposed to be the same as **38a**. However the small difference in the second monomeric unit **39b** was that the chemical shift of H-3' upfield shifted from  $\delta_H$  7.72 in **38** to  $\delta_H$  7.40 in **39** (Table 2.3 & 2.5) suggested that the relative configurations in the partial **39b**, implying the central and axial chirality elements or preferred helicities of **39** will be differed from those of **38**. The axial chiralities were deduced on the basis of an ECD exciton chirality method [105]. The anticlockwise manner of two benzoyl chromophores in **39** resulted in negative exciton couplings near 218 nm, allowing assignment of axial chirality as *aS* (Fig. 2.10).[107] In contrast, the axial chirality in **38** was assigned to *aR* by positive exciton coupling near 213 nm (Fig. 2.10).

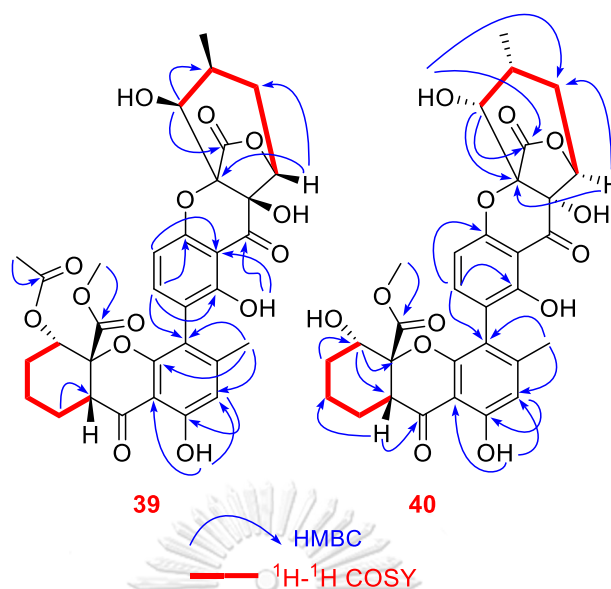


Fig. 2.14 The key COSY, HMBC correlations of **39** and **40**

Moreover, with the aid of the single crystals, the absolute configurations of **39** were directly determined as (5*S*,8*aR*,10*aS*,5'*S*,6'*S*,8'*R*,8'*aR*,10'*S*) by X-ray diffraction analysis with Cu  $K\alpha$  radiation [Flack parameter = 0.05 (Fig. 2.15)]. Therefore, the structure of **39** was elucidated and named usneaxanthone B.

#### New dimeric xanthone Usneaxanthone C (**40**)

Usneaxanthone C (**40**) was obtained as colorless needles. The molecular formula of **40** was assigned as  $C_{31}H_{30}O_{13}$  by negative HRESIMS analysis ( $[M-H]^-$   $m/z$  609.1607, calcd 609.1608), which was 42 units less than those of **38** and **39**. The comparison of the  $^{13}C$  and  $^1H$  NMR spectroscopic data of **38** and **40** (Tables 2.3 -2.6) indicated that the acetoxy group at C-5 in **38** was disappeared in **40**. These data, in conjunction with its molecular formula, suggested that the acetoxy moiety was

replaced by a hydroxyl moiety in **40**, confirmed by the corresponding proton at  $\delta_{\text{H}}$  3.80 (-CH-OH) and  $^{13}\text{C}$  NMR spectra data of **40**.

The comparison ECD method was used to assign axial chirality of **40**. The ECD curves of **40** were almost identical to those of **38**, particularly the similar patterns of positive exciton coupling near 215 nm indicated an *aR* axial configuration for **40** (Fig. 2.10), which is in agreement with **38**. The absolute configurations in two monomeric units of **40** were proposed to be the same as those in **38**, as indicated by similar NMR data (Tables 2.3 & 2.5), and the coupling constants.

Moreover, its absolute configurations were finally deduced as (5*S*,8*aR*,10*aS*,5'*R*,6'*R*,8'*S*,8'*aS*,10'*R*) by X-ray diffraction (CCDC 1854042, Fig. 2.15) with a Flack parameter of 0.07. Therefore, **40** was a new dimeric tetrahydroxanthone and was named usneaxanthone C.

#### New dimeric xanthone Usneaxanthone E (**41**)

Usneaxanthone E (**41**), colorless crystal (in EtOH), had a molecular formula of  $\text{C}_{34}\text{H}_{34}\text{O}_{14}$  as determined by the HRESIMS through the protonated molecular ion at  $m/z$  689.1894  $[\text{M} + \text{Na}]^+$  (calcd for  $\text{C}_{33}\text{H}_{32}\text{O}_{14}$  653.1870) and the sodium adduct ion at  $m/z$  675.1681  $[(\text{M}+\text{Na})^+]$ , (calcd for  $\text{C}_{34}\text{H}_{34}\text{O}_{14}\text{Na}$ , 689.1846).

Table 2.5  $^1\text{H}$  Spectroscopic Data of 39–41

No.	39	40	41
	$\delta_{\text{H}}$ , mult, ( $J$ in Hz)	$\delta_{\text{H}}$ , mult, ( $J$ in Hz)	$\delta_{\text{H}}$ , mult, ( $J$ in Hz)
2	6.49, 1H, s	6.52, 1H, s	6.46, 1H, s
5	4.98, 1H, dd, 4.4, 10.8	3.80, 1H, dd, 4.4, 10.0	5.00, 1H, dd, 4.8, 11.6
6	1.88, 2H, m	1.44, 1H, m	1.74, 2H, m
		1.84, 1H, m	
7	1.51, 1H, m	1.44, 1H, m	1.49, 1H, m
	1.88, 1H, m	1.84, 1H, m	1.86, 1H, m
8	1.51, 1H, m	1.44, 1H, m	1.49, 1H, m
	1.84, 1H, m	1.84, 1H, m	1.86, 1H, m
8a	3.00, 1H, dd, 4.8, 12.0	2.92, 1H, dd, 4.4, 12.0	2.97, 1H, dd, 4.4, 14.4
11	2.15, 3H, s	2.16, 3H, s	2.11, 3H, s
13	3.54, 3H, s	3.74, 3H, s	3.64, 3H, s
15	1.70, 3H, s	-	1.98, 3H, s
1-OH	11.44 s	11.54 s	11.44, 1H, s
3'	7.40, 1H, d, 8.0	7.86, 1H, d, 8.8	7.74, 1H, d, 8.8
4'	6.73, 1H, d, 8.0	6.80, 1H, d, 8.8	6.62, 1H, d, 8.4
5'	5.30, 1H, d, 3.6	5.29, 1H, d, 4.4	4.46, 1H, d, 3.2
6'	2.21, 1H, m	2.20, 1H, m	2.89, 1H, m
7'	2.09, 1H, m	2.10, 2H, m	2.22, 1H, m
	2.21, 1H, m		2.95, 1H, m
8'	4.40, 1H, d, 2.8	4.41, 1H, d, 3.2	-
8'a	-	-	3.07, 1H, m
			3.22, 1H, m
11'	1.21, 3H, d, 5.2	1.19, 3H, d, 6.4	1.28, 3H, d, 6.4
13'	-	-	3.68, 3H, s
1'-OH	11.71, 1H, s	11.76, 1H, s	11.74, 1H, s
5'-OH	-	6.55, 1H, s	-

Table 2.6.  $^{13}\text{C}$  NMR spectroscopic data of 39–41 (100 MHz,  $\text{CDCl}_3$ ,  $\delta$  ppm)

No.	39	40	41	No.	39	40	41
	$\delta_{\text{C}}$	$\delta_{\text{C}}$	$\delta_{\text{C}}$		$\delta_{\text{C}}$	$\delta_{\text{C}}$	$\delta_{\text{C}}$
1	161.8	162.0	161.7	1'	161.0	160.6	159.4
2	111.2	111.6	111.2	2'	118.1	117.6	117.2
3	150.9	150.9	150.8	3'	143.0	143.3	142.9
4	115.6	114.9	115.4	4'	107.2	107.8	107.2
4a	156.5	156.2	156.4	4a'	157.8	158.3	158.9
5	72.5	72.8	72.5	5'	77.0	76.1	87.6
6	26.5	29.8	26.0	6'	29.4	29.5	30.0
7	25.4	25.6	25.2	7'	27.5	27.5	36.2
8	22.2	22.6	22.3	8'	74.8	74.5	175.2
8a	48.5	48.9	48.6	8a'	76.0	77.0	39.8
9	197.6	197.8	197.5	9'	191.5	191.9	194.3
9a	104.7	105.0	104.8	9a'	106.6	106.9	107.4
10a	83.3	85.2	83.4	10a'	82.5	82.8	84.6
11	21.3	21.3	21.1	11'	15.4	15.4	20.8
12	169.7	170.6	169.7	12'	169.8	169.7	168.8
13	53.3	53.3	53.3	13'	-	-	53.3
14	170.3	-	170.2				
15	20.5	-	20.8				

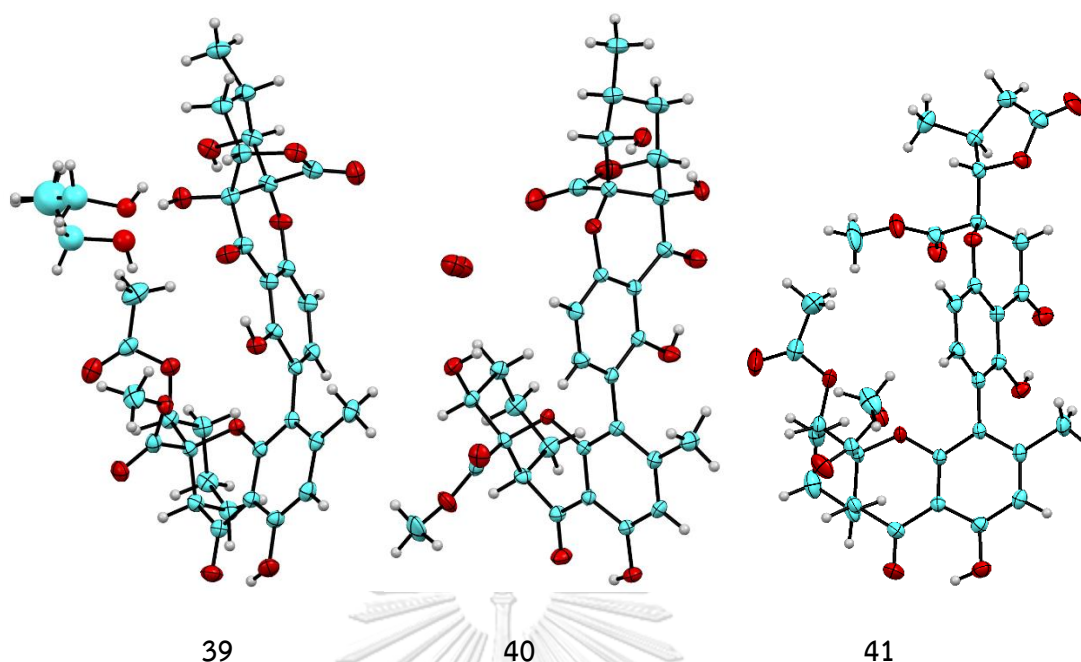


Fig. 2.15 ORTEP diagram for the single crystals X-ray geometry of 39–41.

The  $^1\text{H}$  and  $^{13}\text{C}$  NMR spectra displayed characteristic resonances for the dimeric tetrahydroxanthone skeleton of **41**, including the presence of two conjugated ketone carbonyls ( $\delta_{\text{C}}$  197.5, 194.3) and two phenolic hydroxyl protons at  $\delta_{\text{H}}$  11.44 (1H, s) and 11.74 (1H, s), three aromatic protons at  $\delta_{\text{H}}$  6.46 (1H, s), 6.57 (1H, d,  $J = 8.4$  Hz), and 7.72 (1H, d,  $J = 8.4$  Hz) (Table 1). Further comparison of its 1D NMR data and HMBC correlations (Fig. 2.16) with those of usneaxanthone A-D, the planar structure of **41** was established by assembling two partial structures **41a–41b**. The comparison of the 1D NMR data of **41** (Tables 2.5-2.6) with those of usneaxanthone A-D suggested a similar substructure **41a** for these compounds, which was further corroborated by 2D NMR correlations (Fig. 2.16).

The relative configuration of tetrahydroxanthone monomer was readily established to be the same as that of usneaxanthone A-D by similar chemical shifts and coupling constants (Tables 2.5–2.6). In partial **41a**, the large coupling constants between proton H-5 and H-6 ( $^3J_{5-6ax} = 11.6$  Hz;  $^3J_{5-6eq} = 4.8$  Hz) and between H-8a and H-8 ( $^3J_{8a-8ax} = 11.6$  Hz;  $^3J_{8a-8eq} = 4.0$  Hz) suggested H-5 and H-8a be in the *cis*-diaxial positions and the pseudoequatorial *trans* orientation for acetoxy group at C-5 and methoxycarbonyl group at C-10a. For partial **41b**, the small coupling constants between H-5' and H-6' ( $^3J_{H-5'-H-6'} = 3.6$  Hz) suggested the *trans*-diaxial configuration of H-5' and H-6' in the  $\gamma$ -butyrolactone moiety.

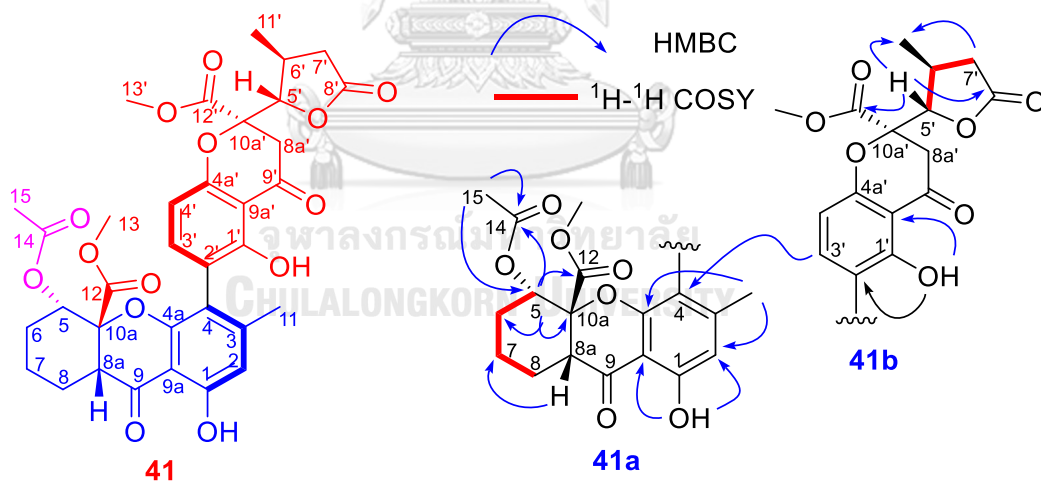


Fig. 2.16 Structure and the key COSY, HMBC correlations of **41**

The axial chiralities were deduced on the basis of an ECD exciton chirality method [105]. The anticlockwise manner of the two benzoyl chromophores in **41** resulted in positive exciton couplings near 212 nm, allowing the assignment of axial



chirality *aR* (Fig. 2.17) [107]. Finally, the absolute configuration of **41** was unambiguously determined by using single-crystal X-ray diffraction analysis with Cu  $K\alpha$  radiation as *5S,8aR,10aS,5'S,6'S,10'aS* (Fig. 2.15). Therefore, the structure of **41** was elucidated and named usneaxanthone E.

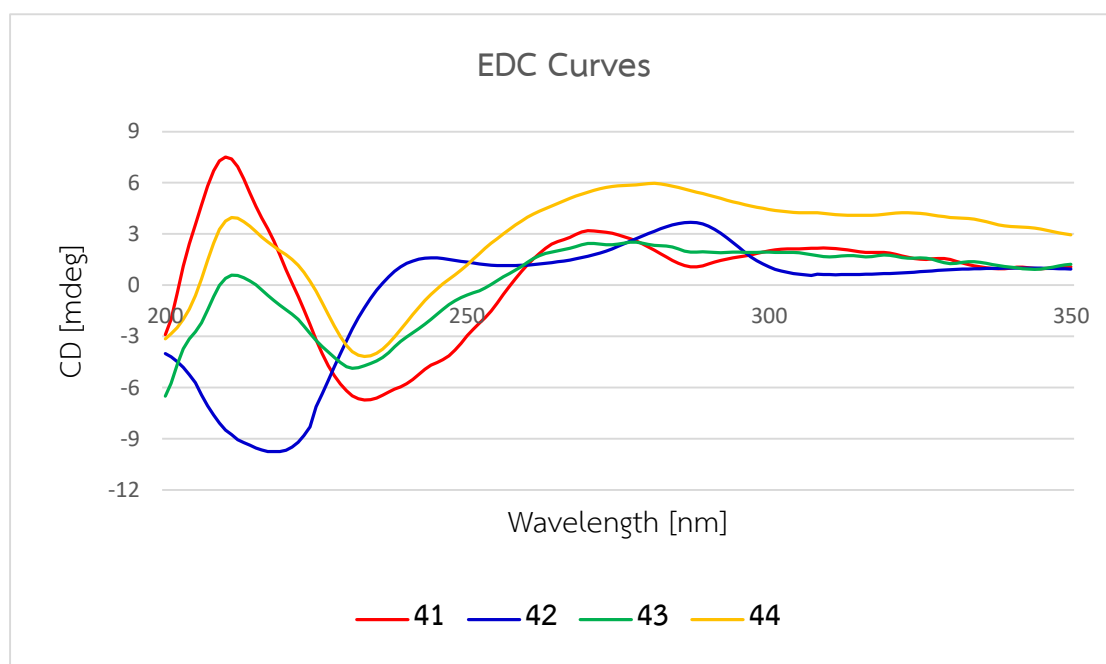


Fig. 2.17 Experimental ECD spectra of 41–44

#### New dimeric xanthone Usneaxanthone F (42)

Usneaxanthone F (**42**) was obtained as colorless needles, shared the same molecular formula of  $C_{34}H_{34}O_{14}$ , determined to be identical to that of **41** by HRESIMS with  $m/z$  689.1854  $[M + Na]^+$  (calcd for  $C_{34}H_{32}O_{14}Na$ , 689.1846). The typically doubled NMR data (Tables 2.7–2.8), especially the presence of two conjugated ketone carbonyls ( $\delta_C$  197.8, 195.3) and two enolic groups ( $\delta_H$  11.44, 1H, s and  $\delta_C$  161.7;  $\delta_H$

11.74, 1H, s and  $\delta_c$  161.9), revealed the dimeric tetrahydroxanthone skeleton of **42**. Further comparison of IR, UV, and NMR spectra suggested that **42** be an additional analogue of **41**.

The  $^1\text{H}$  and  $^{13}\text{C}$  NMR shift values in rings A and B of **42** were similar to those of **41** (Tables 2.7 and 2.8) with small differences in four chemical shift values. Interestingly, **41** and **42** displayed opposite signs for optical rotation data: whereas **41** was levorotatory ( $[\alpha]_D^{25} = -74$ ), **42** was dextrorotary ( $[\alpha]_D^{25} = +81$ ). The relative configurations of two units in **42** were confirmed to be the same as those in **41**, due to the similar NOESY of H-5/OCH<sub>3</sub>-13, H-5'/CH<sub>3</sub>-11', H-6'/OCH<sub>3</sub>-13' (Fig. 2.18). Putting these data together, the distinction of their axial chiralities could be suggested [108, 109]. Moreover, the anticlockwise manner of the two benzoyl chromophores in **42** resulted in negative exciton couplings near 218 nm, allowing the assignment of axial chirality as *aS* (Fig. 2.16) [105]. Combining all the data together suggested **42** as the atropisomer [110] of **41** with *aS*\* configuration, rather than the *aR*\* in **41**. Thus, the structure of **42** was elucidated and named usneaxanthone F.

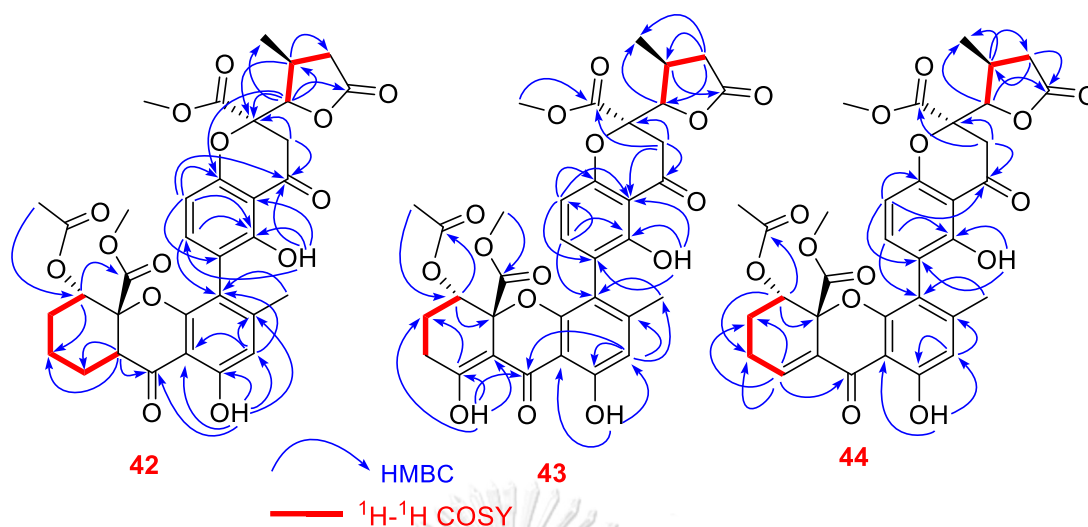


Fig. 2.18 The key COSY, HMBC correlations of 42–44

#### New dimeric xanthone Usneaxanthone G (43)

Usneaxanthone G (**43**) was obtained as yellow crystals. Its molecular formula was deduced to be  $\text{C}_{34}\text{H}_{32}\text{O}_{15}$  (19 DBEs) by HRESIMS ( $m/z$  703.1627  $[\text{M} + \text{Na}]^+$ , calcd 703.1639). The comparison of the  $^{13}\text{C}$  and  $^1\text{H}$  NMR spectroscopic data of **43** and **41** (Tables 2.7 and 2.8) indicated that **43** was a dimeric tetrahydroxanthone with structural similarity to those of **41** and **42**. However, key differences were the appearance of the hydrogen-bonded phenolic proton at C-8 in **43**, confirmed by the corresponding proton at  $\delta_{\text{H}}$  13.92 (8-OH) and HMBC correlations of **43** (Fig. 2.17).

The relative configurations of the tetrahydroxanthone monomeric units in **43** were found to be (5*R*,10*aS*,5'*S*,6'*S*,10'*aS*), deduced from NOESY correlations, coupling constants and ECD experiment. The NOESY signals between H-5' and CH<sub>3</sub>-11' revealed their *cis* configuration and the absent NOESY cross – peaks of OCH<sub>3</sub>-13/H-5,

OCH<sub>3</sub>-13'/H-5' indicated the orientation of COOCH<sub>3</sub>-10a and COOCH<sub>3</sub>-10a' in **43** (Fig. 2.18). In addition, the ECD curves of **43** were almost identical to those of **41** particularly the similar patterns of positive exciton coupling near 215 nm indicated an *aR* axial configuration for **43** (Fig. 2.16), which is in agreement with **41**. Therefore, structure of **43** elucidated and named as usneaxanthone G.

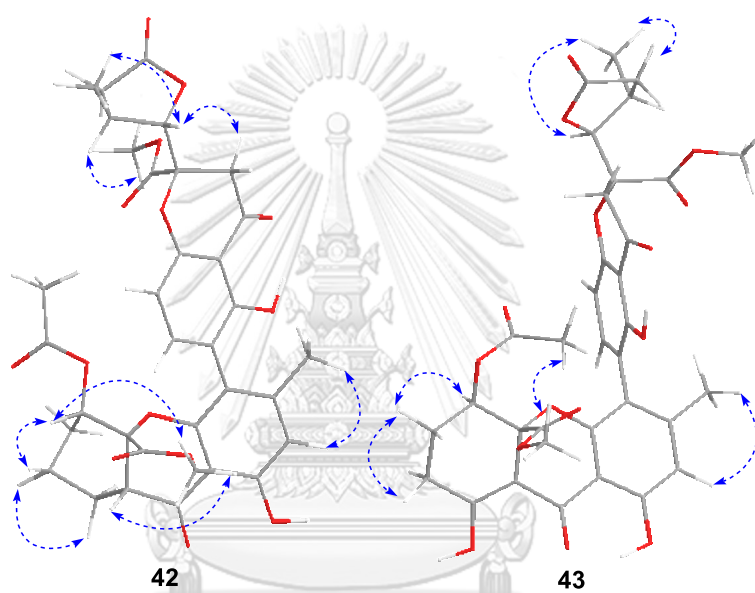


Fig. 2.19 Conformations and key NOESY correlations of **42** and **43**

#### New dimeric xanthone Usneaxanthone H (**44**)

Usneaxanthone H (**44**) was assigned by the molecular formula of C<sub>34</sub>H<sub>32</sub>O<sub>14</sub> by positive HRESIMS analysis ([M+Na]<sup>+</sup> *m/z* 687.1712, calcd 687.1690), which was two units less than those of **41** and **42**. The 1D and 2D NMR spectra of **44** highly resembled those of **43**, and the gross structure of **44** was achieved by <sup>1</sup>H-<sup>1</sup>H COSY and HMBC analyses in the same manner as described for **43**. The main difference

between **44** and **43** was the replacement of the hydrogen-bonded phenolic proton in **43** ( $\delta_{\text{H}}$  13.92 ppm) by an olefinic proton (H-8) in **44**, supported by signals of an olefinic proton H-8 ( $\delta_{\text{H}}$  7.32), and two olefinic carbons C-8 ( $\delta_{\text{C}}$  141.9), C-8a ( $\delta_{\text{C}}$  129.0), and the HMBC correlations from H-8 to C-6/C-10a/C-9 and from H<sub>2</sub>-7 to C-8/C-8a (Fig. 2.17).

The relative configurations of **44** were found to be (5*R*,10*aS*,5'*S*,6'*S*,10*a'S*), the same as that of **43**, as indicated by similar NMR data (Tables 2.7–2.8), and coupling constants. The comparison ECD method was used to assign axial chirality of **44**. The ECD curves of **44** were almost identical to those of **43**, particularly the similar patterns of positive exciton coupling near 213 nm indicated an *aR* axial configuration for **44** (Fig. 2.16), which is in agreement with **43**. Finally, the structure of **44** was elucidated and named as usneaxanthone H.

Table 2.7.  $^1\text{H}$  NMR spectroscopic data of 42–44

No.	42	43	44
	$\delta_{\text{H}}$ mult, ( $J$ in Hz)	$\delta_{\text{H}}$ mult, ( $J$ in Hz)	$\delta_{\text{H}}$ mult, ( $J$ in Hz)
2	6.50, 1H, s	6.47, 1H, s	6.49, 1H, s
5	5.03, 1H, dd, 4.8, 11.6	5.34, 1H, s	5.41, 1H, s
6	1.76, 2H, m	2.40, 1H, dd, 11.2, 19.2	1.95, 2H, m
	1.95, 1H, m	2.50, 1H, dd, 6.0, 19.2	
7	1.47, 1H, m	1.91, 1H, m	2.47, 1H, m
	1.76, 1H, m	2.06, 1H, m	2.51, 1H, m
8	1.53, 1H, m	-	7.32, 1H, m
	1.88, 1H, m	-	
8a	2.98, 1H, dd, 4.4, 12.4	-	-
11	2.07, 3H, s	2.08, 3H, s	2.06, 3H, s
13	3.64, 3H, s	3.68, 3H, s	3.80, 3H, s
15	1.98, 3H, s	1.89, 3H, s	1.84, 3H, s
1-OH	11.46, 1H, s	11.26, 1H, s	12.03, 1H, s
8-OH	-	13.92, 1H, s	-
3'	7.69, 1H d, 8.8	7.27, 1H d, 10.0	7.30, 1H d, 8.8
4'	6.61, 1H, d 8.4	6.62, 1H, d, 8.0	6.63, 1H, d 8.4
5'	4.21, 1H, d, 2.0	4.48, 1H, d, 2.8	4.49, 1H, d, 2.8
6'	2.22, 1H, m	2.88, 1H, m	2.88, 1H, m
7'	1.90, 1H, m	2.25, 1H, m	2.25, 1H, m
	2.30, 1H, m	2.50, 1H, m	2.93, 1H, m
8'a	3.08, 1H, d, 17.2	3.06, 1H, d, 16.8	3.07, 1H, d, 16.8
	3.54, 1H, d, 17.2	3.27, 1H, d, 16.8	3.27, 1H, d, 16.8
11'	1.00, 3H, d, 2.8	1.28, 3H, d, 6.4	1.28, 3H, d, 6.4
13'	3.70, 3H, s	3.79, 3H, s	3.68, 3H, s
1'-OH	11.64, 1H, s	11.68, 1H, s	11.69, 1H, s

Table 2.8  $^{13}\text{C}$  NMR spectroscopic data of 42–44 (100 MHz,  $\text{CDCl}_3$ ,  $\delta$  ppm)

No.	42	43	44	No.	42	43	44
	$\delta_{\text{C}}$	$\delta_{\text{C}}$	$\delta_{\text{C}}$		$\delta_{\text{C}}$	$\delta_{\text{C}}$	$\delta_{\text{C}}$
1	161.7	161.3	162.3	1'	161.9	159.8	159.6
2	110.7	111.7	111.5	2'	114.8	117.4	117.3
3	151.2	149.5	150.2	3'	142.9	141.1	141.4
4	115.9	115.9	115.7	4'	110.1	107.5	107.6
4a	156.3	155.6	156.2	4a'	156.7	158.8	158.8
5	72.8	66.1	66.4	5'	86.3	87.8	87.8
6	25.2	24.8	23.5	6'	29.2	30.2	30.2
7	25.4	22.7	22.1	7'	35.5	36.3	36.3
8	22.7	177.8	142.0	8'	175.8	175.2	175.2
8a	48.8	100.8	129.0	8a'	40.9	39.8	39.7
9	197.8	187.4	184.8	9'	195.3	194.4	194.9
9a	104.7	105.0	105.8	9a'	107.5	107.7	107.3
10a	83.6	81.7	81.3	10a'	84.5	84.6	84.6
11	21.1	21.2	21.3	11'	20.9	20.8	20.6
12	169.7	170.9	169.8	12'	168.1	169.0	169.1
13	53.3	53.6	53.9	13'	53.3	53.9	53.6
14	170.1	169.2	169.1				
15	21.1	20.7	20.7				

### Bailexanthone (45)

Compound **45** was obtained as yellow crystals. The HRESIMS of **45** showed a positive HRESIMS analysis ( $[\text{M}+\text{Na}]^+$   $m/z$  633.1909, calcd 633.1948), consistent with a molecular formula of  $\text{C}_{32}\text{H}_{34}\text{O}_{12}$ . The  $^{13}\text{C}$  NMR in accordance with the HSQC spectra of **45** revealed the existence of 16 carbon signals. The presence of only 16 carbons

signals in the  $^{13}\text{C}$  NMR spectrum indicated a symmetric, homodimer structure. Analysis of  $^1\text{H}$  and  $^{13}\text{C}$  NMR, MS and HSQC spectra revealed that half of the molecule  $\text{C}_{16}\text{H}_{17}\text{O}_6$ , possessed a conjugated ketone carbonyl ( $\delta_{\text{C}}$  197.4), five quaternary carbons ( $\delta_{\text{C}}$  159.0 (2C), 117.6, 107.6 and 87.6), two  $\text{sp}^2$  methine carbons ( $\delta_{\text{C}}$  140.4,  $\delta_{\text{H}}$  7.49 (1H, d, 8.4 Hz) and  $\delta_{\text{C}}$  107.3, 6.62 (1H, d, 8.8 Hz), one oxymethine ( $\delta_{\text{C}}$  80.3, one ester carbonyl carbon ( $\delta_{\text{C}}$  169.3), one methoxy group ( $\delta_{\text{C}}$  53.0),  $\delta_{\text{H}}$  3.72 (1H, d,  $J=10.8$  Hz)), two methylenes ( $\delta_{\text{C}}$  31.2,  $\delta_{\text{H}}$  1.96 and 1.20, and  $\delta_{\text{C}}$  20.4,  $\delta_{\text{H}}$  2.15), one methyl group attached to methine carbon ( $\delta_{\text{C}}$  18.5,  $\delta_{\text{H}}$  1.11, d,  $J=6.4$  Hz) and one methoxy ( $\delta_{\text{C}}$  53.0,  $\delta_{\text{H}}$  3.67), and also observed a proton signal of a chelated phenolic hydroxy ( $\delta_{\text{H}}$  11.85).

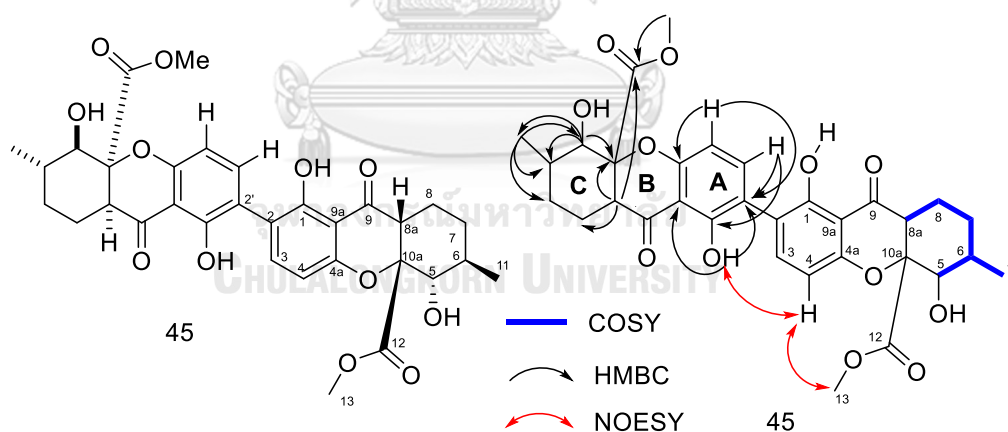


Fig. 2.20 Structure and key COSY, HMBC, NOESY correlations of 45

The COSY correlations revealed the connectivity of C-5 to C-8, and the tetrahydroxanthone structure was established on the basis of the HMBC correlations. In addition, the HMBC correlations of 1-OH to three quaternary carbons C-1, C-2, and



C-9a supported the 2,2'-linkage of **45**. Thus, the planar structure of **45** was determined.

Table 2.9  $^1\text{H}$  and  $^{13}\text{C}$  NMR spectroscopic data of **45**

No.	$\delta_{\text{H}}$ , J (Hz)	$\delta_{\text{C}}$	No.	$\delta_{\text{H}}$ , J (Hz)	$\delta_{\text{C}}$
1		159.0	1'		159.0
2		117.6	2'		117.6
3	7.49, 1H, d, 8.4	140.4	3'	7.49, 1H, d, 8.4	140.4
4	6.62, 1H, d, 8.8	107.3	4'	6.62, 1H, d, 8.8	107.3
4a		159.0	4a'		159.0
5	3.72, 1H, d, 10.8	80.3	5'	3.72, 1H, d, 10.8	80.3
6	1.83, 1H, m	34.3	6'	1.83, 1H, m	34.3
7	1.96, 1H, m	31.2	7'	1.96, 1H, m	31.2
	1.20, 1H, m			1.20, 1H, m	
8	2.15, 2H, m	20.4	8'	2.15, 2H, m	20.4
8a	2.98, 1H, dd, 11.6, 4.4	51.2	8a'	2.98, 1H, dd, 11.6, 4.4	51.2
9		197.4	9'		197.4
9a		107.6	9a'		107.6
10a		87.6	10'		87.6
11	1.11, 3H, d, 6.4	18.4	11'	1.11, 3H, d, 6.4	18.4
12		169.3	12'		169.3
13	3.67, 3H, s	53.0	13'	3.67, 3H, s	53.0
1-OH	11.85, 1H, s		1'-OH	11.85, 1H, s	

The relative configuration of **45** was established by analysis of 1D and 2D NMR data, especially by coupling constants together with comparison with literature review [86]. The large coupling constant of H-5 ( $\delta_{\text{H}}$  3.72, d,  $J = 10.8$  Hz) revealed the antiperiplanar of these protons (both pseudoaxial), therefore the *trans* configuration of 5-OH and H<sub>3</sub>-11. Moreover, the coupling constants of H-8a ( $\delta_{\text{H}}$  2.98, dd,  $J = 11.6, 4.4$

Hz) in **45** led to define the axial position of H-8a. In the case of eumitrin A2 (**34**), the configurations of H-5'/H-8a' and of H<sub>3</sub>-13'/H<sub>3</sub>-15' defined their *syn* relationships, respectively. These data confirmed the *anti*-relationship of H-8a and H<sub>3</sub>-13 in **45**. Furthermore, these spectroscopic data were compatible with the published ones in the literature [86], therefore **45** was elucidated as bailexanthone.

## 2.4 Biological activities

### 2.4.1 Antibacteria activity

The antibacterial activity of isolated compounds (**12**, **13**, **28**, **33**) towards pathogenic bacteria was determined by using agar well diffusion. The antibacterial activity of isolated compounds was displayed in Table 2.10.

Followed the literature reviews about bioactivities of lichen metabolites, the antibacterial activity of four isolated compounds were determined. As presented in Table 2.10, usnic acid (**28**), the dibenzofuran as well as the major compound of lichen *U. aciculifera* showed very good activity towards all types of bacteria. The second major compounds, two depsides barbatinic (**12**) and diffractaic acid (**13**) showed very good activity towards to *P.acnes* and *S. aureus*, and promising activity towards *S. mutans* and *S. sobrinus* with diameter zone inhibition around 9.67 to 17.67 mm while dimeric xanthone eumitrin B (**33**) showed moderated activity.

This result embarks the interesting point to develop these bioactive compounds as potent antibacterial agents. Further works, will continue investigating of MIC

(minimum inhibitory concentration) and MBC (minimum bactericidal concentration) of all isolated compounds.



Table 2.10 Antibacterial activity of isolated compounds

Compounds	Concentration	Inhibition zone (mm)				
		<i>S. typhi</i>	<i>P. acnes</i>	<i>S. aureus</i>	<i>S. sobrinus</i>	<i>S. mutans</i>
(+) Chloramphenicol	0.5 mM	ATCC 422 19.00±0.44	KCCM4147 25.00±0.44	ATCC 25923 31.00±0.57	KCCM 11898 22.00±0.50	ATCC 25175 26.00±0.50
<b>12</b>	1 mM	14.00±0.01	23.00±0.82	20.00±0.00	16.00±0.82	17.67±1.25
<b>13</b>	1 mM	10.67±0.47	23.33±0.94	20.00±0.00	9.67±0.94	11.67±0.94
<b>28</b>	1 mM	20.00±0.82	29.33±0.94	27.33±0.94	22.67±1.70	22.67±0.94
<b>33</b>	1 mM	9.67±0.37	13.67±0.47	10.00±0.00	11.33±0.47	9.67±0.47

Criteria of clear zone inhibition (including the diameter of well in mm) 6.0 = no activity; 6.1–8.0 = weak; 8.1–10 = moderate; 10.1–13 = Good; 13.1–15 = very good; > 15 = excellent.

## 2.4.2 Anti-dengue activity

The inhibition of infection DENV2 was conducted under the collaboration with Department of Microbiology, Faculty of Medicine, Chulalongkorn University. Isolated compounds (**1**, **12**, **13**, **19**, **20**, **21** and **33**) were evaluated the inhibition of dengue infection. The percentage of inhibition, percentage of cell viability, EC<sub>50</sub>, CC<sub>50</sub> and TI value are presented in Table 2.11.

**Table 2.1 Anti-dengue results of isolated compounds**

Entry	Cpds	% Plaque inhibition (at 10 $\mu$ M)	% Cell viability (at 10 $\mu$ M)	EC <sub>50</sub> ( $\mu$ M)	CC <sub>50</sub> ( $\mu$ M)	TI
1	<b>1</b>	No inhibition	106.62 $\pm$ 8.05	-	-	-
2	<b>12</b>	99.99 $\pm$ 0.02	113.31 $\pm$ 7.29	2.43 $\pm$ 0.32	50.13 $\pm$ 7.45	20.59
3	<b>13</b>	99.98 $\pm$ 0.04	114.72 $\pm$ 5.88	0.91 $\pm$ 0.26	11.78 $\pm$ 0.56	12.97
4	<b>19</b>	78.00 $\pm$ 7.55	111.18 $\pm$ 5.63	-	-	-
5	<b>20</b>	No inhibition	108.02 $\pm$ 4.34	-	-	-
6	<b>21</b>	-	insoluble	-	-	-
7	<b>33</b>	No inhibition	119.68 $\pm$ 11.66	-	-	-

Data represent means  $\pm$  standard error mean (SEM) of three independent experiment. The results were reported from three independent experiments. Compound **12** was used as positive control.

EC<sub>50</sub> = Effective concentrations, the molar concentration of an agonist that produced 50% of the maximal possible effect of that agonist;

CC<sub>50</sub> = Cytotoxic concentrations, the concentration of compound required for the reduction of 50% cell viability

TI = Therapeutic Indices;

The tabular results of biological indices of isolated compounds pointed out some promising candidates for further studying on dengue inhibitors. The first preliminary screening of plaque inhibition at 10  $\mu\text{M}$  displayed the efficiency of depsides (**12** and **13**). Both depsides exhibited excellent inhibitory value of more than 90% of virus infection (entries 2 and 3). On the other hand, other compounds showed no inhibition.

To estimate the toxicity of tested compounds at 10  $\mu\text{M}$ , the percentage of cell viability was accounted. The results showed that all isolated compounds were relatively non-toxic with the cell as specific concentration. Most of the cases, more than 100% of cells were viable, except for the case of (**21**) because of solubility

Based on the preliminary screening results, to further evaluate the cytotoxicity and effective concentration of these isolated compounds, appropriate experiments were conducted to determine  $\text{EC}_{50}$  and  $\text{CC}_{50}$  value.

In accordance with the inhibitory results, both depsides (**12** and **13**) displayed competitive  $\text{EC}_{50}$  and  $\text{CC}_{50}$  and could be considered as good anti-dengue agents. Both depsides will be considered to study intensely in the future.

#### 2.4.2 Cytotoxic activity

All xanthone dimers were evaluated for their *in vitro* cytotoxic activity against five human cancer cell lines [HCT116 colorectal cancer, MCF-7 breast cancer, A549

lung cancer and OVCAR-3 ovarian cancer] using the MTT reduction assay [111], and 5-fluorouracil and cisplatin were used as the positive control.

#### 2.4.2.1 HT-29 human colorectal cancer cell evaluation

The purified xanthone dimers were evaluated for their *in vitro* cytotoxicity against HT-29 human colorectal cancer cell line using the MTT reduction assay [111], and 5-fluorouracil was used as a positive control. The IC<sub>50</sub> value are presented in Table 2.12.

Table 2.12 IC<sub>50</sub> value of 33-45 and 5-fluorouracil on HT-29 cells<sup>a</sup>

Compound	IC <sub>50</sub> ± SD	Compound	IC <sub>50</sub> ± SD
<b>33</b>	>30	<b>39</b>	>10
<b>34</b>	>30	<b>40</b>	10.68 ± 0.96
<b>35</b>	3.49 ± 0.21	<b>41</b>	16.17 ± 3.71
<b>36</b>	2.41 ± 0.33	<b>42</b>	9.51 ± 0.92
<b>37</b>	18.74 ± 1.60	<b>43</b>	7.78 ± 1.32
<b>38</b>	>30	<b>44</b>	5.74 ± 0.09
5-Fluorouracil <sup>b</sup>	>30	<b>45</b>	4.15 ± 0.34

<sup>a</sup> Cytotoxicity was expressed as the mean values of three experiments ± SD; the other isolated compounds were inactive (IC<sub>50</sub> > 10–30 μM).

<sup>b</sup> 5-Fluorouracil was tested as a positive control

The tabular results of cytotoxic activity against HT-29 human colorectal cancer cell of isolated xanthone dimers pointed out some promising candidates for further studying on cytotoxicity. Xanthone dimers **35**, **36**, **42-45** showed strong cytotoxicity against HT-29 cell line with IC<sub>50</sub> values ranging from 3.37 to 4.53 μM. Other compounds possessed low cytotoxicity towards to cells. To discover the exact

target and understand the important interactions of compound with protein in the cell, other computational calculation and bio-assays are necessary in the future.

#### 2.4.2.2 Cytotoxic activity against other four cancer cell lines

The new xanthone dimers **41–44** were evaluated for their *in vitro* cytotoxic activity against four human cancer cell lines [HCT116 colorectal cancer, MCF-7 breast cancer, A549 lung cancer and OVCAR-3 ovarian cancer] using the MTT reduction assay, and cisplatin was used as a positive control [111]. The  $IC_{50}$  value are presented in Table 2.13.

The tabular results of cytotoxic activity against four cancer cell of isolated xanthone dimers **41–44** showed that all compounds exhibited highly potent cytotoxicity against HCT116 cell line with  $IC_{50}$  values ranging from 3.37 to 4.53  $\mu\text{M}$ . Usneaxanthone E (**41**) and usneaxanthone H (**44**) showed strong cytotoxicity against MCF7 cell line with  $IC_{50}$  values of 9.86 and 8.33  $\mu\text{M}$ , respectively. Usneaxanthone H (**44**) also exhibited cytotoxicity against A549 cancer cell line with  $IC_{50}$  value of 7.99  $\mu\text{M}$ . However, all compounds were found ineffectively in controlling the growth of OVCAR3 ovarian cancer cells.



Table 2.13 IC<sub>50</sub> values of 41–44 and cisplatin on human cancer cells<sup>a</sup>

Compounds	IC <sub>50</sub> (mean ± SD)			
	HCT116	MCF7	A549	OVCAR3
	(colorectal cancer)	(breast cancer)	(lung cancer)	(ovarian cancer)
41	4.53 ± 1.23	9.86 ± 2.12	31.41 ± 3.06	NA
42	3.37 ± 0.30	10.94 ± 0.37	23.41 ± 4.21	68.47 ± 7.04
43	3.66 ± 0.67	14.01 ± 0.47	7.99 ± 0.82	70.33 ± 16.73
44	3.47 ± 0.31	8.33 ± 1.72	12.23 ± 2.99	NA
cisplatin <sup>b</sup>	10.88 ± 1.04	5.46 ± 0.74	17.7 ± 2.41	43.83 ± 6.14

<sup>a</sup> Cytotoxicity was expressed as the mean values of three experiments ± SD; the other isolated compounds were inactive (IC<sub>50</sub> > 10–30 μM).

<sup>b</sup> Cisplatin was tested as positive control

NA: not active

Based on the cytotoxicity results of new xanthone dimers, these compounds may have potential as lead compounds for the development of new anti-cancer agents and will be considered to study intensely in the future.

## 2.5 Conclusion

Phytochemical investigation of lichen *Usnea aciculifera* Vain (Parmeliaceae) led to the isolation of nine new dimeric xanthenes, usneaxanthenes A-I (36–44), along with thirty-six known compounds including four known dimeric xanthenes (33–35, 45), eleven monocyclic compounds (1–11), seven depsides (12–18), nine

depsidones (19–27), one dibenzofuran (28), one steroid (29) and three terpenoids (30–32). The chemical structures of the isolated compounds were elucidated by a combination spectroscopic data (1D, 2D NMR, HRESIMS), electronic circular dichroism (ECD) experiments, and single-crystal X-ray crystallographic analyses as well as comparison of their NMR data with those in the literature. The biological activities of isolated compounds were evaluated for antibacterial, anti-dengue, and cytotoxic activities. The results revealed that depsides may have potential as lead compounds for the development of new antibacterial and anti-dengue agents. Furthermore, dimeric xanthones exhibited highly potent cytotoxicity against HT-29, HCT116, MCF-7 and A549 cancer cell lines with  $IC_{50}$  values ranging from 2.41 to 9.86  $\mu\text{M}$ . These compounds will be considered to study intensely in the future.

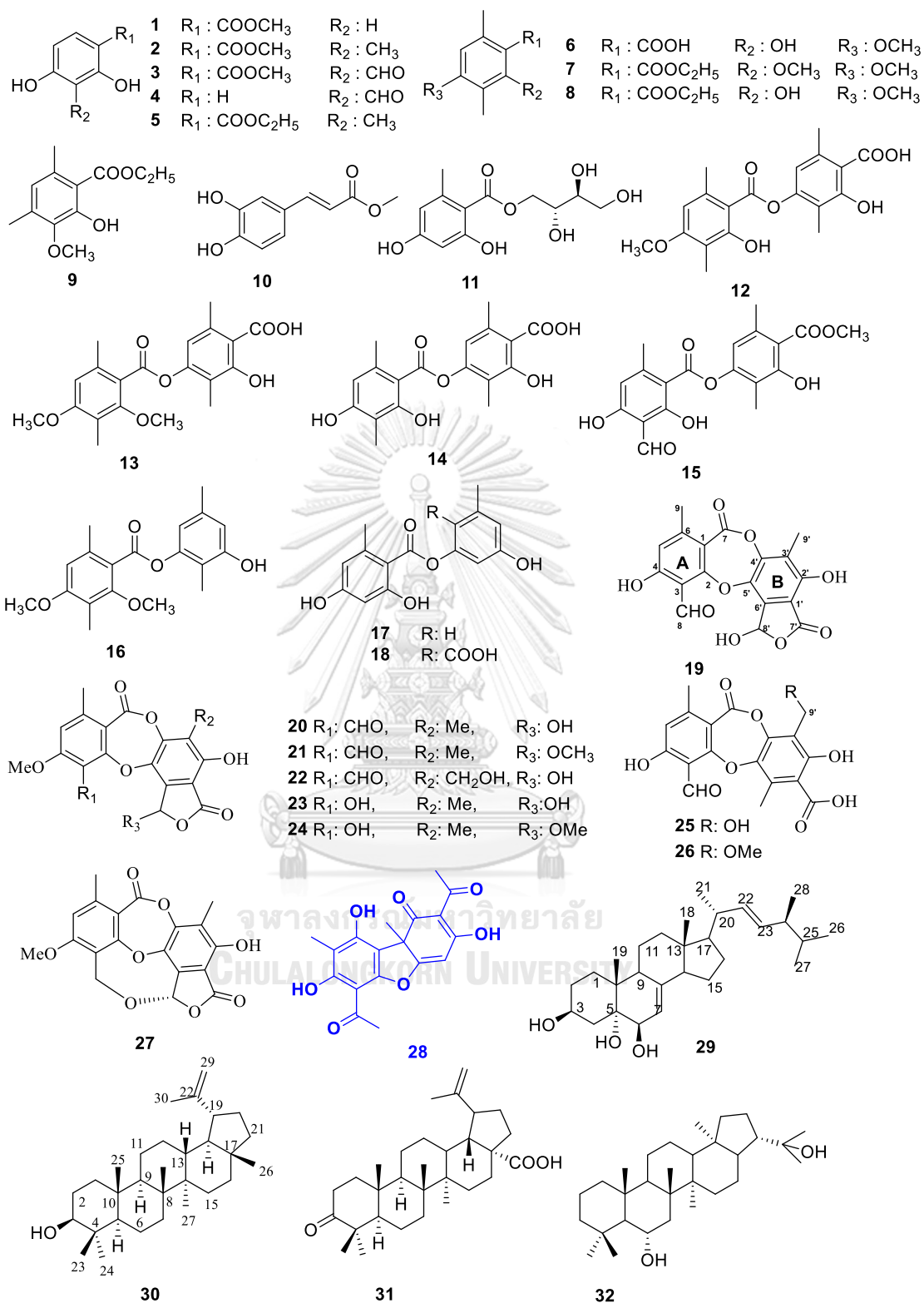


Fig. 2.21 Chemical structures of 1-32

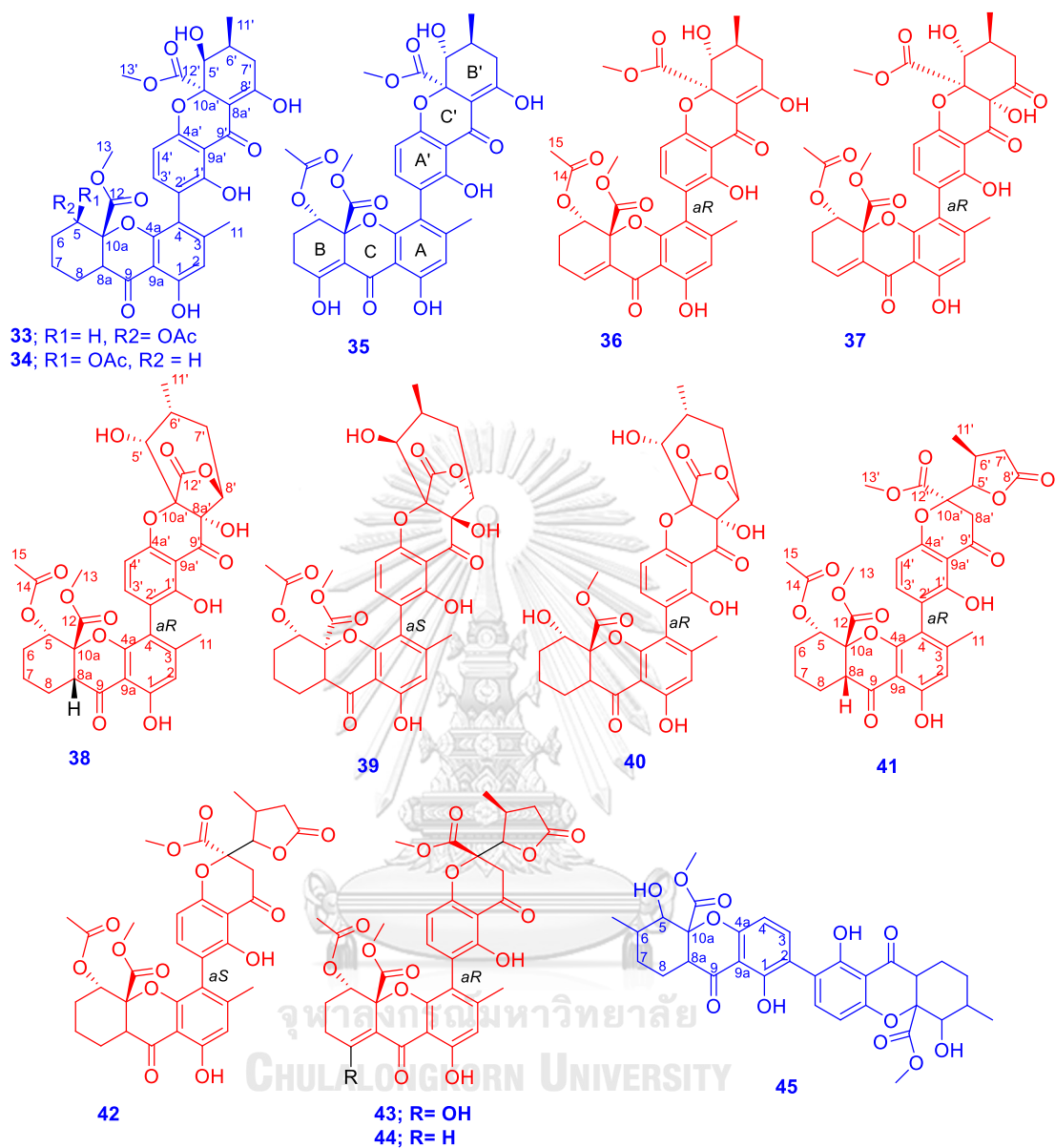


Fig. 2.22 Chemical structures of 33–45

## CHAPTER 3

USNIC ACID CONJUGATES AND THEIR  $\alpha$ -GLUCOSIDASE INHIBITORY

## 3.1 Introduction

Usnic acid (2,6-diacetyl-7,9-dihydroxy-8,9bdimethyldibenzo[b,d]furan-1,3(2H,9bH)-dione) (UA) is a secondary metabolite of lichens with a unique dibenzofuran scaffold, found in numerous lichen species such as *Cladonia* (Cladoniaceae), *Usnea* (Usneaceae), *Lecanora* (Lecanoraceae), *Ramalina* (Ramalinaceae), *Evernia*, *Parmelia* (Parmeliaceae), *Alectoria* (Alectoriaceae) with the highest isolated yield of 26%. [112] It occurs in nature as both (-) and (+) isomers as well as a racemic mixture and is one of the few lichen secondary metabolites that are commercially available. UA has been of interest to chemist and pharmacologists owing to the broad range of its biological activity, such as antitumor, antiviral, antimicrobial, anti-inflammatory, and insecticidal effects. [31, 34, 113] It is one of a few commercially available lichen metabolites and has been the most extensively investigated. Nevertheless, its adverse effects, particularly severe liver damage, greatly limit its use in medical applications. [31, 114, 115] Over the past few decades, significant efforts have been made to reduce the side effects of UA by encapsulating it in microspheres or nanocapsules [116, 117] and by searching for derivatives through synthesis [118-121] or phytochemical isolation from natural resources. [69, 122, 123] These efforts have ultimately led to the discovery of lead compounds with better pharmacological and toxicity profiles. [124] Thus, the synthesis of new UA

derivatives and the investigation of their biological activity contributes much to the understanding of the biological action of UA itself and opens up fresh opportunities for the pharmacological use of this metabolite (Table 3.1).

**Table 3.1 Biological activities of usnic acid [31, 34, 114, 120]**

Antioxidant and pro-oxidant activities	<p>UA exhibits antioxidant effect in gastric ulcers in rats with dose 25, 50, 100 and 200 mg/kg</p> <p>UA displays variable redox-active properties from 2 ng/mL to 20 µg/mL for 4 and 24 h.</p>	
Antimicrobial activity	Gram positive bacteria	<p><i>Enterococcus faecalis</i>, <i>Enterococcus faecium</i>, <i>Staphylococcus aureus</i>, <i>Streptococcus mutans</i> <i>Streptococcus pyogenes</i>.</p>
	Anaerobic bacteria	<p><i>Bacteroides fragilis</i>, <i>Bacteroides ruminicola</i> ssp. <i>brevis</i>, <i>Bacteroides thetaiotaomicron</i>, <i>Bacterioides vulgatus</i>, <i>Clostridium perfringens</i>, <i>Propionibacterium acnes</i>.</p>
	Mycobacteria	<p><i>M. aurum</i>, <i>M. avium</i>, <i>M. smegmatis</i>, <i>M. tuberculosis</i> var. <i>bovis</i>, <i>M. tuberculosis</i> var. <i>hominis</i>.</p>
Antiviral activity	<p>(+)-UA: inhibited against herpes simplex type 1 and polio type 1 viruses.</p> <p>Inhibited against <i>Epstein-Barr</i> virus with ED<sub>50</sub> of 1.0 µg/mL</p>	
Antiproliferative activity	<p>(-)-UA: exhibit P388 leukaemia, L1210 cells.</p> <p>(+)-UA: inhibit K-562 leukemic, endometrial carcinoma cell</p>	

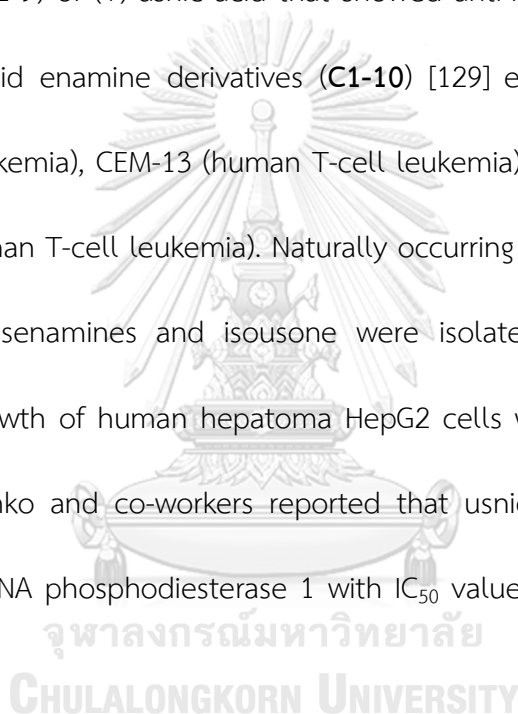
	lines, against HaCaT.
Antimalarial activity	(+)-UA and its conjugates showed <i>in vitro</i> and <i>in vivo</i> antimalarial activity against <i>Plasmodium falciparum</i> (K1) and cytotoxicity against L6 cells with $IC_{50}$ 0.0014 to 15.28 $\mu$ M.
Cytotoxicity	Cytotoxic activity on cancer cell lines: 3LL, L1210, DU145, MCF7, K-562, U251  Cytotoxicity on p53 breast cancer cell lines: MCF7, MDA-MB-231.  Lung cancer cell line H1299.  Significant cytotoxicity against MM98 malignant mesothelioma cells, A431 vulvar carcinoma cells.

With an effort to improve UA biological properties, a series of UA derivatives were synthesized by conjugating UA to a variety of amines and amino acids.

### 3.1.1 Usnic acid derivatives and biological activities

In previous studies, Takai *et al.* [68] synthesized a series of usnic acid derivatives to improve their bioavailability by increasing water solubility and indicated the importance of its lipophilicity and  $\beta$ -triketone moiety of usnic acid on cytotoxicity. Acylhydrazones of usnic acid coordinated with Pd(II) and Cu(II) were found to be cytotoxic *in vitro* towards HeLa cells with  $IC_{50}$  values ranging from 1.8 to 86.0  $\mu$ M.[125] Synthetic usnic acid derivatives (**A1-9**) obtained by conjugation of the acetyl group to a polyamine chain were shown to be more active than usnic acid in cancer cells, with  $IC_{50}$  values from 3 to 14  $\mu$ M in the case of 1,8-diaminooctane.[119]

Furthermore, synthetic and enamine derivatives of both enantiomers of usnic acid showed cytotoxic effects on blood tumor cell lines, especially the cyanoethyl derivative, for which the activity against human T cell leukemia (MT-4) cells was 2 times higher than that of (+)-usnic acid, while derivatives with a quaternized nitrogen atom were inactive against all cell lines tested.[126, 127] Vanga *et al.* synthesized triazole hybrids (**B1-9**) of (+)-usnic acid that showed anti-inflammatory activity. [128] Series of usnic acid enamine derivatives (**C1-10**) [129] exhibited good cytotoxicity against L1210 (leukemia), CEM-13 (human T-cell leukemia), U-937 (human monocyte tumor), MT-4 (human T-cell leukemia). Naturally occurring in *U. longissima*, the usnic acid derivatives usnamines and isousone were isolated and showed inhibitory effects on the growth of human hepatoma HepG2 cells with  $IC_{50}$  values of 3.3–6.0  $\mu\text{M}$ . [124] Zakharenko and co-workers reported that usnic acid enamines (**D1-D11**) revealed tyrosyl-DNA phosphodiesterase 1 with  $IC_{50}$  values in the range of 0.16–2.0  $\mu\text{M}$ . [130]





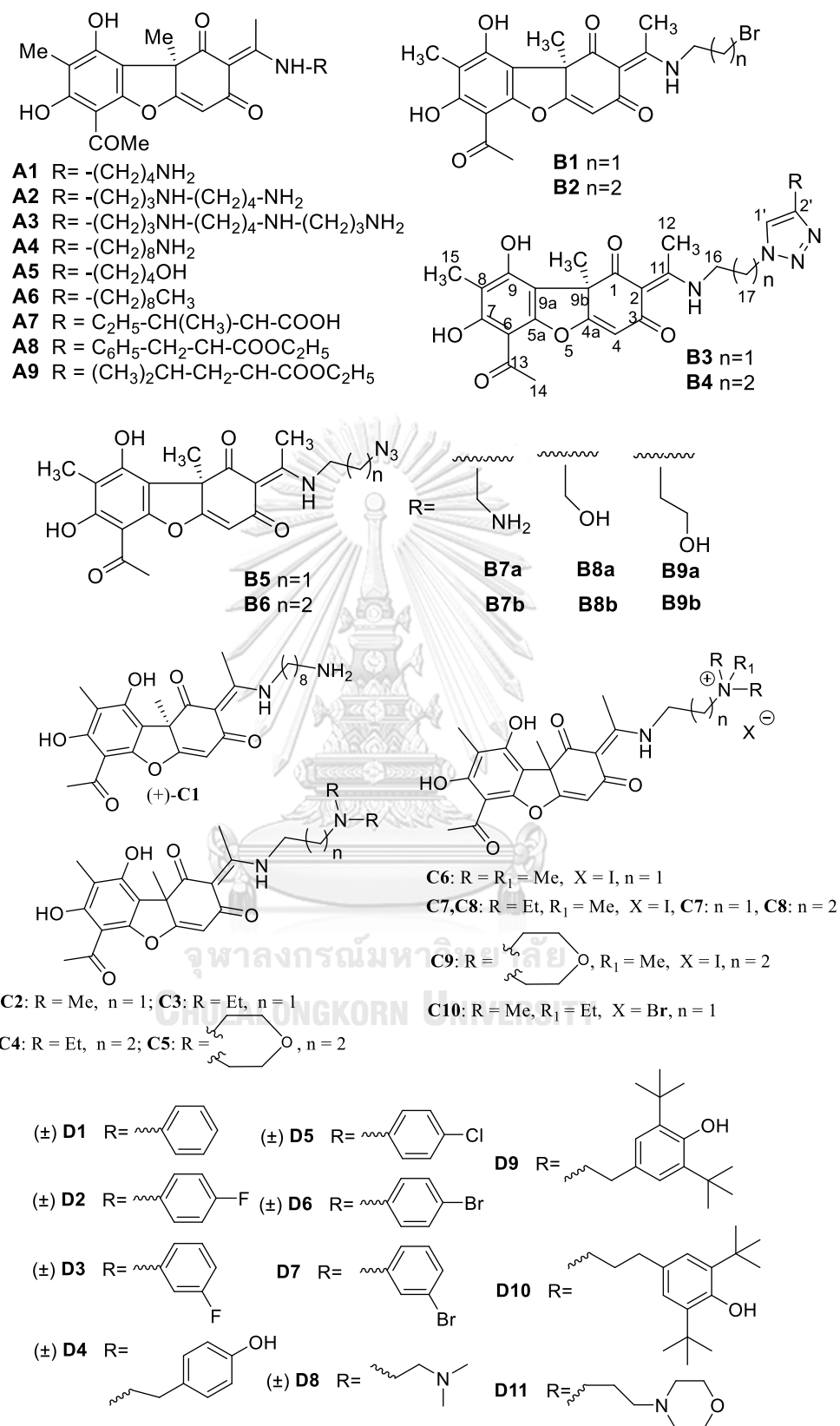


Fig. 3.1 Reported of usnic acid derivatives

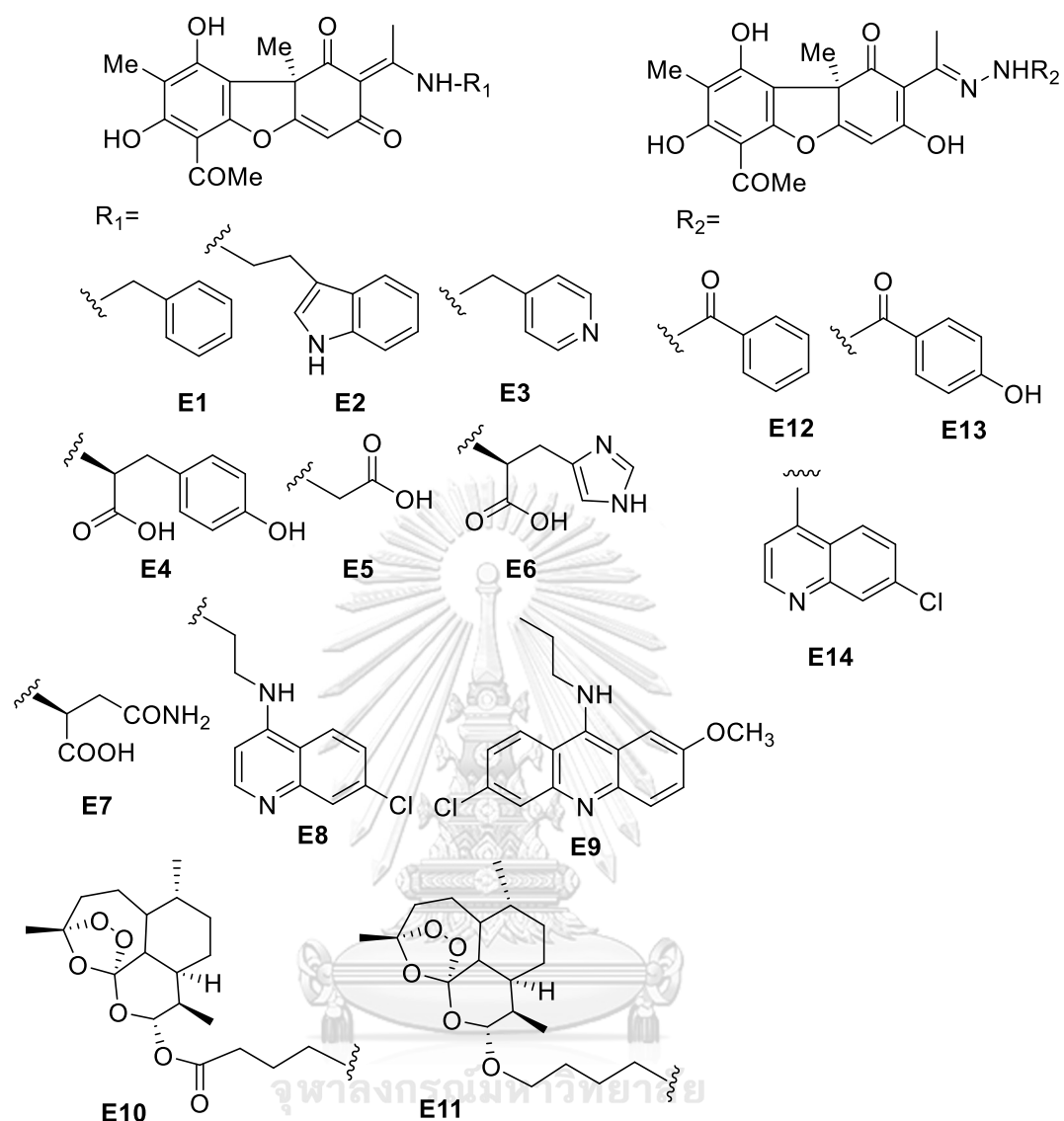


Fig. 3.1 Reported of usnic acid derivatives (continued)

Moreover, these compounds enhanced the cytotoxicity of camptothecin by an order of magnitude.[130] Bruno *et al.* reported the synthesis of a potent antimalarial agent through natural products conjugation (E1-E14).[131] Thus, some modifications to the structure of usnic acid have been shown to improve the potency of its bioactivity.

A few studies have discovered the positive potential of lichens extracts as potent antidiabetic agents. Verma *et al.* [92] found three potent alpha glucosidase inhibitors and antihyperglycemic effect on salazinic acid from *Ramalina celastri*, sekikaic acid from *R. nervulosa*, and usnic acid from *R. pacifica*. In another study, usnic acid had shown high antidiabetic activity (alpha glucosidase and antiglycation) (Thadhani and Karunaratne 2017). [132] Our extensive literature survey with respect to glucosidase inhibition potential of lichens or their metabolites, we found hardly one or two reports. It implies that there were not much work done in this aspects of lichens or their metabolites. Therefore, we have undertaken this study to find out lichen metabolites or their derivatives having glucosidase inhibitory activity, especially the lichen metabolites usnic acid and its derivatives.

### 3.1.2 Objectives

The usnic acid derivatives were synthesized as described by Pavan *et al.* [133] and Tazetdinova *et al.* [120]. The structure of products were elucidated using NMR spectroscopic and HRESIMS. The evaluation on enzyme  $\alpha$ -glucosidase inhibitory of all synthesized compounds was carried out.

## 3.2 Experimental

### 3.2.1 Instrument and equipment

The NMR experiments using residual solvent signal as internal reference: acetone- $d_6$   $\delta_H$  2.05, 2.84,  $\delta_C$  29.84, 206.26, chloroform- $d$   $\delta_H$  7.24,  $\delta_C$  77.23 and dimethyl sulfoxide- $d_6$   $\delta_H$  2.50, 3.33,  $\delta_C$  39.52 were performed with a Bruker 400

Avance spectrometer (400 MHz for  $^1\text{H}$  and 100 MHz for  $^{13}\text{C}$ ) or a JEOL 500 (500 MHz for  $^1\text{H}$  and 125 MHz for  $^{13}\text{C}$ -NMR) spectrometer. High resolution mass spectra (HR-MS) were recorded on a Bruker Daltonics microTOF using electron spray ionization (ESI).

### 3.2.2 Chemicals

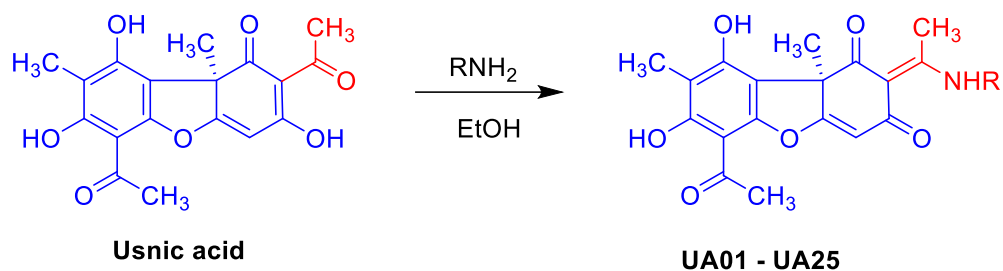
All solvents used in this research were distilled prior to use except those which were reagent grades. Thin layer chromatography (TLC) was carried out on precoated silica gel 60 F<sub>254</sub> (Merck) and precoated 60 RP-18 F<sub>254</sub>S (Merck). Silica gel (No. 7729, 7734, and 9385, Merck or Silicycle) was used as stationary phase on open column chromatography and quick column chromatography.

### 3.2.3 General procedure

The products **UA01–25** were prepared by the reaction of (+)-usnic acid with appropriate amines or amino acid [120, 133]. (Scheme 3.1).

**UA01–22** were synthesized as described by Tazetdinova et al. [120]

**UA23–25** were synthesized as described by Pavan et al.[133] after prolonging reflux but the precipitate from the reaction with **UA23–25** were finely dispersed. Therefore, the reaction mixture was extracted with EtOAc (3x 50 mL). The extracts were dried over anhydrous  $\text{Na}_2\text{SO}_4$ . The solvent was distilled *in vacuo*. All compounds were isolated by column chromatography over silica gel with a gradient elution of MeOH in  $\text{CH}_2\text{Cl}_2$  (from 5 to 50%).



**Scheme 3.1. Synthesis of usnic acid derivatives**

The desired UA enamine derivatives were prepared by reacting 1.5 mmol of appropriate amine with 1 mmol of (+)-usnic acid in 10 mL of EtOH. The reaction mixture was refluxed in an oil bath for 5 h and cooled, and then 10 mL of cold distilled water was added. The precipitate was formed, which was collected upon a filtration, washed with cold water, and dried in air. The precipitate was chromatographed on a silica gel column (fraction 60-200  $\mu\text{m}$  Merck) by a mixture of *n*-hexane with  $\text{CH}_2\text{Cl}_2$  (30 to 95%) for **UA1–22**, and  $\text{CH}_2\text{Cl}_2$  with MeOH (5 to 50%) for **UA23–25**.

The structures of synthesized compounds were confirmed by NMR spectroscopy and mass spectrometry.

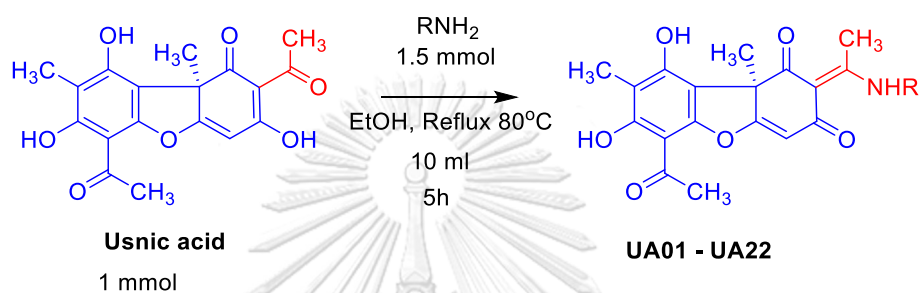
### 3.3 Results and discussion

Structural modification of usnic acid has been investigated for improvement biological activity along with penetration ability. Bioactive usnic acid enamine-conjugated products were proved as promising agents for further study. In this research, usnic acid derivatives with aromatic substitution containing halogenated

compounds were conducted to obtain a range of derivatives as new candidates for  $\alpha$ -glucosidase inhibitory.

### 3.3.1 Synthesis of usnic acid enamine-conjugated 1–22

The usnic acid enamine-conjugated **UA01–UA22** were prepared by reaction of (+)-usnic acid with appropriate amines [120]. (Scheme 3.2).



Scheme 3.2 Synthesis of UA01–UA22

After purification by silica gel column, the desired products were obtained as shown in Table 3.2.



Table 3.2 The yields and characteristics of usnic acid derivatives UA01-22

Products	Appearance	% isolated yield	Remarks
UA01	Yellow solid	56	Known
UA02	White amorphous powder	59	New
UA03	Yellow solid	58	Known
UA04	Yellow solid	56	Known
UA05	Yellow solid	70	Known
UA06	White amorphous powder	61	New
UA07	Yellow oil	64	Known
UA08	White solid	66	New
UA09	Yellow solid	61	New
UA10	Yellow amorphous powder	79	Known
UA11	Yellow amorphous powder	86	New
UA12	Yellow amorphous powder	82	New
UA13	Yellow amorphous powder	89	New
UA14	Yellow amorphous powder	70	New
UA15	Yellow solid	22	New
UA16	White solid	58	New
UA17	White solid	61	New
UA18	Yellow solid	85	Known
UA19	Yellow solid	72	New
UA20	Yellow solid	71	New
UA21	White amorphous powder	81	Known
UA22	Yellow solid	70	Known

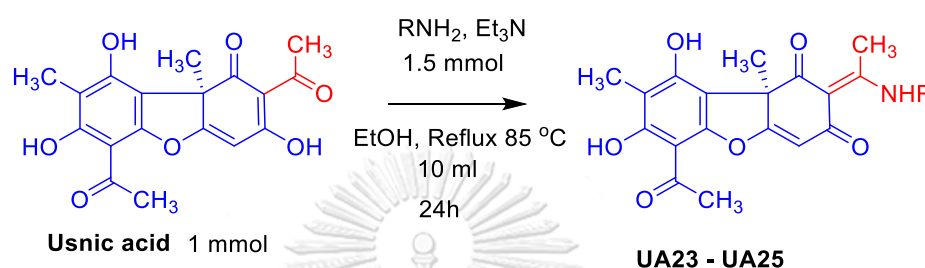
As presented in Table 3.2, the usnic acid enamine-conjugates could be achieved in moderate to excellent isolated yields (56-89 %) (UA01–UA22), except for UA15 with poor isolated yield (22 %).



### 3.3.2 Synthesis of usnic acid conjugates UA23–25

The usnic acid conjugates **UA3–25** were prepared by the reaction of (+)-usnic acid with selected amines or amino acid in the presence of Et<sub>3</sub>N for 24 h [133].

(Scheme 3.3).



Scheme 3.3 Synthesis of compounds

After purification by silica gel column, the desired products were obtained as shown in Table 3.3.

Table 3.3 The yields and characteristics of usnic acid derivatives UA23–25

Products	Appearance	% isolated yield	Remarks
UA23	Yellow solid	45	Known
UA24	Yellow oil	42	New
UA25	white solid	51	New

As presented in Table 3.3, the usnic acid conjugates were obtained in poor isolated yields (42-51 %).

### 3.4 $\alpha$ -glucosidase inhibitory activity of usnic acid conjugates

Compounds were evaluated for  $\alpha$ -glucosidase inhibitory activity using enzymes from baker's yeast (type I) according to [134]. The enzymatic activity was calculated by measuring absorbance at 405 nm (ALLSHENG micro plate reader AMR-

100). All samples were analyzed in triplicates at various concentrations to obtain the  $IC_{50}$  value of each compound. The mean values and standard deviation were also determined.

**Table 3.4  $\alpha$ -Glucosidase inhibitory assay of usnic acid conjugates**

Compounds	$IC_{50} \pm SD$ ( $\mu M$ )	Compounds	$IC_{50} \pm SD$ ( $\mu M$ )
Usnic acid	>200	UA13	14.51 $\pm$ 1.75
UA01	99.04 $\pm$ 4.74	UA14	>200
UA02	>200	UA15	>200
UA03	98.9 $\pm$ 1.75	UA16	>200
UA04	76.32 $\pm$ 0.65	UA17	73.46 $\pm$ 0.76
UA05	>200	UA18	53.04 $\pm$ 3.15
UA06	104.82 $\pm$ 4.03	UA19	160.48 $\pm$ 2.44
UA07	> 200	UA20	>200
UA08	112.84 $\pm$ 4.10	UA21	>200
UA09	116.20 $\pm$ 4.20	UA22	>200
UA10	>200	UA23	ND
UA11	89.68 $\pm$ 0.81	UA24	159.74 $\pm$ 11.65
UA12	59.24 $\pm$ 0.39	UA25	>200
Acarbose <sup>b</sup>	93.60 $\pm$ 0.49		

All usnic acid conjugates (UA01-UA25) were tested with  $\alpha$ -glucosidase inhibitory activity. All derivatives exhibited the same or higher activity comparing with starting material (usnic acid >200  $\mu M$  and no activity (NA) for  $\alpha$ -glucosidase). Especially, UA04, UA11-13 and UA17-18 showed excellent  $\alpha$ -glucosidase activity with  $IC_{50}$  values ranging from 14.51 to 89.68  $\mu M$ . These analogues not only displayed higher activity than its parent compounds, but also with that of positive control, acarbose

( $IC_{50}$   $93.60 \pm 0.49 \mu M$ ) as showed in Table 3.4. Noticeably, **UA13** displayed the strongest activity with  $IC_{50}$   $14.51 \pm 1.75$ . These results revealed that usnic acid conjugates may have potential as lead compounds for the development of new  $\alpha$ -glucosidase inhibitory agents. The search for new  $\alpha$ -glucosidase inhibitors and other antidiabetic drugs from natural sources has increased notably in recent years, considering that type II diabetes mellitus is one of the most challenging health problems of the 21st century. Therefore, as part of an effort to discover new  $\alpha$ -glucosidases inhibitors useful for the development of antidiabetic agents, we now report the series of usnic acid conjugates that showed potential as  $\alpha$ -glucosidase inhibitory agent.

To discover the exact target and to understand the important interactions of compound with protein in the cell, or the relationship between structure and bioactivity, other computational calculation study and bio-assays are necessary in the future.

### 3.5 Conclusion

According to the biological activities of usnic acid and reported usnic acid derivatives, twenty-five usnic acid derivatives were synthesized. Their chemical structures were elucidated by 1D NMR and HRESIMS as well as comparison with those of literature. Among them, fifteen compounds were obtained as new compounds. Noticeably, all derivatives exhibited the same or higher activity

comparing with starting material, usnic acid for  $\alpha$ -glucosidase activity. Especially, **UA04**, **UA11-13** and **UA17-18** showed excellent activity with  $IC_{50}$  values ranging from 14.51 to 89.68  $\mu$ M. These usnic acid derivatives can be further studied for the interaction mechanism with enzyme and the relationship between structure and bioactivity in the future.



## Chapter 4

### CONCLUSIONS

#### 4.1 Chemical constituents of lichen *Usnea aciculifera*

Nine new dimeric xanthenes, usneaxanthenes A-I (**36–44**), along with thirty-six known compounds (**1–35**, **45**) were successfully isolated from hexane and dichloromethane extracts. The chemical structures of the isolated compounds were elucidated by a combination spectroscopic data (1D, 2D NMR, HRESIMS), electronic circular dichroism (ECD) experiments, and single-crystal X-ray crystallographic analyses as well as comparison of their NMR data with those in the literature. The biological activities of isolated compounds were evaluated for antibacterial, anti-dengue and cytotoxic activities. The results revealed that usnic acid (**28**) and depsides (**12** and **13**) may have potential as lead compounds for the development of new antibacterial agents. On the other hand, depsides (**12** and **13**) also displayed competitive  $EC_{50}$  and  $CC_{50}$  and could be considered as good anti-dengue agents. Both depside will be considered to study intensely in the future.

Moreover, dimeric xanthenes exhibited highly potent cytotoxicity against HT-29, HCT116, MCF-7 and A549 cancer cell lines with  $IC_{50}$  values ranging from 2.41 to 9.86  $\mu\text{M}$ .

## 4.2 Synthesis of usnic acid conjugates

Twenty-five usnic acid derivatives were synthesized and evaluated on  $\alpha$ -glucosidase inhibitory activity. Interestingly, **UA04**, **UA11-13** and **UA17-18** showed excellent  $\alpha$ -glucosidase activity with  $IC_{50}$  values ranging from 14.51 to 89.68  $\mu$ M. These analogues not only displayed higher activity than its parent, usnic acid, but also with that of acarbose, a positive control. The results revealed that usnic acid conjugates may have potential as lead compounds for the development of new  $\alpha$ -glucosidase inhibitory agents.

### Suggestion for future work

The further research would be continued to the chemical constituents from the remaining dichloromethane fractions, hexane, ethyl acetate and methanol extracts. Furthermore, the synthesis of derivatives from other major compounds such as depsides (barbatinic acid (**12**) and diffractaic acid (**13**)), depsidones (stictic acid (**20**), 8-*O*-methylstictic acid (**21**)) should be studied. Other biological activities such as cytotoxic and some inhibitory activities such as tyrosinase, acetylcholinesterase should be conducted on the isolated compounds and derivatives. Computational calculation study and bio-assays are necessary to discover the exact target and understand the important interactions of compound with protein in the cell, or the relationship between structure and bioactivity.

APPENDIX



จุฬาลงกรณ์มหาวิทยาลัย  
**CHULALONGKORN UNIVERSITY**

## CONTENT OF SUPPORTING INFORMATION

Table A1. Crystal data and refinement parameters of compounds 33, 35–36 and 38–41. ....	143
Figure A1. <sup>1</sup> H NMR spectrum of usneaxanthone D (36) in CDCl <sub>3</sub> .....	145
Figure A2. <sup>13</sup> C NMR spectrum of usneaxanthone D (36) in CDCl <sub>3</sub> .....	145
Figure A3. COSY spectrum of usneaxanthone D (36) in CDCl <sub>3</sub> .....	146
Figure A4. HSQC spectrum of usneaxanthone D (36) in CDCl <sub>3</sub> .....	146
Figure A5. HMBC spectrum of usneaxanthone D (36) in CDCl <sub>3</sub> .....	147
Figure A6. HRESIMS spectrum of usneaxanthone D (36) .....	148
Figure A7. <sup>1</sup> H NMR spectrum of usneaxanthone I (37) in CDCl <sub>3</sub> .....	149
Figure A8. <sup>13</sup> C NMR spectrum of usneaxanthone I (37) in CDCl <sub>3</sub> .....	149
Figure A9. COSY spectrum of usneaxanthone I (37) in CDCl <sub>3</sub> .....	150
Figure A10. HSQC spectrum of usneaxanthone I (37) in CDCl <sub>3</sub> .....	150
Figure 11 HMBC spectrum of usneaxanthone I (37) in CDCl <sub>3</sub> .....	151
Figure A12. HRESIMS spectrum of usneaxanthone I (37).....	152
Figure A13. <sup>1</sup> H NMR spectrum of usneaxanthone A (38) in CDCl <sub>3</sub> .....	153
Figure A14. <sup>13</sup> C NMR spectrum of usneaxanthone A (38) in CDCl <sub>3</sub> .....	153
Figure A15. COSY spectrum of usneaxanthone A (38) in CDCl <sub>3</sub> .....	154
Figure A16. HSQC spectrum of usneaxanthone A (38) in CDCl <sub>3</sub> .....	154
Figure A17. HMBC spectrum of usneaxanthone A (38) in CDCl <sub>3</sub> .....	155
Figure A18. HRESIMS spectrum of usneaxanthone A (38) .....	156
Figure A19. <sup>1</sup> H NMR spectrum of usneaxanthone B (39) in CDCl <sub>3</sub> .....	157
Figure A20. <sup>13</sup> C NMR spectrum of usneaxanthone B (39) in CDCl <sub>3</sub> .....	157
Figure A21. COSY spectrum of usneaxanthone B (39) in CDCl <sub>3</sub> .....	158



Figure A22. HSQC spectrum of usneaxanthone B (39) in CDCl <sub>3</sub> .....	158
Figure A23. HMBC spectrum of usneaxanthone B (39) in CDCl <sub>3</sub> .....	159
Figure A24. HRESIMS spectrum of usneaxanthone B (39) .....	160
Figure A25. <sup>1</sup> H NMR spectrum of of usneaxanthone C (40) in CDCl <sub>3</sub> .....	161
Figure A26. <sup>13</sup> C NMR spectrum of usneaxanthone C (40) in CDCl <sub>3</sub> .....	161
Figure A27. COSY spectrum of usneaxanthone C (40) in CDCl <sub>3</sub> .....	162
Figure A28. HSQC spectrum of usneaxanthone C (40) in CDCl <sub>3</sub> .....	162
Figure A29. HMBC spectrum of usneaxanthone C (40) in CDCl <sub>3</sub> .....	163
Figure A30. HRESIMS spectrum of usneaxanthone C (40) .....	164
Figure A31. <sup>1</sup> H NMR spectrum of usneaxanthone E (41) in CDCl <sub>3</sub> .....	165
Figure A32. <sup>13</sup> C NMR spectrum of usneaxanthone E (41) in CDCl <sub>3</sub> .....	165
Figure A33. COSY spectrum of usneaxanthone E (41) in CDCl <sub>3</sub> .....	166
Figure A34. HSQC spectrum of usneaxanthone E (41) in CDCl <sub>3</sub> .....	166
Figure A35. HMBC spectrum of usneaxanthone E (41) in CDCl <sub>3</sub> .....	167
Figure A36. NOESY spectrum of usneaxanthone E (41) in CDCl <sub>3</sub> .....	167
Figure A37. HRESIMS spectrum of usneaxanthone E (41).....	168
Figure A38. <sup>1</sup> H NMR spectrum of usneaxanthone F (42) in CDCl <sub>3</sub> .....	169
Figure A39. <sup>13</sup> C NMR spectrum of usneaxanthone F (42) in CDCl <sub>3</sub> .....	169
Figure A40. COSY spectrum of usneaxanthone F (42) in CDCl <sub>3</sub> .....	170
Figure A41. HSQC spectrum of usneaxanthone F (42) in CDCl <sub>3</sub> .....	170
Figure A42. HMBC spectrum of usneaxanthone F (42) in CDCl <sub>3</sub> .....	171
Figure A43. NOESY spectrum of usneaxanthone F (42) in CDCl <sub>3</sub> .....	171
Figure A44. HRESIMS spectrum of usneaxanthone F (42).....	172
Figure A45. <sup>1</sup> H NMR spectrum of of usneaxanthone G (43) in CDCl <sub>3</sub> .....	173

Figure A46. $^{13}\text{C}$ NMR spectrum of usneaxanthone G (43) in $\text{CDCl}_3$ .....	173
Figure A47. COSY spectrum of usneaxanthone G (43) in $\text{CDCl}_3$ .....	174
Figure A48. HSQC spectrum of usneaxanthone G (43) in $\text{CDCl}_3$ .....	174
Figure A49. HMBC spectrum of usneaxanthone C (43) in $\text{CDCl}_3$ .....	175
Figure A50. NOESY spectrum of usneaxanthone G (43) in $\text{CDCl}_3$ .....	175
Figure A51. HRESIMS spectrum of usneaxanthone G (43) .....	176
Figure A52. $^1\text{H}$ NMR spectrum of usneaxanthone H (44) in $\text{CDCl}_3$ .....	177
Figure A53. $^{13}\text{C}$ NMR spectrum of usneaxanthone H (44) in $\text{CDCl}_3$ .....	177
Figure A54. COSY spectrum of usneaxanthone H (44) in $\text{CDCl}_3$ .....	178
Figure A55. HSQC spectrum of usneaxanthone H (44) in $\text{CDCl}_3$ .....	178
Figure A56. HMBC spectrum of usneaxanthone H (44) in $\text{CDCl}_3$ .....	179
Figure A57. HRESIMS spectrum of usneaxanthone H (44) .....	180
Figure A58. $^1\text{H}$ NMR spectrum of UA02 in $\text{CDCl}_3$ .....	181
Figure A59. $^{13}\text{C}$ NMR spectrum of UA02 in $\text{CDCl}_3$ .....	181
Figure A60. HRESIMS spectrum of UA02 .....	182
Figure A61. $^1\text{H}$ NMR spectrum of UA06 in $\text{CDCl}_3$ .....	183
Figure A62. $^{13}\text{C}$ NMR spectrum of UA06 in $\text{CDCl}_3$ .....	183
Figure A63. HRESIMS spectrum of UA06 .....	184
Fig. A64. $^1\text{H}$ NMR spectrum of UA08 in $\text{CDCl}_3$ .....	185
Fig. A65. $^{13}\text{C}$ NMR spectrum of UA08 in $\text{CDCl}_3$ .....	185
Fig. A67. $^1\text{H}$ NMR spectrum of UA09 in $\text{CDCl}_3$ .....	186
Fig. A69. $^1\text{H}$ NMR spectrum of UA11 in $\text{CDCl}_3$ .....	187
Fig. A70. $^{13}\text{C}$ NMR spectrum of UA11 in $\text{CDCl}_3$ .....	187
Figure A71. HRESIMS spectrum of UA11 .....	188

Fig. A72. $^1\text{H}$ NMR spectrum of UA12 in $\text{CDCl}_3$ .....	189
Fig. A73. $^{13}\text{C}$ NMR spectrum of UA12 in $\text{CDCl}_3$ .....	189
Fig. A74. HRESIMS spectrum of UA12 .....	190
Fig. A75. $^1\text{H}$ NMR spectrum of UA13 in $\text{CDCl}_3$ .....	191
Fig. A76. $^{13}\text{C}$ NMR spectrum of UA13 in $\text{CDCl}_3$ .....	191
Fig. 77 HRESIMS spectrum of UA13.....	192
Fig. A78. $^1\text{H}$ NMR spectrum of UA14 in $\text{CDCl}_3$ .....	193
Fig. A79. $^{13}\text{C}$ NMR spectrum of UA14 in $\text{CDCl}_3$ .....	193
Fig. A80. HRESIMS spectrum of UA14 .....	194
Fig. A81. $^1\text{H}$ NMR spectrum of UA15 in $\text{CDCl}_3$ .....	195
Fig. A82. $^{13}\text{C}$ NMR spectrum of UA15 in $\text{CDCl}_3$ .....	195
Fig. A83. $^1\text{H}$ NMR spectrum of UA16 in $\text{CDCl}_3$ .....	196
Fig. A84. $^{13}\text{C}$ NMR spectrum of UA16 in $\text{CDCl}_3$ .....	196
Figure A85. HRESIMS spectrum of UA16 .....	197
Fig. A86. $^1\text{H}$ NMR spectrum of UA17 in $\text{CDCl}_3$ .....	198
Fig. 87 $^{13}\text{C}$ NMR spectrum of UA17 in $\text{CDCl}_3$ .....	198
Figure A88. HRESIMS spectrum of UA17 .....	199
Fig. A89. $^1\text{H}$ NMR spectrum of UA20 in $\text{CDCl}_3$ .....	200
Fig. A91. $^1\text{H}$ NMR spectrum of UA24 in $\text{CDCl}_3$ .....	201
Fig. 92 $^{13}\text{C}$ NMR spectrum of UA24 in $\text{CDCl}_3$ .....	201
Figure A93. HRESIMS spectrum of UA24 .....	202
Fig. 94. $^1\text{H}$ NMR spectrum of UA25 in $\text{CDCl}_3$ .....	203
Fig. A95. $^{13}\text{C}$ NMR spectrum of UA25 in $\text{CDCl}_3$ .....	203

**Methyl orsellinate (1)**

White needles (recrystallized in chloroform), mp. 143 – 144 °C

$^1\text{H-NMR}$  ( $\text{CDCl}_3$ , 500 MHz),  $\delta$  : 11.59 (s, 1H, 2-OH), 9.08 (s, 1H, 4-OH), 6.29 (d (2.0 Hz), 1H, H-5), 6.24 (d (2.0 Hz), 1H, H-2), 3.92 (s, 3H, H-9), 2.46 (s, 3H, H-8)

$^{13}\text{C NMR}$  ( $\text{CDCl}_3$ , 125 MHz)  $\delta$  173.2 (C-7), 166.6 (C-2), 163.6 (C-4), 144.6 (C-6), 112.6 (C-5), 105.8 (C-1), 102.0 (C-3), 52.4 (C-9), 24.4 (C-8).

**Methyl  $\beta$ -orsellinate (2)**

Colorless needles (recrystallized in chloroform), mp. 140 – 141 °C

$^1\text{H-NMR}$  ( $\text{CDCl}_3$ , 500 MHz),  $\delta$  : 12.03 (s, 1H, 2-OH), 5.25 (s, 1H, 4-OH), 6.20 (s, 1H, H-5), 3.92 (s, 3H, H-10), 2.45 (s, 3H, H-9), 2.10 (1H, s, H-8)

$^{13}\text{C NMR}$  ( $\text{CDCl}_3$ , 125 MHz)  $\delta$  172.8 (C-7), 163.3 (C-2), 158.3 (C-4), 140.3 (C-6), 110.7 (C-5), 108.7 (C-3), 105.4 (C-1), 51.9 (C-10), 24.1 (C-9), 7.8 (C-8).

**Methyl haematommate (3)**

Colorless needles (recrystallized in chloroform), mp. 141 °C

$^1\text{H-NMR}$  ( $\text{CDCl}_3$ , 500 MHz),  $\delta$  : 12.87 (s, 1H, 4-OH), 12.41 (s, 1H, 2-OH), 10.34 (s, 1H, H-8), 6.29 (s, 1H, H-5), 3.96 (s, 3H, H-10), 2.53 (s, 3H, H-9)

$^{13}\text{C NMR}$  ( $\text{CDCl}_3$ , 125 MHz)  $\delta$  : 193.9 (C-8), 171.9 (C-7), 168.3 (C-2), 166.7 (C-4), 152.2 (C-6), 112.1 (C-5), 108.5 (C-3), 104.2 (C-1), 52.2 (C-10), 25.1 (C-9).

**Atranol (4)**

Yellow needles (recrystallized in acetone), mp. 124 °C

$^1\text{H-NMR}$  ( $\text{CDCl}_3$ , 500 MHz),  $\delta$  : 10.67 (br, 1H, 6-OH), 10.67 (br, 1H, 2-OH), 10.28 (s, 1H, H-8), 6.25 (s, 1H, H-5), 6.25 (s, 1H, H-3), 2.23 (s, 3H, H-7)

$^{13}\text{C NMR}$  ( $\text{CDCl}_3$ , 125 MHz)  $\delta$  : 194.2 (C-8), 163.1 (C-6), 163.1 (C-2), 151.5 (C-4), 109.4 (C-1), 108.5 (C-6), 108.5 (C-6), 22.4 (C-7).

**Ethyl  $\beta$ -orsellinate (5)**

Colorless needles (recrystallized in chloroform), mp. 129 °C

$^1\text{H-NMR}$  ( $\text{CDCl}_3$ , 500 MHz),  $\delta$  : 12.05 (s, 1H, 2-OH), 6.14 (s, 1H, H-5), 5.02 (s, 1H, 4-OH), 4.32 (q, 2H,  $J=7$ , H-1'), 2.41 (s, 3H, 6- $\text{CH}_3$ ), 2.03 (s, 3H, 3- $\text{CH}_3$ ), 1.34 (t, 3H, 2'- $\text{CH}_3$ )

$^{13}\text{C NMR}$  ( $\text{CDCl}_3$ , 125 MHz)  $\delta$  : 172.1 (C-7), 163.2 (C-2), 157.9 (C-4), 140.2 (C-6), 110.5 (C-5), 108.5 (C-3), 105.4 (C-1), 61.2 (C-1'), 24.2 (6-Me), 14.2 (C-2'), 7.6 (3-Me).

#### 4-hydroxy-2-methoxy-3,6-dimethylbenzoic acid (6)

Orange needles (recrystallized in chloroform), mp. 184 °C

$^1\text{H-NMR}$  ( $\text{CDCl}_3$ , 500 MHz),  $\delta$  : 13.53 (1H, OH), 6.86 (2H, d), 3.90 (s, 3H, O- $\text{CH}_3$ ), 3.91 (s, 3H, O- $\text{CH}_3$ ), 2.95 (s, 3H,  $\text{CH}_3$ )

$^{13}\text{C NMR}$  ( $\text{CDCl}_3$ , 125 MHz)  $\delta$  : 183.1 (CO, C-9), 165.3 (Cq, C-3), 163.9 (Cq, C-13), 162.9 (Cq, C-6), 159.4 (C-OH, C-1), 156.9 (Cq, C-11), 143.9 (Cq, C-8), 115.7 (CH, C-7), 113.1 (C-10), 104.6 (C-12), 98.1 (CH-5), 96.3 (CH-4), 98.1 (CH-2), 55.3 (O- $\text{CH}_3$ ), 55.1 (O- $\text{CH}_3$ ), 23.8 (C-8,  $\text{CH}_3$ ).

#### Ethyl 2-hydroxy-3-methoxy-4,6-dimethylbenzoate (9).

White crystals (recrystallized in chloroform), mp. 85 °C

$^1\text{H-NMR}$  ( $\text{CDCl}_3$ , 500 MHz),  $\delta$ : 11.90 (1H, s, 2-OH), 6.25 (1H, s, H-5), 4.38 (q, 2H,  $J=7$  Hz, H-1') 3.80 (s, 3H, H-10), 2.50 (s, 3H, H-8), 2.08 (s, 3H, H-9), 1.40 (t, 3H,  $J=7$  Hz, 2'- $\text{CH}_3$ ).

$^{13}\text{C NMR}$  ( $\text{CDCl}_3$ , 125 MHz)  $\delta$  : 172.4 (C-7), 162.0 (C-2), 161.2 (C-3), 140.0 (C-1), 110.0 (C-4), 105.7 (C-6), 105.4 (C-5), 61.1 (C-1'), 55.3 (C-10), 24.6 (C-8), 14.1 (C-2'), 7.7 (C-9).

#### Methyl (*E*)-3-(3,4-dihydroxyphenyl)acrylate (10)

Orange oil. HRESIMS analysis  $m/z$ : 193.39 [M-H]<sup>-</sup> (calcd. for [C<sub>10</sub>H<sub>10</sub>O<sub>4</sub>-H]<sup>-</sup> 193.18)

$^1\text{H-NMR}$  ( $\text{DMSO-}d_6$ , 500 MHz),  $\delta$  : 7.48 (d,  $J=16$  Hz, 1H, H-7), 7.05 (d,  $J=1.6$  Hz, 1H, H-2), 6.99 (dd,  $J=1.6$ ; 8.0 Hz, 1H, H-6), 6.76 (d,  $J=8.0$  Hz, 1H, H-5), 6.27 (d,  $J=16$  Hz, 1H, H-8), 3.68 (s, 3H, H-10).

$^{13}\text{C NMR}$  ( $\text{DMSO-}d_6$ , 125 MHz)  $\delta$  : 167.1 (C-9), 148.6 (C-4), 145.7 (C-3), 145.2 (C-7), 125.6 (C-1), 115.2 (C-5), 114.8 (C-2), 113.8 (C-8), 51.3 (C-10).

#### (+)-D-Montagnetol (11)

Yellow oil.  $[\alpha]_D^{25} = +184$  ( $c = 0.002$ , MeOH)

$^1\text{H-NMR}$  (DMSO- $d_6$ , 500 MHz),  $\delta$  : 6.18 (*d*,  $J=2.4$  Hz, 1H, H-5'), 6.14 (*d*,  $J=2.4$  Hz, 1H, H-3'), 4.38 (*dd*,  $J=11.2; 2.4$  Hz, 1H, H-1), 4.24 (*dd*,  $J=11.2; 7.2$  Hz, 1H, H-1'), 3.72 (*m*, 1H, H-2), 3.72 (*m*, 1H, H-3), 2.08 (*s*, 3H, 6'-CH<sub>3</sub>).

$^{13}\text{C NMR}$  (DMSO- $d_6$ , 125 MHz)  $\delta$  : 170.0 (C-7'), 161.9 (C-2'), 161.4 (C-4'), 141.9 (C-6'), 110.6 (C-5'), 106.7 (C-1'), 100.5 (C-3'), 72.5 (C-3), 69.7 (C-2), 66.7 (C-1), 63.0 (C-4), 22.6 (6'-CH<sub>3</sub>).

### Barbatinic acid (12)

Colorless needles (recrystallized in acetone). Mp: 181 – 183 °C.

$^1\text{H-NMR}$  (Acetone- $d_6$ , 500 MHz),  $\delta$  : 11.43 (*s*, 1H, 2-OH), 6.70 (*s*, 1H, H-5'), 6.61 (*s*, 1H, H-5), 3.93 (*s*, 3H, 4-OCH<sub>3</sub>), 2.69 (*s*, 3H, H-9), 2.60 (*s*, 3H, H-9'), 2.05 (*s*, 3H, H-8'), 2.04 (*s*, 3H, H-8).

$^{13}\text{C NMR}$  (Acetone- $d_6$ , 125 MHz)  $\delta$  : 174.3 (C-7'), 170.8 (C-7), 164.0 (C-2), 163.4 (C-4), 163.2 (C-2'), 153.5 (C-4'), 141.8 (C-6), 141.0 (C-6'), 117.1 (C-3'), 111.3 (C-1), 110.6 (C-1'), 107.5 (C-5), 105.3 (C-3), 56.1 (4-OCH<sub>3</sub>), 24.8 (C-9), 23.7 (C-9'), 9.3 (C-8'), 7.9 (C-8).

### Diffraitaic acid (13)

Colorless needles (recrystallized in acetone). Mp: 191 – 194 °C. HRESIMS analysis  $m/z$ :  $m/z$  397.1258 [M+Na]<sup>+</sup> (calcd for (C<sub>20</sub>H<sub>22</sub>O<sub>7</sub> + Na): 397.1258).

$^1\text{H-NMR}$  (Acetone- $d_6$ , 500 MHz),  $\delta$  : 6.73 (*s*, 1H, H-5'), 6.69 (*s*, 1H, H-5), 3.88 (*s*, 3H, 4-OCH<sub>3</sub>), 3.84 (*s*, 3H, 2-OCH<sub>3</sub>), 2.61 (*s*, 3H, H-9'), 2.44 (*s*, 3H, H-9), 2.14 (*s*, 3H, H-8'), 2.13 (*s*, 3H, H-8).

$^{13}\text{C NMR}$  (Acetone- $d_6$ , 125 MHz)  $\delta$  : 174.3 (C-7'), 166.4 (C-7), 164.0 (C-2'), 160.8 (C-4), 157.8 (C-2), 154.4 (C-4'), 140.9 (C-6'), 135.9 (C-6), 120.8 (C-1), 117.8 (C-3), 117.4 (C-1'), 117.0 (C-5'), 110.2 (C-3'), 109.0 (C-5), 62.2 (2-OCH<sub>3</sub>), 56.1 (4-OCH<sub>3</sub>), 23.8 (C-9'), 19.9 (C-9), 9.2 (C-8'), 9.0 (C-9).

### Demethylbarbatinic acid (14)

Colorless needles (recrystallized in acetone). Mp: 176 – 177 °C.

$^1\text{H-NMR}$  (Acetone- $d_6$ , 500 MHz),  $\delta$  : 6.48 (s, 1H, H-5), 6.41 (s, 1H, H-5'), 2.62 (s, 3H, H-9'), 2.60 (s, 3H, H-9), 2.08 (s, 3H, H-8), 2.0 (s, 3H, H-8').

$^{13}\text{C NMR}$  (Acetone- $d_6$ , 125 MHz)  $\delta$  174.8 (C-7'), 171.1 (C-7), 161.5 (C-2), 164.3 (C-4), 163.7 (C-2'), 151.0 (C-4'), 140.8 (C-6), 140.5 (C-6'), 115.3 (C-3'), 103.9 (C-1), 115.3 (C-1'), 111.8 (C-5), 109.8 (C-3), 24.3 (C-9), 23.4 (C-9'), 9.4 (C-8'), 7.8 (C-8).

### Atranorin (15)

Colorless needles (recrystallized in acetone). Mp: 195 – 197 °C.

$^1\text{H-NMR}$  ( $\text{CDCl}_3$ , 500 MHz),  $\delta$  : 12.55 (s, 1H, 4-OH), 12.49 (s, 1H, 2-OH), 11.94 (s, 1H, 2'-OH), 10.36 (s, 1H, H-8), 6.52 (s, 1H, H-5'), 6.40 (s, 1H, H-5), 3.98 (s, 3H, H-10'), 2.69 (s, 3H, H-9), 2.54 (s, 3H, H-9'), 2.09 (s, 3H, H-8').

$^{13}\text{C NMR}$  ( $\text{CDCl}_3$ , 125 MHz)  $\delta$  193.8 (C-8), 172.2 (C-7'), 169.7 (C-7), 169.1 (C-2), 167.5 (C-4), 162.9 (C-2'), 152.4 (C-6), 152.0 (C-4'), 139.9 (C-6'), 116.8 (C-3'), 116.0 (C-5'), 112.8 (C-5), 110.3 (C-1'), 108.6 (C-3), 102.9 (C-1), 52.3 (C-10'), 25.5 (C-9), 24.0 (C-9'), 9.4 (C-8').

### Aceculiferin A (16)

Colorless needle (acetone). HRESIMS analysis  $m/z$ :  $m/z$  353.1387  $[\text{M}+\text{Na}]^+$  (calcd for (calcd for  $\text{C}_{19}\text{H}_{22}\text{O}_5 + \text{Na}$ ): 353.1359).

$^1\text{H-NMR}$  (Acetone- $d_6$ , 500 MHz),  $\delta$  : 8.34 (s, 1H, H-2'), 6.73 (s, 1H, H-5), 6.64 (s, 1H, H-5'), 6.53 (s, 1H, H-1'), 3.88 (s, 3H, 4-OCH<sub>3</sub>), 3.83 (s, 3H, 2-OCH<sub>3</sub>), 2.43 (s, 3H, H-9), 2.25 (s, 3H, H-8'), 2.13 (s, 3H, H-8), 2.11 (s, 3H, H-7').

$^{13}\text{C NMR}$  (Acetone- $d_6$ , 125 MHz)  $\delta$  167.1 (C-7), 160.7 (C-4), 157.8 (C-2), 157.2 (C-4'), 151.5 (C-2'), 137.2 (C-6'), 135.7 (C-6), 121.8 (C-1), 117.8 (C-3), 115.5 (C-3'), 114.1 (C-5'), 114.6 (C-1'), 109.1 (C-5), 62.3 (4-OCH<sub>3</sub>), 56.2 (2-OCH<sub>3</sub>), 21.1 (C-7'), 20.0 (C-9), 9.4 (C-8'), 9.1 (C-8).

### Lecanorin (17)

Yellow amorphous powder.

$^1\text{H-NMR}$  ( $\text{CDCl}_3$ , 500 MHz),  $\delta$  : 11.31 (s, 1H, 2-OH), 9.33 (s, 1H, 4-OH), 8.60 (s, 1H, 2'-OH), 6.63 (s, 1H, H-1'), 6.58 (s, 1H, H-3'), 6.58 (s, 1H, H-5'), 6.38 (d,  $J=2.5$ , 1H, H-5), 6.29 (d,  $J=2.5$ , 1H, H-3), 2.59 (s, 3H, H-8), 2.29 (s, 3H, H-7).

$^{13}\text{C}$  NMR ( $\text{CDCl}_3$ , 125 MHz)  $\delta$  171.1 (C-7), 164.0 (C-4), 166.8 (C-2), 159.1 (C-2'), 151.9 (C-4'), 144.7 (C-6), 141.1 (C-6'), 114.7 (C-1'), 114.4 (C-5'), 112.8 (C-5), 107.4 (C-3') 105.1 (C-1), 101.8 (C-3), 24.4 (C-8), 21.4 (C-7').

#### Isolecanoric acid (18)

Yellow amorphous powder.

$^1\text{H}$ -NMR ( $\text{CDCl}_3$ , 500 MHz),  $\delta$  : 6.53 (*d*,  $J=2.5$ , 1H, H-5'), 6.49 (*d*,  $J=2.0$ , 1H, H-3'), 6.29 (*d*,  $J=2.5$ , 1H, H-5), 6.22 (*d*,  $J=2.5$ , 1H, H-3), 2.60 (*s*, 3H, H-8'), 2.54 (*s*, 3H, H-8).

$^{13}\text{C}$  NMR ( $\text{CDCl}_3$ , 125 MHz)  $\delta$  167.6 (C-7), 164.5 (C-4), 164.3 (C-2), 153.5 (C-2'), 166.2 (C-4'), 144.6 (C-6), 144.8 (C-6'), 116.4 (C-1'), 116.2 (C-5'), 112.9 (C-5), 106.5 (C-3') 108.5 (C-1), 101.9 (C-3), 23.5 (C-8), 175.3 (C-7'), 24.2 (C-8').

#### Norstictic acid (19)

White powder. Mp : 286 – 287 °C.

$^1\text{H}$ -NMR ( $\text{DMSO-}d_6$ , 500 MHz),  $\delta$  : 12.07 (*s*, 1H, 2'-OH), 10.45 (*s*, 1H, 8-OH), 10.16 (*s*, 1H, 4-OH), 8.28 (*s*, 1H, 9'-OH), 6.84 (*s*, 1H, H-5), 6.78 (*s*, 1H, H-9'), 2.44 (*s*, 3H, H-9), 2.22 (*s*, 3H, H-8').

$^{13}\text{C}$  NMR ( $\text{DMSO-}d_6$ , 125 MHz)  $\delta$  192.7, 164.0, 163.6, 160.3, 152.3, 137.4, 135.7, 120.8, 117.3, 111.8, 110.6, 21.4, 9.5.

#### Stictic acid (20)

White powder. Mp : 286 – 287 °C.

$^1\text{H}$ -NMR ( $\text{DMSO-}d_6$ , 500 MHz),  $\delta$  : 10.49 (*s*, 1H, H-8), 10.14 (*s*, 1H, 2'-OH), 8.19 (*s*, 1H, 9'-OH), 7.11 (*s*, 1H, H-5), 6.63 (*s*, 1H, H-9'), 3.94 (*s*, 3H, H-10), 2.52 (*s*, 3H, H-9), 2.22 (*s*, 3H, H-8').

$^{13}\text{C}$  NMR ( $\text{DMSO-}d_6$ , 125 MHz)  $\delta$  186.6 (C-8), 166.3 (C-7'), 163.0 (C-4), 162.3 (C-2), 160.6 (C-7), 151.8 (C-2'), 150.8 (C-6), 147.9 (C-4'), 137.4 (C-6'), 135.8 (C-5'), 120.7 (C-3'), 114.3 (C-3), 113.0 (C-1), 112.7 (C-5), 109.1 (C-1'), 95.0 (C-9'), 56.7 (C-10), 21.4 (C-9), 9.5 (C-8').

#### 8'-O- Methylstictic acid (21)

White powder. Mp : 286 – 287 °C.

$^1\text{H}$ -NMR ( $\text{DMSO-}d_6$ , 500 MHz),  $\delta$  : 10.40 (*s*, 1H, 2'-OH), 7.10 (*s*, 1H, H-5), 6.47 (*s*, 1H, H-9'), 3.92 (*s*, 3H, H-10), 3.48 (*s*, 3H, H-10'), 2.51 (*s*, 3H, H-9), 2.19 (*s*, 3H, H-8').



$^{13}\text{C}$  NMR (DMSO- $d_6$ , 125 MHz)  $\delta$  186.6 (C-8), 166.0 (C-7'), 162.9 (C-4), 162.5 (C-2), 160.7 (C-7), 152.4 (C-2'), 151.1 (C-6), 148.4 (C-4'), 137.7 (C-6'), 133.2 (C-5'), 121.8 (C-3'), 114.4 (C-3), 113.3 (C-1), 113.0 (C-5), 109.0 (C-1'), 100.0 (C-9'), 56.9 (C-10), 56.4 (C-10'), 21.6 (C-9), 9.8 (C-8').

#### Hypoconstictic acid (22)

White powder. Mp : 260–262 °C.

$^1\text{H}$ -NMR (DMSO- $d_6$ , 400 MHz),  $\delta$  : 8.30 (*br*, 1H, 9'-OH), 6.87 (*s*, 1H, H-5), 6.67 (*br*, 1H, H-9'), 4.60 (*s*, 3H, H-8'), 3.85 (*s*, 3H, 4-OCH<sub>3</sub>), 2.39 (*s*, 3H, H-9), 2.23 (*s*, 3H, H-8).

$^{13}\text{C}$  NMR (DMSO- $d_6$ , 100 MHz)  $\delta$  110.8 (C-1), 166.1 (C-2), 114.5 (C-3), 161.1 (C-4), 112.5 (C-5), 148.3 (C-6), 158.7 (C-7), 8.6 (C-8), 20.7 (C-9), 56.2 (4-OCH<sub>3</sub>), 109.1 (C-1'), 152.3 (C-2'), 122.1 (C-3'), 141.8 (C-4'), 137.8 (C-5'), 136.9 (C-6'), 161.1 (C-7'), 52.7 (C-8'), 95.3 (C-9').

#### Cryptostictic acid (23)

White powder. Mp : 241–243 °C.

$^1\text{H}$ -NMR (DMSO- $d_6$ , 400 MHz),  $\delta$  : 8.22 (*br*, 1H, 9'-OH), 6.95 (*s*, 1H, H-5), 4.80 (*d*,  $J = 11.2$  Hz, 1H, H-8a), 4.62 (*d*,  $J = 11.2$  Hz, 1H, H-8b), 3.87 (*s*, 3H, 4-OCH<sub>3</sub>), 2.45 (*s*, 3H, H-9), 2.19 (*s*, 3H, H-8').

$^{13}\text{C}$  NMR (DMSO- $d_6$ , 100 MHz)  $\delta$  111.6 (C-1), 166.5 (C-2), 118.5 (C-3), 161.7 (C-4), 112.7 (C-5), 148.2 (C-6), 158.9 (C-7), 51.3 (C-8), 20.8 (C-9), 56.2 (4-OCH<sub>3</sub>), 109.0 (C-1'), 151.5 (C-2'), 120.3 (C-3'), 144.2 (C-4'), 137.9 (C-5'), 135.8 (C-6'), 161.4 (C-7'), 9.5 (C-8'), 95.4 (C-9').

#### 8'-O-methylmenegazziaic acid (24)

White powder. Mp : 231 – 232 °C.

$^1\text{H}$ -NMR (CDCl<sub>3</sub>, 500 MHz),  $\delta$  : 2.26 (3H, *s*, 8'-Me), 2.44 (3H, *s*, 8-Me), 3.76 (3H, *s*, 8'-OMe), 3.91 (3H, *s*, 4-OMe), 6.40 (1H, *s*, 3-OH), 6.51 (1H, *s*, H-8'), 6.61 (1H, *s*, H-5), and 7.67 (1H, *s*, 2'-OH)

$^{13}\text{C}$  NMR (CDCl<sub>3</sub>, 125 MHz)  $\delta$  114.2 (C-1), 147.2 (C-2), 113.5 (C-3), 151.7 (C-4), 111.4 (C-5), 134.5 (C-6), 160.8 (C-7), 20.7 (C-8), 56.4 (4-OMe), 107.2 (C-1'), 152.1 (C-2'), 121.2 (C-

3'), 149.6 (C-4'), 163.7 (C-5'), 138.7 (C-6'), 168.7 (C-7'), 9.1 (C-9'), 102.0 (C-8') and 57.4 (8'-OMe).

#### Protocetraric acid (25)

White powder. Mp : 245 – 250 °C.

$^1\text{H-NMR}$  ( $\text{CDCl}_3$ , 500 MHz),  $\delta$  : 10.59 (1H, s, 4-CHO), 6.83 (1H, s, H-5), 4.60 (2H, s, H-9'), 2.43 (3H, s, 6- $\text{CH}_3$ ), 2.40 (3H, s, 6'- $\text{CH}_3$ ).

$^{13}\text{C NMR}$  ( $\text{CDCl}_3$ , 125 MHz)  $\delta$  112.4 (C-1), 161.2 (C-2), 111.8 (C-3), 163.8 (C-4), 117.0 (C-5), 152.0 (C-6), 164.0 (C-7), 21.3 (C-8), 191.7 (C-9), 116.6 (C-1'), 155.0 (C-2'), 118.6 (C-3'), 144.5 (C-4'), 141.7 (C-5'), 131.4 (C-6'), 170.1 (C-7'), 14.3 (C-8'), 52.9 (C-9').

#### 8'-O-methylprotocetraric acid (26)

White powder. Mp : 286 – 287 °C.

$^1\text{H-NMR}$  ( $\text{CDCl}_3$ , 500 MHz),  $\delta$  : 10.54 (s, 1H, CHO), 6.78 (s, 1H, H-5), 4.43 (s, 1H, H-8'), 3.19 (s, 3H,  $\text{OCH}_3$ ), 2.45 (s, 3H, H-9), 2.34 (s, 3H, H-9').

$^{13}\text{C NMR}$  ( $\text{CDCl}_3$ , 125 MHz)  $\delta$  191.8 (C-8), 170.4 (C-7'), 163.8 (C-4), 164.4 (C-2), 161.3 (C-7), 158.2 (C-2'), 151.8 (C-6), 145.1 (C-4'), 131.2 (C-6'), 141.2 (C-5'), 115.1 (C-3'), 112.3 (C-3), 111.8 (C-1), 119.6 (C-5), 111.5 (C-1'), 14.4 (C-9'), 57.3 (C-10'), 21.3 (C-9), 62.4 (C-8').

#### Lobarientalone B (27)

White amorphous powder;  $[\alpha]_{\text{D}}^{25} = -83$  ( $c = 0.002$ , MeOH). HR-ESI-MS  $m/z$  371.0772 [ $\text{M} + \text{H}]^+$  (calcd. for  $\text{C}_{19}\text{H}_{14}\text{O}_8$ , 371.0767).

$^1\text{H-NMR}$  ( $\text{DMSO-}d_6$ , 500 MHz),  $\delta$  : 10.04 (s, 1H, 4-OH), 6.95 (s, 1H, H-1), 6.95 (s, 1H, H-9), 4.80 (d,  $J = 9.0$ , 1H, H-13a), 4.61 (d,  $J = 9.0$ , 1H, H-13b), 3.87 (s, 3H, 10- $\text{OCH}_3$ ), 2.45 (s, 3H,  $\text{CH}_3$ -8), 2.18 (s, 3H, 5- $\text{CH}_3$ ).

$^{13}\text{C NMR}$  ( $\text{DMSO-}d_6$ , 125 MHz)  $\delta$  166.6 (C-3), 161.6 (C-10), 163.0 (C-4), 159.0 (C-11a), 151.6 (C-4), 148.8 (C-5a), 144.3 (C-8), 138.0 (C-1a), 135.9 (C-12a), 132.2 (C-12a), 120.4 (C-5), 118.5 (C-11), 115.1 (C-11), 112.7 (C-7a), 112.7 (C-5), 111.6 (C-9), 109.0 (C-3a), 95.4 (C-1), 56.3 (C-11), 51.4 (C-13), 20.9 (8- $\text{CH}_3$ ), 9.5 (5- $\text{CH}_3$ ).

#### (+) (12R) - Usnic acid (28)

Yellow prisms (chloroform). Mp 204 °C.  $[\alpha]^{25} -0.4922$  ( $c$  10.5,  $\text{CHCl}_3$  : MeOH (1:1)).

$^1\text{H-NMR}$  ( $\text{CDCl}_3$ , 500 MHz),  $\delta$  : 13.30 (s, 1H, 8-OH), 11.02(s, 1H, 10-OH), 5.97 (s, 1H, H-4), 2.68 (s, 3H, H-18), 2.66 (s, 3H, H-15), 2.11 (s, 3H, H-16), 1.76 (s, 3H, H-13)

$^{13}\text{C NMR}$  ( $\text{CDCl}_3$ , 125 MHz)  $\delta$  : 201.9 (C-17), 200.4 (C-14), 198.2 (C-1), 191.9 (C-3), 179.5 (C-5), 164.1 (C-8), 157.7 (C-10), 155.4 (C-6), 109.5 (C-9), 105.4 (C-2), 104.1 (C-11), 101.7 (C-7), 98.5 (C-4), 59.3 (C-12), 32.3 (C-18), 31.4 (C-13), 28.0 (C-15), 7.7 (C-16).

### Lupeol (29)

White powder. Mp: 213–215 °C.

$^1\text{H-NMR}$  ( $\text{CDCl}_3$ , 500 MHz),  $\delta$  : 4.56-4.68 (d,  $J$ = 2.5, 2H, H-29), 3.18 (dd,  $J$ = 11.0; 5.0, 1H, H-3), 2.37 (dd,  $J$ = 11.0; 5.5, 1H, H-19), 1.68 (s, 3H, H-30), 1.03 (s, 3H, H-26), 0.96 (s, 3H, H-23), 0.94 (s, 3H, H-27), 0.83 (s, 3H, H-25), 0.79 (s, 3H, H-28), 0.76 (s, 3H, H-24).

$^{13}\text{C NMR}$  ( $\text{CDCl}_3$ , 125 MHz)  $\delta$  : 38.3 (C-1), 25.4 (C-2), 79.2 (C-3), 39.0 (C-4), 55.6 (C-5), 18.5 (C-6), 34.5 (C-7), 41.1 (C-8), 50.7 (C-9), 37.4 (C-10), 21.2 (C-11), 27.6 (C-12), 39.1 (C-13), 43.1 (C-14), 27.7 (C-15), 35.8 (C-16), 43.2 (C-17), 48.6 (C-18), 48.2 (C-19), 151.1 (C-20), 30.1 (C-21), 40.2 (C-22), 28.2 (C-23), 15.5 (C-24), 16.3 (C-25), 16.2 (C-26), 14.8 (C-27), 18.2 (C-28), 109.5 (C-29), 19.5 (C-30).

### Zeorin (31)

White powder, mp 238 °C.

$^1\text{H-NMR}$  ( $\text{CDCl}_3$ , 500 MHz),  $\delta$  : 3.88 (d,  $J$ = 6.5, 1H, 6-OH), 3.81 (s, 1H, 22-OH), 3.74 (m, 1H, H-6), 2.10 (dd,  $J$ = 20.0; 9.0, 1H, H-21), 1.93 (d,  $J$ = 13, 1H, H-7a), 1.37 (d,  $J$ = 3.6, 1H, H-7b), 1.12 (s, 1H, H-23), 0.94 (s, 1H, H-24), 0.81 (s, 3H, H-25), 0.98 (s, 3H, H-26), 0.92 (s, 3H, H-27), 0.71 (s, 3H, H-28), 1.03 (s, 3H, H-29), 1.07 (s, 3H, H-30).

$^{13}\text{C NMR}$  ( $\text{CDCl}_3$ , 125 MHz)  $\delta$  : 40.0 (C-1), 18.0 (C-2), 43.5 (C-3), 33.3 (C-4), 59.9 (C-5), 66.5 (C-6), 44.7 (C-7), 42.1 (C-8), 49.3 (C-9), 38.5 (C-10), 21.3 (C-11), 23.6 (C-12), 48.9 (C-13), 41.4 (C-14), 33.9 (C-15), 20.6 (C-16), 53.8 (C-17), 43.5 (C-18), 40.9 (C-19), 26.0 (C-20), 50.3 (C-21), 71.5 (C-22), 36.6 (C-23), 21.9 (C-24), 16.8 (C-25), 18.0 (C-26), 16.9 (C-27), 15.8 (C-28), 28.9 (C-29), 30.7 (C-30).

### Cerevisterol (32)

White amorphous powder, mp 258 °C.

$^1\text{H-NMR}$  ( $\text{CDCl}_3$ , 500 MHz),  $\delta$  : 5.24 (*dd*,  $J = 15.0, 7.0$ , 1H, H-23), 5.17 (*dd*,  $J = 15.0, 8.0$ , 1H, H-22), 5.08 (*dd*,  $J = 5.5, 3.0$ , 1H, H-7), 4.49 (*d*,  $J = 5.5$ , 1H, 6-OH), 4.22 (*d*,  $J = 5.5$ , 1H, 3-OH), 3.76 (*ddd*, 1H,  $J = 11.0, 5.5$ , H-3), 3.58 (*s*, 1H, 5-OH), 3.37 (*s*, 1H, H-6), 0.99 (*d*,  $J = 6.5$ , 3H, H-21), 0.91 (*s*, 3H, H-19), 0.89 (*d*,  $J = 7.0$ , 3H, H-28), 0.81 (*d*,  $J = 6.5$ , 3H, H-26), 0.80 (*d*,  $J = 6.5$ , 3H, H-27).

$^{13}\text{C NMR}$  ( $\text{CDCl}_3$ , 125 MHz)  $\delta$  : 32.4 (C-1), 31.2 (C-2), 65.9 (C-3), 40.2 (C-4), 74.2 (C-5), 72.1 (C-6), 119.4 (C-7), 139.6 (C-8), 42.2 (C-9), 36.6 (C-10), 21.3 (C-11), 38.9 (C-12), 43.0 (C-13), 54.1 (C-14), 22.6 (C-15), 27.7 (C-16), 55.3 (C-17), 12.0 (C-18), 17.7 (C-19), 39.9 (C-20), 20.9 (C-21), 135.4 (C-22), 131.4 (C-23), 42.0 (C-24), 32.4 (C-25), 19.4 (C-26), 19.7 (C-27), 17.2 (C-28).

**Eumitrin B (33)** light yellow needles;  $[\alpha]_D^{25} = -40$  (c 0.1,  $\text{CHCl}_3$ ); mp 234 °C; UV (MeOH)  $\lambda_{\text{max}}$  (log  $\epsilon$ ) 251(3.79), 272 (4.11), 293 (3.62) and 335 (4.21) nm; IR (KBr)  $\nu_{\text{max}}$ : 3523, 1755, 1614, 1582, 1563  $\text{cm}^{-1}$ ; HRESIMS  $m/z$  689.1901 [ $\text{M} + \text{Na}$ ] $^+$  (calcd for  $\text{C}_{34}\text{H}_{34}\text{O}_{14}\text{Na}$ , 689.1847).

**Eumitrin A2 (34)** light yellow needles;  $[\alpha]_D^{25} = -82$  (c 0.1,  $\text{CHCl}_3$ ); mp 214 °C; UV (MeOH)  $\lambda_{\text{max}}$  (log  $\epsilon$ ) 261(4.09), 281 (4.10), 299 (4.12) and 339 (4.41) nm; IR (KBr)  $\nu_{\text{max}}$ : 3481, 1754, 1611, 1580, 1440  $\text{cm}^{-1}$ ; HRESIMS  $m/z$  667.2022 [ $\text{M} + \text{H}$ ] $^+$  (calcd for  $\text{C}_{34}\text{H}_{34}\text{O}_{14}\text{H}$ , 667.2027).

**Eumitrin A1 (35)** light yellow needles;  $[\alpha]_D^{25} = -61$  (c 0.1,  $\text{CHCl}_3$ ); mp 241-245 °C; UV (MeOH)  $\lambda_{\text{max}}$  (log  $\epsilon$ ) 271(3.9), 280 (4.2), 287 (4.12) and 340 (5.1) nm; IR (KBr)  $\nu_{\text{max}}$ : 3478, 1755, 1616, 1584, 1441  $\text{cm}^{-1}$ ; HRESIMS  $m/z$  681.1809 [ $\text{M} + \text{H}$ ] $^+$  (calcd for  $\text{C}_{34}\text{H}_{32}\text{O}_{15}\text{H}$ , 681.1819).

**Usneaxanthone D (36)**. light yellow crystals;  $[\alpha]_D^{25} = -209$  (c 0.002, MeOH); mp 192 °C; UV (MeOH)  $\lambda_{\text{max}}$  (log  $\epsilon$ ) 220 (2.1), 270 (1.0), 310 (0.7) nm; ECD ( $\Delta\epsilon$ ) ( $3 \times 10^{-4}$  M, MeOH) 345 (−0.75), 311 (+3.67), 287 (−1.56), 270 (+3.19), 236 (−26.3), 211 (+29.7); IR (KBr)  $\nu_{\text{max}}$ : 3727, 3631, 1742, 1700, 1606, 1298  $\text{cm}^{-1}$ ; HRESIMS  $m/z$  687.1733 [ $\text{M} + \text{Na}$ ] $^+$  (calcd for  $\text{C}_{34}\text{H}_{32}\text{O}_{14}\text{Na}$ , 687.1690).

**Usneaxanthone A (38).** light yellow crystals;  $[\alpha]_D^{25} = -232$  (c 0.002, MeOH); mp 175 °C; UV (MeOH)  $\lambda_{\max}$  (log  $\epsilon$ ) 238 (2.8), 270 (1.3), 315 (0.8) nm; ECD ( $\Delta\epsilon$ ) ( $3 \times 10^{-4}$  M, MeOH, MeOH) 319 (+5.94), 293 (+0.50), 274 (+8.00), 234 (−21.37), 213 (+15.36); IR (KBr)  $\nu_{\max}$ : 3419, 3377, 1733, 1613, 1309  $\text{cm}^{-1}$ ; HRESIMS  $m/z$  653.1862  $[M + H]^+$  (calcd for  $\text{C}_{33}\text{H}_{33}\text{O}_{14}$ , 653.1865) and  $m/z$  675.1681  $[M + \text{Na}]^+$ , calcd 675.1645).

**Usneaxanthone B (39).** light yellow crystals;  $[\alpha]_D^{25} = +286$  (c 0.002, MeOH); mp 176 °C; UV (MeOH)  $\lambda_{\max}$  (log  $\epsilon$ ) 218 (4.2), 235 (4.0), 270 (2.5), 309 (2.4) nm; ECD ( $\Delta\epsilon$ ) ( $3 \times 10^{-4}$  M, MeOH, MeOH) 313 (+2.08), 288 (+14.63), 244 (+6.41), 257 (+4.60), 218 (−39.59); IR (KBr)  $\nu_{\max}$ : 3424, 1733, 1607, 1299  $\text{cm}^{-1}$ ; HRESIMS  $m/z$  675.1711  $[M + \text{Na}]^+$  (calcd for  $\text{C}_{33}\text{H}_{32}\text{O}_{14}\text{Na}$ , 675.1690).

**Usneaxanthone C (40).** colorless needles;  $[\alpha]_D^{25} = -238$  (c 0.002, MeOH); mp 180 °C; UV (MeOH)  $\lambda_{\max}$  (log  $\epsilon$ ) 220 (4.2) and 330 (1.2) nm; ECD ( $\Delta\epsilon$ ) ( $3 \times 10^{-4}$  M, MeOH) 317 (+6.00), 294 (+2.43), 276 (+14.18), 239 (−39.55), 215 (+26.61); IR (KBr)  $\nu_{\max}$ : 3418, 1725, 1606, 1294  $\text{cm}^{-1}$ ; HRESIMS  $m/z$  609.1607  $[M - H]^-$  (calcd for  $\text{C}_{31}\text{H}_{29}\text{O}_{13}$ , 609.1608).

**Usneaxanthone E (41).** Colorless crystal (EtOH);  $[\alpha]_D^{25} = -74$  (c 0.1,  $\text{CHCl}_3$ ); mp 196 °C; UV (MeOH)  $\lambda_{\max}$  (log  $\epsilon$ ) 224 (1.8), 255 (3.76), 333 (3.60) nm; ECD ( $\Delta\epsilon$ ) (0.005 mg/mL, MeOH) 307 (1.78), 270 (3.18), 234 (−6.72), 270 (8.63), 210 (7.52); IR (KBr)  $\nu_{\max}$ : 3537, 3439, 1740, 1611, 1090  $\text{cm}^{-1}$ ; HRESIMS  $m/z$  689.1894  $[M + \text{Na}]^+$  (calcd for  $\text{C}_{34}\text{H}_{34}\text{O}_{14}\text{Na}$ , 689.1846).

**Usneaxanthone F (42).** light yellow needles;  $[\alpha]_D^{25} = +81$  (c 0.05,  $\text{CHCl}_3$ ); mp 197 °C; UV (MeOH)  $\lambda_{\max}$  (log  $\epsilon$ ) 228 (2.2), 275 (2.52) and 344 (2.1) nm; ECD ( $\Delta\epsilon$ ) (0.01 mg/mL, MeOH) 312 (0.52), 286 (3.66), 241 (1.42), 218 (−9.90); IR (KBr)  $\nu_{\max}$ : 3430, 1744, 1613, 1136  $\text{cm}^{-1}$ ; HRESIMS  $m/z$  689.1854  $[M + \text{Na}]^+$  (calcd for  $\text{C}_{34}\text{H}_{32}\text{O}_{14}\text{Na}$ , 689.1846).

**Usneaxanthone G (43).** colorless needles;  $[\alpha]_D^{25} = -238$  (c 0.1,  $\text{CHCl}_3$ ); mp 207 °C; UV (MeOH)  $\lambda_{\max}$  (log  $\epsilon$ ) 220 (4.2) and 330 (1.2) nm; ECD ( $\Delta\epsilon$ ) ( $3 \times 10^{-4}$  M, MeOH) 317 (+6.00), 294 (+2.43), 276 (+14.18), 239 (−39.55), 215 (+26.61); IR (KBr)  $\nu_{\max}$ : 3448, 2945,

1796, 1744, 1357, 1214  $\text{cm}^{-1}$ ; HRESIMS  $m/z$  609.1607  $[\text{M}-\text{H}]^-$  (calcd for  $\text{C}_{31}\text{H}_{29}\text{O}_{13}$ , 609.1608).

**Usneaxanthone H (44).** light yellow needles;  $[\alpha]_D^{25} = -128$  (c 0.1,  $\text{CHCl}_3$ ); mp 202  $^\circ\text{C}$ ; UV (MeOH)  $\lambda_{\text{max}}$  (log  $\epsilon$ ) 230 (3.9), 275 (2.2) and 340 (1.1) nm; ECD ( $\Delta\epsilon$ ) (0.3 mg/mL, MeOH) 343 (-8.15), 315 (-9.40), 303 (-10.54), 293 (-9.71), 272 (-10.07), 251 (+7.40), 231 (+5.24), 208 (+11.95); IR (KBr)  $\nu_{\text{max}}$ : 3418, 1725, 1606, 1294  $\text{cm}^{-1}$ ; HRESIMS  $m/z$  687.1712  $[\text{M} + \text{Na}]^+$  (calcd for  $\text{C}_{34}\text{H}_{32}\text{O}_{14}\text{Na}$ , 687.1690).

**Bailexanthone (45).** yellow crystals;  $[\alpha]_D^{25} +137.7$  (c 0.7,  $\text{CHCl}_3$ ). mp 186  $^\circ\text{C}$ . ECD (0.3,  $\text{CHCl}_3$ ) ( $\Delta\epsilon$ ) 208 (+ 24.0), 214 (-9.2), 224 (+10.8), 265 (-17.5), 275 (- 15.5) 311 (+36.0).. HR-ESI-MS  $m/z$  ( $[\text{M}+\text{Na}]^+$   $m/z$  633.1909, calcd 633.1948).

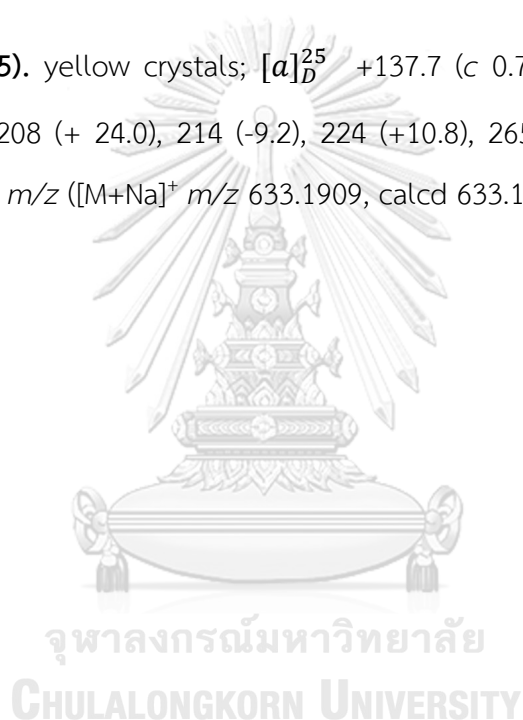


Table A1. Crystal data and refinement parameters of compounds 33, 35–36 and 38–41.

	35	33	41	36	38	39	40
Crystal habit	Block, light yellow	Block, light yellow	Rod, colorless	Rod, light yellow	Rod, light yellow	Rod, light yellow	Rod, colorless
Crystal size [mm <sup>3</sup> ]	0.26×0.42×0.50	0.42×0.46×0.50	0.20×0.24×0.50	0.14×0.24×0.40	0.14×0.28×0.48	0.18×0.20×0.38	0.12×0.18×0.32
Empirical formula	C <sub>34</sub> H <sub>32</sub> O <sub>15</sub>	C <sub>34</sub> H <sub>34</sub> O <sub>14</sub>	C <sub>34</sub> H <sub>34</sub> O <sub>14</sub>	C <sub>34</sub> H <sub>32</sub> O <sub>14</sub>	C <sub>33</sub> H <sub>32</sub> O <sub>14</sub>	C <sub>33</sub> H <sub>32</sub> O <sub>14</sub>	C <sub>31</sub> H <sub>30</sub> O <sub>13</sub> ·H <sub>2</sub> O
FW	680.59	666.61	666.61	664.6	698.65	698.65	626.55
Crystal system	orthorhombic	orthorhombic	triclinic	orthorhombic	orthorhombic	monoclinic	monoclinic
Space group	P2 <sub>1</sub> -2 <sub>1</sub> -2 <sub>1</sub> (No. 19)	P2 <sub>1</sub> -2 <sub>1</sub> -2 <sub>1</sub> (No. 19)	P1 (No. 1)	P2 <sub>1</sub> -2 <sub>1</sub> -2 <sub>1</sub> (No. 19)	P2 <sub>1</sub> -2 <sub>1</sub> -2 <sub>1</sub> (No. 19)	P2 <sub>1</sub> (No. 4)	P2 <sub>1</sub> (No. 4)
a [Å]	9.4990(3)	9.8414(2)	7.7008(2)	9.5006(2)	8.6564(3)	7.6108(3)	10.9713(3)
b [Å]	17.7716(6)	17.3019(4)	10.4440(2)	17.7560(4)	15.1470(4)	15.8753(6)	7.6377(2)
c [Å]	19.4591(6)	19.5740(4)	11.4532(3)	19.4714(5)	26.7938(7)	14.4697(6)	18.2195(4)
α [°]	90	90	114.437(1)	90	90	90	90
β [°]	90	90	90.076(1)	90	90	101.912(1)	91.876(1)
γ [°]	90	90	97.052(1)	90	90	90	90
V [Å <sup>3</sup> ]	3284.94(18)	3332.96(12)	830.90(4)	3284.68(13)	3513.16(18)	1710.64(12)	1525.89(7)
Z	4	4	1	4	4	2	2
ρ <sub>calcd</sub> [Mg m <sup>-3</sup> ]	1.376	1.329	1.332	1.344	1.321	1.356	1.364

$\mu$ [mm <sup>-1</sup> ]	0.930	0.880	0.883	0.893	0.88	0.904	0.926
<i>F</i> (000)	1424	1400	350	1392	1472	736	656
Diffractometer	PROSPECTOR Kappa CCD (Bruker)						
Wavelength [Å]	CuK $\alpha$ , 1.54178	CuK $\alpha$ , 1.54178	CuK $\alpha$ , 1.54178	CuK $\alpha$ , 1.54178	CuK $\alpha$ , 1.54178	CuK $\alpha$ , 1.54178	CuK $\alpha$ , 1.54178
<i>T</i> [K]	296(2)	296(2)	296(2)	296(2)	296(2)	296(2)	296(2)
$2\sigma_{\text{max}}$	68.5	68.4	68.7	68.4	68.9	68.6	69.1
Resolution [Å]	0.83	0.83	0.83	0.83	0.83	0.83	0.83
Completeness [%],							
<i>R</i> <sub>int</sub>	99.1, 0.0402	99.7, 0.0430	98.1, 0.0484	99.3, 0.0489	99.1, 0.0919	99.4, 0.0502	97.7, 0.0320
Reflns							
collected / unique /	16231 / 5985 /	19019 / 6062 /	12420 / 5659 /	17491 / 5955 /	19250 / 6407 /	16022 / 6150 /	14080 / 5439 /
> $2\sigma(I)$	4506	4823	4046	3885	4420	4400	4083
Data / parameters	5985 / 452	6062 / 446	5659 / 441	5955 / 449	6407 / 460	6150 / 456	5439 / 418
Goodness on fit	1.052	1.117	1.170	1.093	0.995	1.180	1.255
<i>R</i> <sub>1</sub> , <i>wR</i> <sub>2</sub> [ <i>I</i> > $2\sigma(I)$ ]	0.0835, 0.2383	0.0547, 0.1555	0.0617, 0.1619	0.0719, 0.1882	0.0713, 0.1752	0.0717, 0.1909	0.0629, 0.1726
<i>R</i> <sub>1</sub> , <i>wR</i> <sub>2</sub> [all data]	0.0945, 0.2574	0.0634, 0.1641	0.0826, 0.1863	0.0978, 0.2154	0.0904, 0.1870	0.0922, 0.2176	0.0808, 0.2004
$\Delta\rho$ [e Å <sup>-3</sup> ]	-0.42, 0.50	-0.20, 0.21	-0.22, 0.33	-0.22, 0.38	-0.31, 0.32	-0.38, 0.39	-0.29, 0.33
Flack parameter ( <i>x</i> )	0.01(10)	-0.09(9)	-0.06(11)	0.03(8)	-0.10(17)	0.05(9)	0.07(7)
CCDC number	1854036	1854037	1854038	1854039	1854040	1854041	1854042



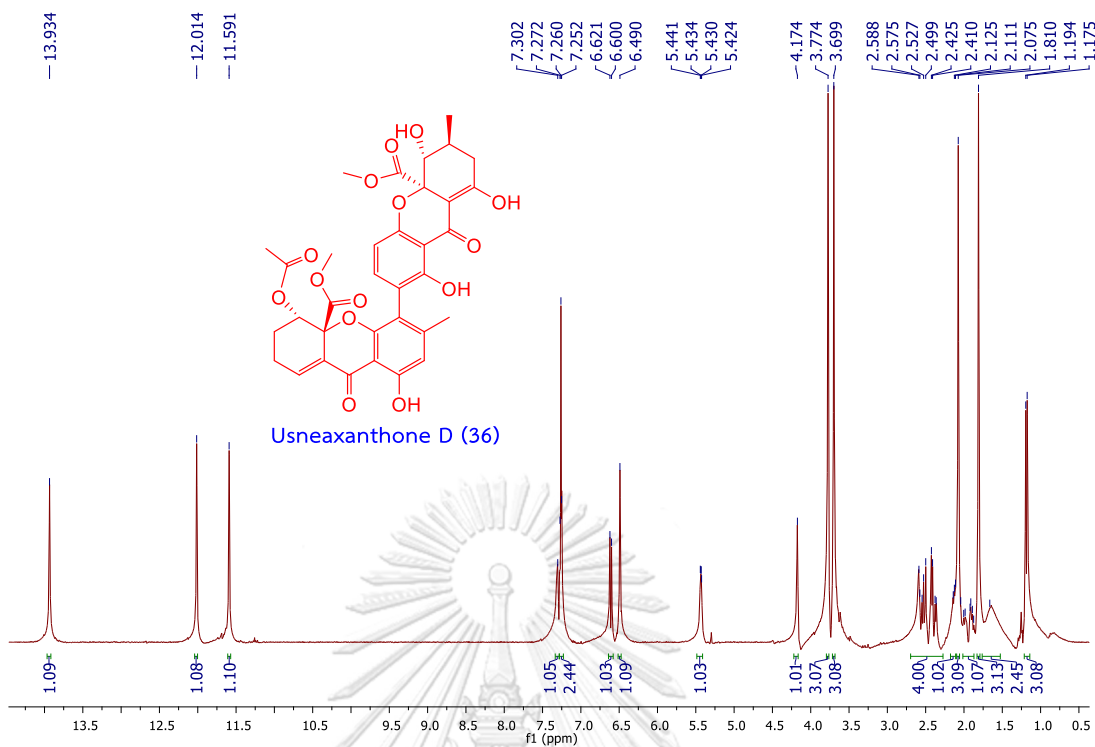


Figure A1.  $^1\text{H}$  NMR spectrum of usneaxanthone D (36) in  $\text{CDCl}_3$

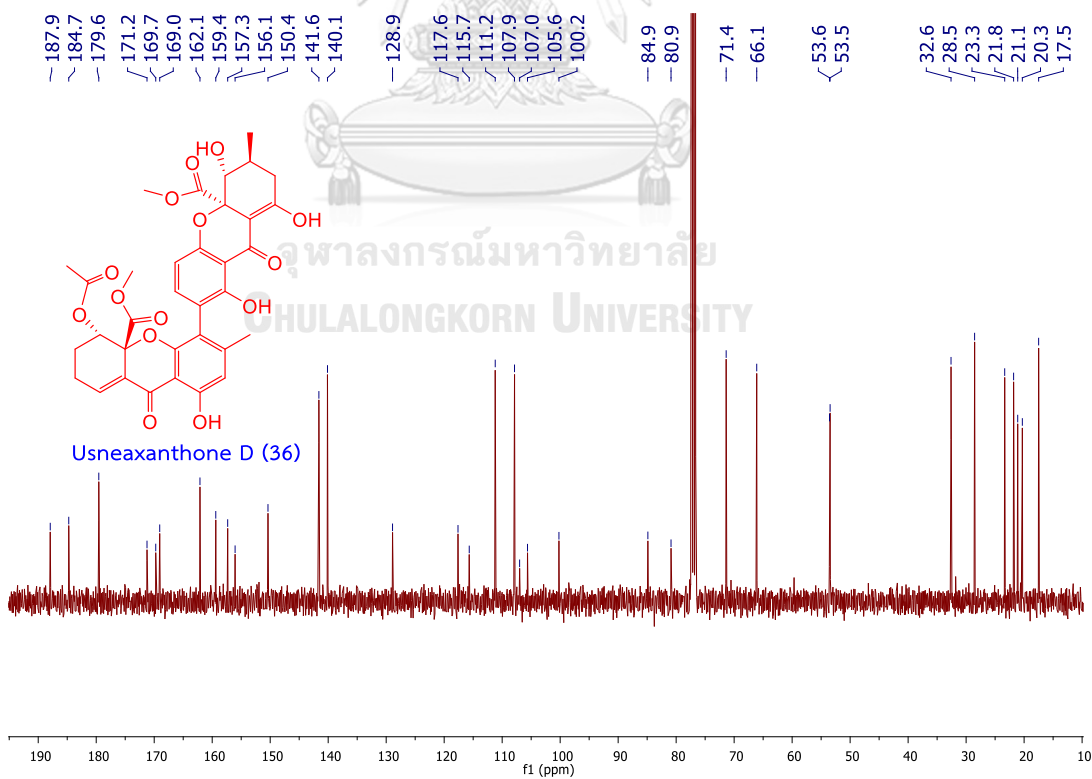
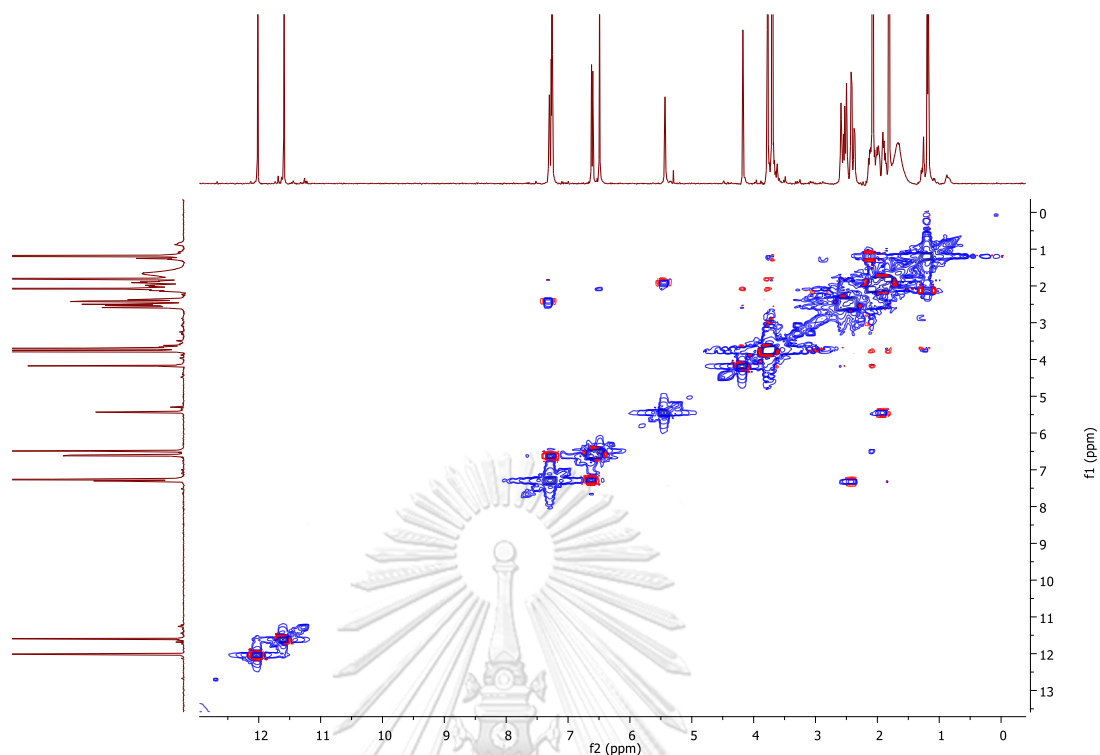
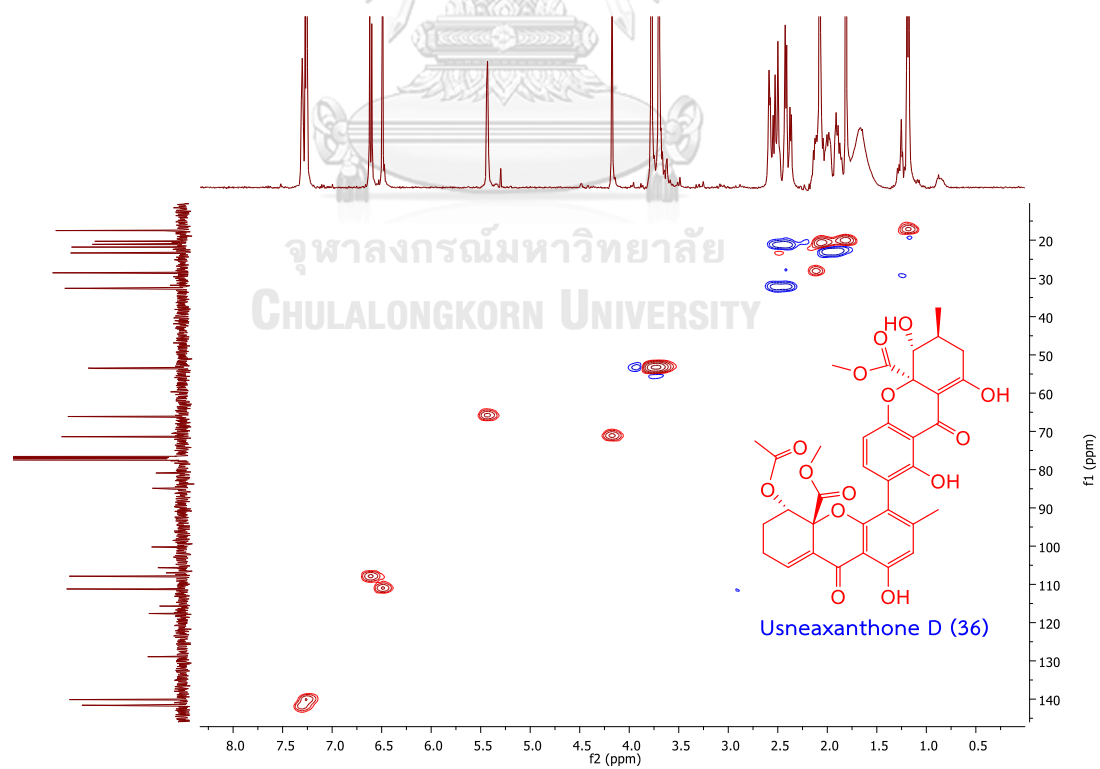


Figure A2.  $^{13}\text{C}$  NMR spectrum of usneaxanthone D (36) in  $\text{CDCl}_3$

Figure A3. COSY spectrum of usneaxanthone D (36) in  $\text{CDCl}_3$ Figure A4. HSQC spectrum of usneaxanthone D (36) in  $\text{CDCl}_3$

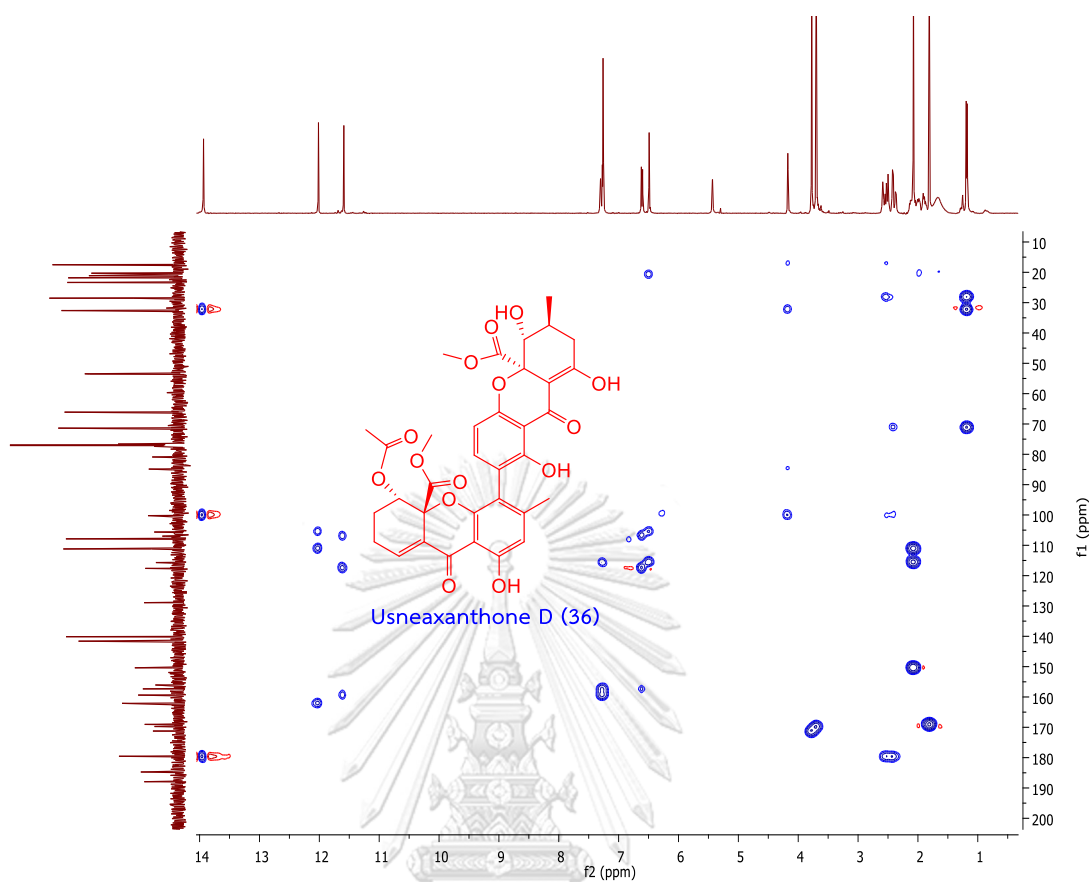


Figure A5. HMBC spectrum of usneaxanthone D (36) in  $\text{CDCl}_3$

## Generic Display Report

## Analysis Info

Analysis Name D:\Data\Data Service\171214\171214\_pos\_TT006.d  
Method NV\_pos\_0.3min\_profile\_1segment\_lowNbulizerDrygas.m  
Sample Name 171214\_pos\_TT006-2  
Comment

Acquisition Date 12/14/2017 12:26:46 PM

Operator CU.  
Instrument microTOF-Q II

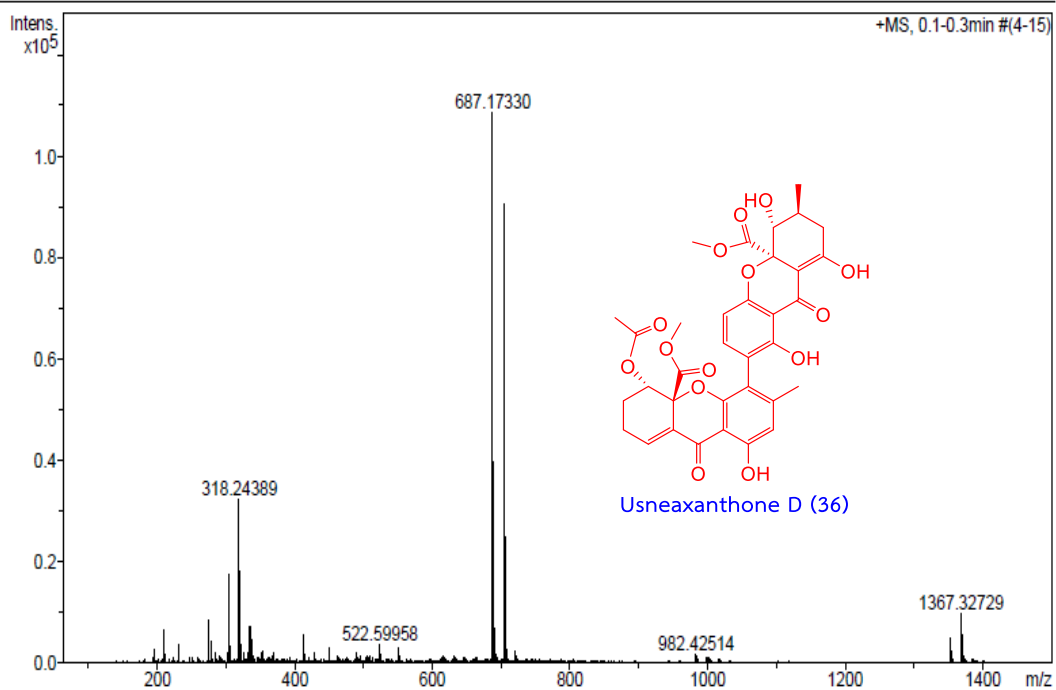


Figure A6. HRESIMS spectrum of usneaxanthone D (36)

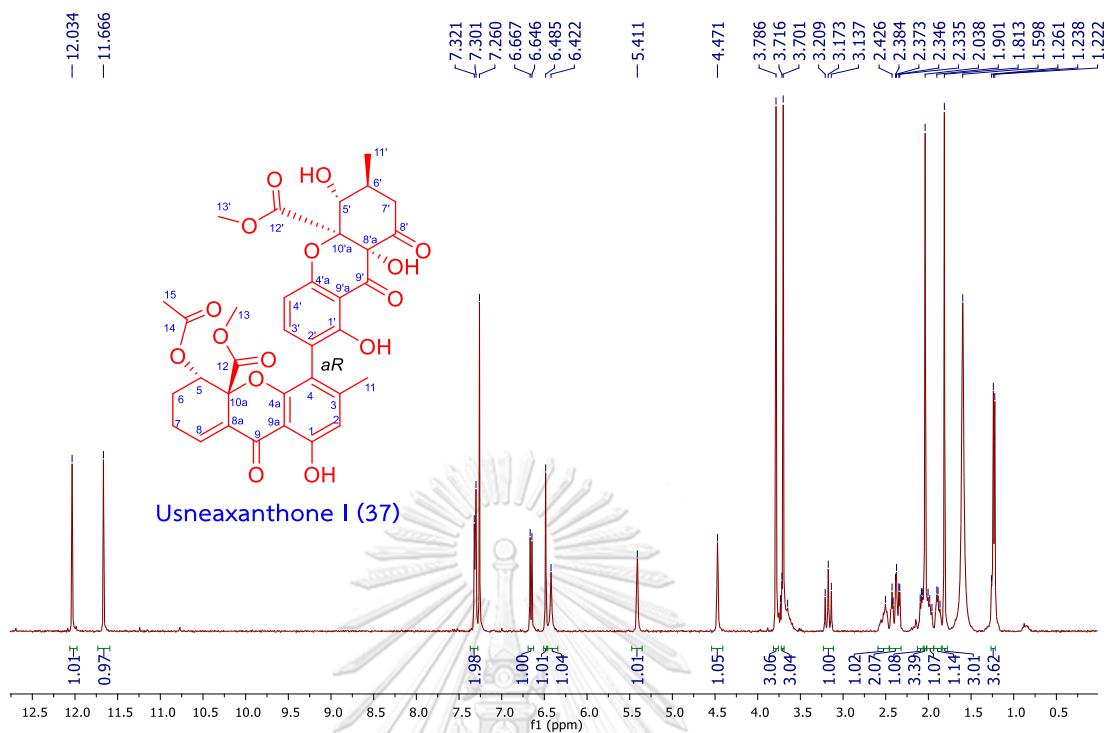


Figure A7.  $^1\text{H}$  NMR spectrum of usneaxanthone I (37) in  $\text{CDCl}_3$

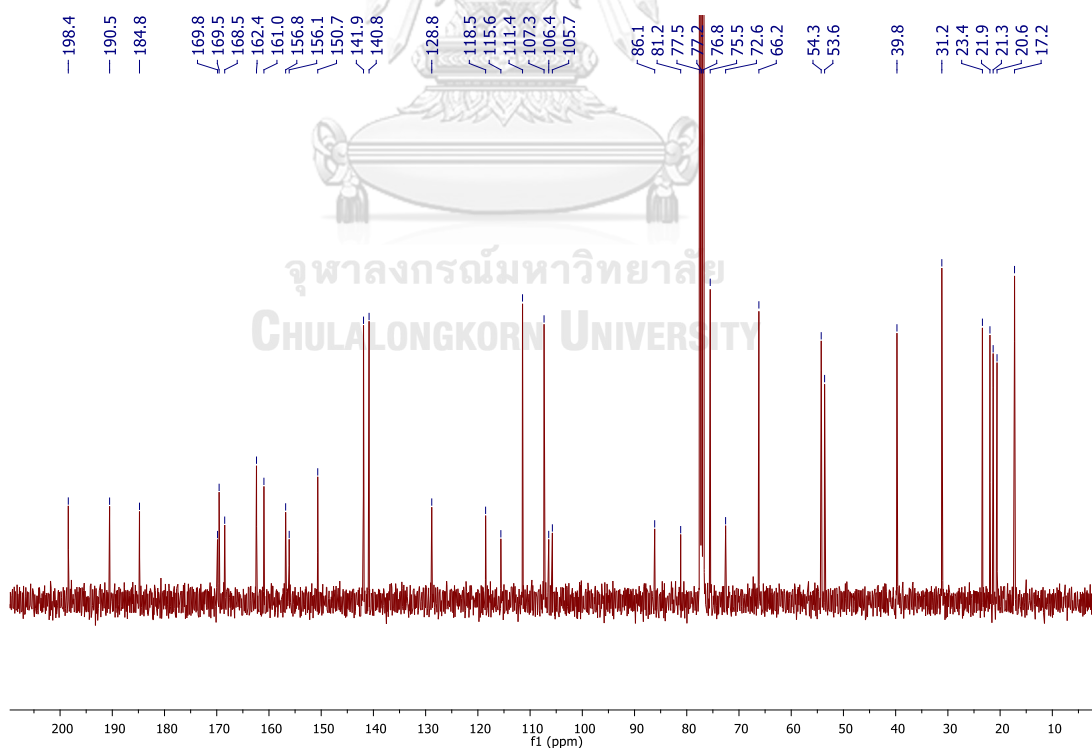


Figure A8.  $^{13}\text{C}$  NMR spectrum of usneaxanthone I (37) in  $\text{CDCl}_3$

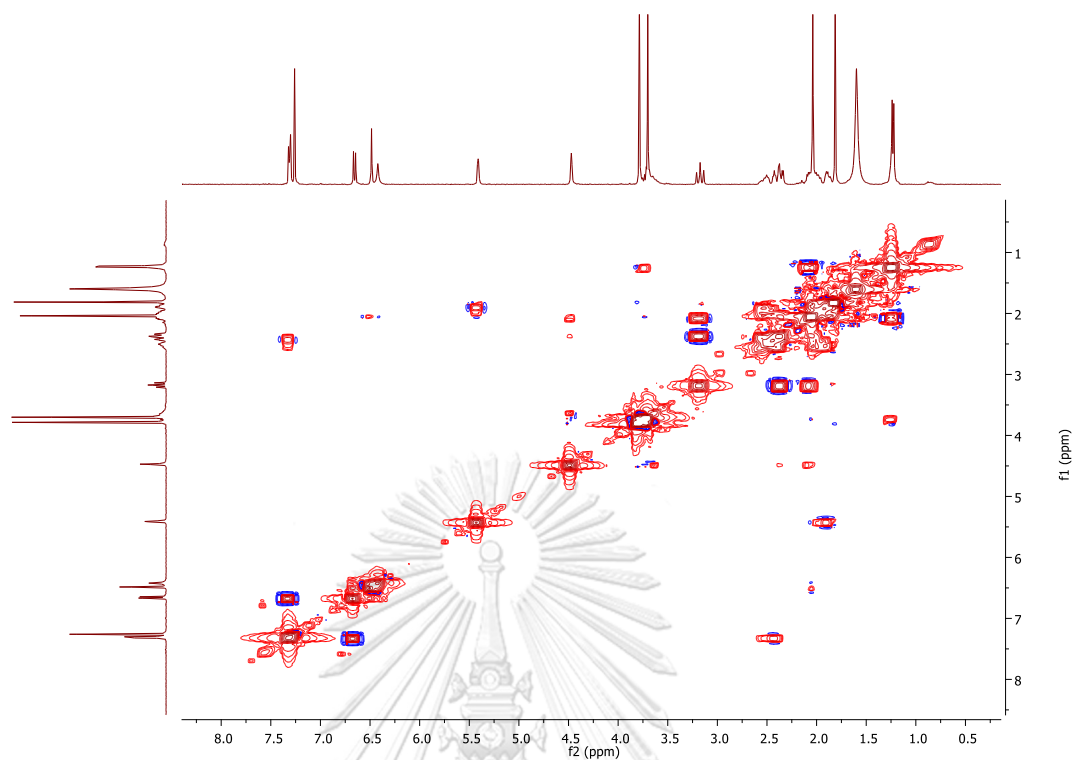


Figure A9. COSY spectrum of usneaxanthone I (37) in  $\text{CDCl}_3$

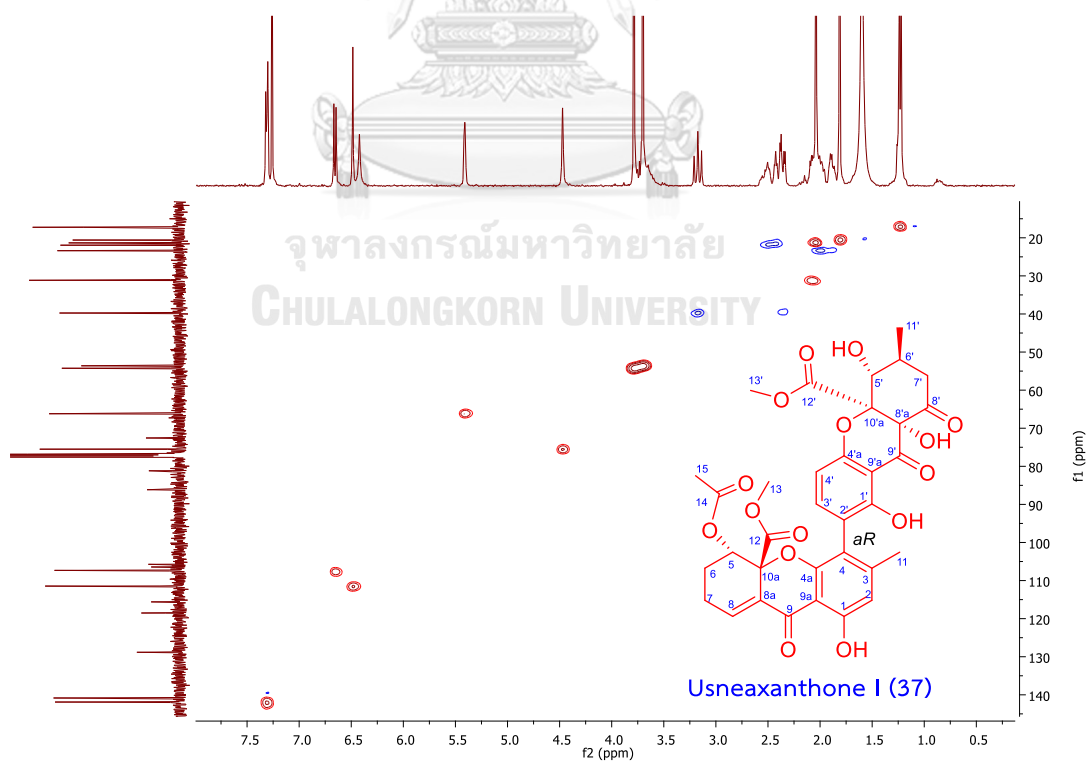


Figure A10. HSQC spectrum of usneaxanthone I (37) in  $\text{CDCl}_3$

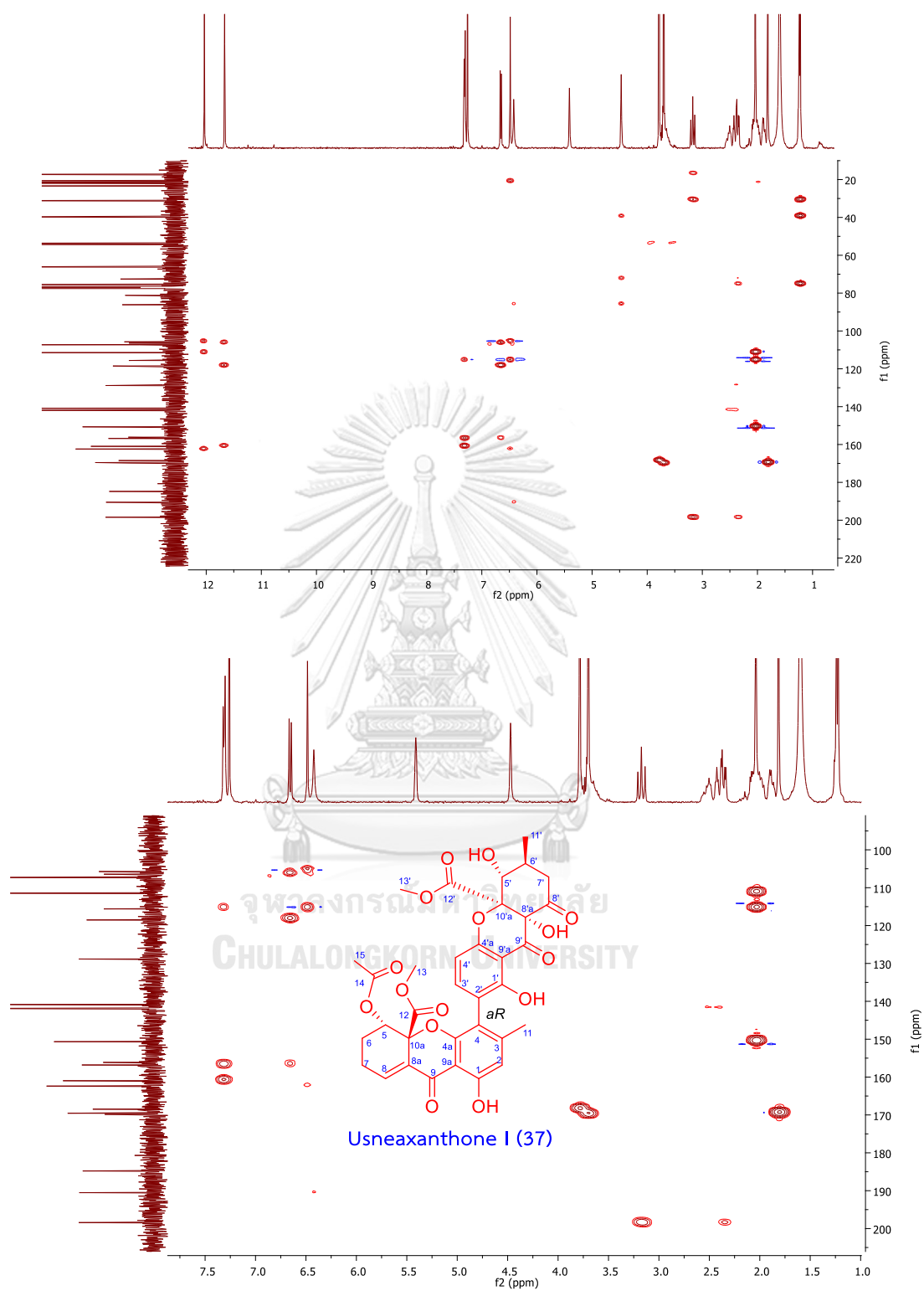


Figure 11 HMBC spectrum of usneaxanthone I (37) in CDCl<sub>3</sub>

## Generic Display Report

## Analysis Info

Analysis Name D:\Data\Data Service\190325\TT-034\_RD5\_01\_2385.d  
Method nv\_pos\_5min\_profile\_190214.m  
Sample Name TT-034  
Comment

Acquisition Date 3/25/2019 7:18:34 PM

Operator CU.  
Instrument microTOF-Q II

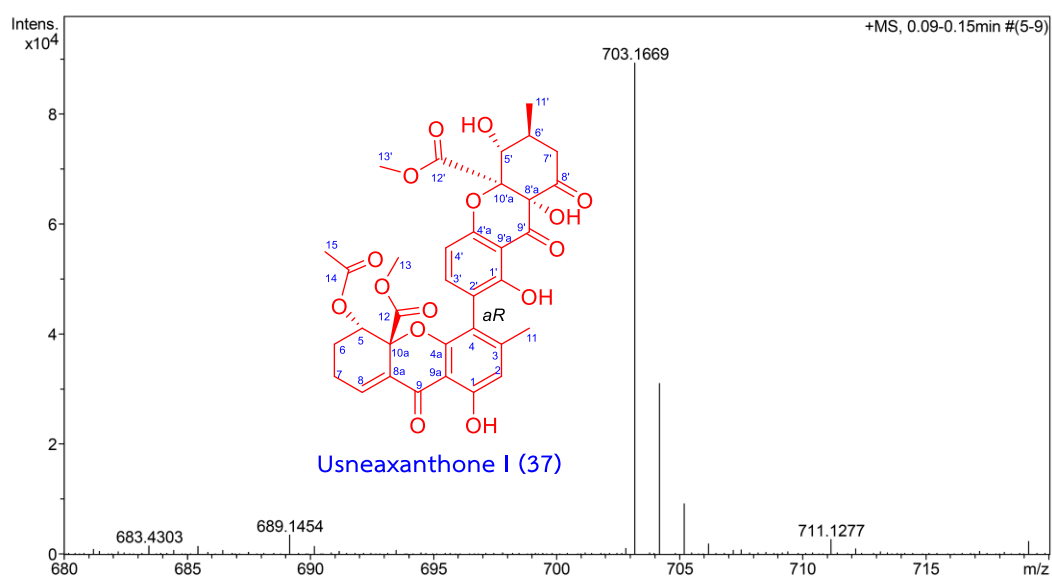
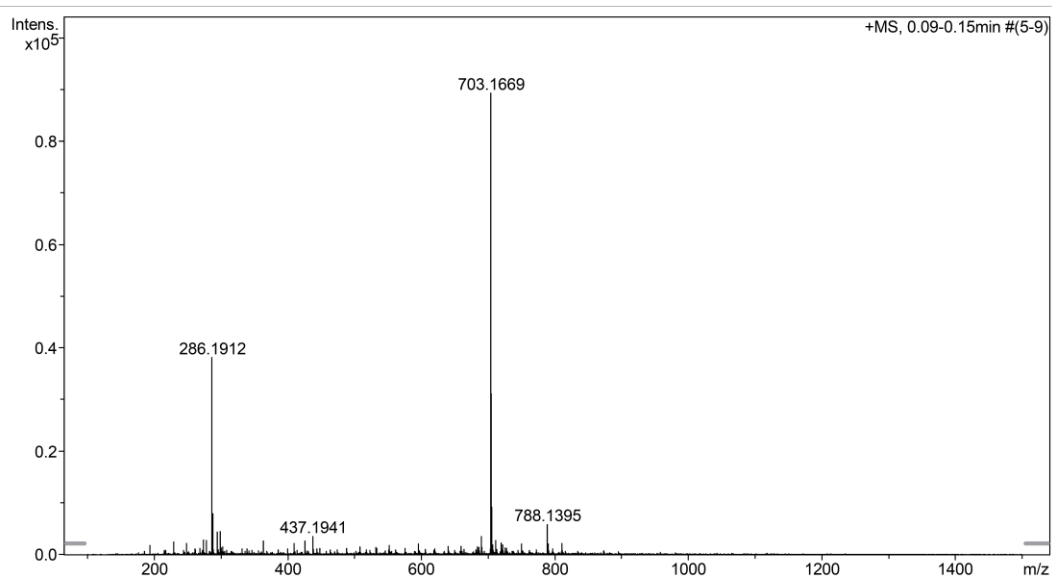


Figure A12. HRESIMS spectrum of usneaxanthone I (37)



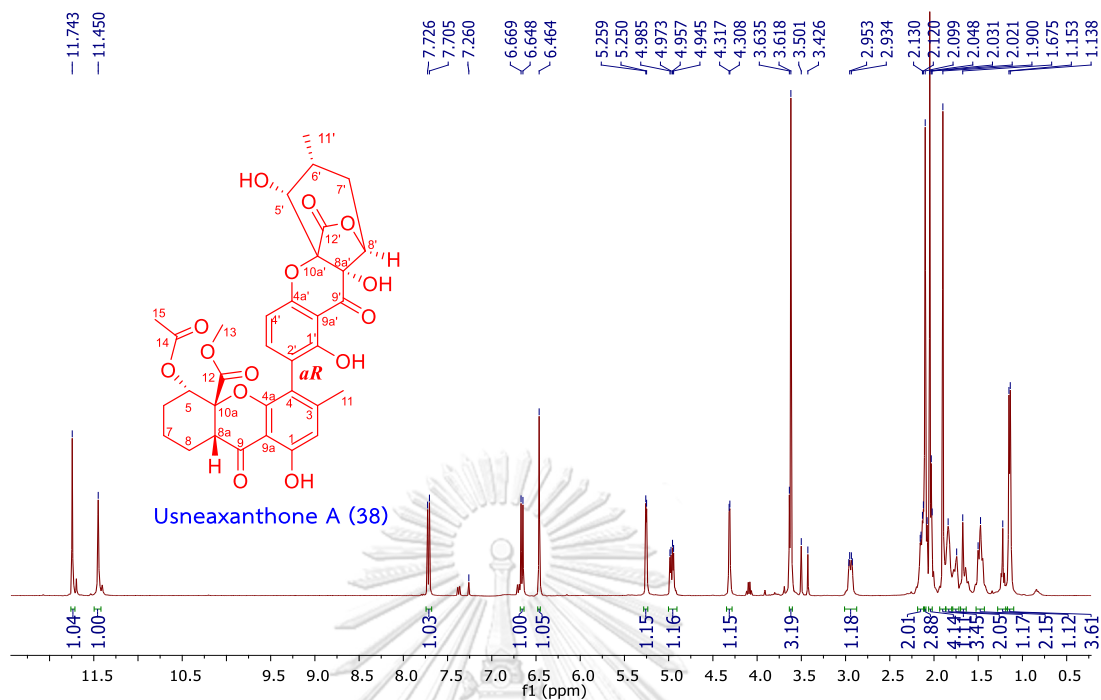


Figure A13.  $^1\text{H}$  NMR spectrum of usneaxanthone A (38) in  $\text{CDCl}_3$

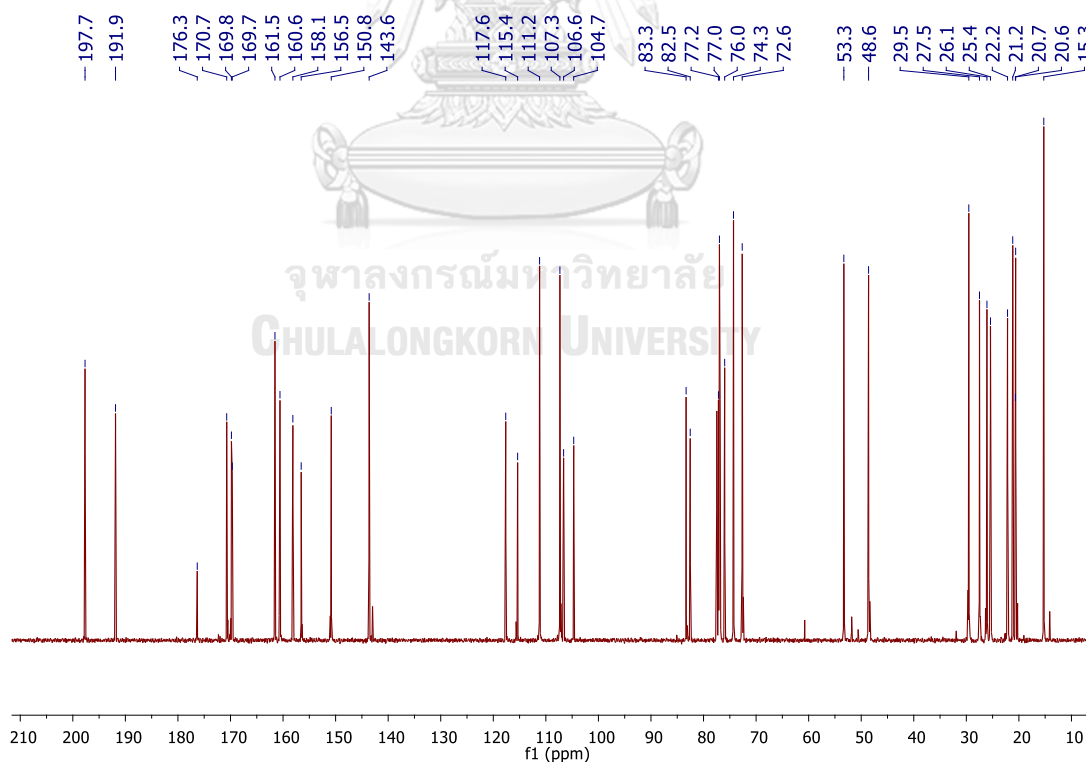
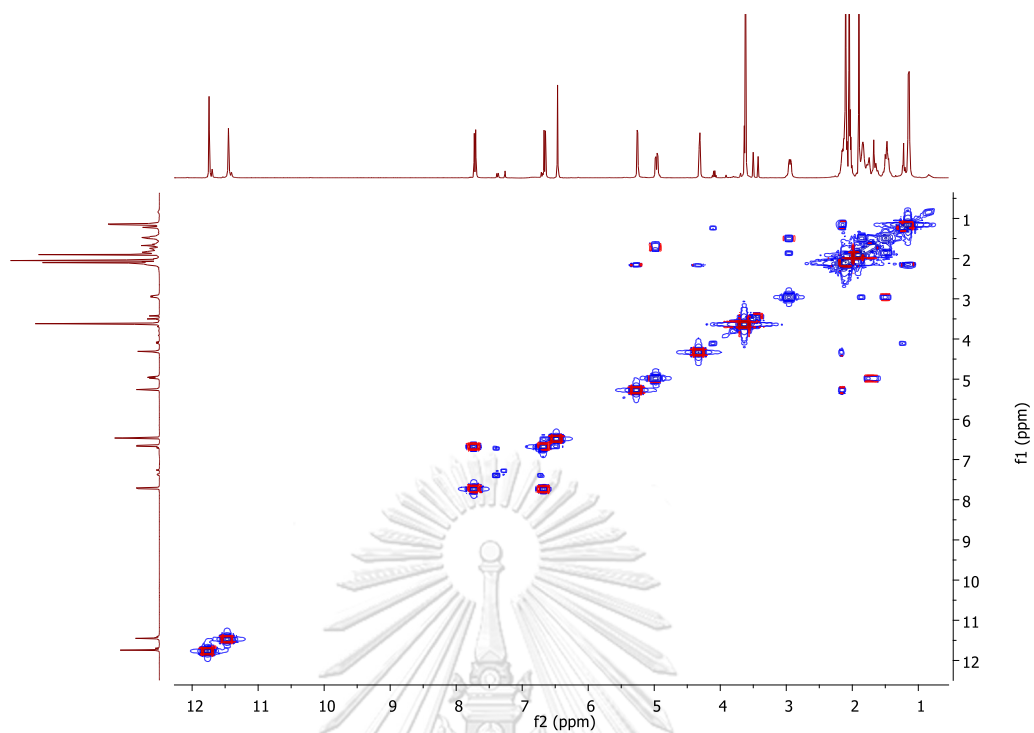
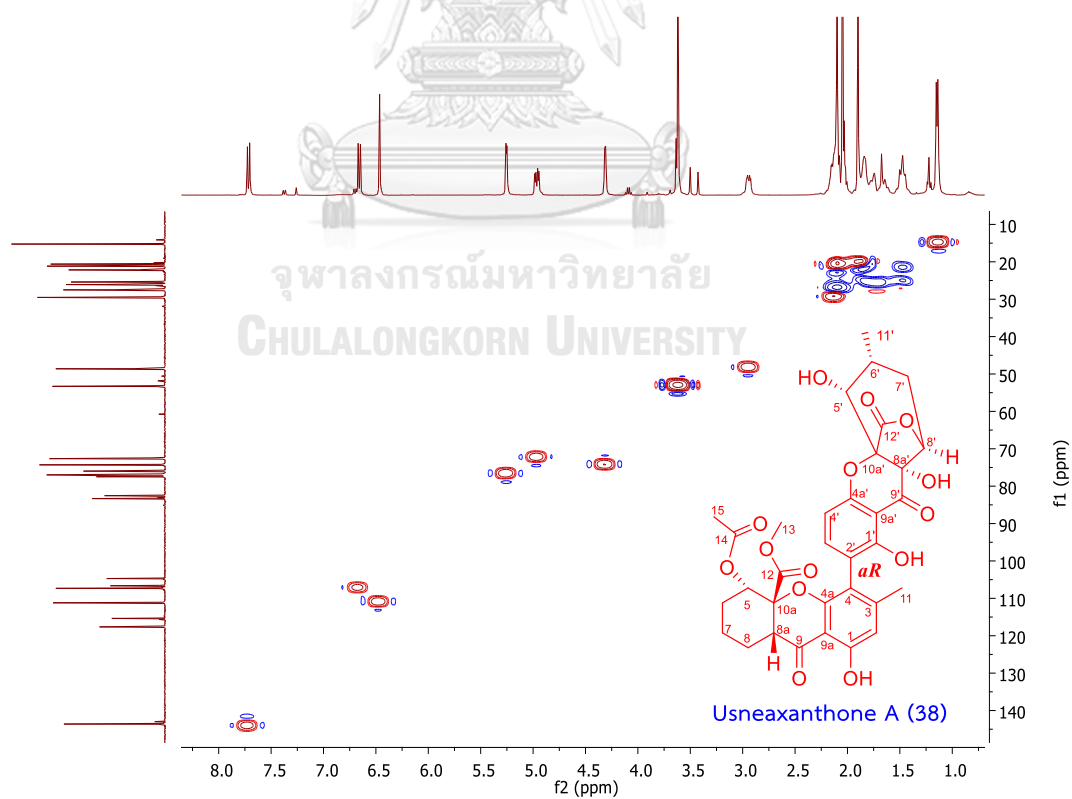
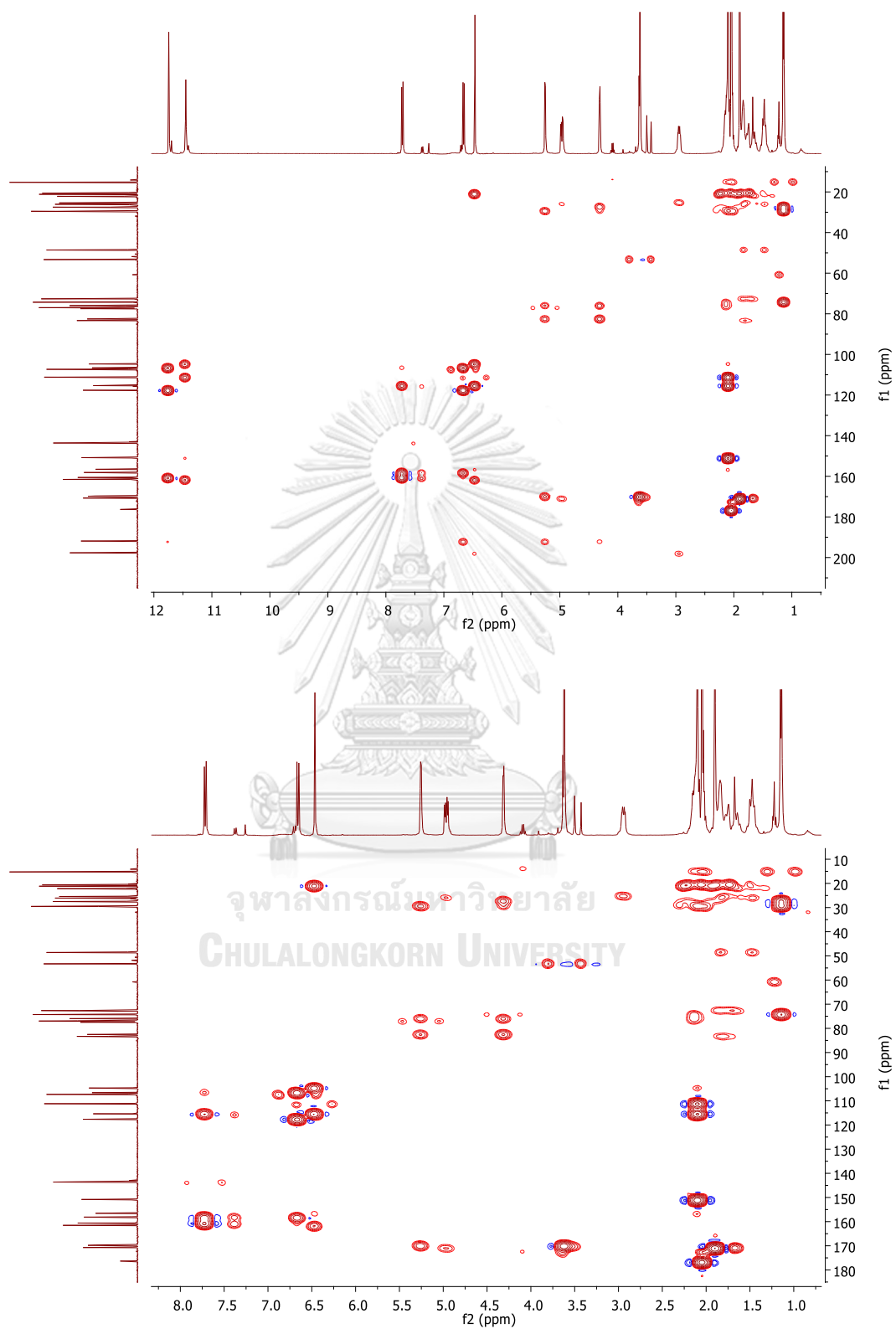


Figure A14.  $^{13}\text{C}$  NMR spectrum of usneaxanthone A (38) in  $\text{CDCl}_3$

Figure A15. COSY spectrum of usneaxanthone A (38) in CDCl<sub>3</sub>Figure A16. HSQC spectrum of usneaxanthone A (38) in CDCl<sub>3</sub>

Figure A17. HMBC spectrum of usneaxanthone A (38) in CDCl<sub>3</sub>

## Display Report

## Analysis Info

Analysis Name D:\Data\cardanol\UDA-29\_1-F,7\_01\_4840.d  
Method dmm 2017.m  
Sample Name UDA-29  
Comment

Acquisition Date 8/11/2017 4:00:56 PM

Operator Anh Mai  
Instrument micrOTOF-Q 10187

## Acquisition Parameter

Source Type	ESI	Ion Polarity	Positive	Set Nebulizer	1.2 Bar
Focus	Active	Set Capillary	4500 V	Set Dry Heater	200 °C
Scan Begin	50 m/z	Set End Plate Offset	-500 V	Set Dry Gas	8.0 l/min
Scan End	3000 m/z	Set Collision Cell RF	250.0 Vpp	Set Divert Valve	Source

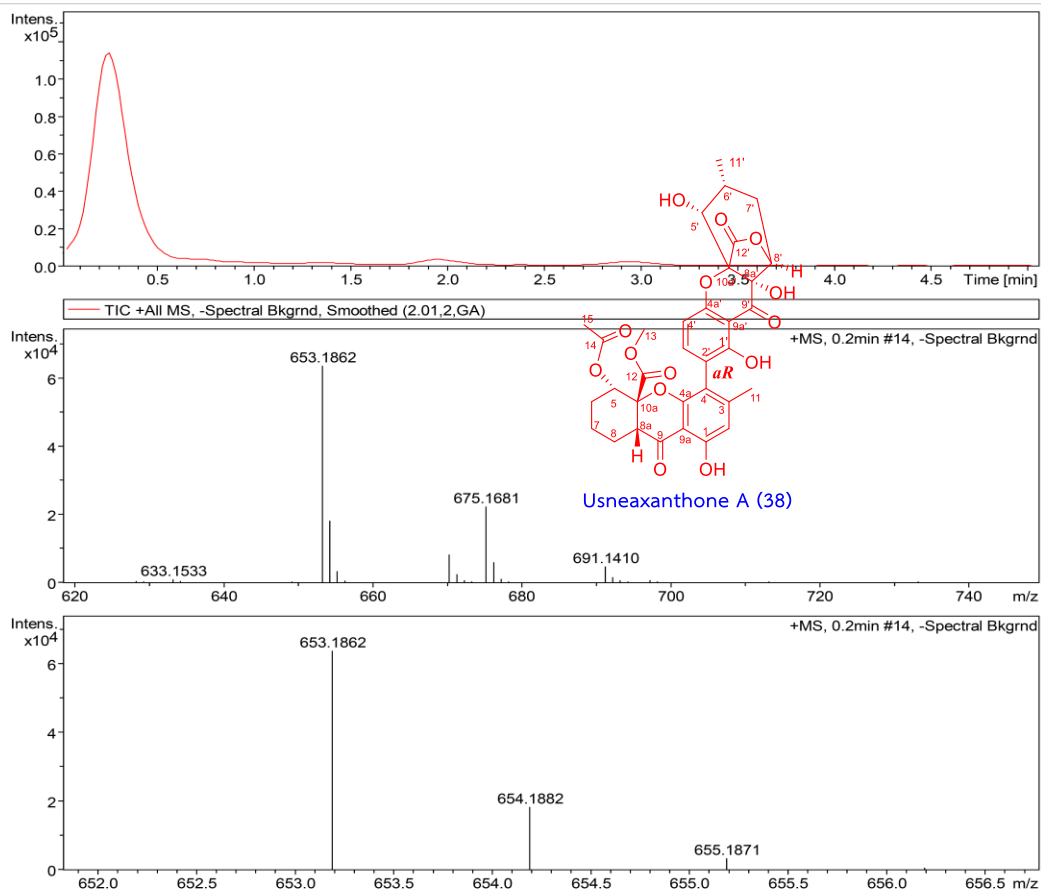


Figure A18. HRESIMS spectrum of usneaxanthone A (38)

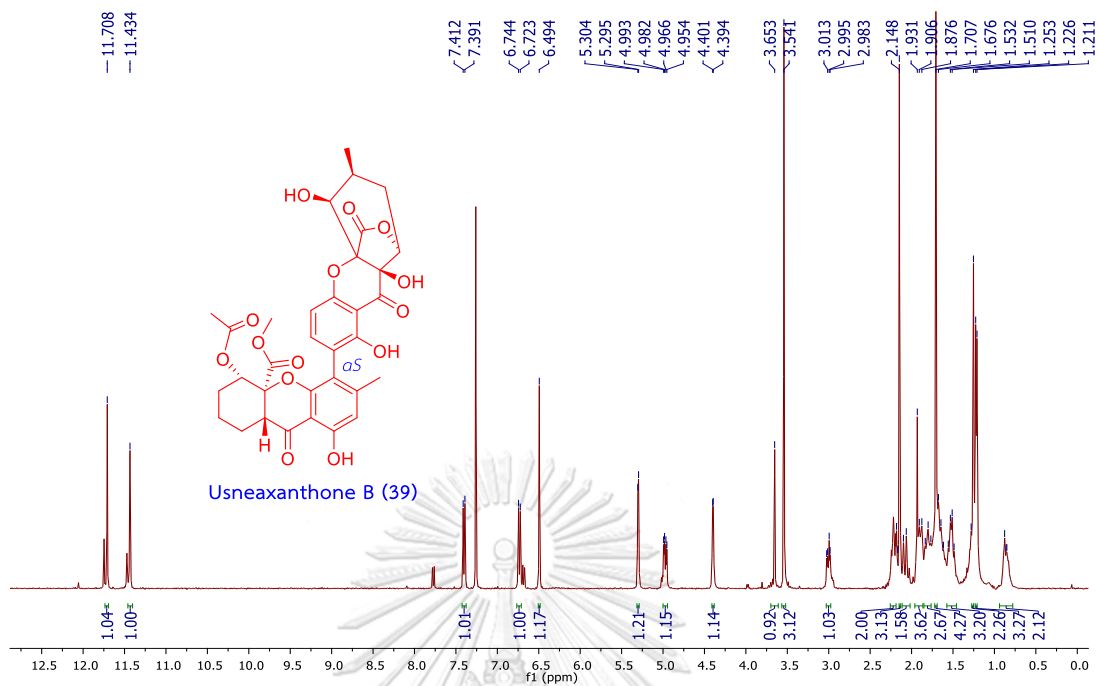


Figure A19. <sup>1</sup>H NMR spectrum of usneaxanthone B (39) in CDCl<sub>3</sub>

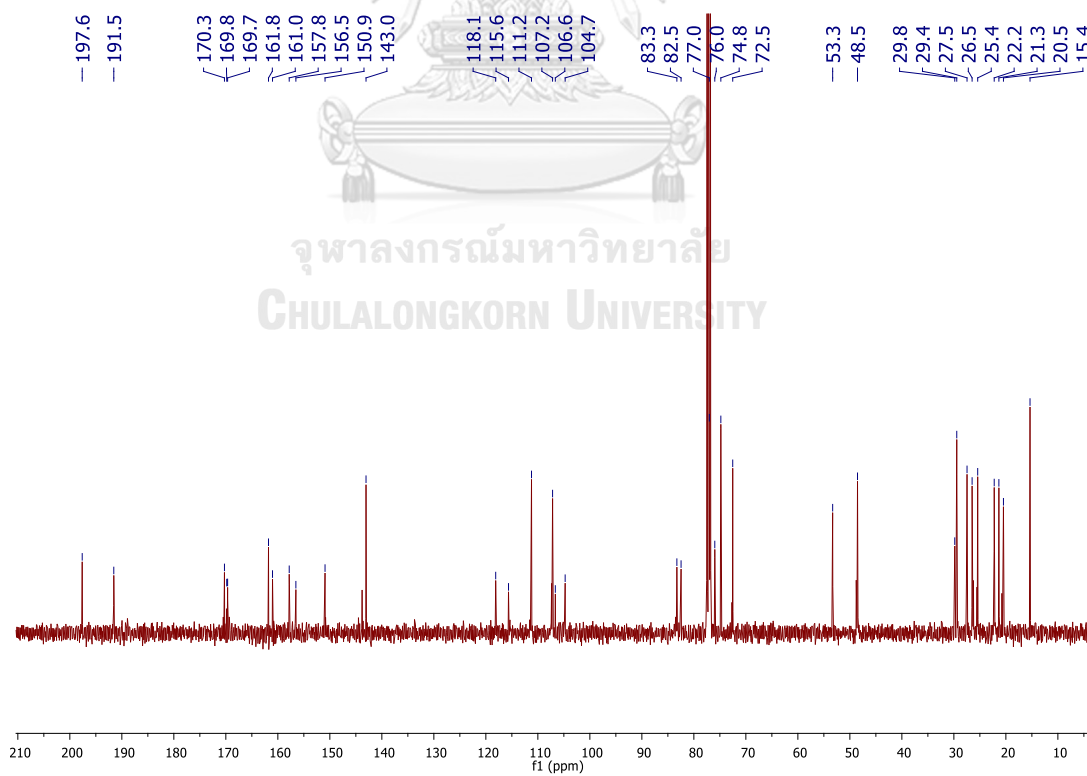
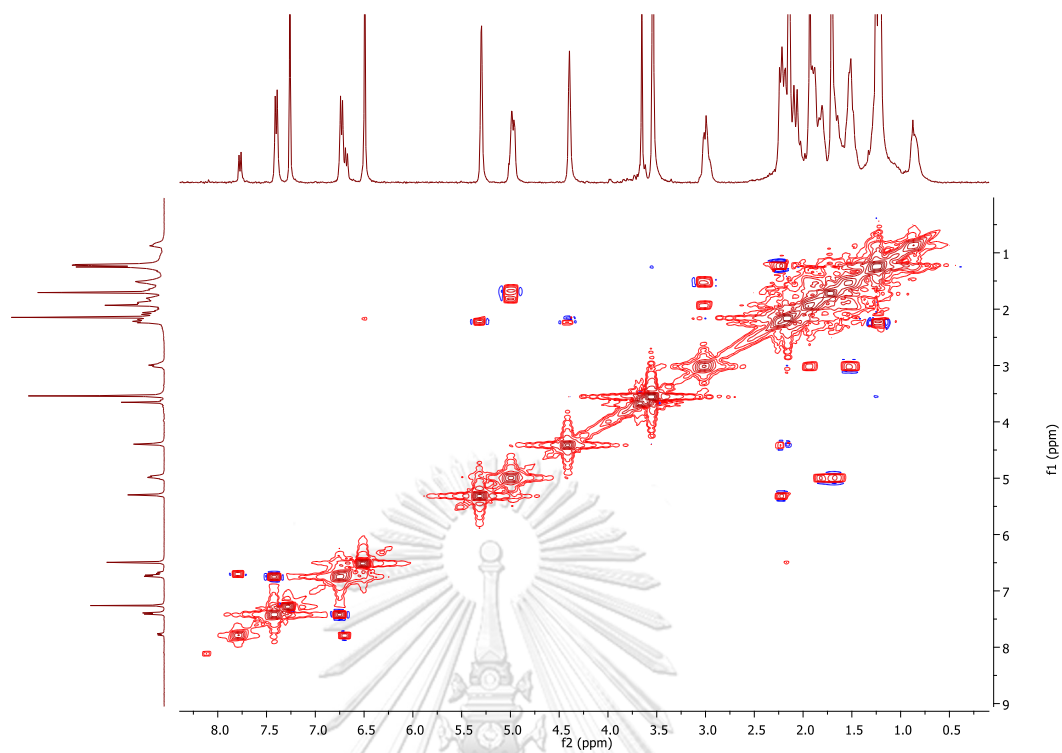
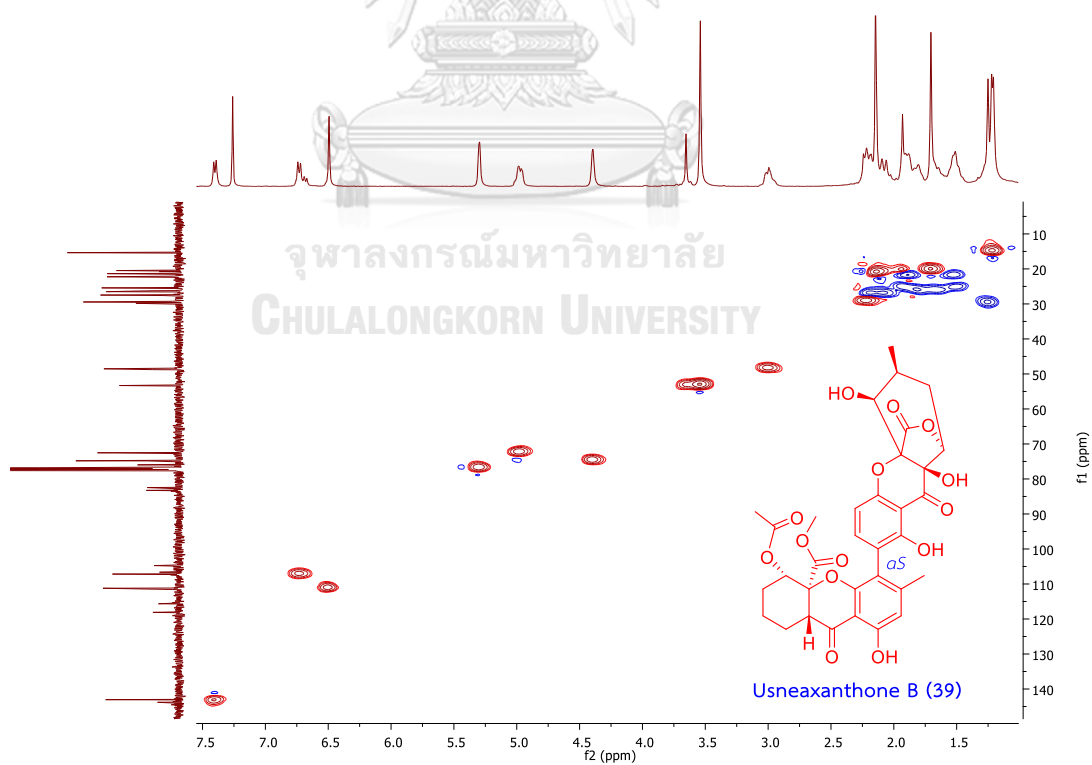
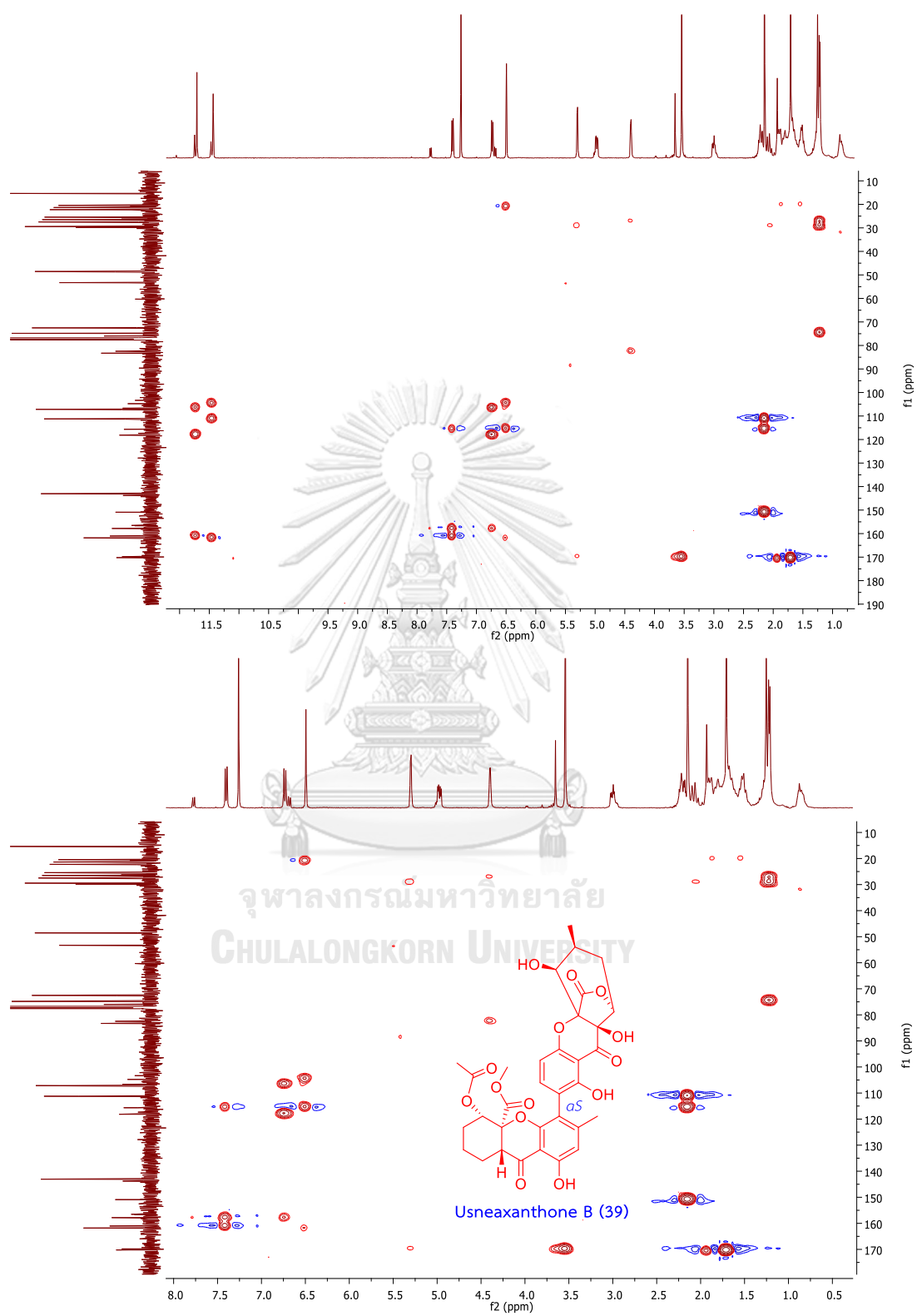


Figure A20. <sup>13</sup>C NMR spectrum of usneaxanthone B (39) in CDCl<sub>3</sub>

Figure A21. COSY spectrum of usneaxanthone B (39) in CDCl<sub>3</sub>Figure A22. HSQC spectrum of usneaxanthone B (39) in CDCl<sub>3</sub>

Figure A23. HMBC spectrum of usneaxanthone B (39) in CDCl<sub>3</sub>

## Generic Display Report

## Analysis Info

Analysis Name	D:\Data\Data Service\171214_pos_TT007.d	Acquisition Date	12/14/2017 12:45:57 PM
Method	NV_pos_0.3min_profile_1segment_lowNubulizerDrygas.m	Operator	CU.
Sample Name	171214_pos_TT007	Instrument	micrOTOF-Q II
Comment			

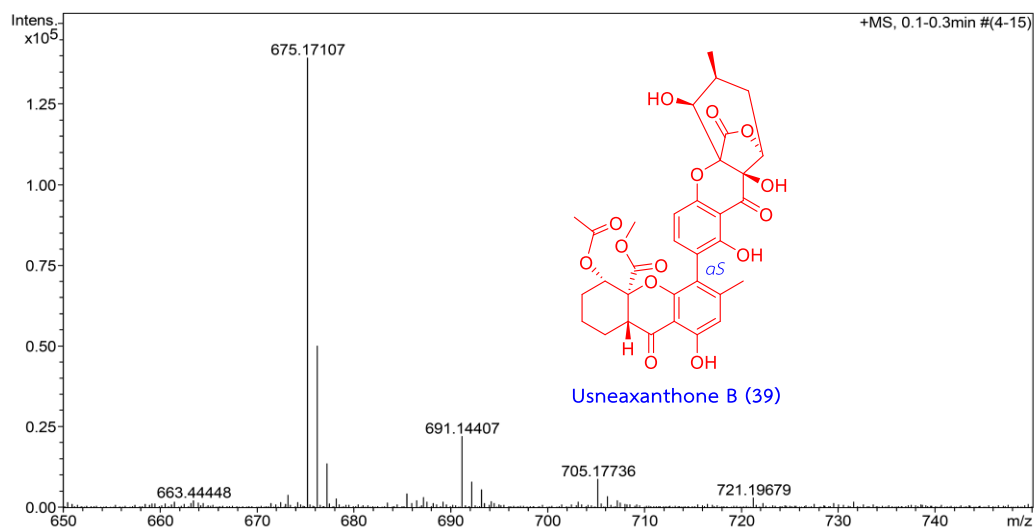
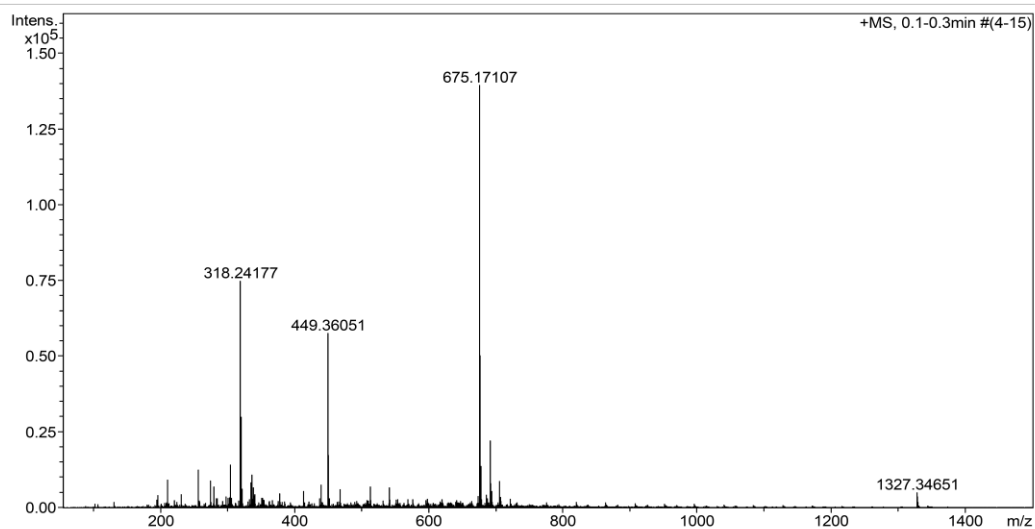


Figure A24. HRESIMS spectrum of usneaxanthone B (39)



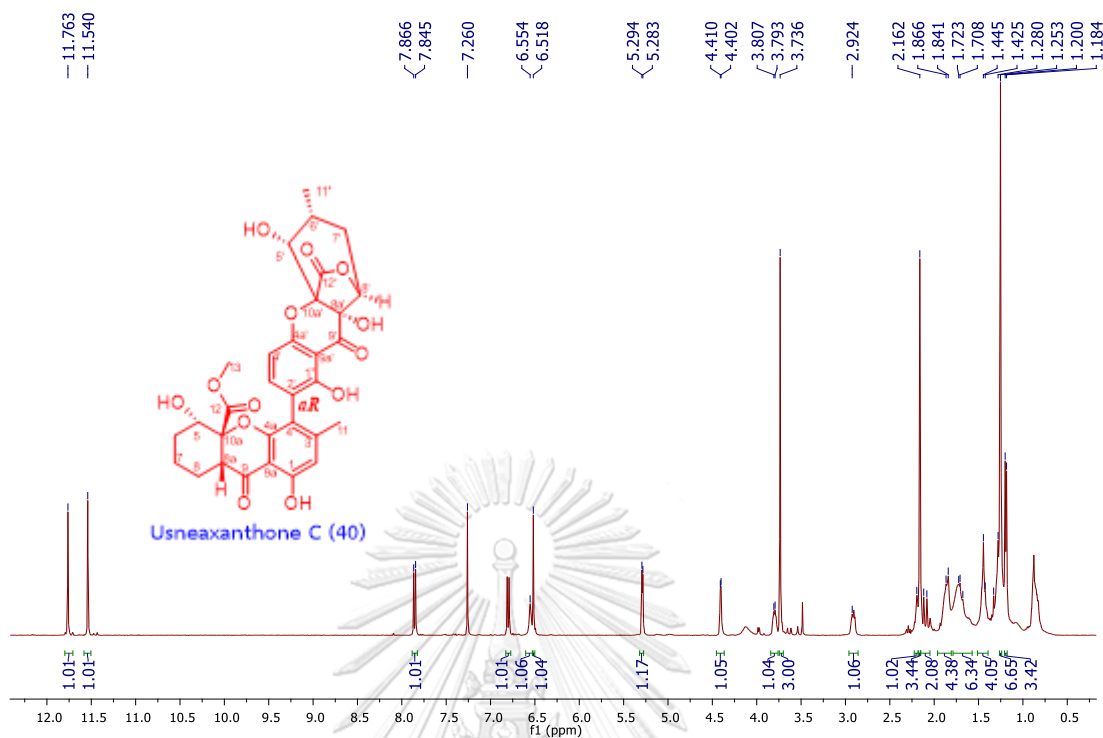


Figure A25.  $^1\text{H}$  NMR spectrum of of usneaxanthone C (40) in  $\text{CDCl}_3$

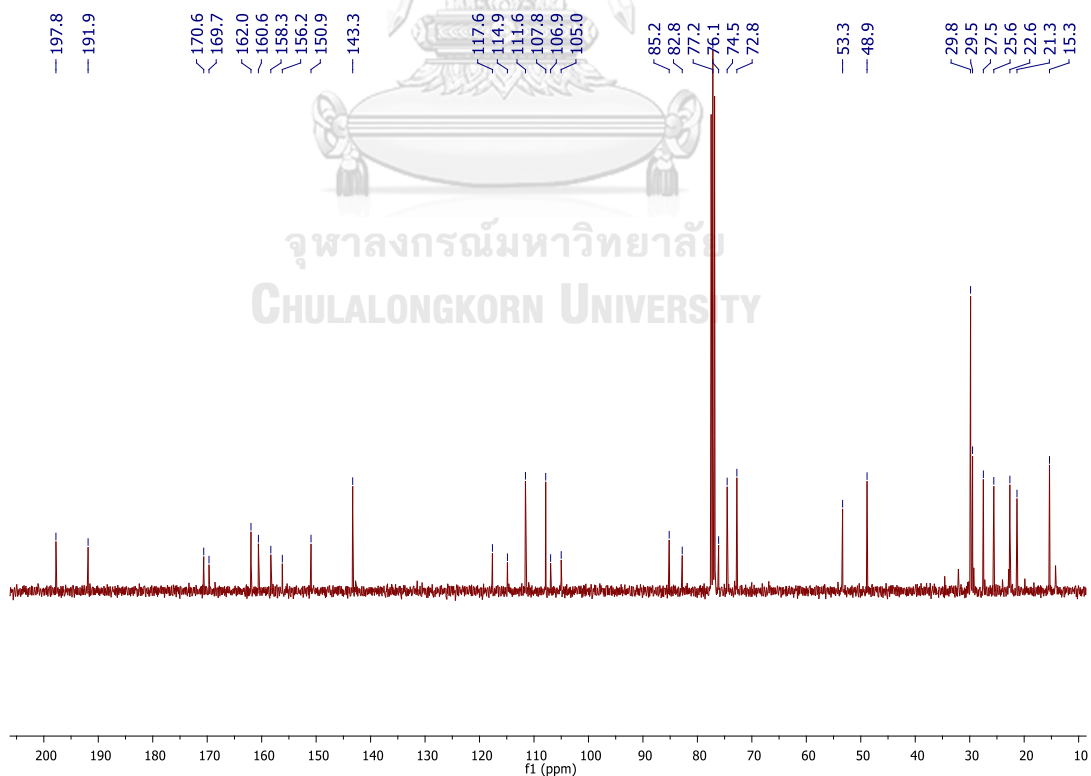
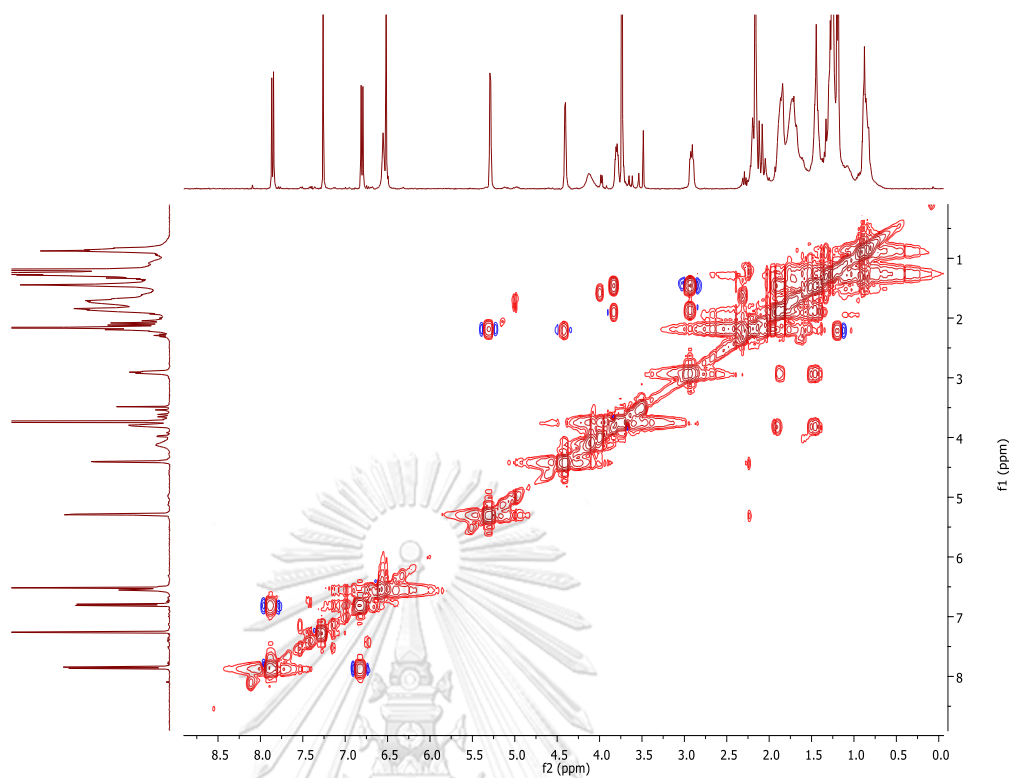
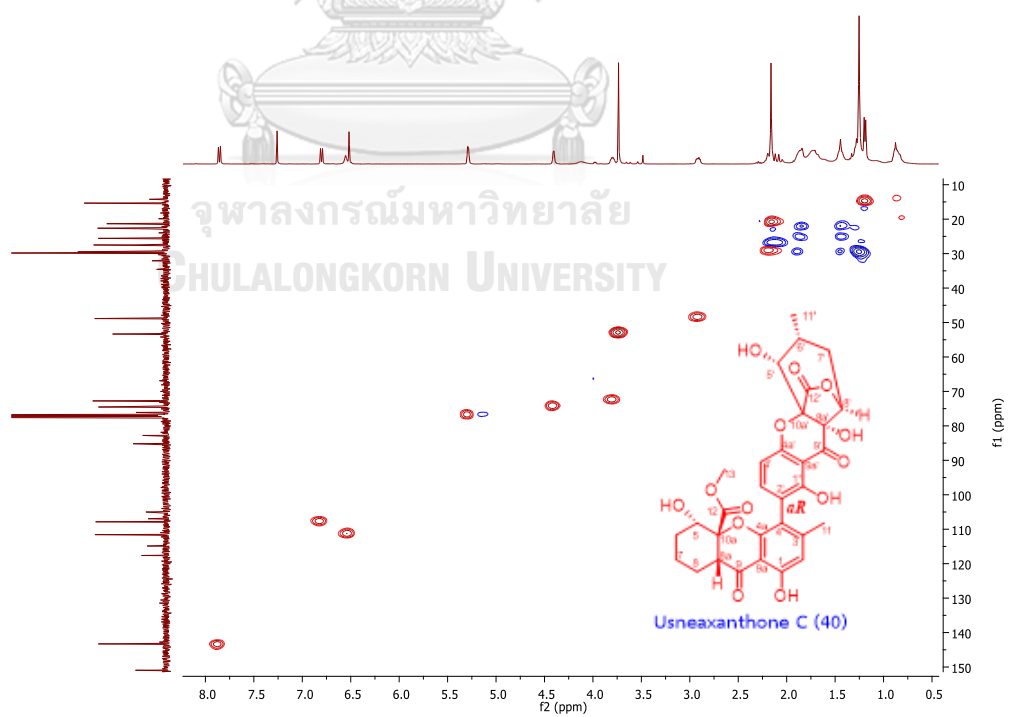
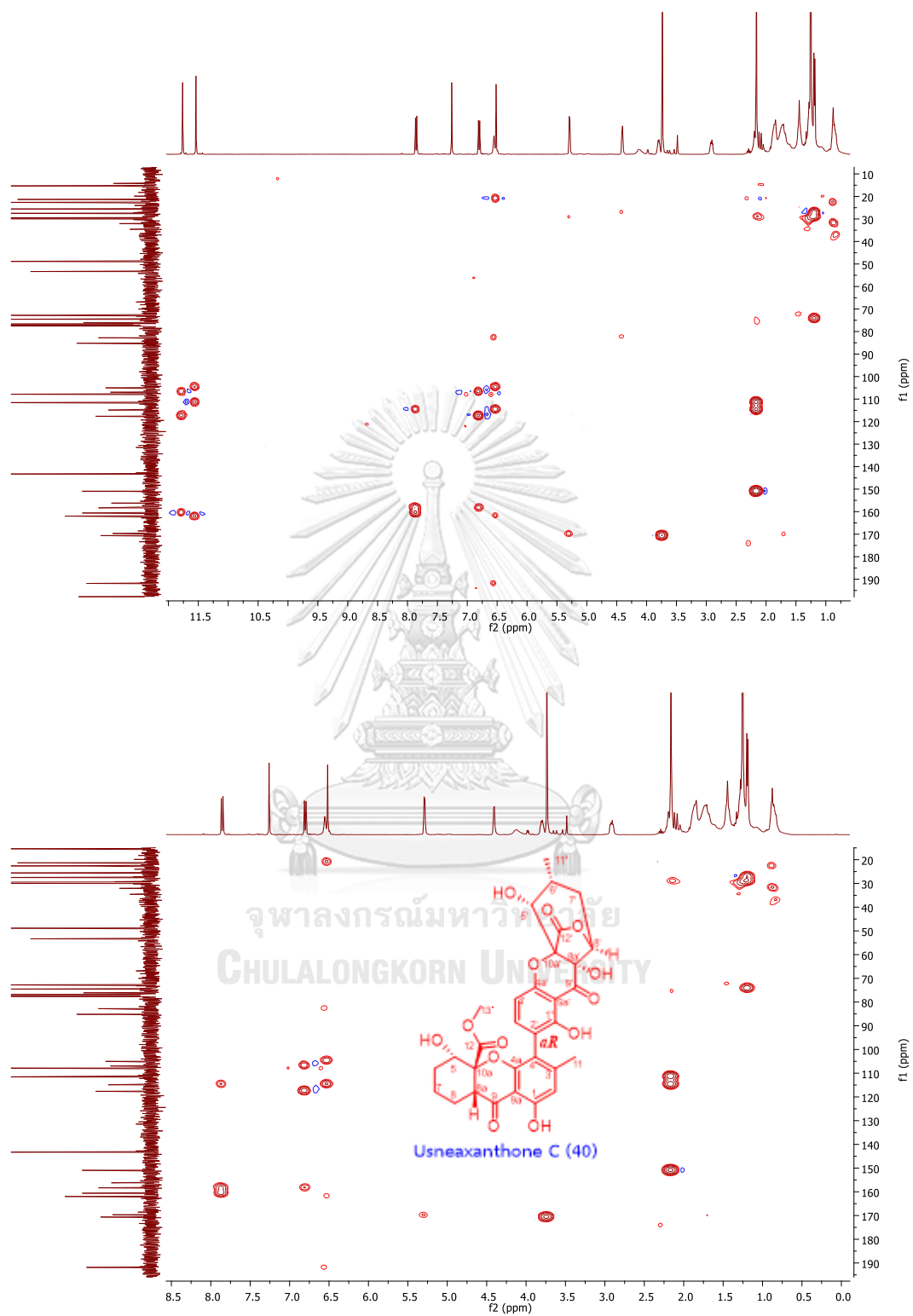


Figure A26.  $^{13}\text{C}$  NMR spectrum of usneaxanthone C (40) in  $\text{CDCl}_3$

Figure A27. COSY spectrum of usneaxanthone C (40) in CDCl<sub>3</sub>Figure A28. HSQC spectrum of usneaxanthone C (40) in CDCl<sub>3</sub>

Figure A29. HMBC spectrum of usneaxanthone C (40) in CDCl<sub>3</sub>

## Generic Display Report

## Analysis Info

Analysis Name D:\Data\Data Service\180209\_neg\_TT009.d Acquisition Date 2/9/2018 12:56:06 PM  
Method NV\_neg\_0.3min\_profile\_1segment\_lowNubulizerDrygas(2).m Operator CU  
Sample Name 180209\_neg\_TT009 Instrument micrOTOF-Q II  
Comment

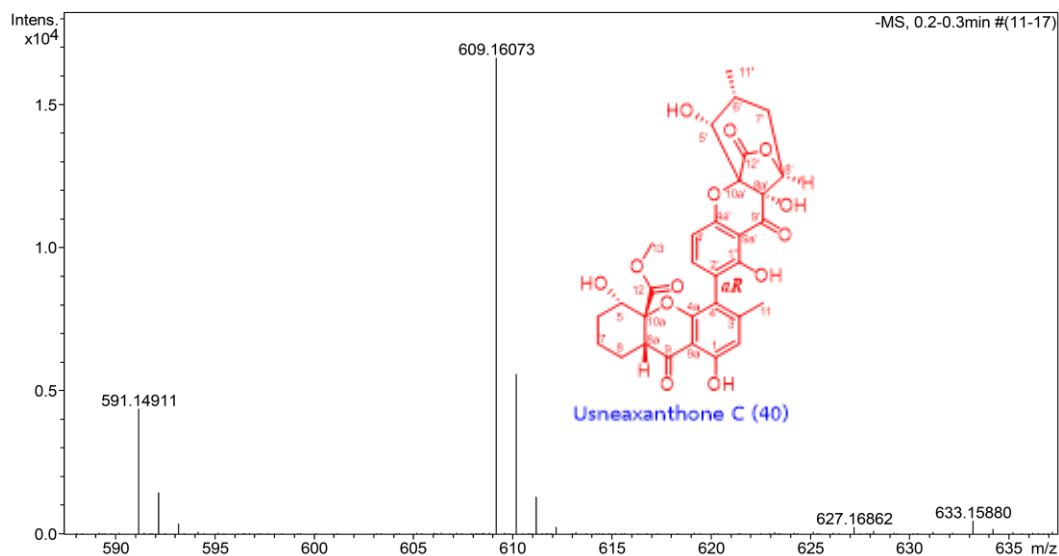
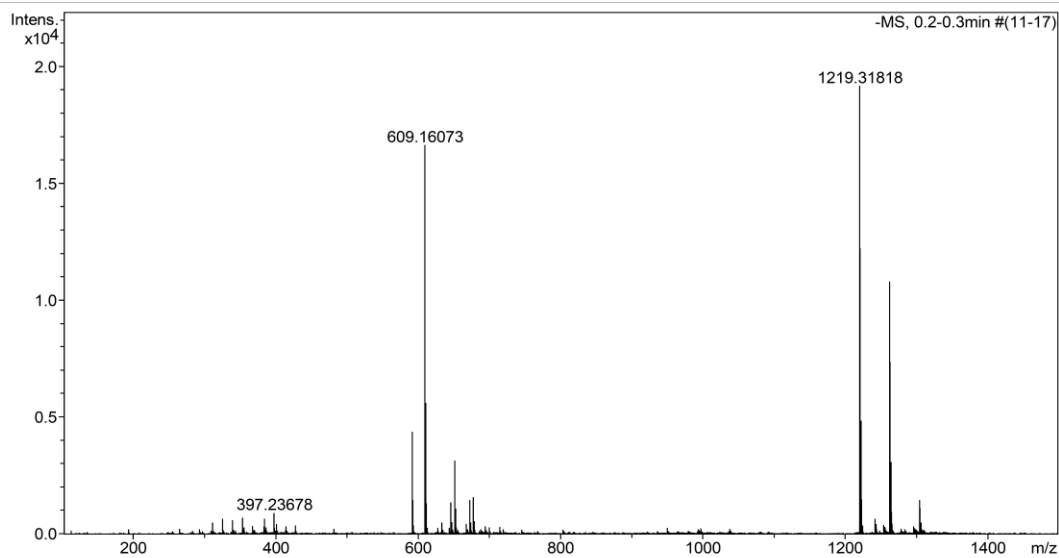


Figure A30. HRESIMS spectrum of usneaxanthone C (40)

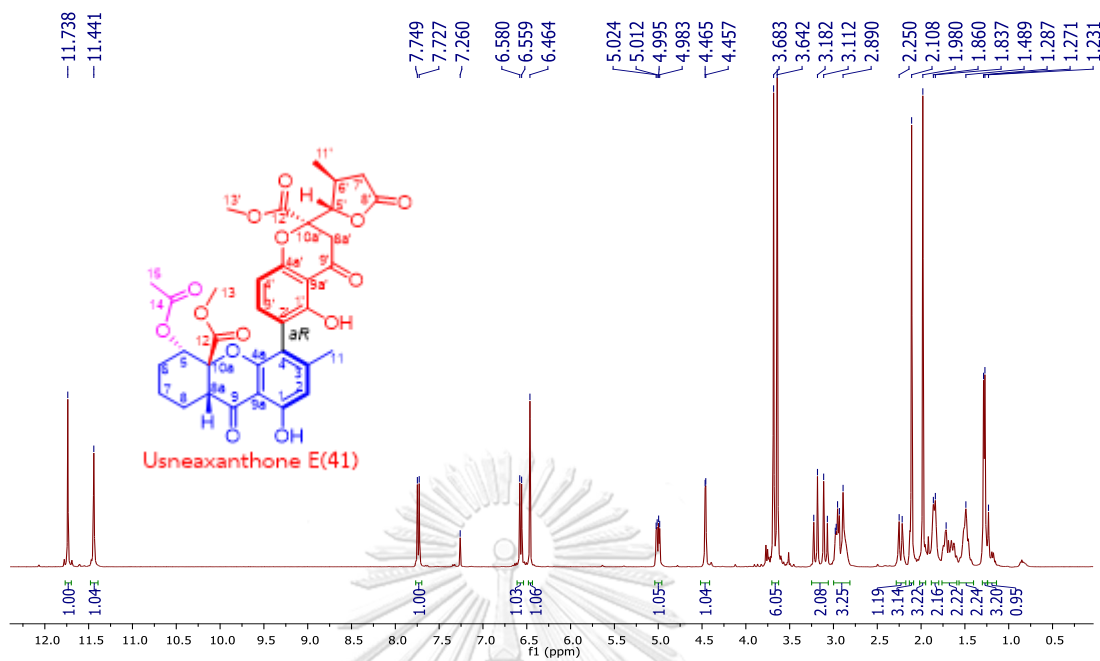


Figure A31. <sup>1</sup>H NMR spectrum of usneaxanthone E (41) in CDCl<sub>3</sub>

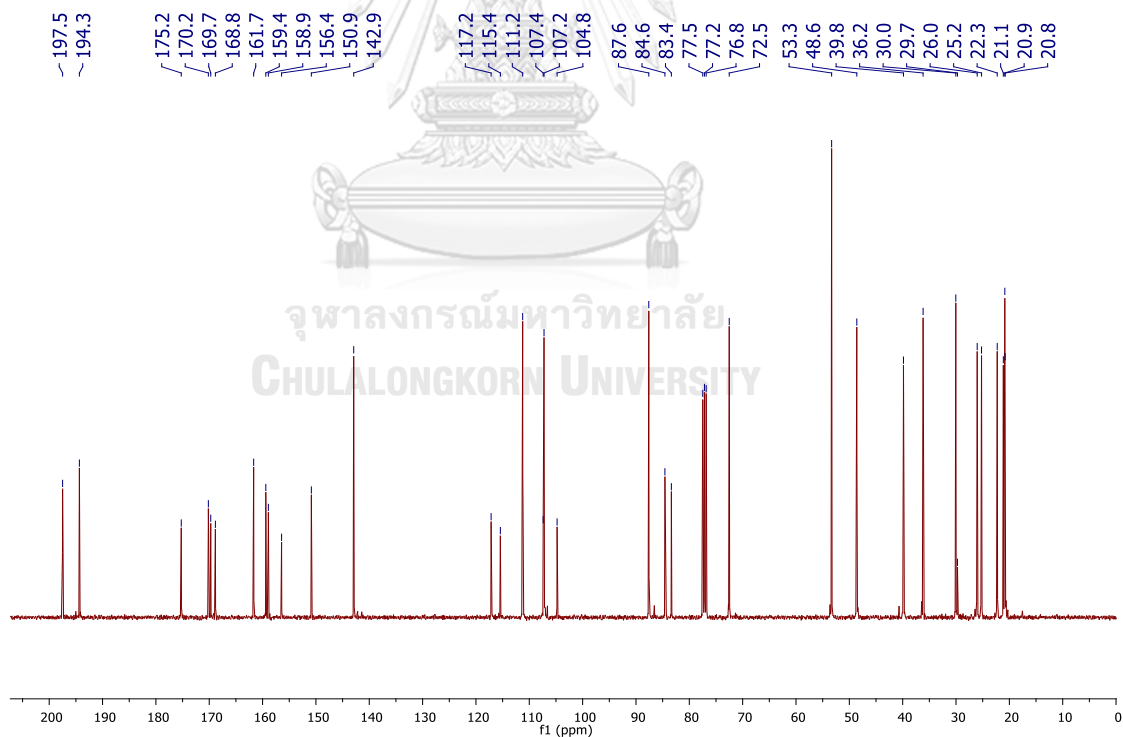
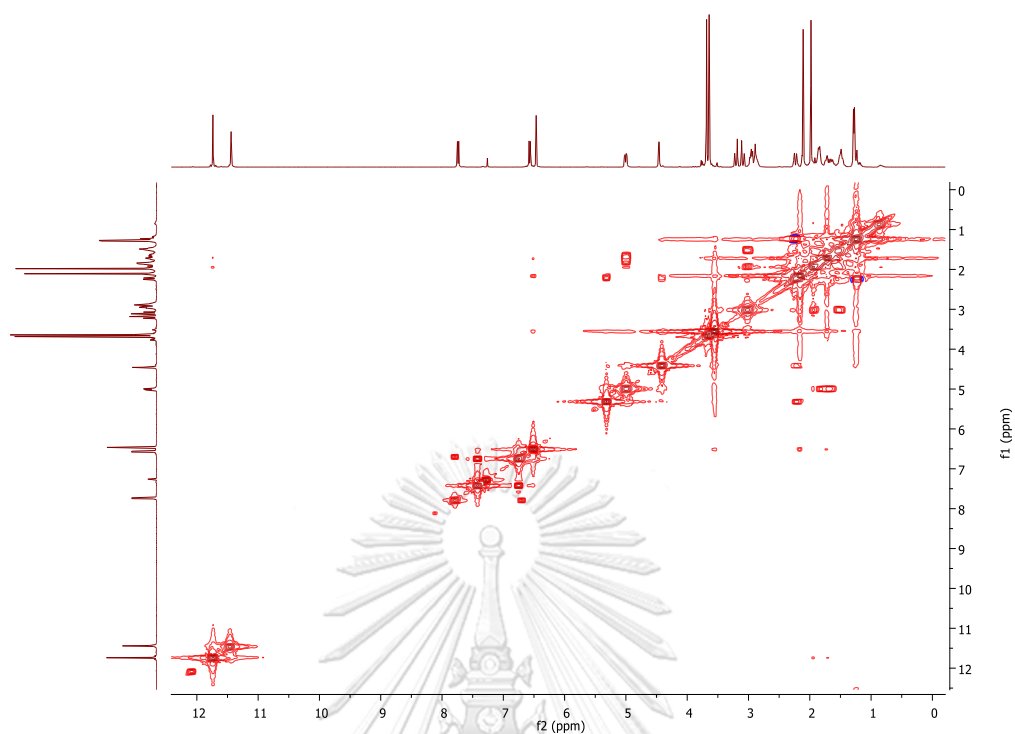
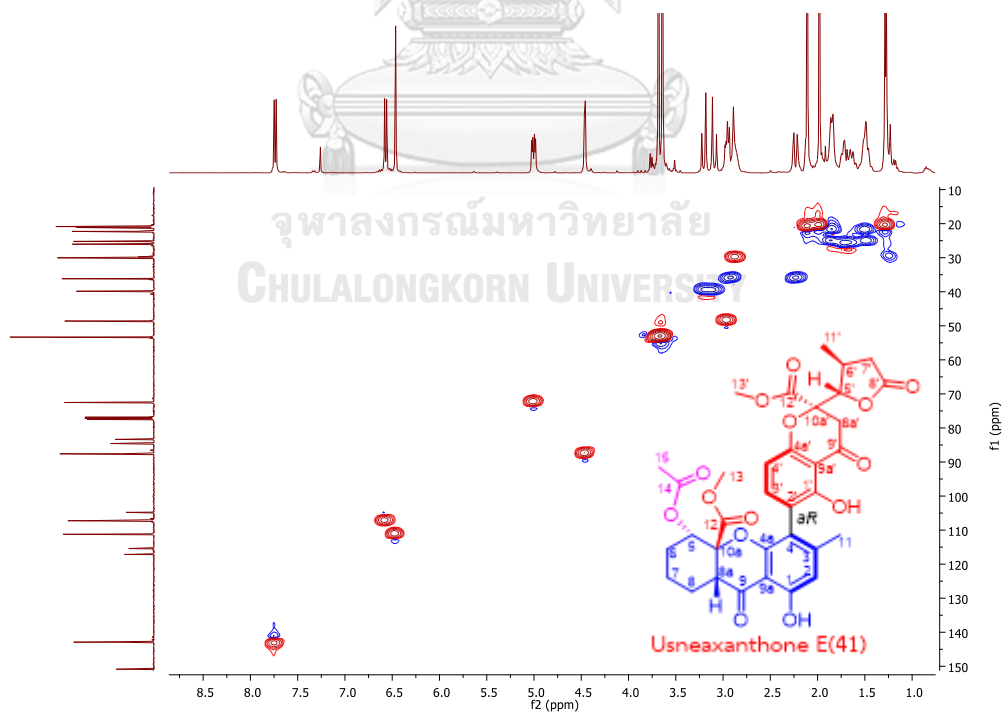
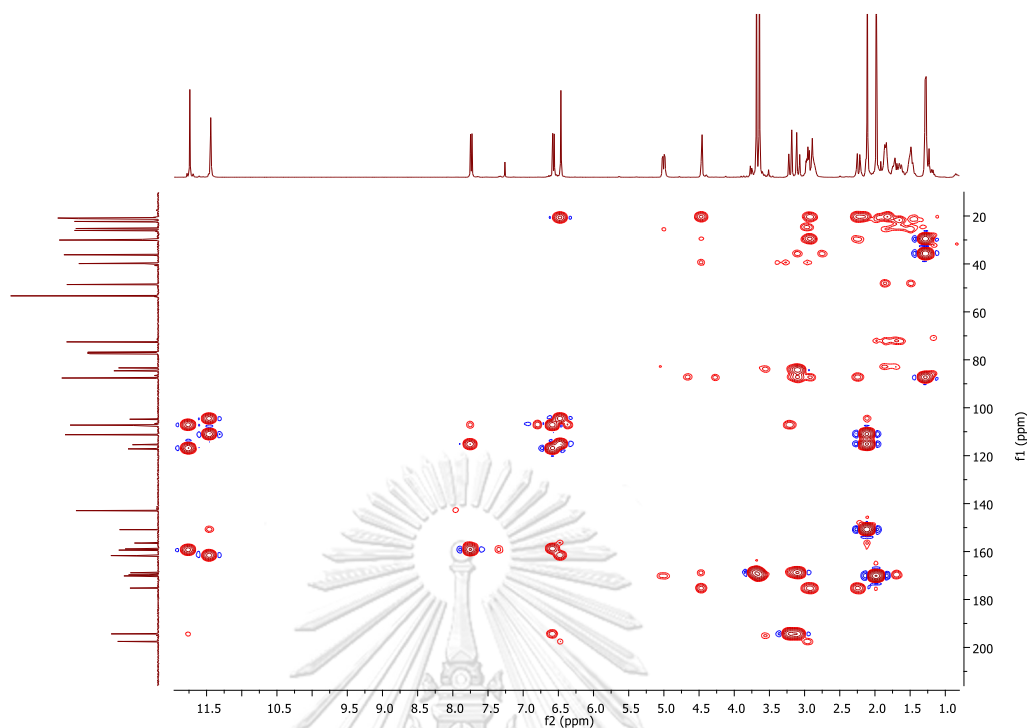
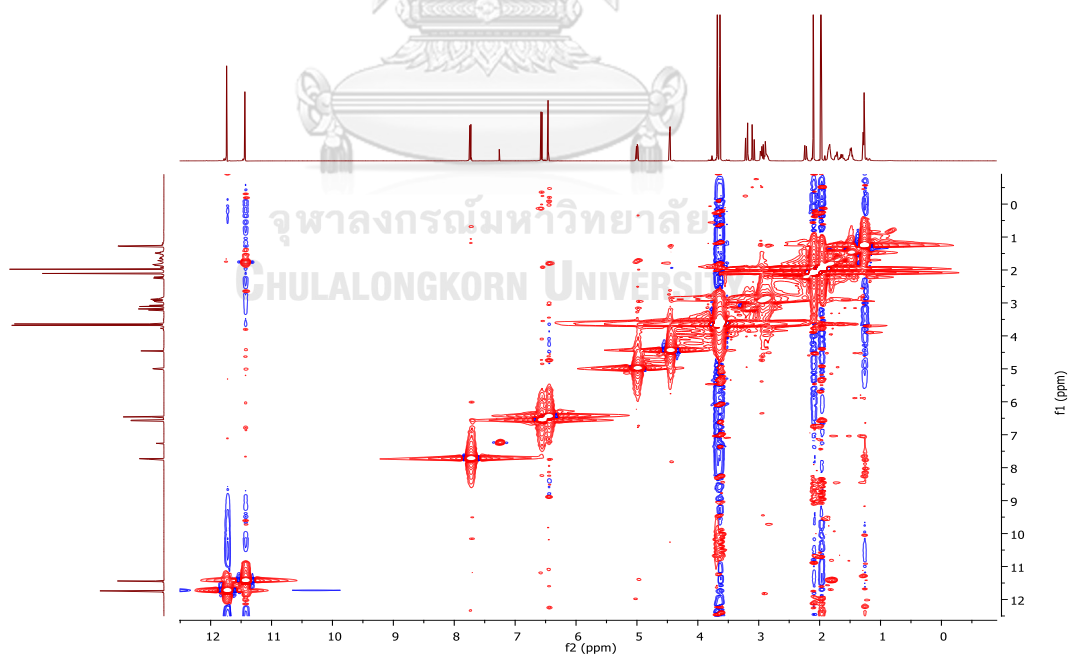


Figure A32. <sup>13</sup>C NMR spectrum of usneaxanthone E (41) in CDCl<sub>3</sub>

Figure A33. COSY spectrum of usneaxanthone E (41) in CDCl<sub>3</sub>Figure A34. HSQC spectrum of usneaxanthone E (41) in CDCl<sub>3</sub>

Figure A35. HMBC spectrum of usneaxanthone E (41) in  $\text{CDCl}_3$ Figure A36. NOESY spectrum of usneaxanthone E (41) in  $\text{CDCl}_3$

## Display Report

## Analysis Info

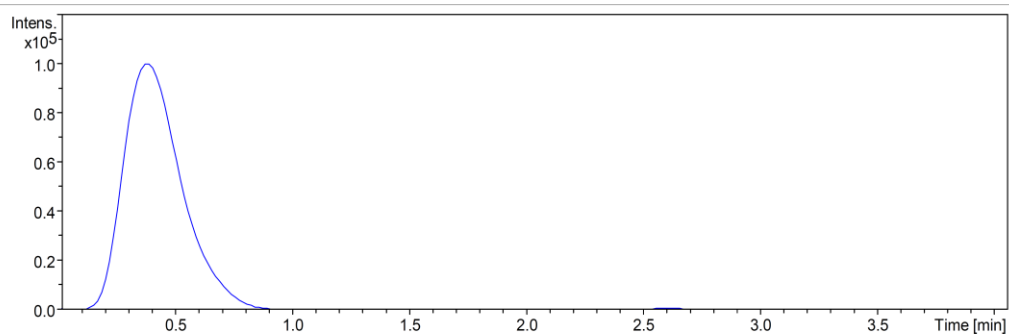
Analysis Name D:\Data\cardano\UAD-25\_1-b,3\_01\_4817.d  
Method dmm 2017.m  
Sample Name UAD-25  
Comment

Acquisition Date 8/9/2017 8:20:43 PM

Operator Anh Mai  
Instrument micrOTOF-Q 10187

## Acquisition Parameter

Source Type	ESI	Ion Polarity	Positive	Set Nebulizer	1.2 Bar
Focus	Active	Set Capillary	4500 V	Set Dry Heater	200 °C
Scan Begin	50 m/z	Set End Plate Offset	-500 V	Set Dry Gas	8.0 l/min
Scan End	3000 m/z	Set Collision Cell RF	250.0 Vpp	Set Divert Valve	Source



— EIC 689.0000 +All MS, -Spectral Bkgrnd, Smoothed (2.01,2,GA)

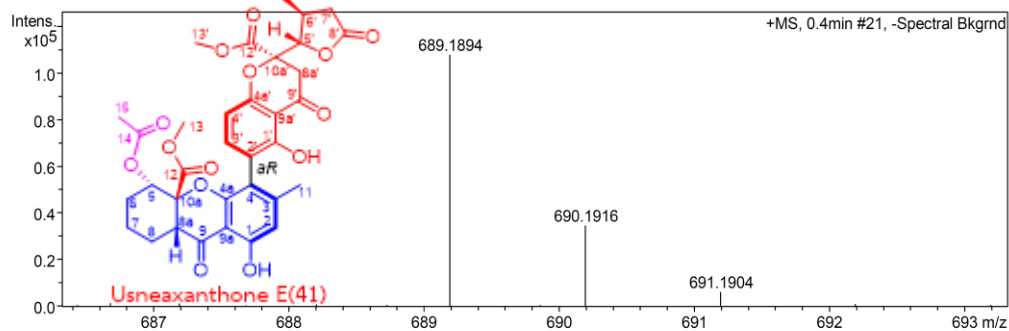
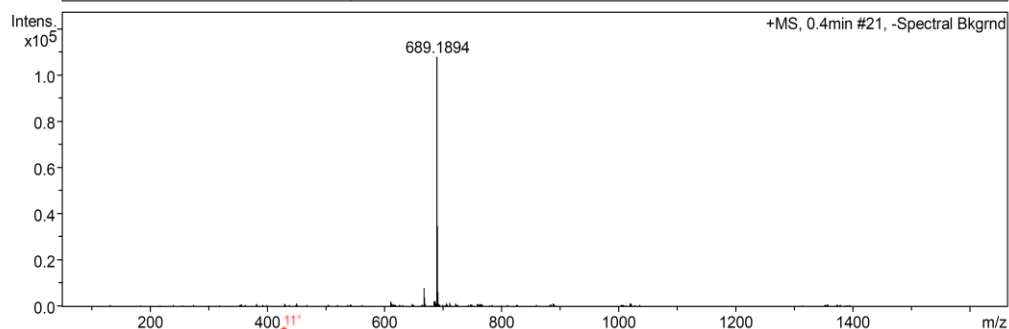
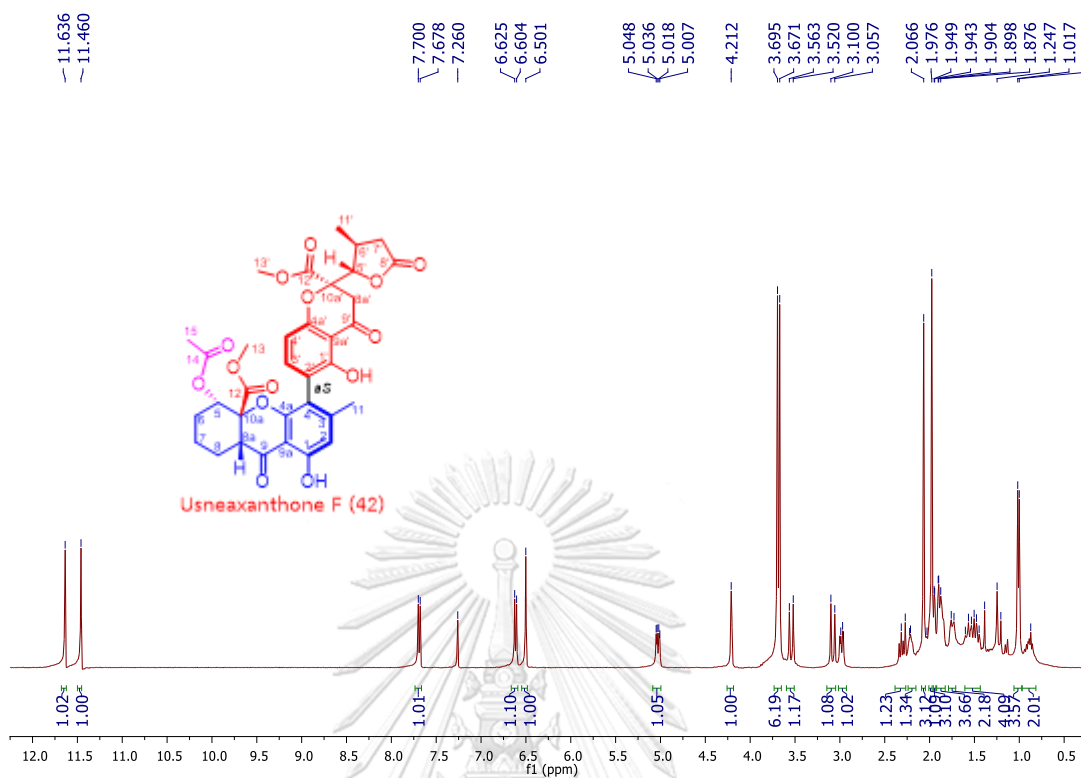
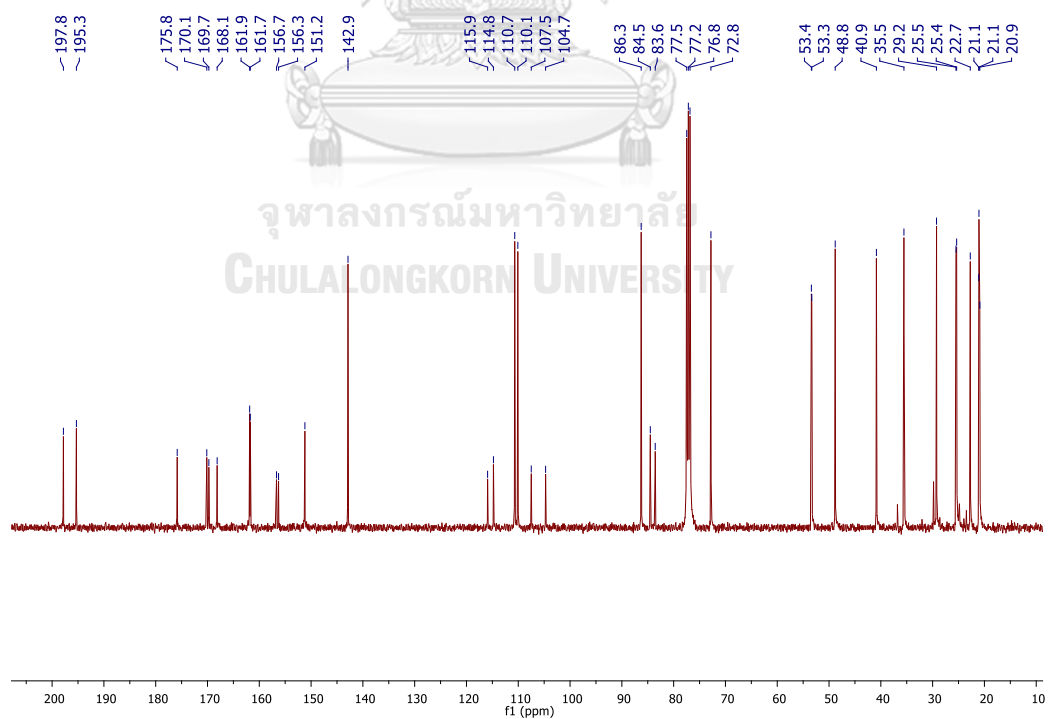
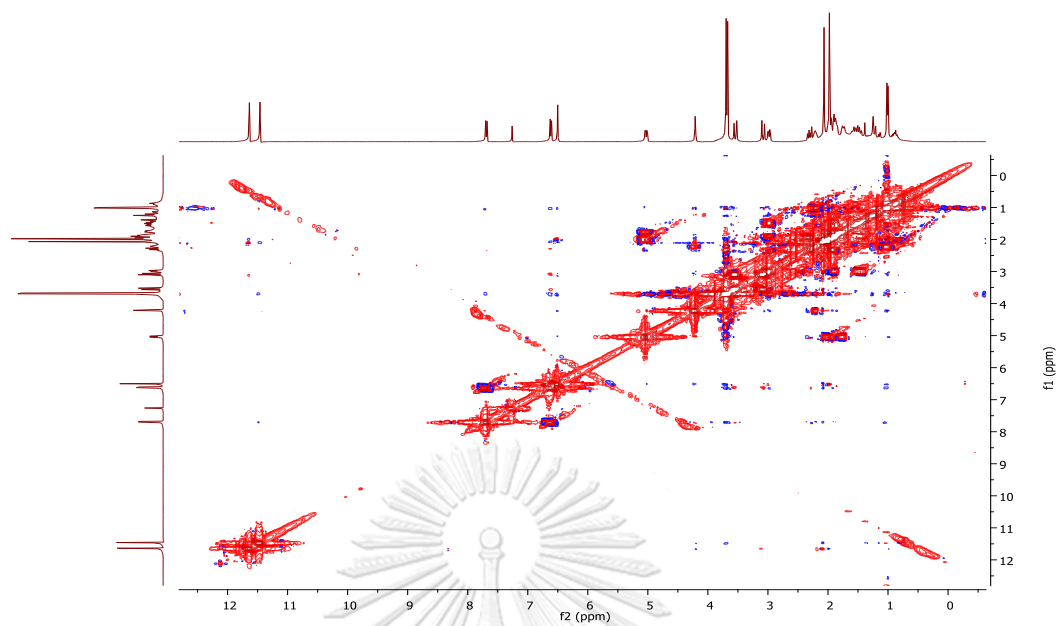
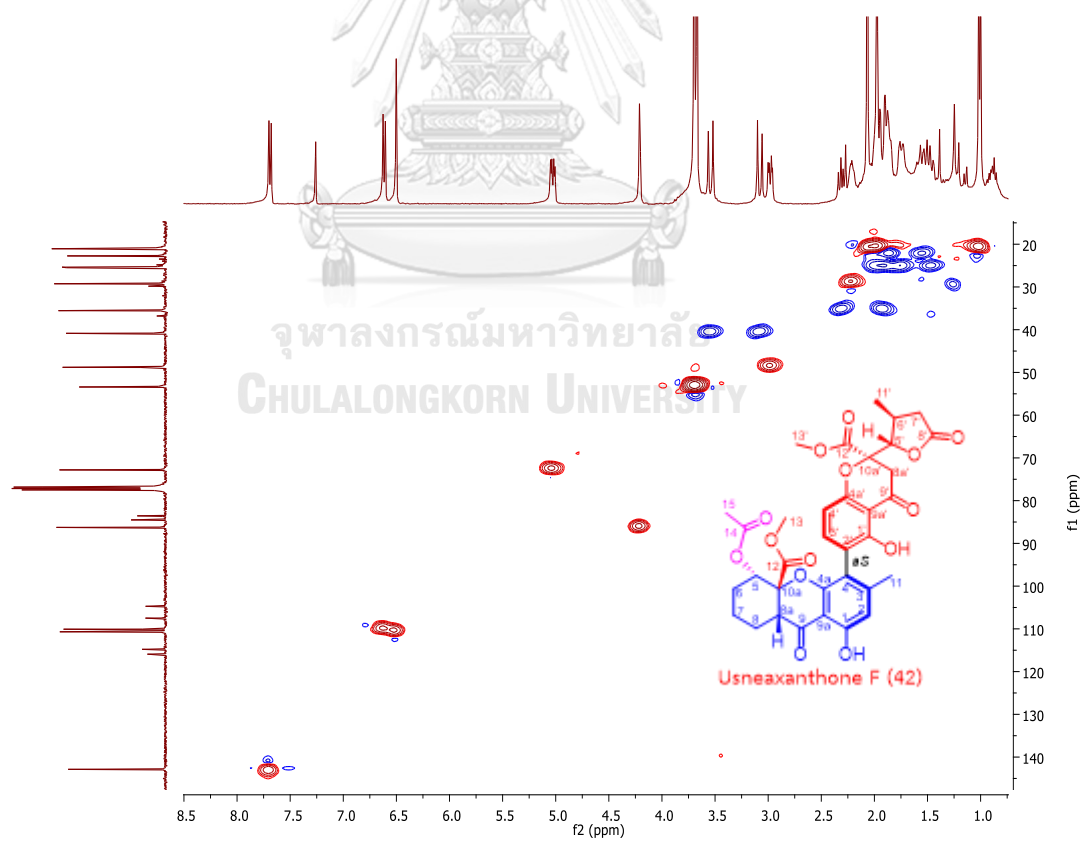
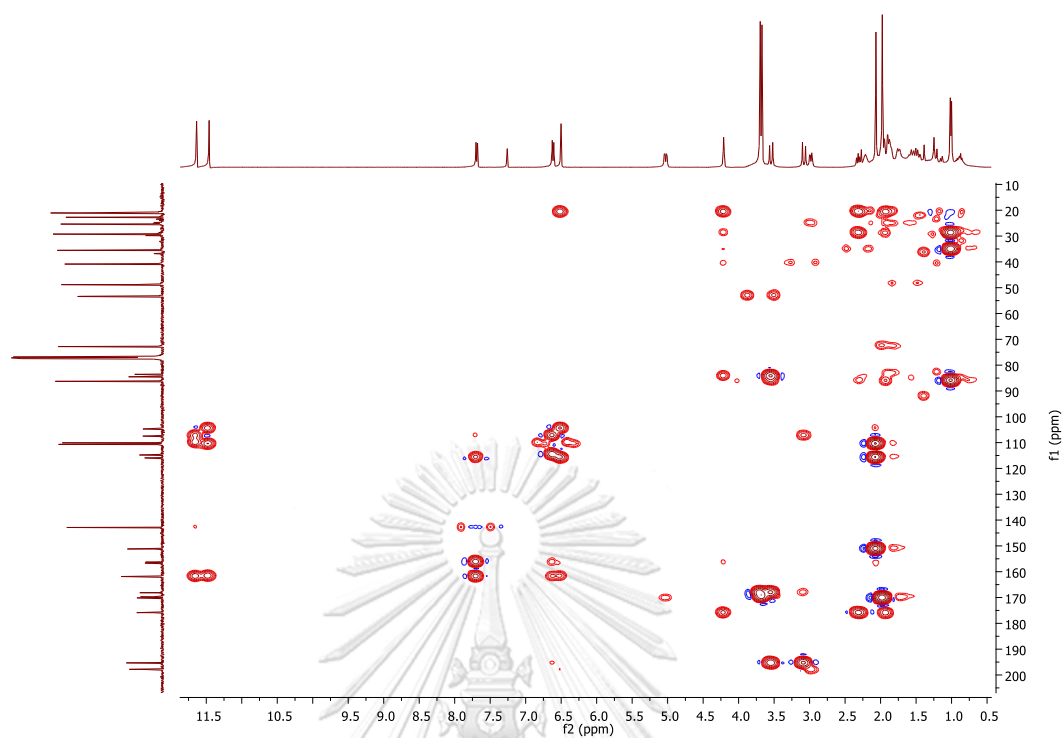
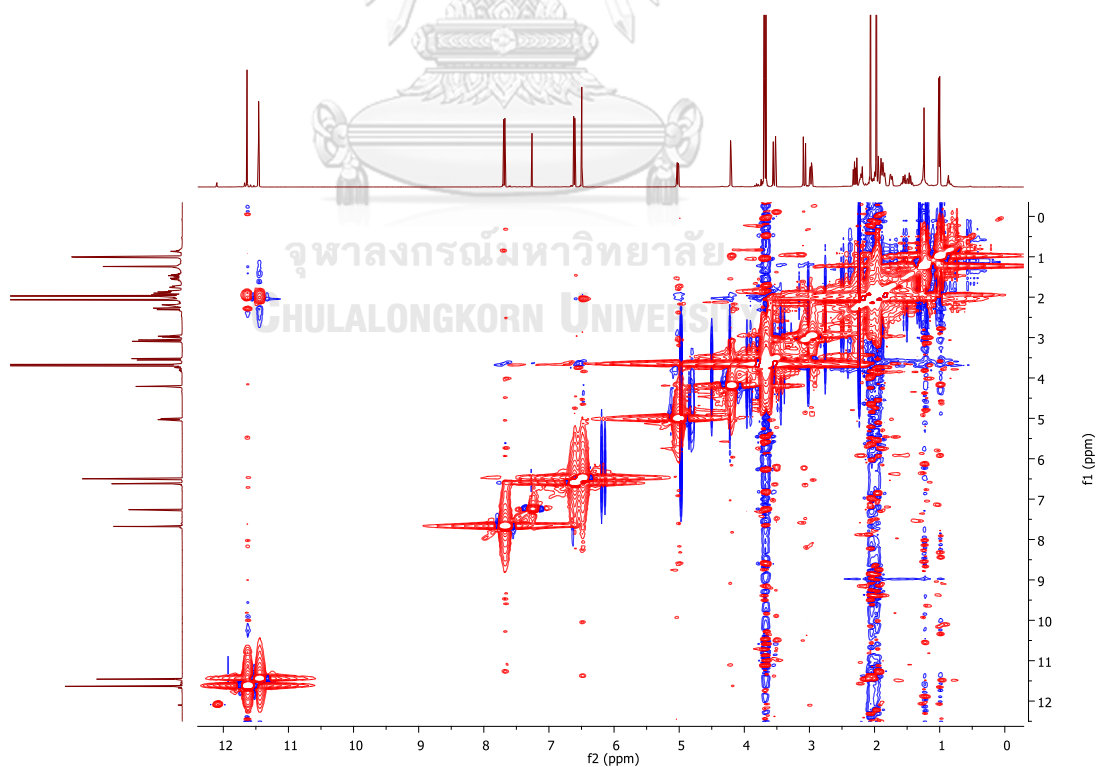


Figure A37. HRESIMS spectrum of usneaxanthone E (41)



Figure A38. <sup>1</sup>H NMR spectrum of usneaxanthone F (42) in CDCl<sub>3</sub>Figure A39. <sup>13</sup>C NMR spectrum of usneaxanthone F (42) in CDCl<sub>3</sub>

Figure A40. COSY spectrum of usneaxanthone F (42) in CDCl<sub>3</sub>Figure A41. HSQC spectrum of usneaxanthone F (42) in CDCl<sub>3</sub>

Figure A42. HMBC spectrum of usneaxanthone F (42) in CDCl<sub>3</sub>Figure A43. NOESY spectrum of usneaxanthone F (42) in CDCl<sub>3</sub>

## Generic Display Report

## Analysis Info

Analysis Name D:\Data\Data Service\190325\TT-039\_RA4\_01\_2400.d  
Method nv\_pos\_5min\_profile\_190214.m  
Sample Name TT-039  
Comment

Acquisition Date 3/27/2019 4:06:40 PM

Operator CU.  
Instrument micrOTOF-Q II

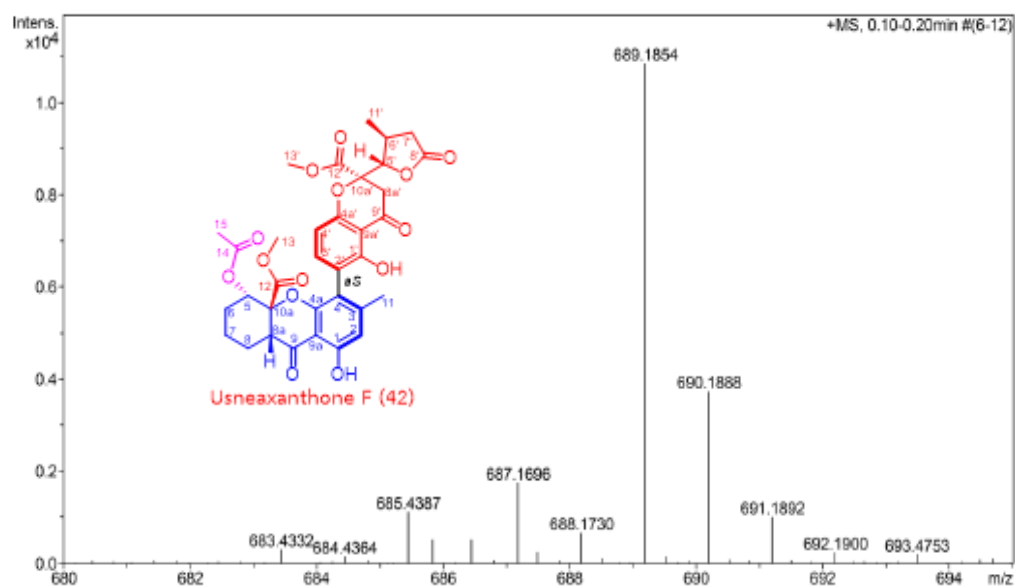
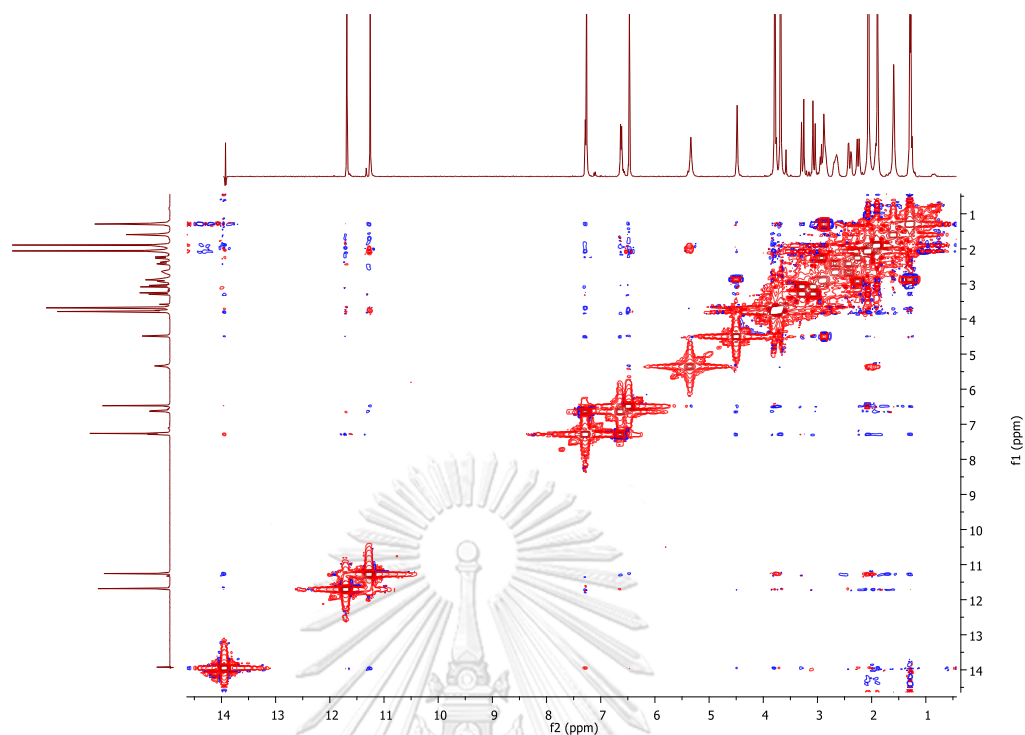
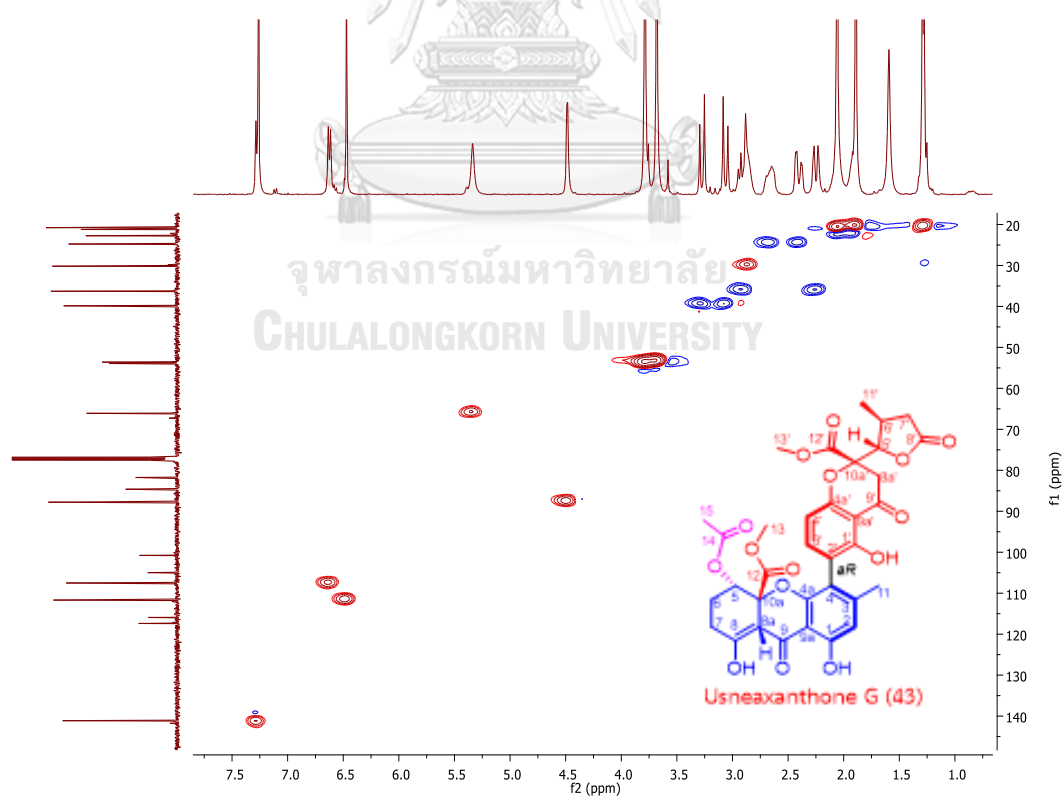


Figure A44. HRESIMS spectrum of usneaxanthone F (42)



Figure A47. COSY spectrum of usneaxanthone G (43) in CDCl<sub>3</sub>Figure A48. HSQC spectrum of usneaxanthone G (43) in CDCl<sub>3</sub>

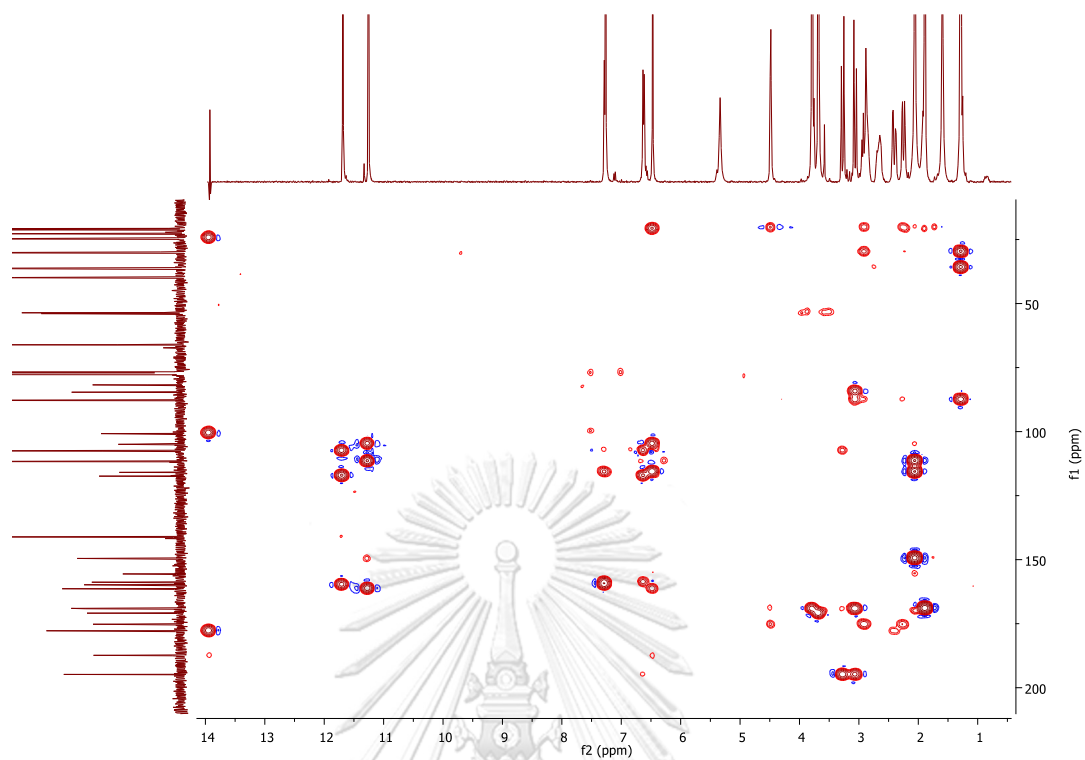


Figure A49. HMBC spectrum of usneaxanthone C (43) in  $\text{CDCl}_3$

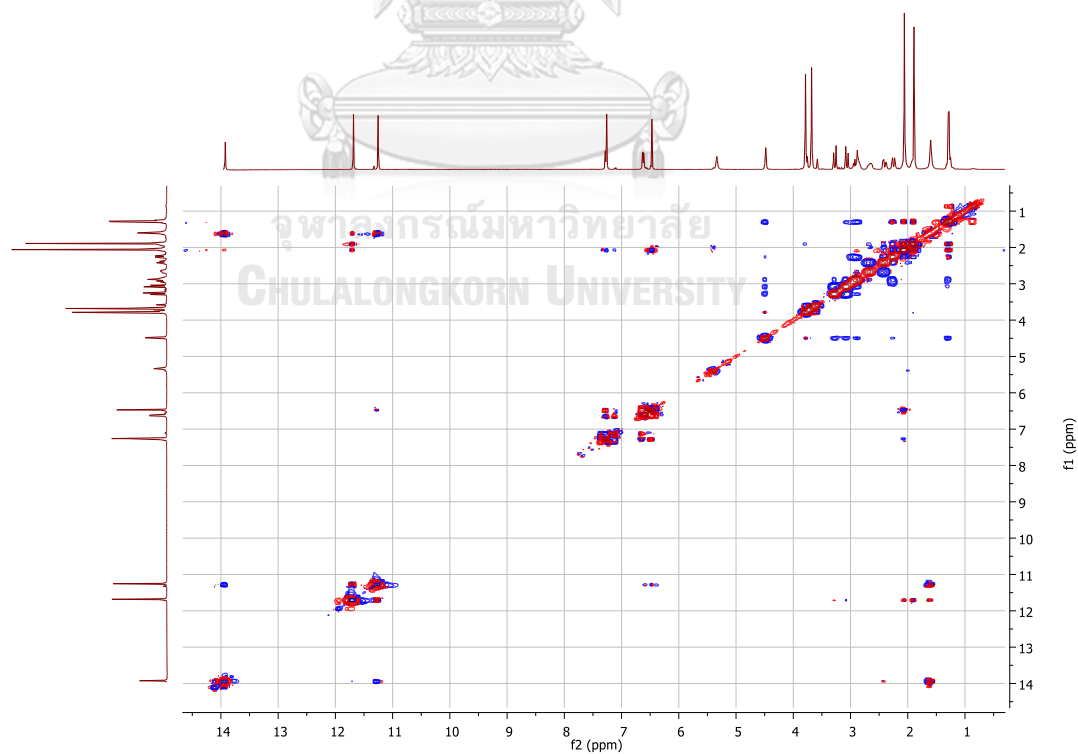


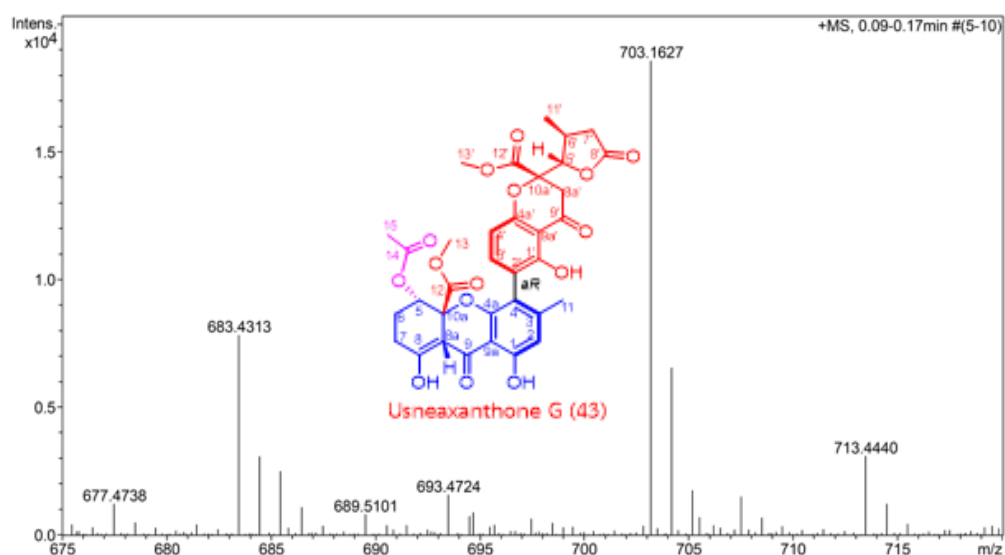
Figure A50. NOESY spectrum of usneaxanthone G (43) in  $\text{CDCl}_3$

## Generic Display Report

## Analysis Info

Analysis Name D:\Data\Data Service\190325\TT-030\_RD4\_01\_2384.d  
Method nv\_pos\_5min\_profile\_190214.m  
Sample Name TT-030  
Comment

Acquisition Date 3/25/2019 7:12:06 PM

Operator CU.  
Instrument micrOTOF-Q II

Bruker Compass DataAnalysis 4.0

printed: 3/25/2019 7:27:44 PM

Page 1 of 1

Figure A51. HRESIMS spectrum of usneaxanthone G (43)





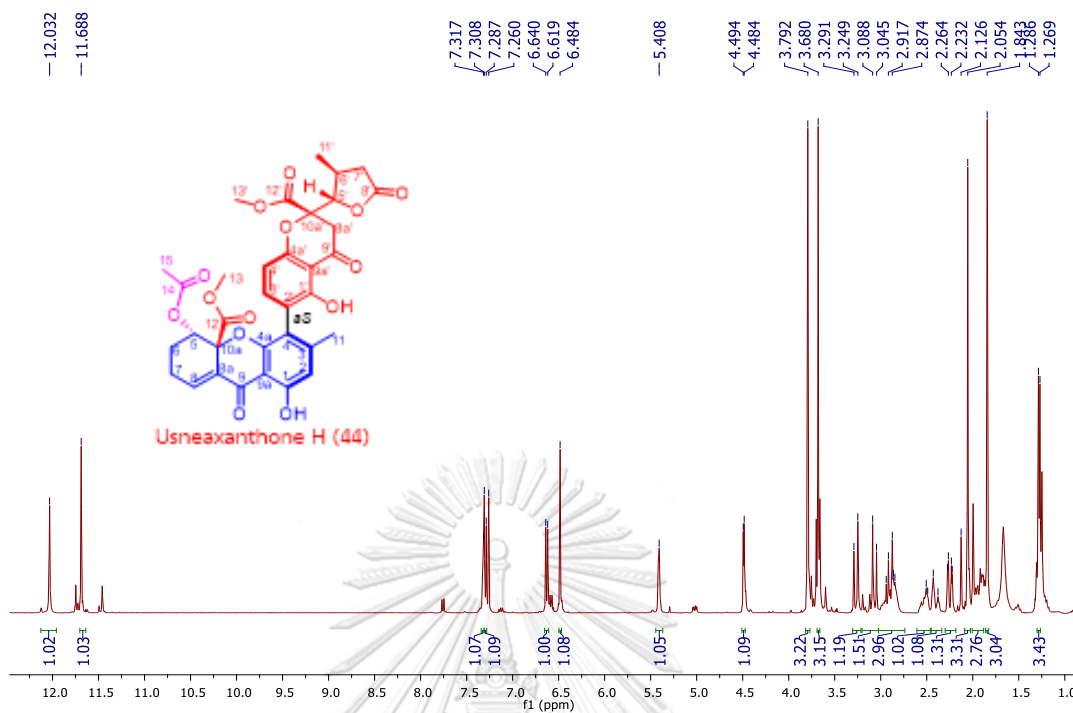


Figure A52.  $^1\text{H}$  NMR spectrum of usneaxanthone H (44) in  $\text{CDCl}_3$

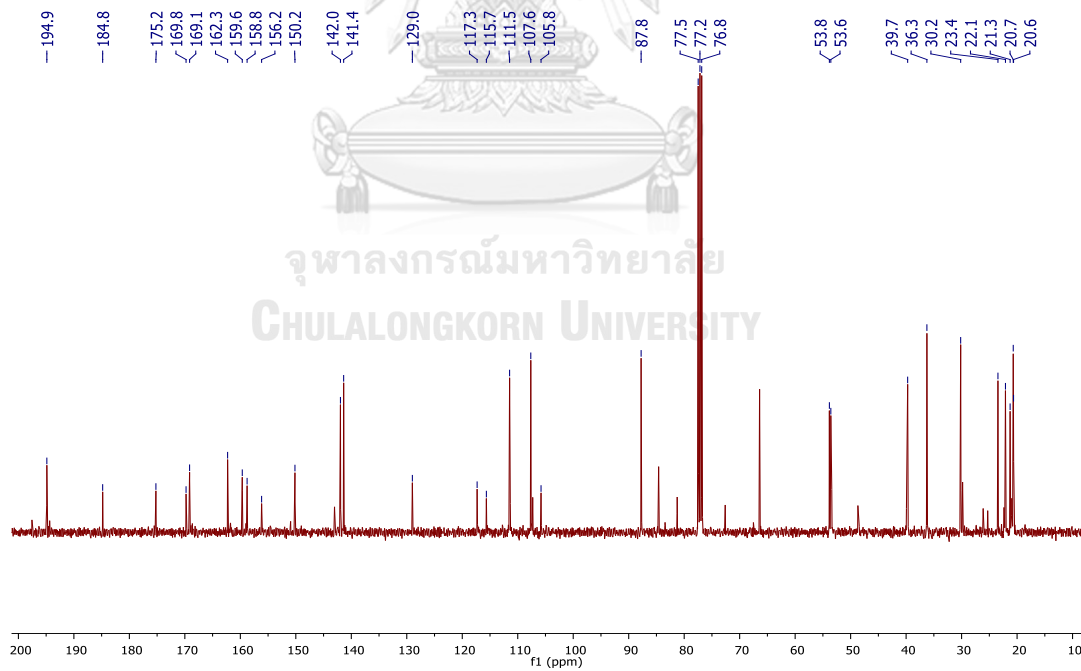
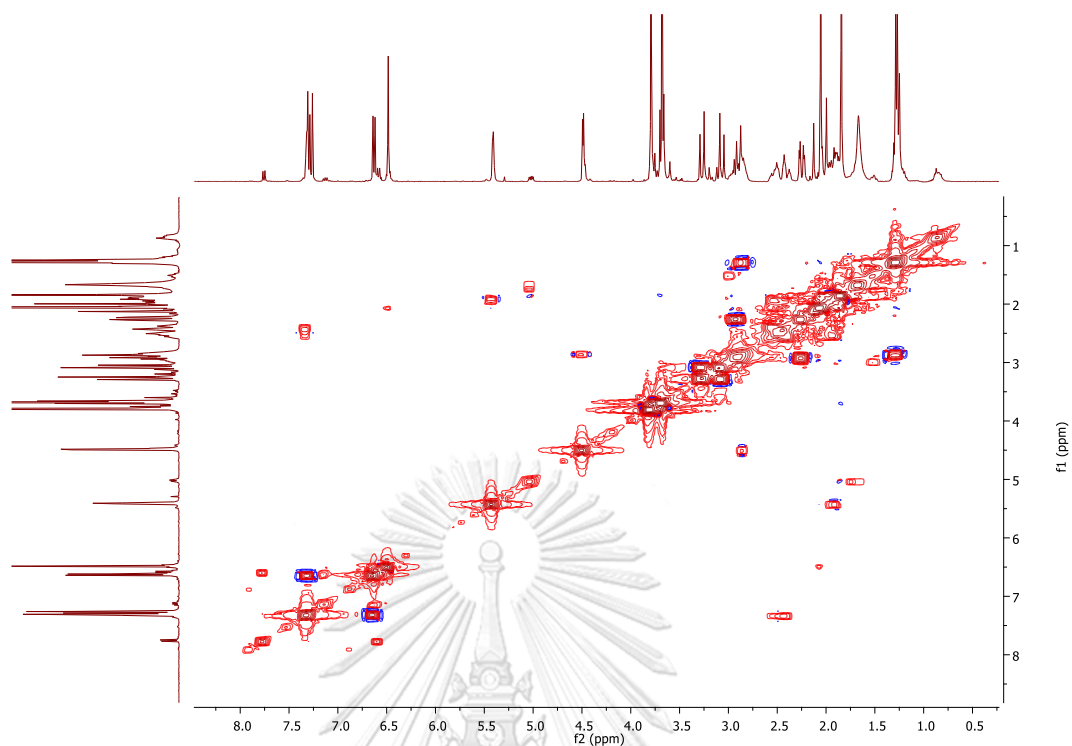
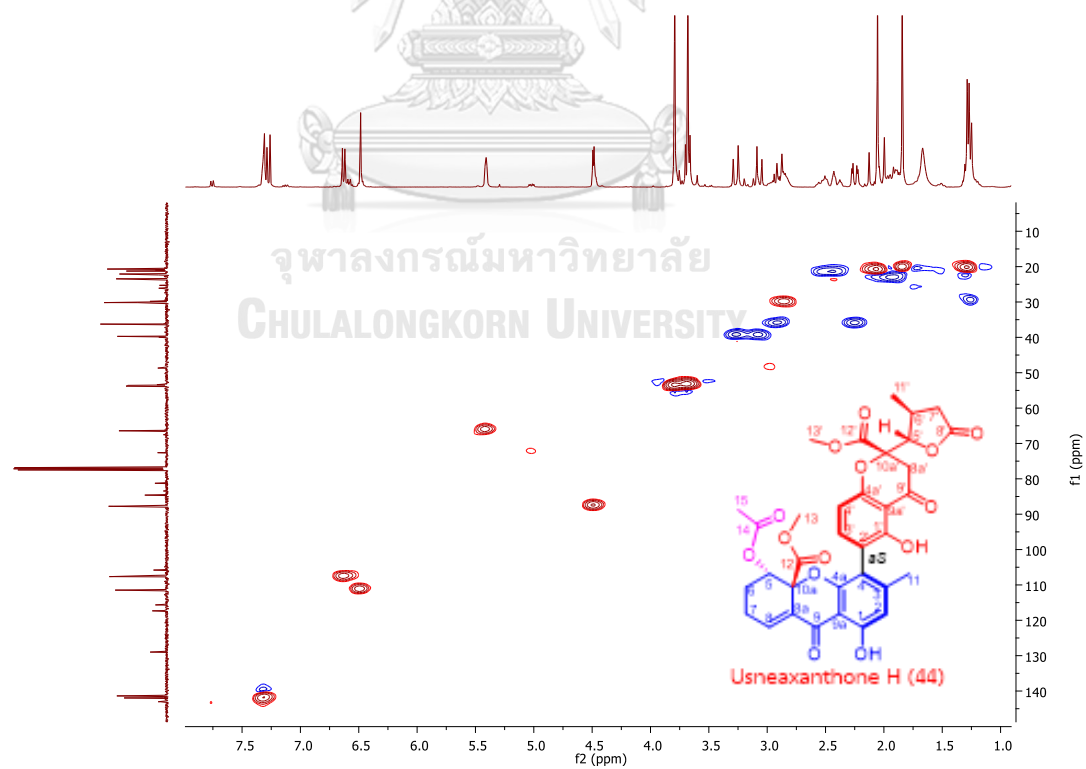


Figure A53.  $^{13}\text{C}$  NMR spectrum of usneaxanthone H (44) in  $\text{CDCl}_3$

Figure A54. COSY spectrum of usneaxanthone H (44) in CDCl<sub>3</sub>Figure A55. HSQC spectrum of usneaxanthone H (44) in CDCl<sub>3</sub>

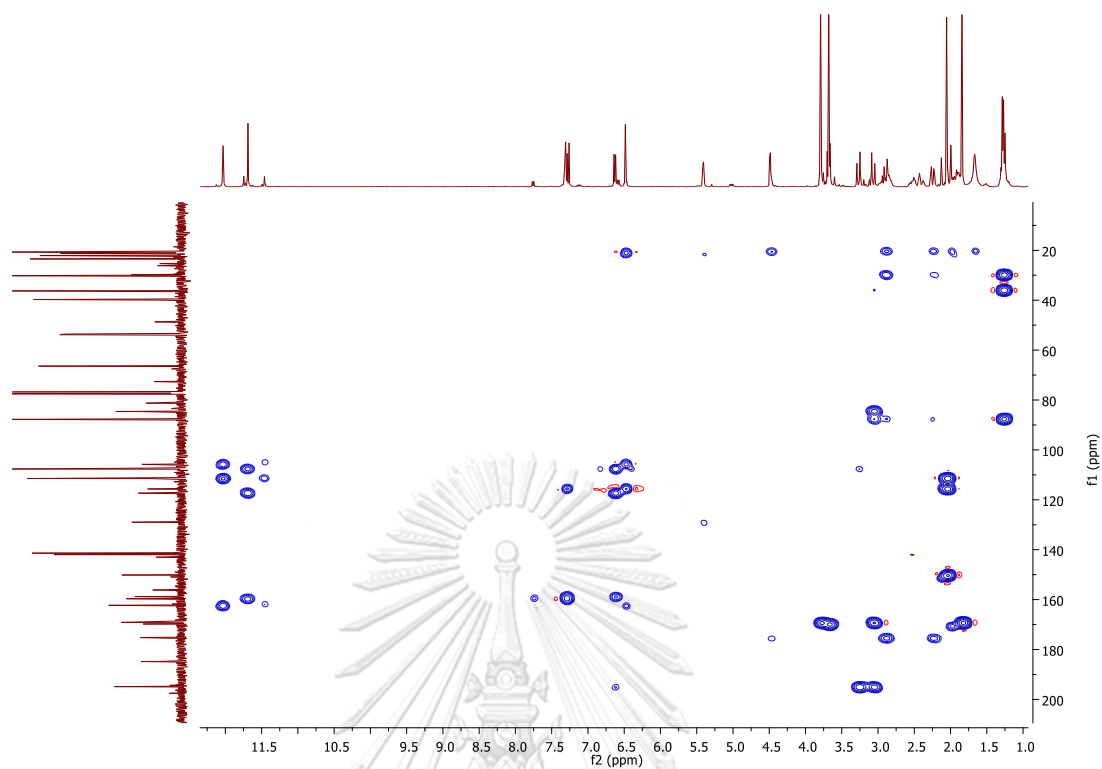


Figure A56. HMBC spectrum of usneaxanthone H (44) in  $\text{CDCl}_3$

## Generic Display Report

<b>Analysis Info</b>	Acquisition Date	12/14/2017 12:20:35 PM	
Analysis Name	D:\Data\Data Service\171214_pos_TT005.d		
Method	NV_pos_0.3min_profile_1segment_lowNubulizerDrygas.m	Operator	CU.
Sample Name	171214_pos_TT005	Instrument	micrOTOF-Q II
Comment			

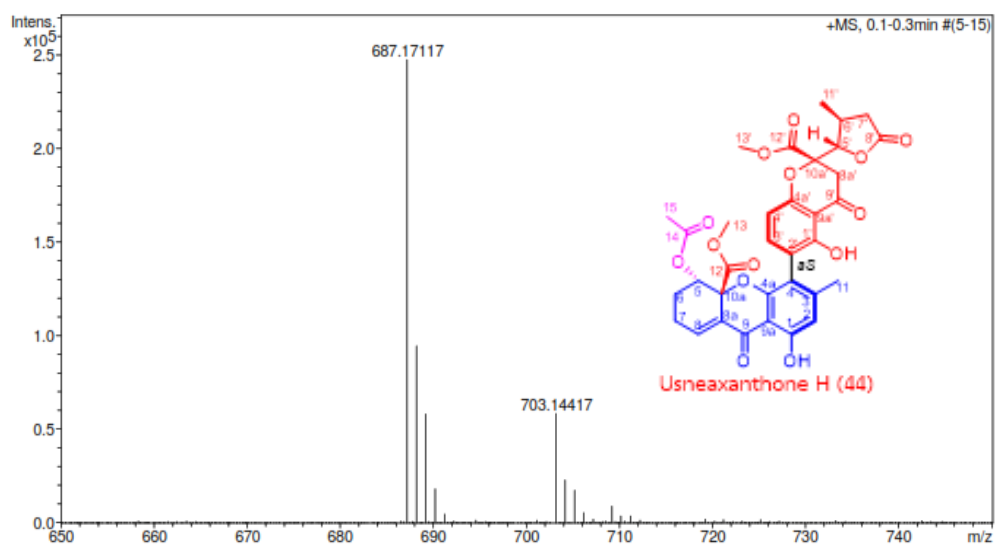
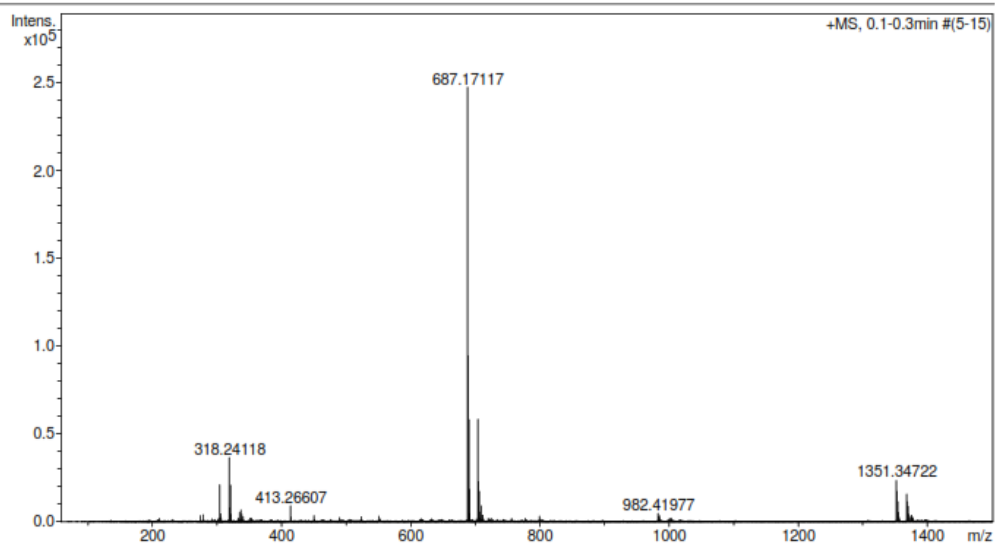
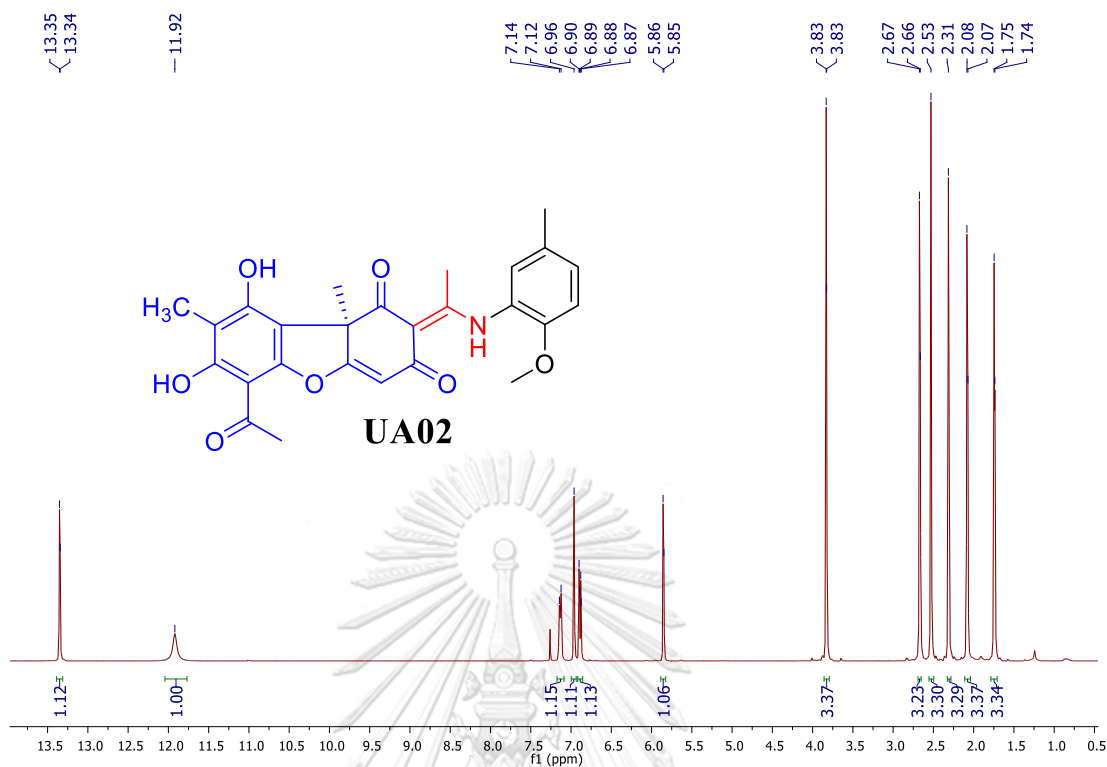
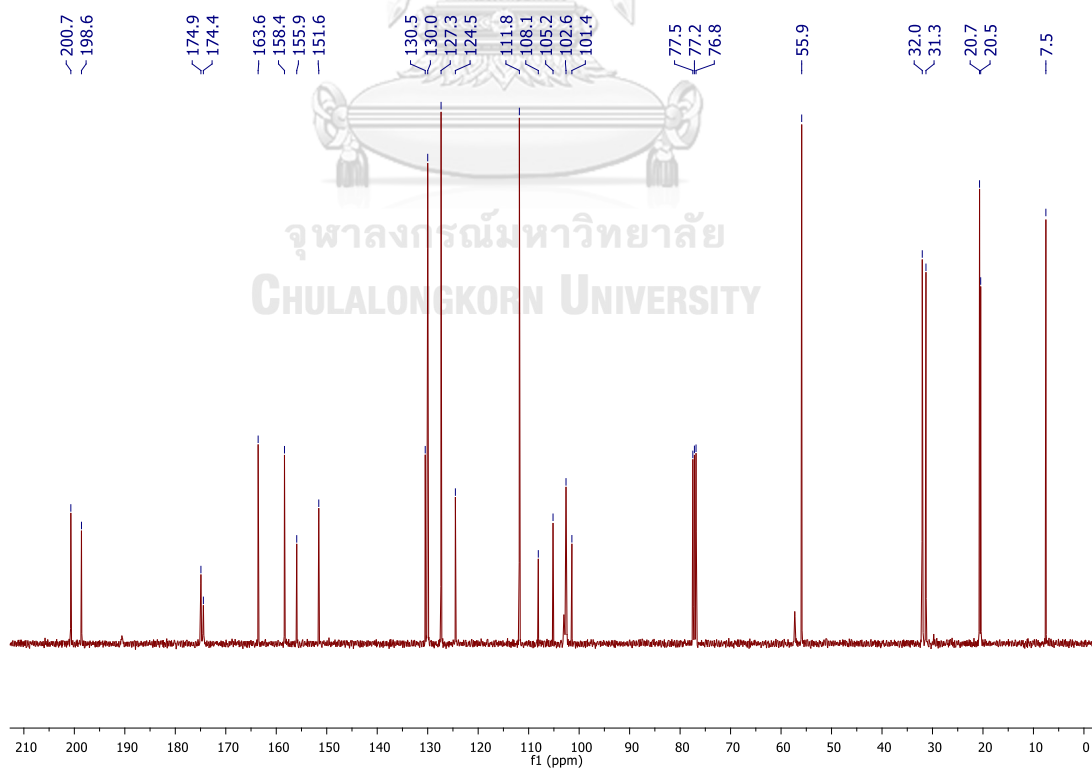


Figure A57. HRESIMS spectrum of usneaxanthone H (44)

Figure A58.  $^1\text{H}$  NMR spectrum of UA02 in  $\text{CDCl}_3$ Figure A59.  $^{13}\text{C}$  NMR spectrum of UA02 in  $\text{CDCl}_3$

## Generic Display Report

## Analysis Info

Analysis Name	D:\Data\Data Service\180730_pos_TT-UA001-3.d	Acquisition Date	7/30/2018 11:10:14 AM
Method	NV_pos_0.3min_profile_1segment_lowNubulizerDrygas.m	Operator	CU.
Sample Name	180730_pos_TT-UA001-3	Instrument	micrOTOF-Q II
Comment			

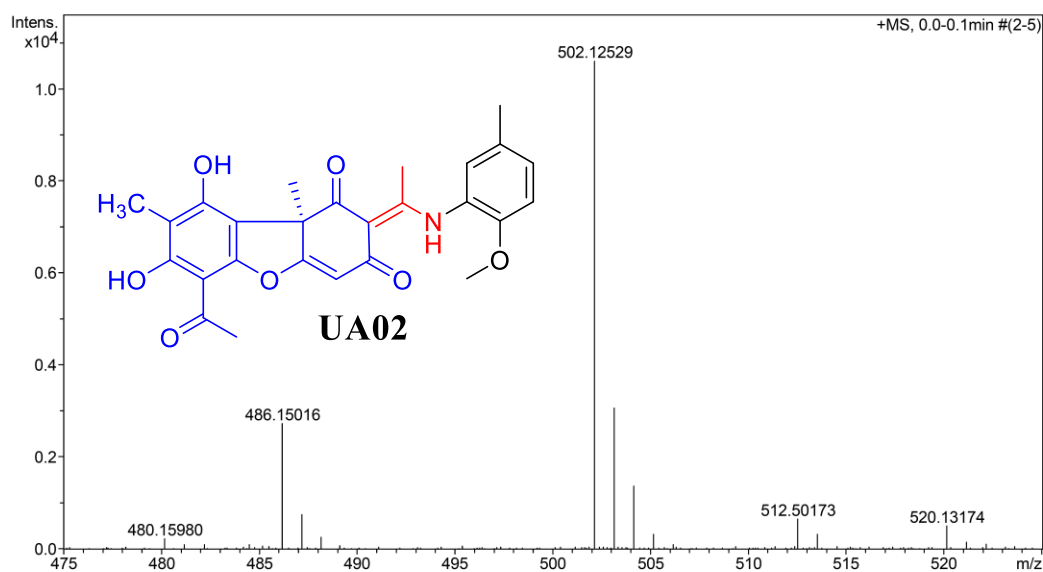
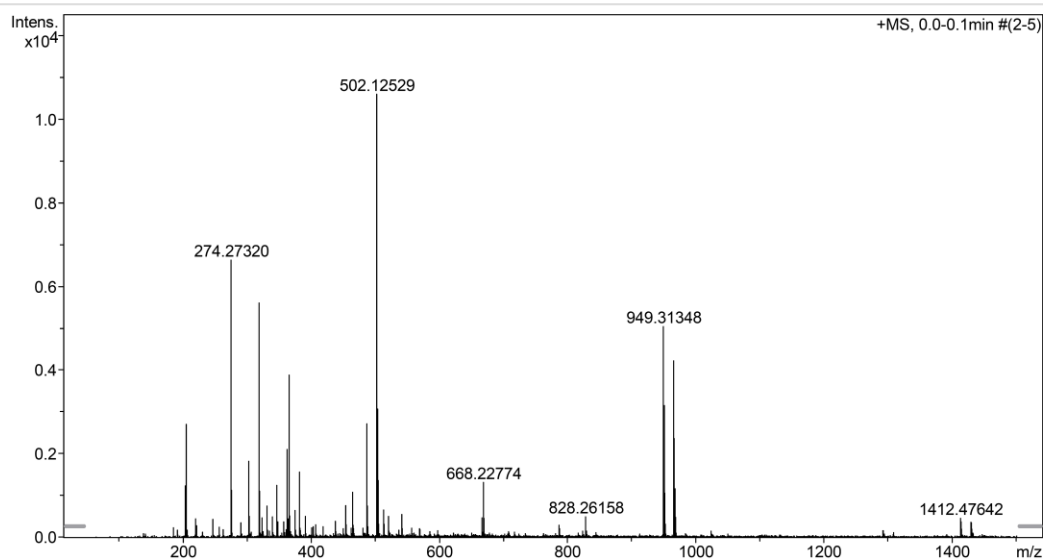
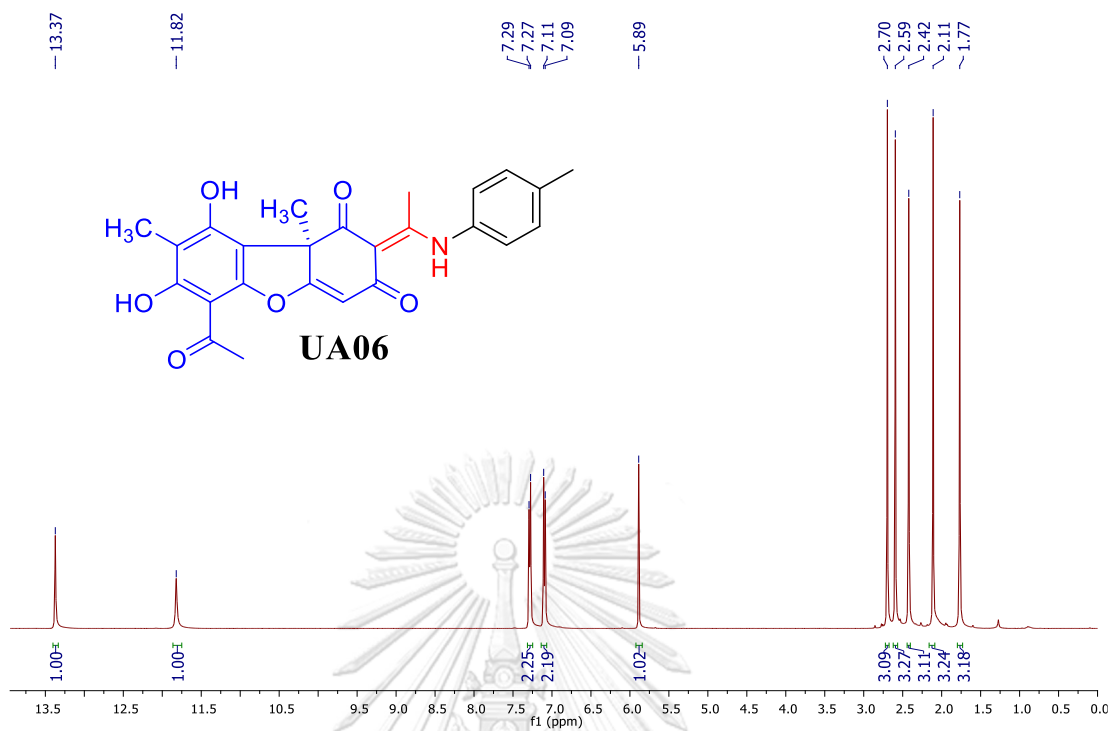
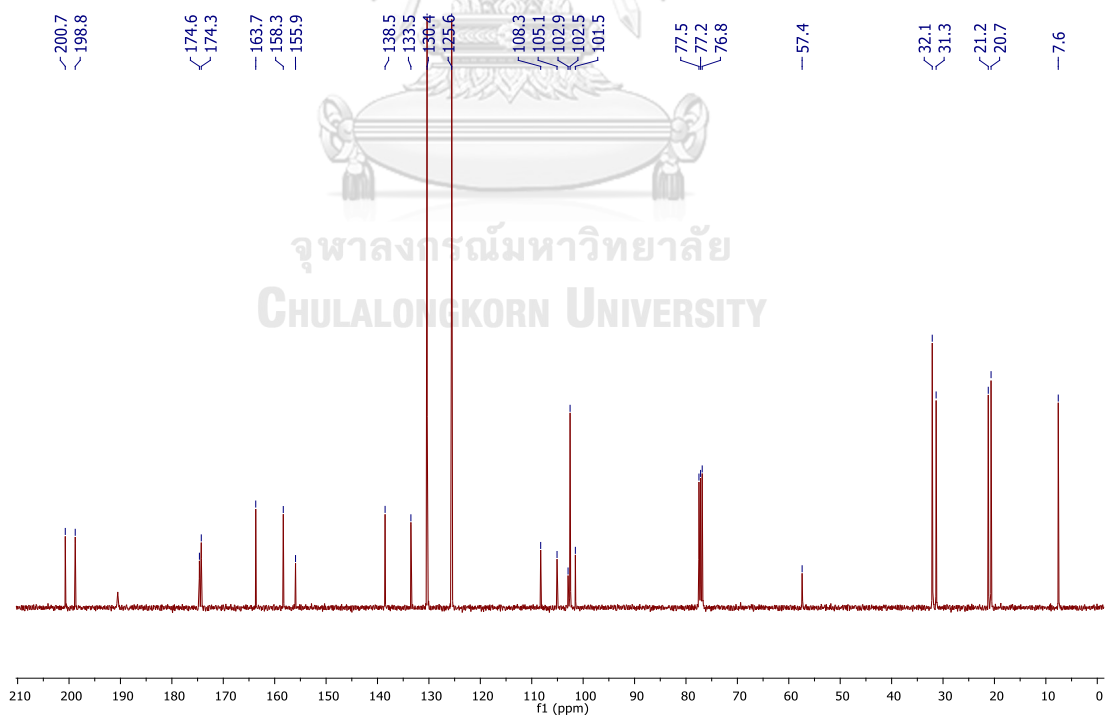


Figure A60. HRESIMS spectrum of UA02

Figure A61.  $^1\text{H NMR}$  spectrum of UA06 in  $\text{CDCl}_3$ Figure A62.  $^{13}\text{C NMR}$  spectrum of UA06 in  $\text{CDCl}_3$

## Generic Display Report

## Analysis Info

Analysis Name D:\Data\Data Service\180730\_pos\_TT-UA005.d  
Method NV\_pos\_0.3min\_profile\_1segment\_lowNbulizerDrygas.m  
Sample Name 180730\_pos\_TT-UA005  
Comment

Acquisition Date 7/30/2018 11:27:05 AM

Operator CU.  
Instrument micrOTOF-Q II

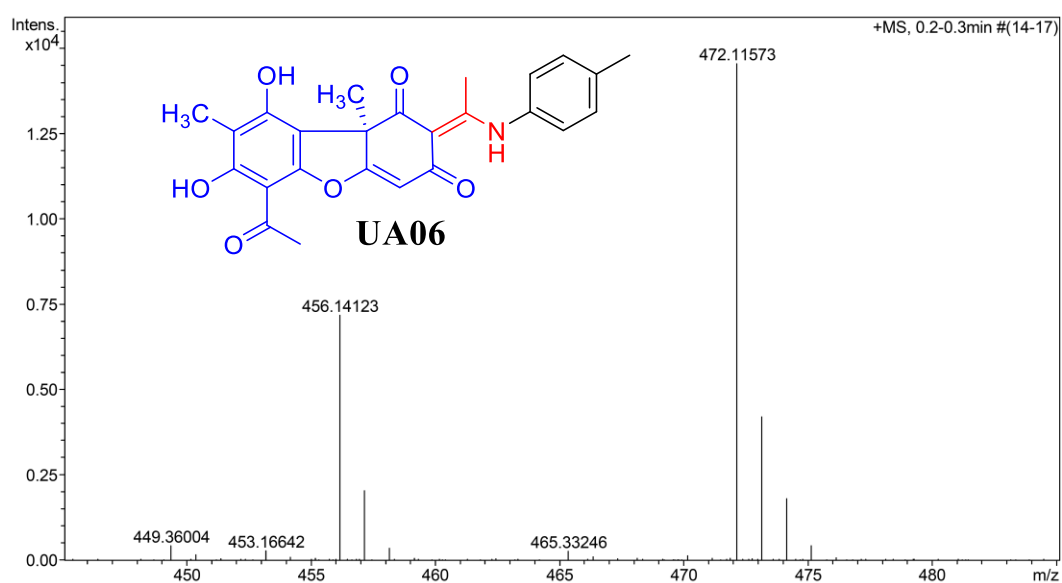
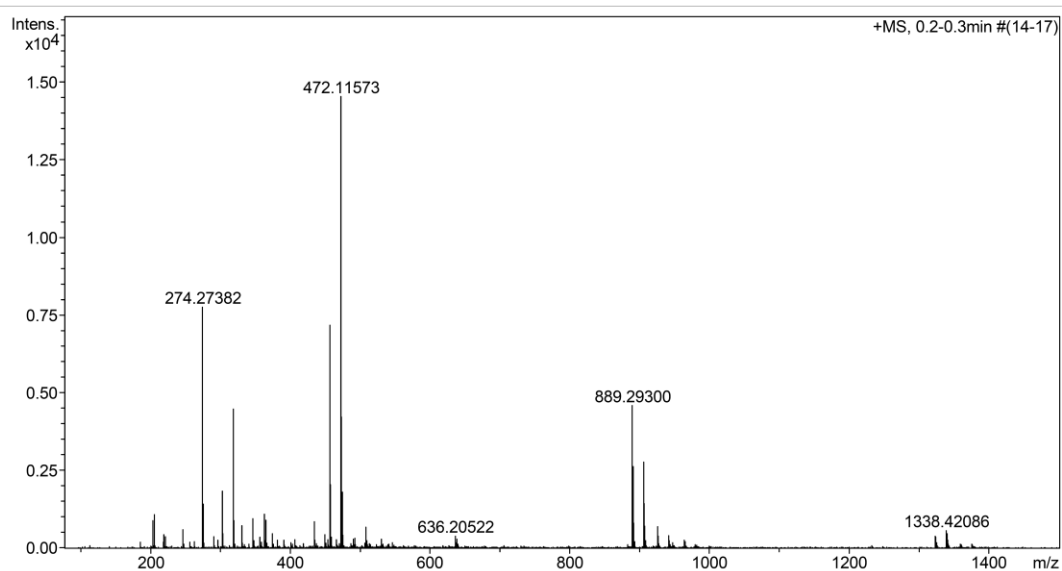
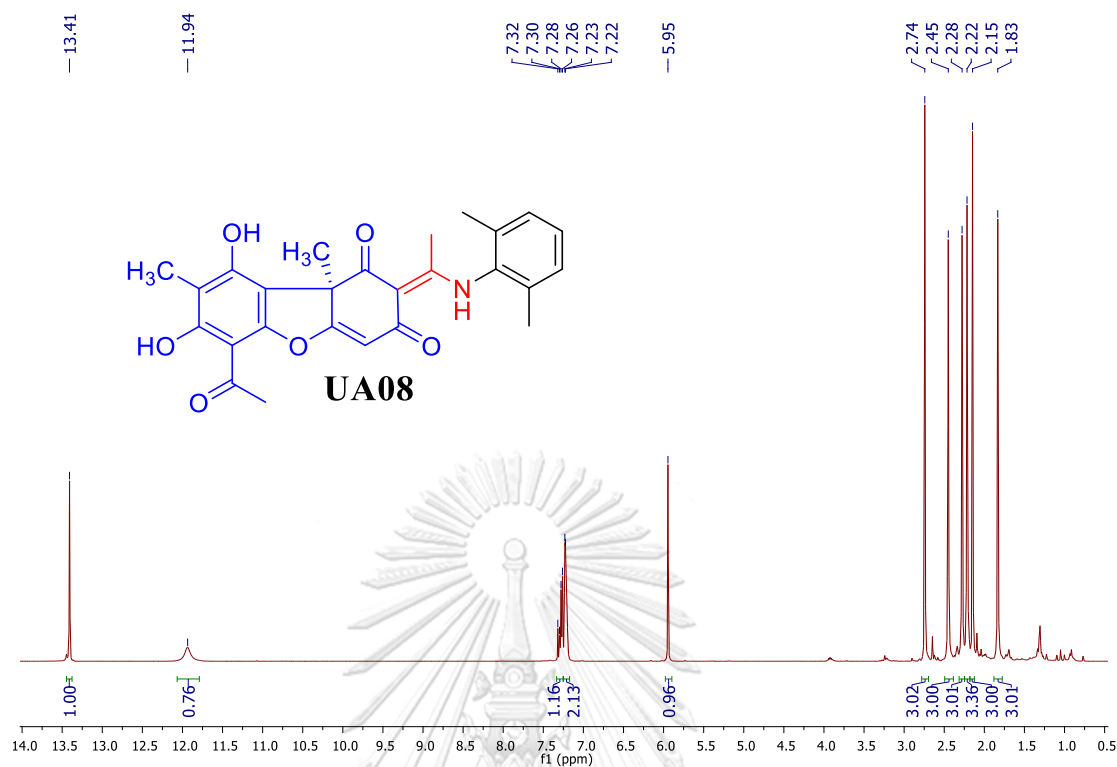
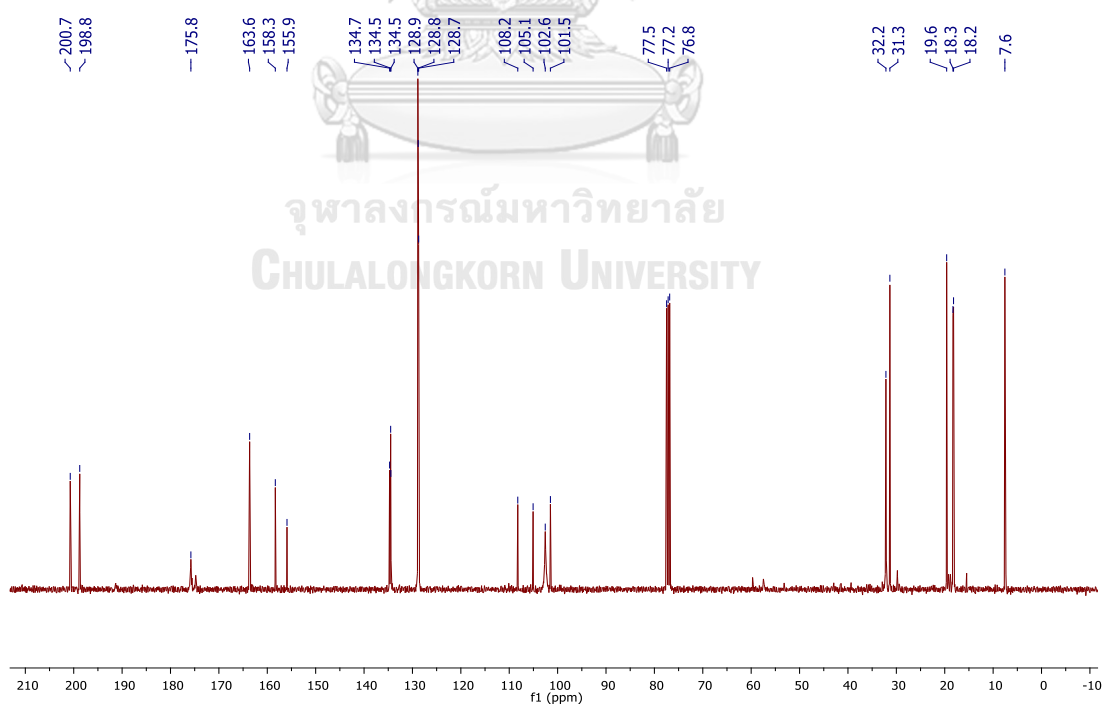
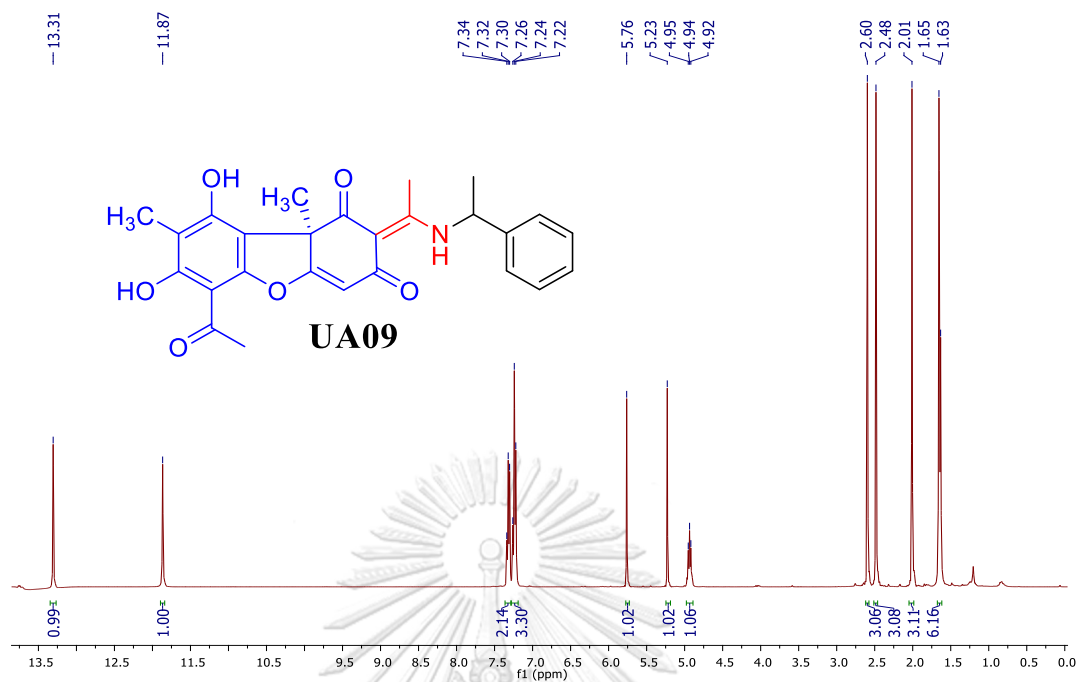
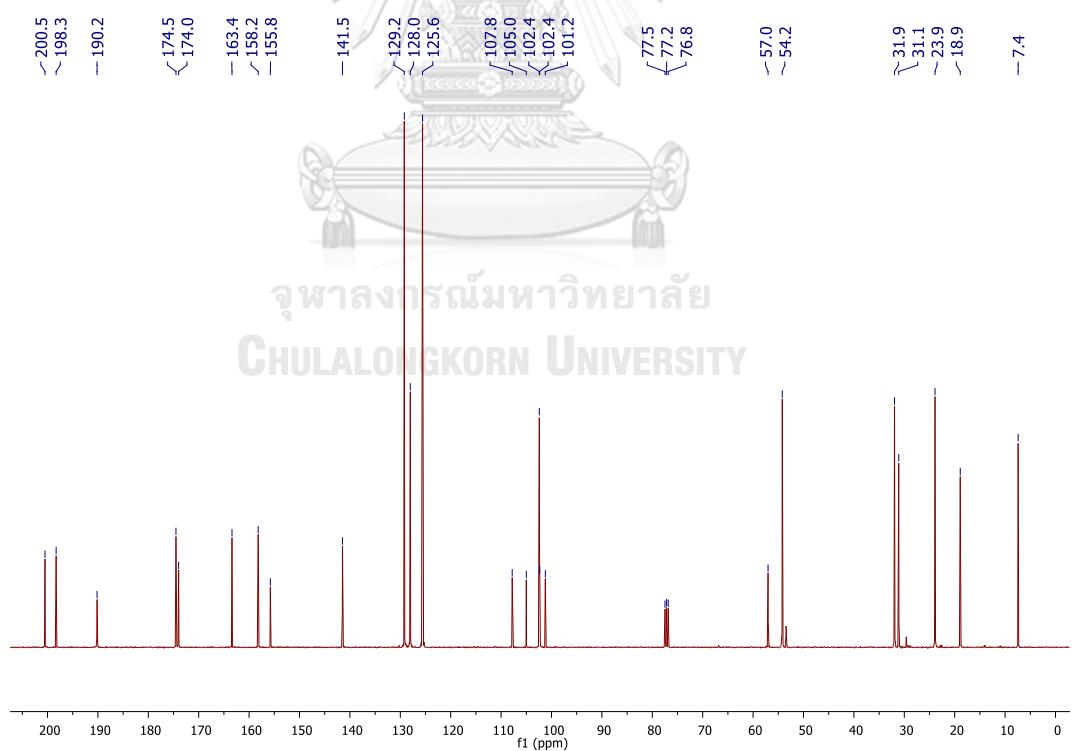
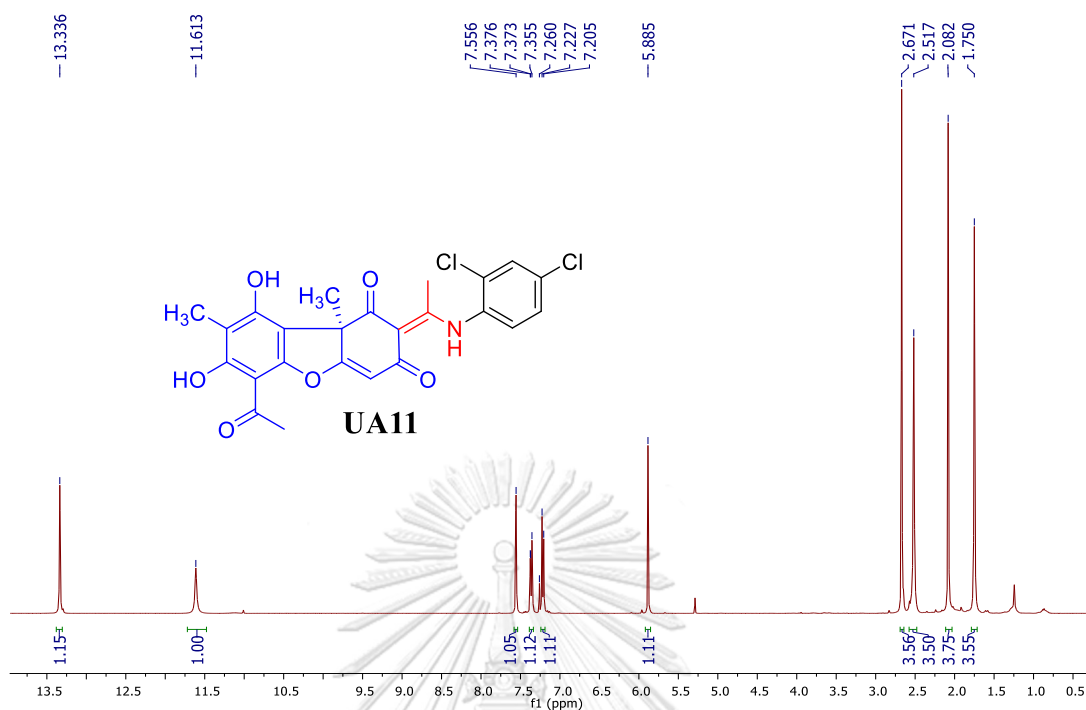
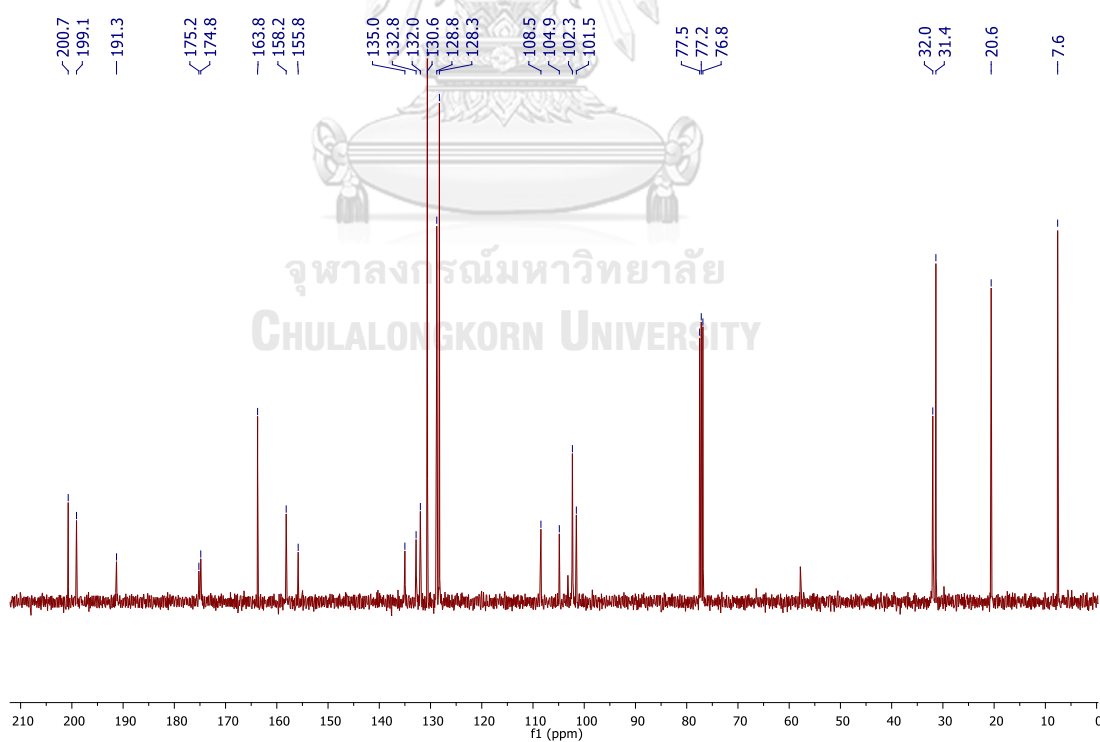


Figure A63. HRESIMS spectrum of UA06



Fig. A64. <sup>1</sup>H NMR spectrum of UA08 in CDCl<sub>3</sub>Fig. A65. <sup>13</sup>C NMR spectrum of UA08 in CDCl<sub>3</sub>

Fig. A67. <sup>1</sup>H NMR spectrum of UA9 in CDCl<sub>3</sub>Fig. A68. <sup>13</sup>C NMR spectrum of UA9 in CDCl<sub>3</sub>

Fig. A69. <sup>1</sup>H NMR spectrum of UA11 in CDCl<sub>3</sub>Fig. A70. <sup>13</sup>C NMR spectrum of UA11 in CDCl<sub>3</sub>

## Generic Display Report

## Analysis Info

Analysis Name D:\Data\Data Service\181112pos\_TT-UA008.d  
Method NV\_pos\_0.3min\_profile\_1segment\_lowNubulizerDrygas.m  
Sample Name 181112pos\_TT-UA008  
Comment

Acquisition Date 11/12/2018 3:36:08 PM

Operator CU.  
Instrument micrOTOF-Q II

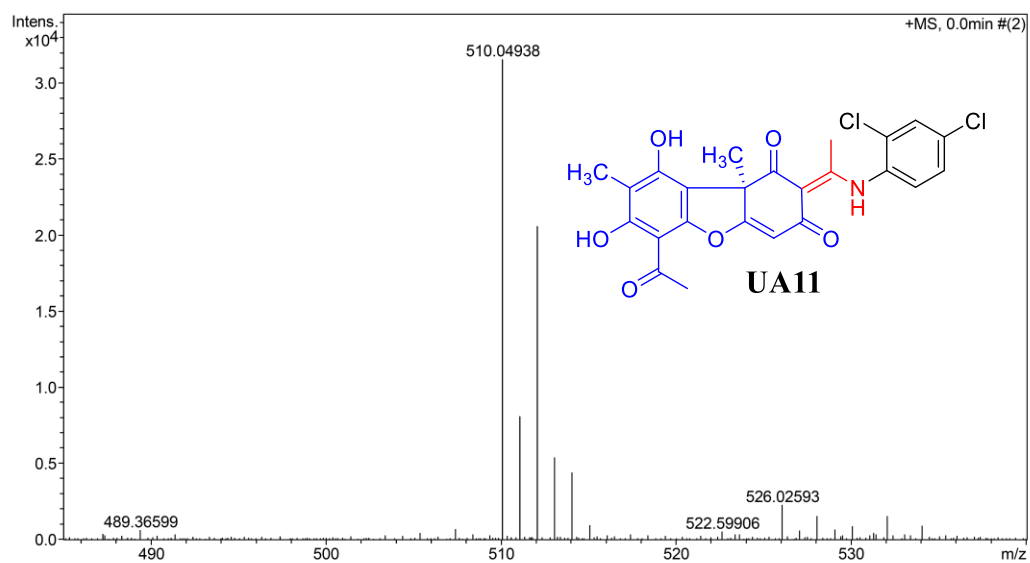
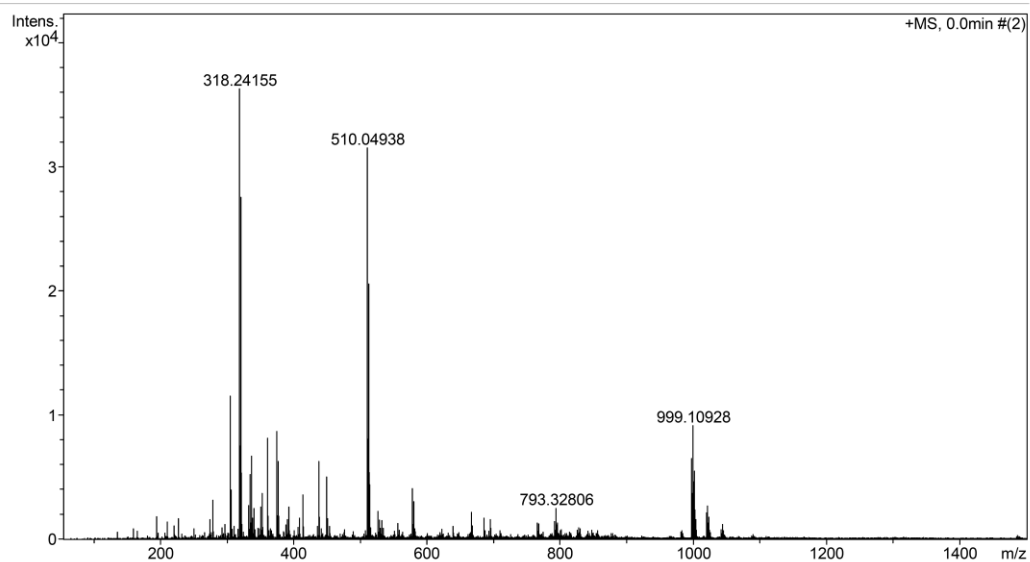
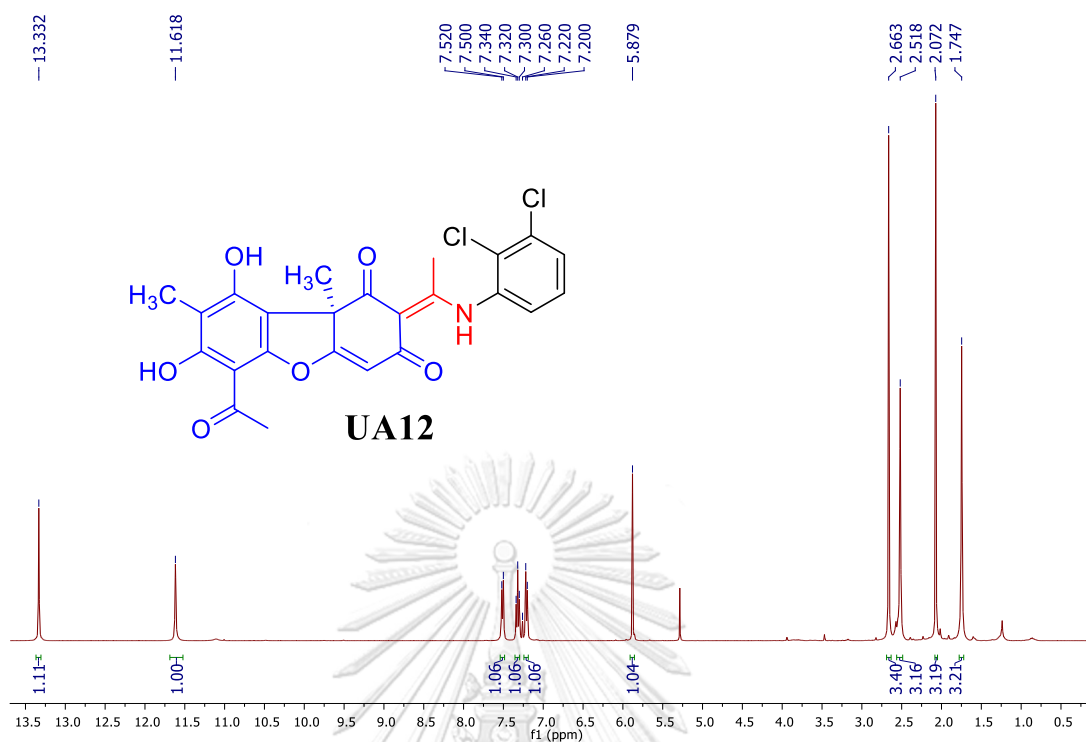
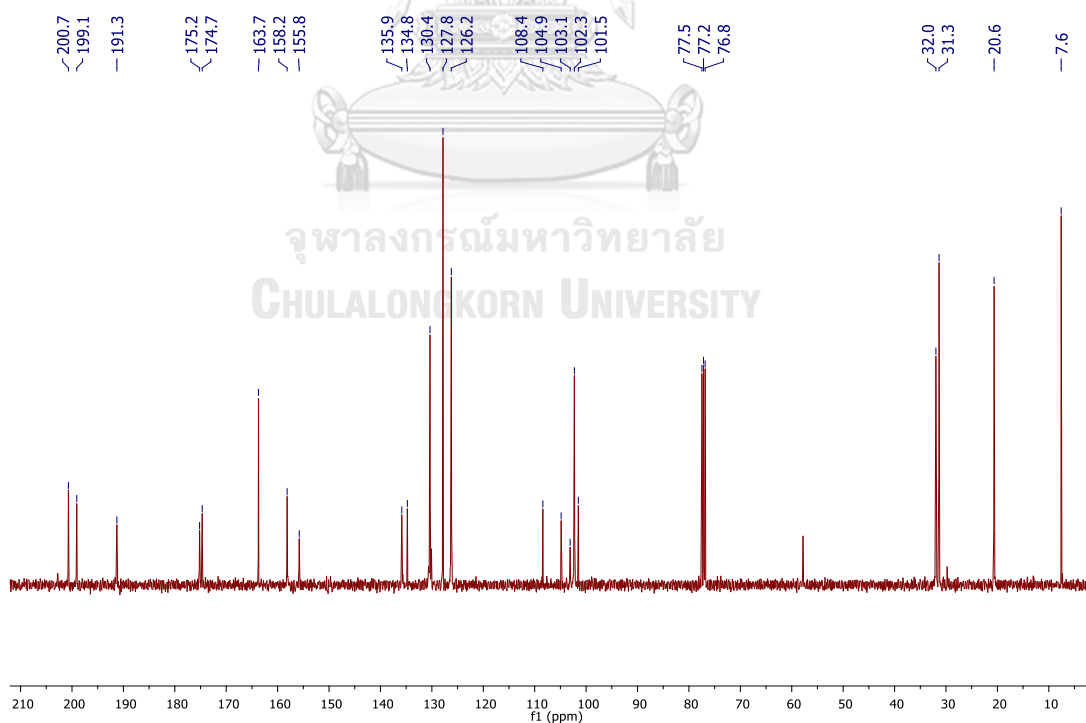


Figure A71. HRESIMS spectrum of UA11

Fig. A72. <sup>1</sup>H NMR spectrum of UA12 in CDCl<sub>3</sub>Fig. A73. <sup>13</sup>C NMR spectrum of UA12 in CDCl<sub>3</sub>

## Generic Display Report

## Analysis Info

Analysis Name D:\Data\Data Service\180730\_pos\_TT-UA003-2.d  
Method NV\_pos\_0.3min\_profile\_1segment\_lowNubulizerDrygas.m  
Sample Name 180730\_pos\_TT-UA003-2  
Comment

Acquisition Date 7/30/2018 11:19:41 AM

Operator CU.  
Instrument micrOTOF-Q II

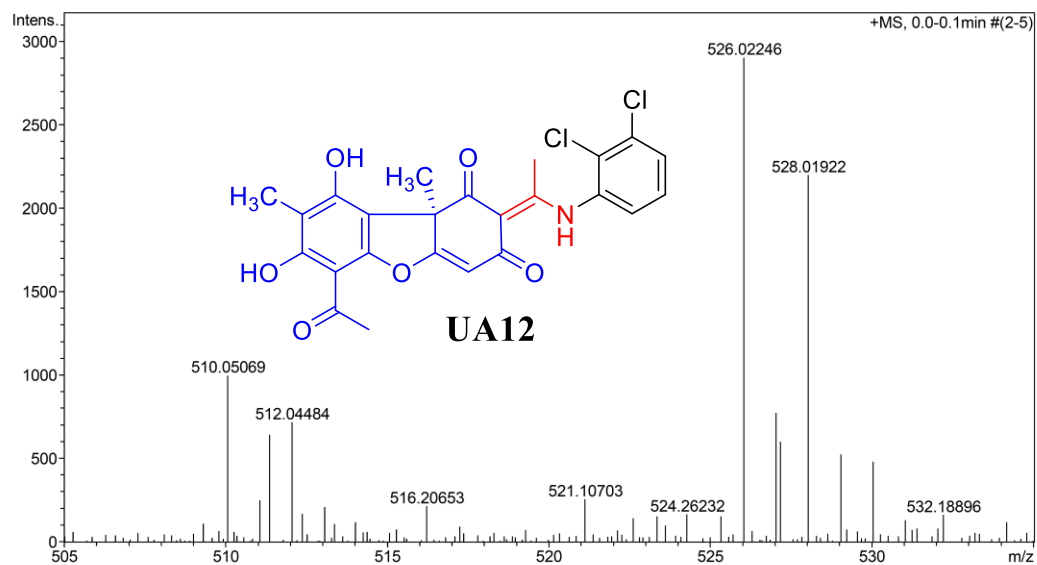
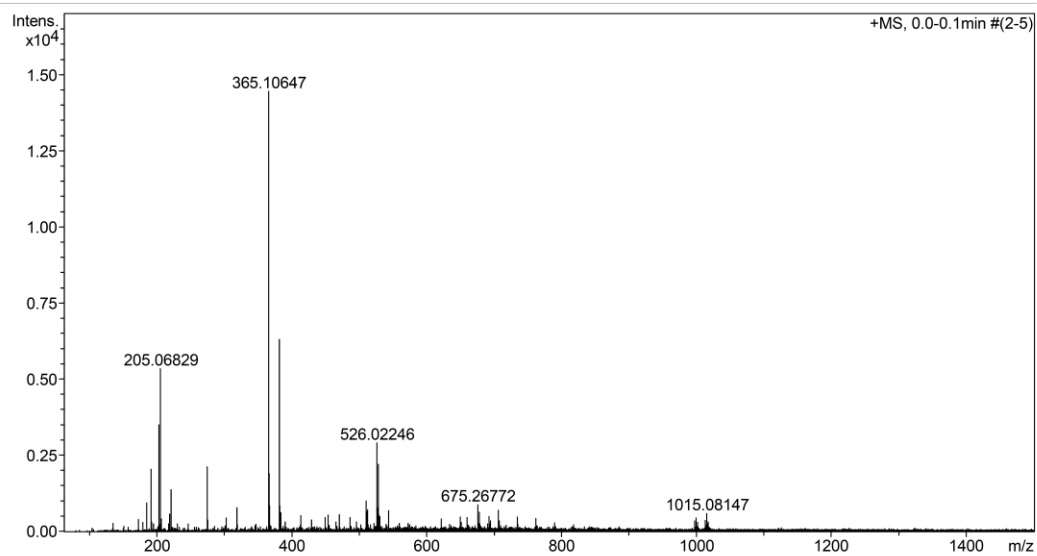
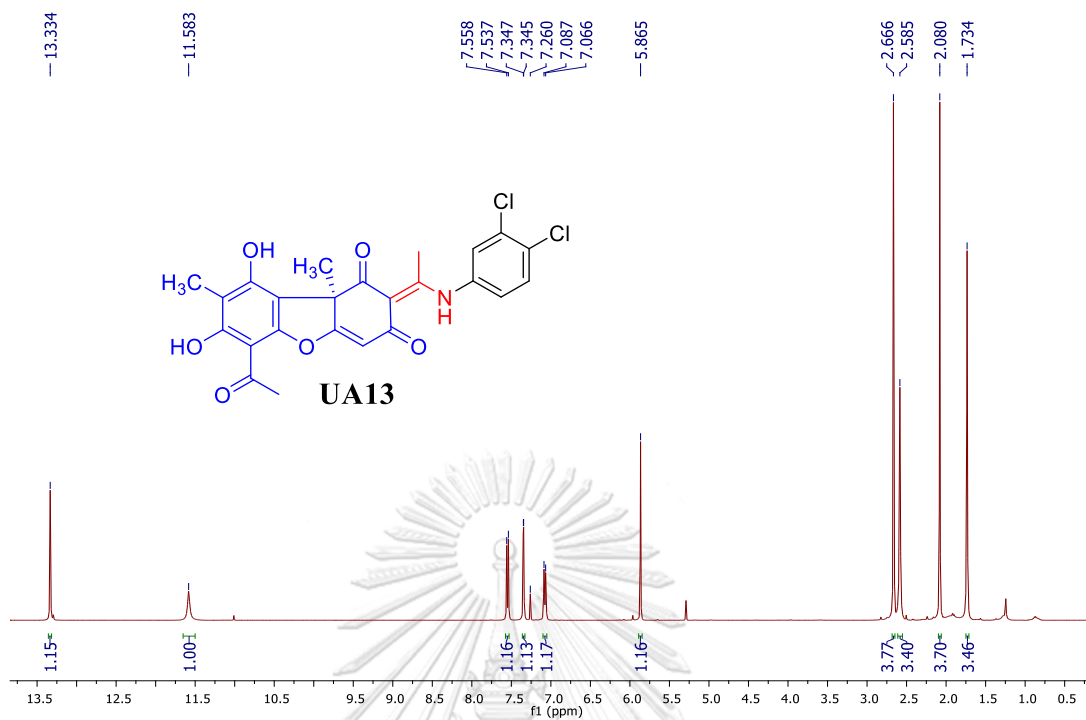
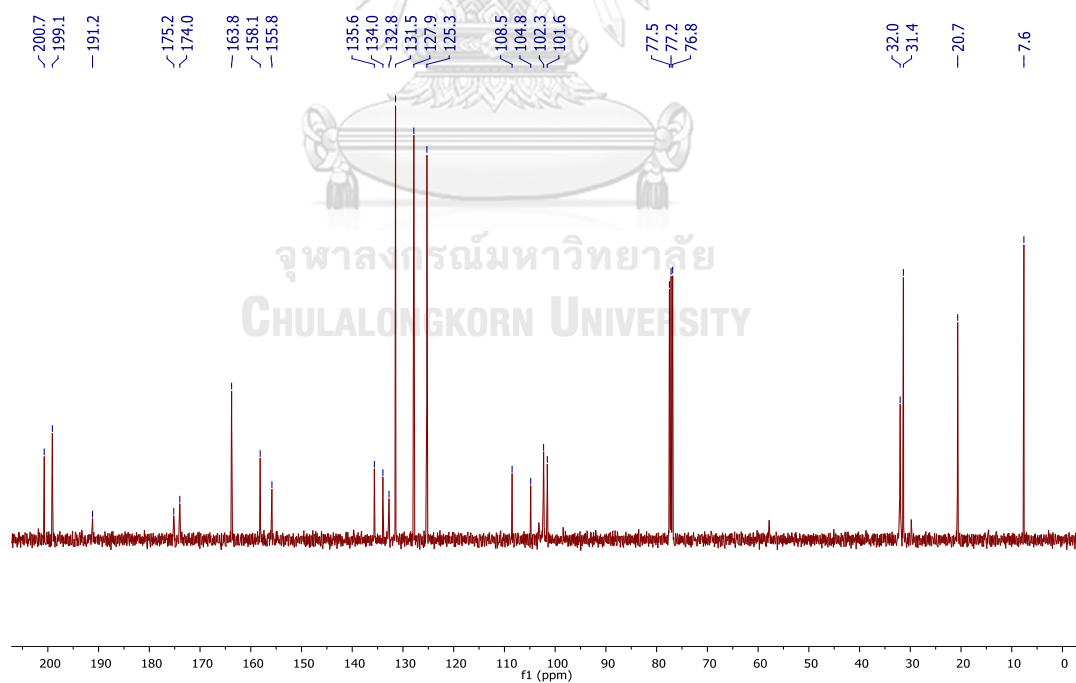


Fig. A74. HRESIMS spectrum of UA12

Fig. A75. <sup>1</sup>H NMR spectrum of UA13 in CDCl<sub>3</sub>Fig. A76. <sup>13</sup>C NMR spectrum of UA13 in CDCl<sub>3</sub>

## Generic Display Report

## Analysis Info

Analysis Name D:\Data\Data Service\181112pos\_TT-UA010.d  
Method NV\_pos\_0.3min\_profile\_1segment\_lowNubulizerDrygas.m  
Sample Name 181112pos\_TT-UA010  
Comment

Acquisition Date 11/12/2018 2:40:27 PM

Operator CU.  
Instrument micrOTOF-Q II

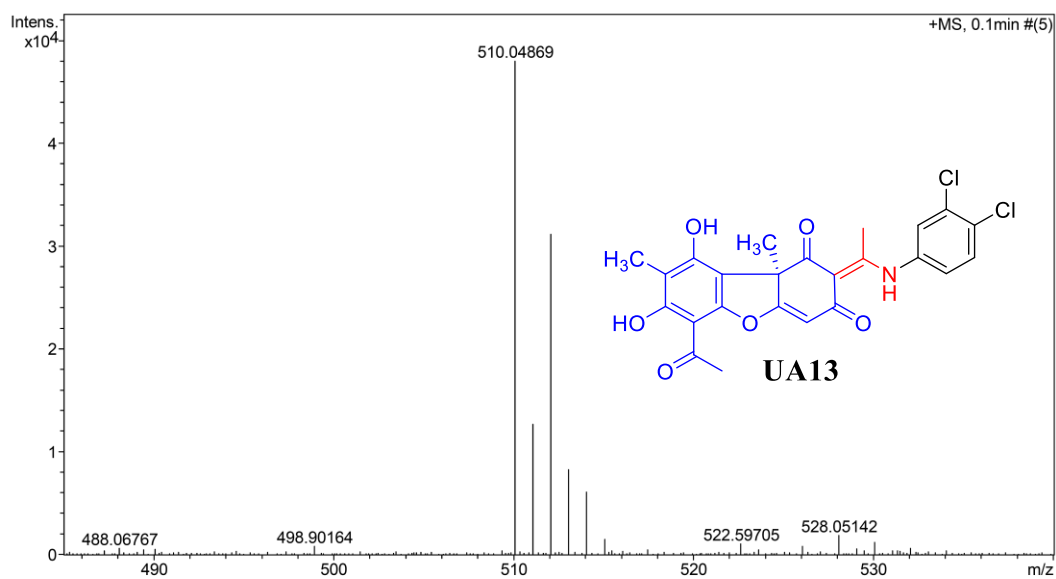
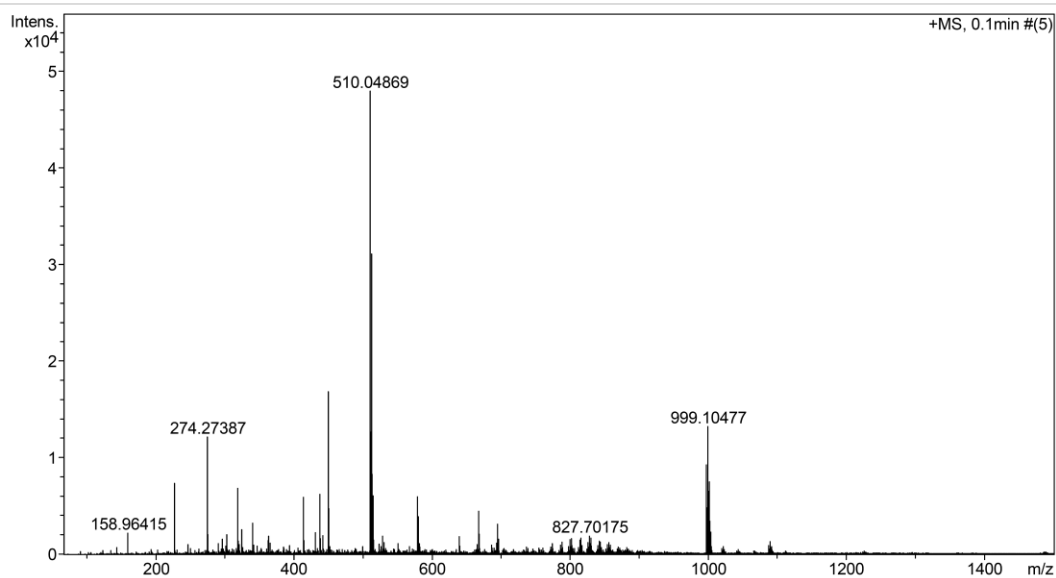
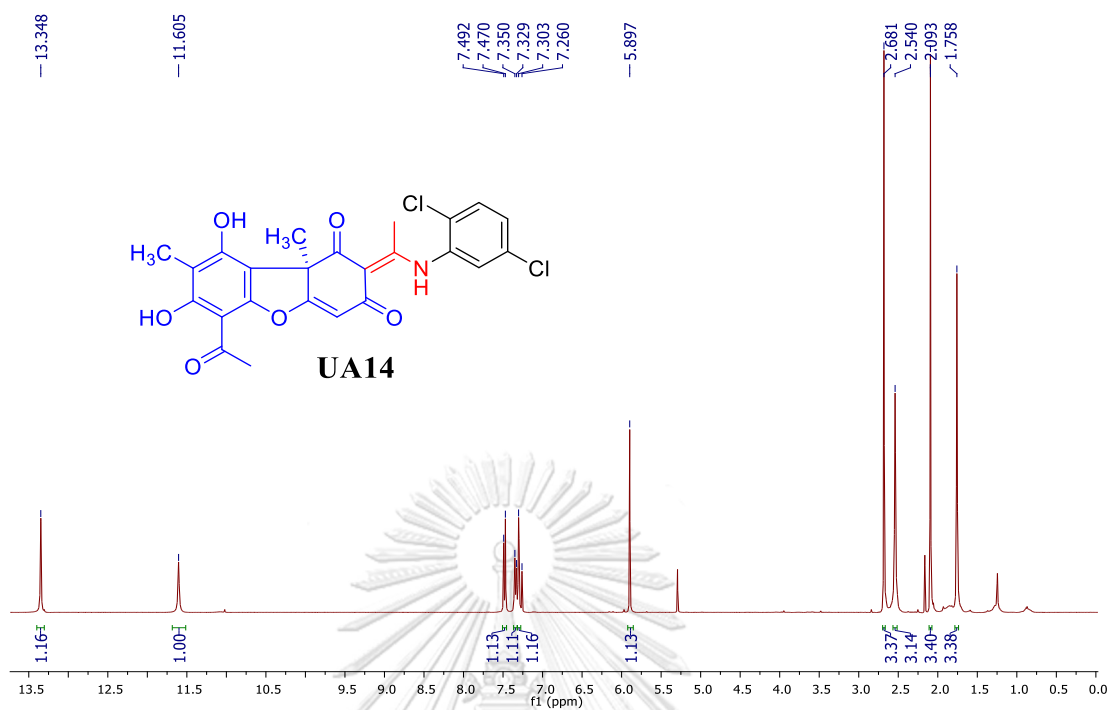
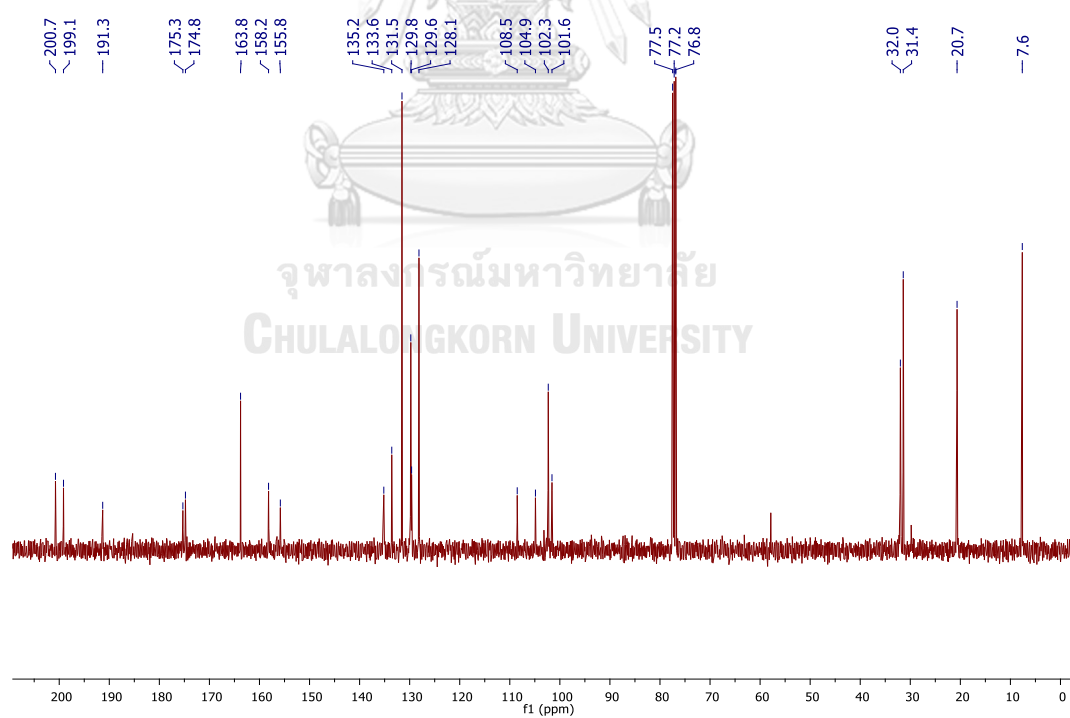


Fig. 77 HRESIMS spectrum of UA13



Fig. A78. <sup>1</sup>H NMR spectrum of UA14 in CDCl<sub>3</sub>Fig. A79. <sup>13</sup>C NMR spectrum of UA14 in CDCl<sub>3</sub>

## Generic Display Report

## Analysis Info

Analysis Name D:\Data\Data Service\181112pos\_TT-UA009.d  
Method NV\_pos\_0.3min\_profile\_1segment\_lowNubulizerDrygas.m  
Sample Name 181112pos\_TT-UA009  
Comment

Acquisition Date 11/12/2018 3:18:17 PM

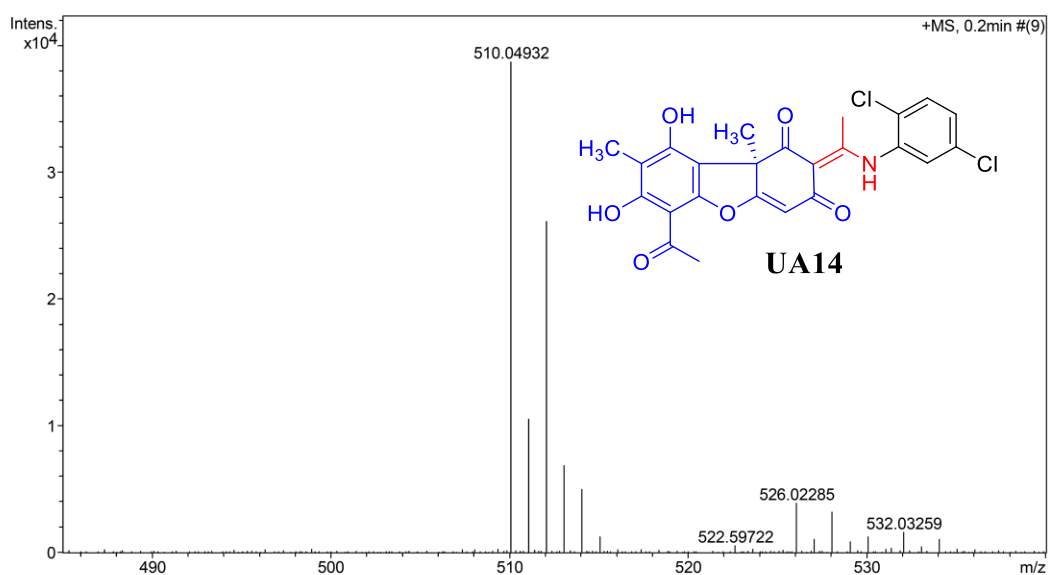
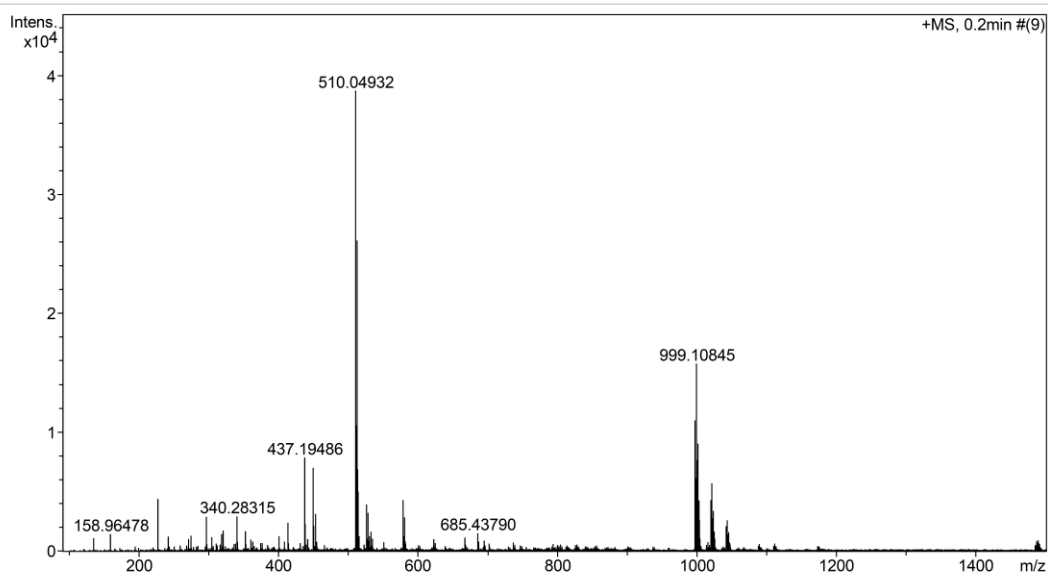
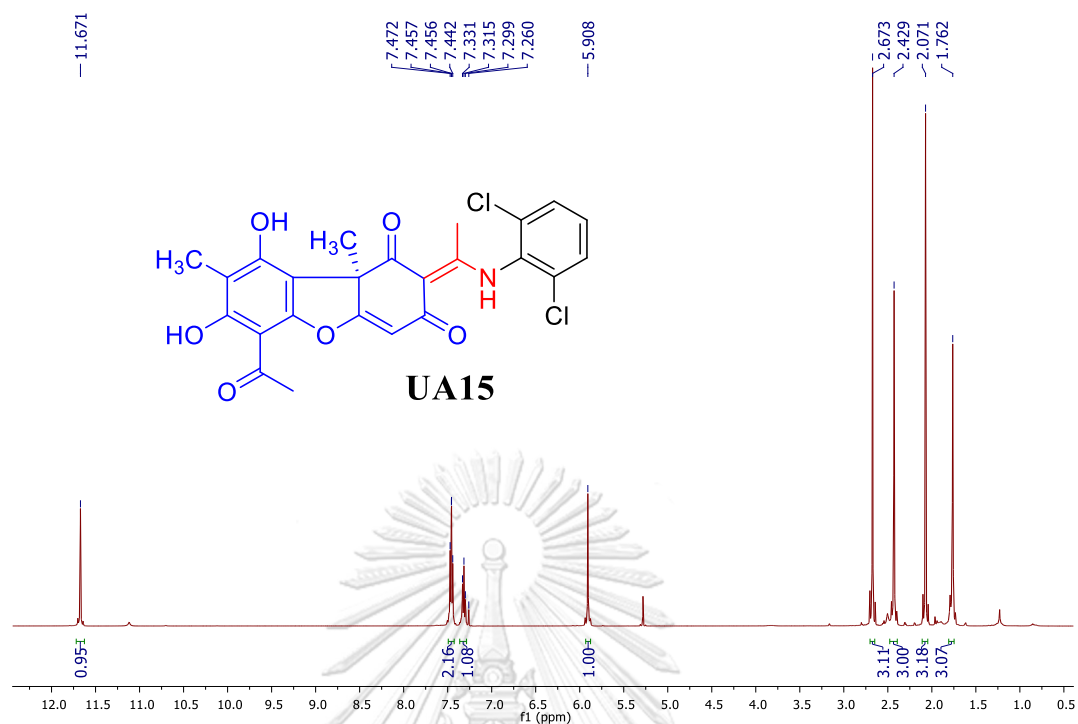
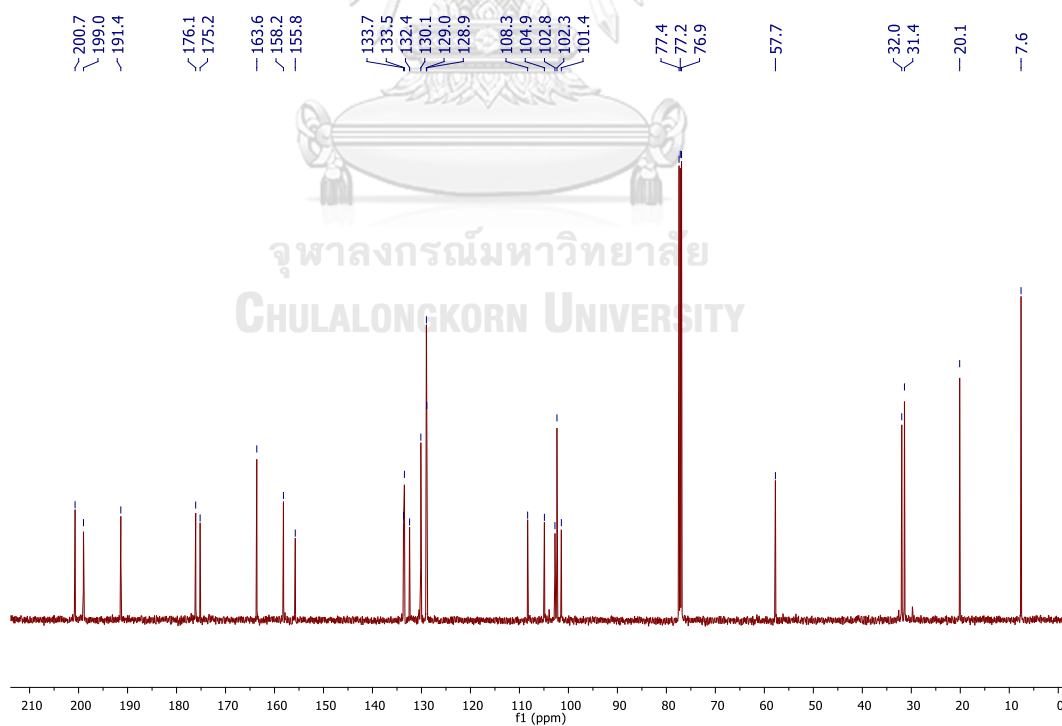
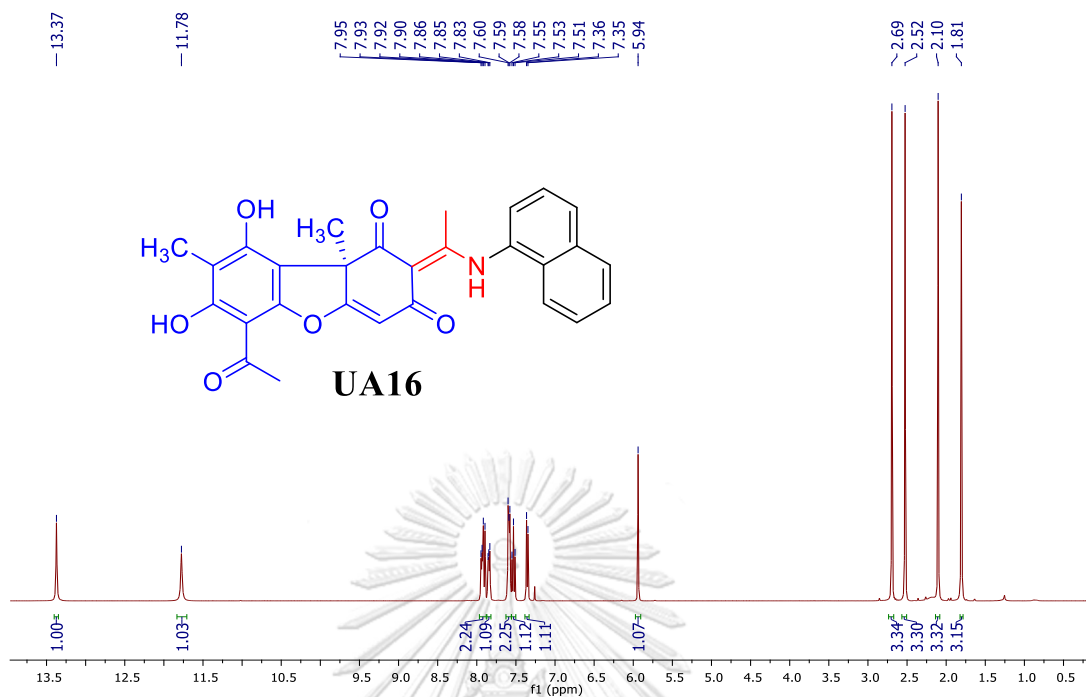
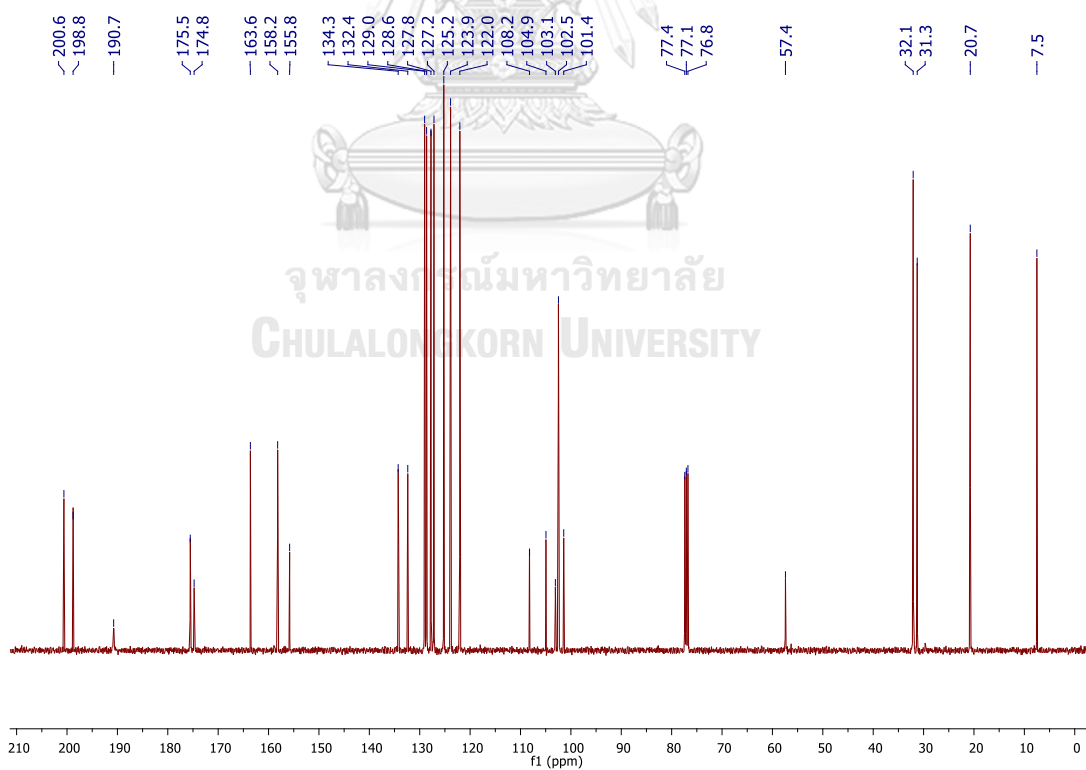
Operator CU.  
Instrument micrOTOF-Q II

Fig. A80. HRESIMS spectrum of UA14

Fig. A81. <sup>1</sup>H NMR spectrum of UA15 in CDCl<sub>3</sub>Fig. A82. <sup>13</sup>C NMR spectrum of UA15 in CDCl<sub>3</sub>

Fig. A83. <sup>1</sup>H NMR spectrum of UA16 in CDCl<sub>3</sub>Fig. A84. <sup>13</sup>C NMR spectrum of UA16 in CDCl<sub>3</sub>

## Generic Display Report

## Analysis Info

Analysis Name D:\Data\Data Service\180730\_pos\_TT-UA004-3.d  
Method NV\_pos\_0.3min\_profile\_1segment\_lowNubulizerDrygas.m  
Sample Name 180730\_pos\_TT-UA004-3  
Comment

Acquisition Date 7/30/2018 11:25:35 AM

Operator CU.  
Instrument micrOTOF-Q II

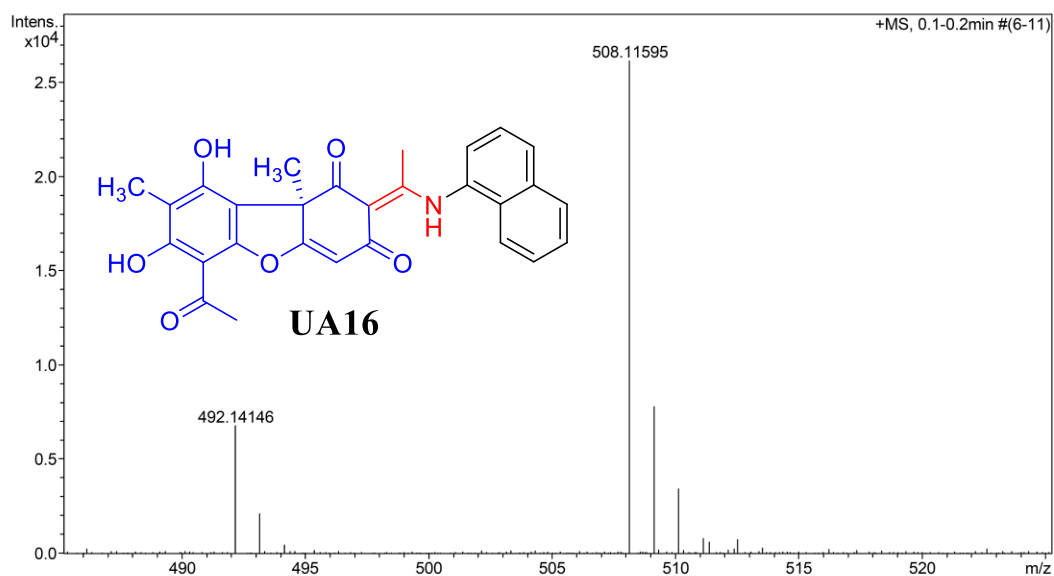
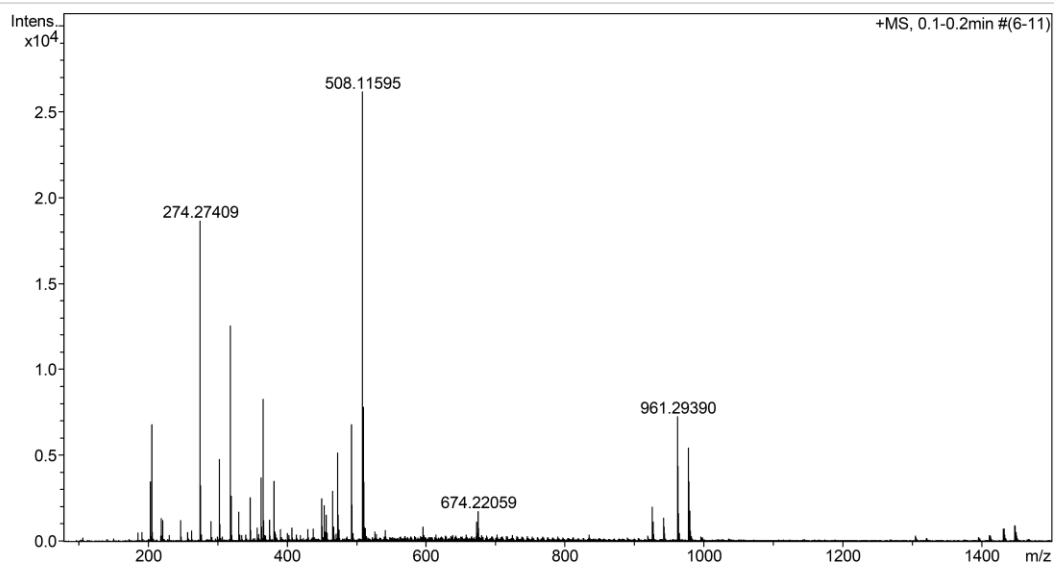
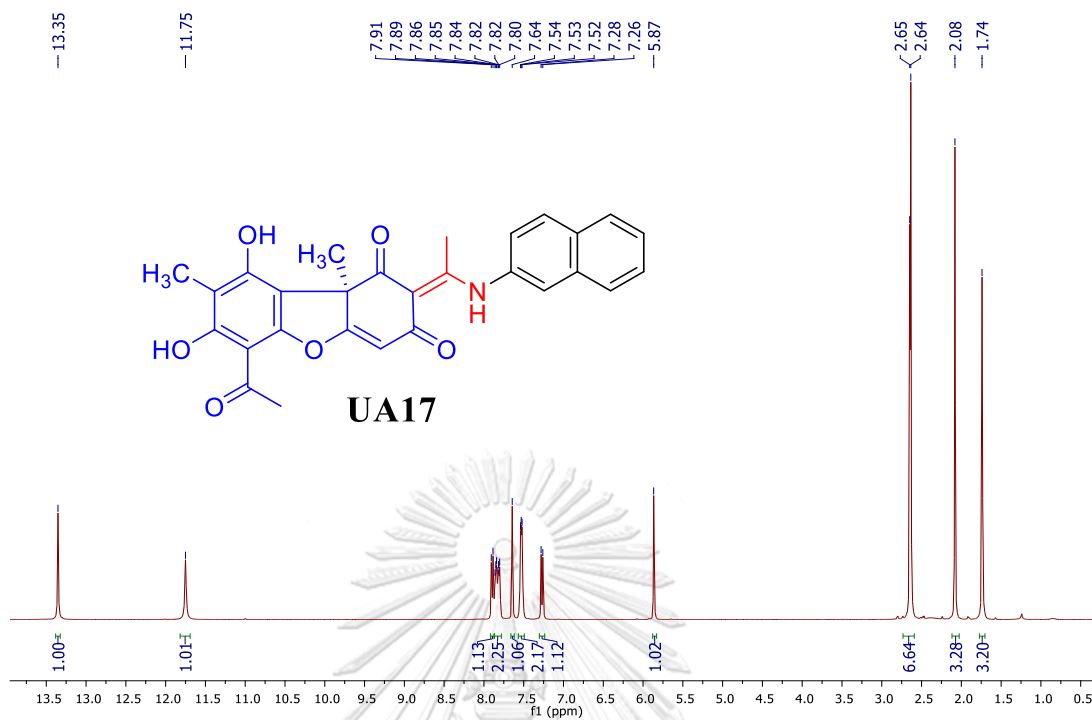
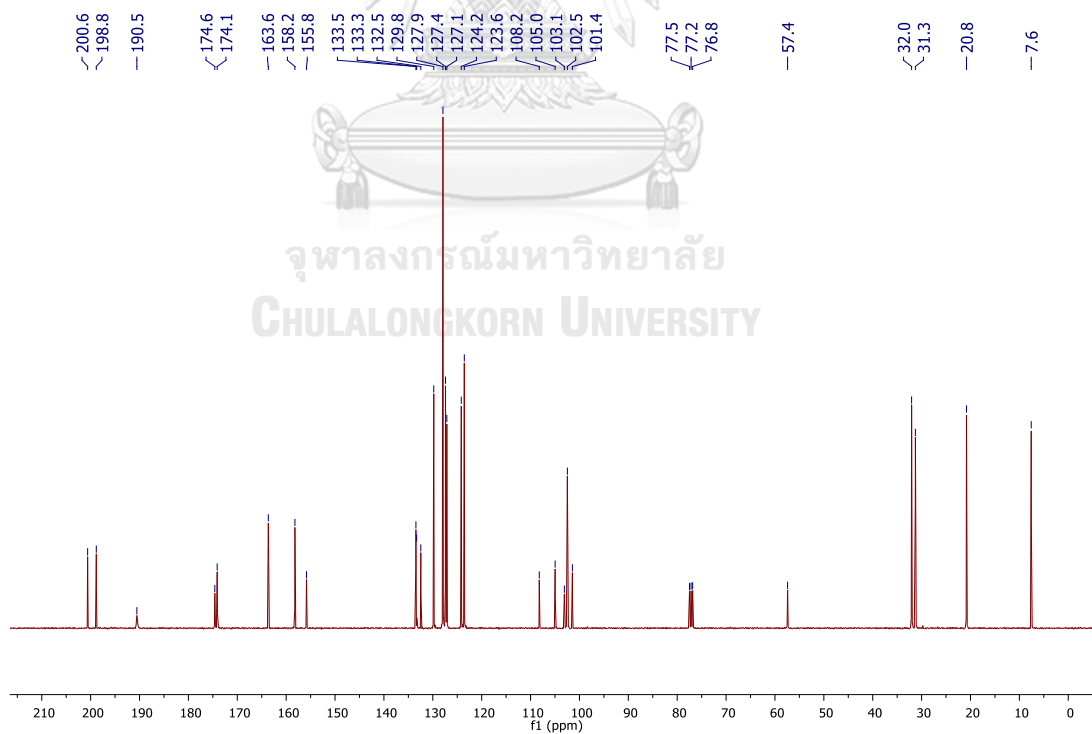


Figure A85. HRESIMS spectrum of UA16

Fig. A86. <sup>1</sup>H NMR spectrum of UA17 in CDCl<sub>3</sub>Fig. 87 <sup>13</sup>C NMR spectrum of UA17 in CDCl<sub>3</sub>

## Generic Display Report

## Analysis Info

Analysis Name D:\Data\Data Service\181112pos\_TT-UA007.d  
Method NV\_pos\_0.3min\_profile\_1segment\_lowNubulizerDrygas.m  
Sample Name 181112pos\_TT-UA007  
Comment

Acquisition Date 11/12/2018 4:17:22 PM

Operator CU.  
Instrument micrOTOF-Q II

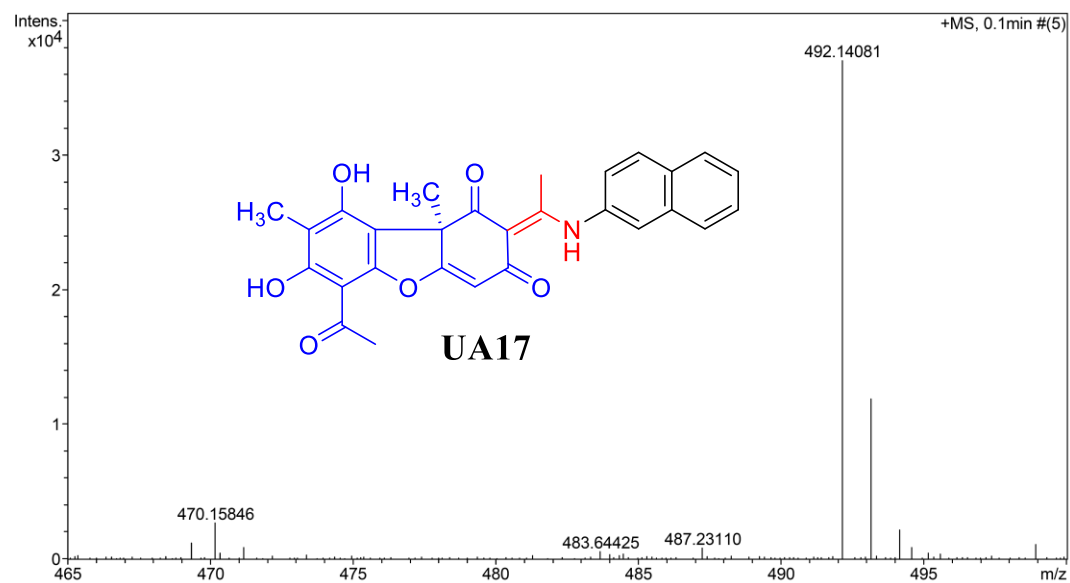
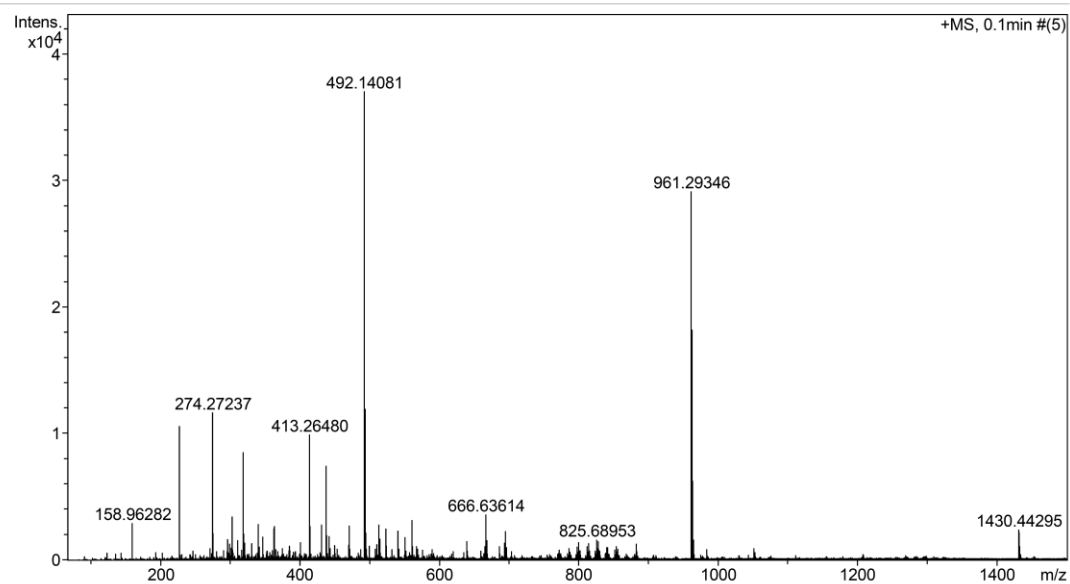
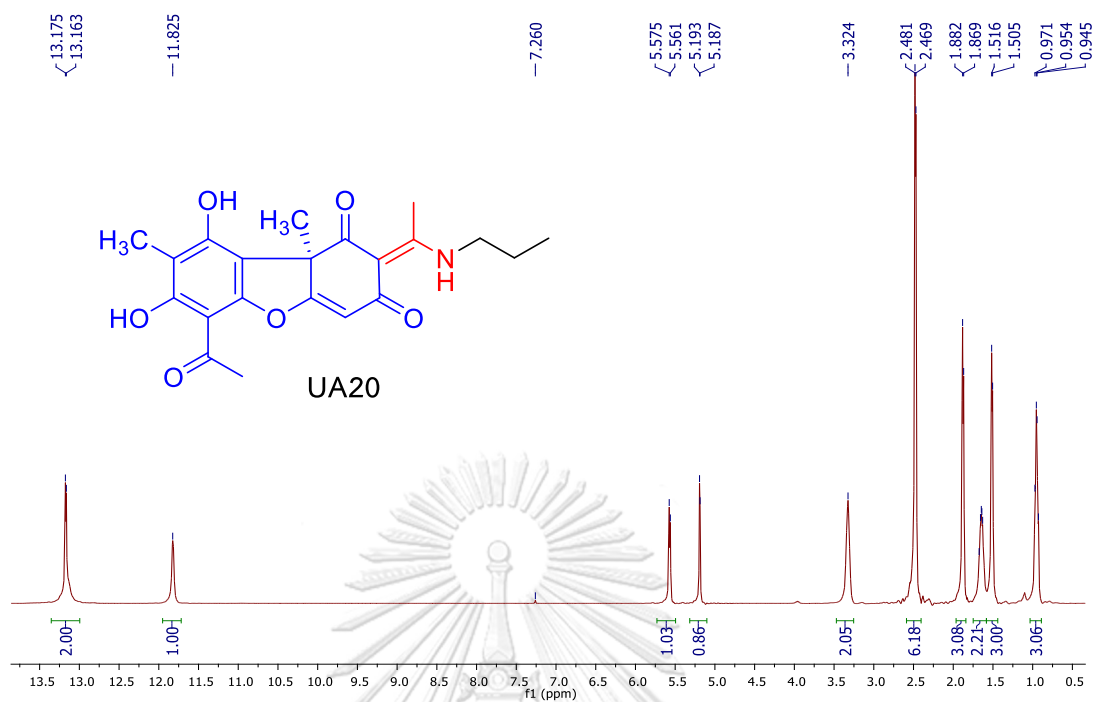
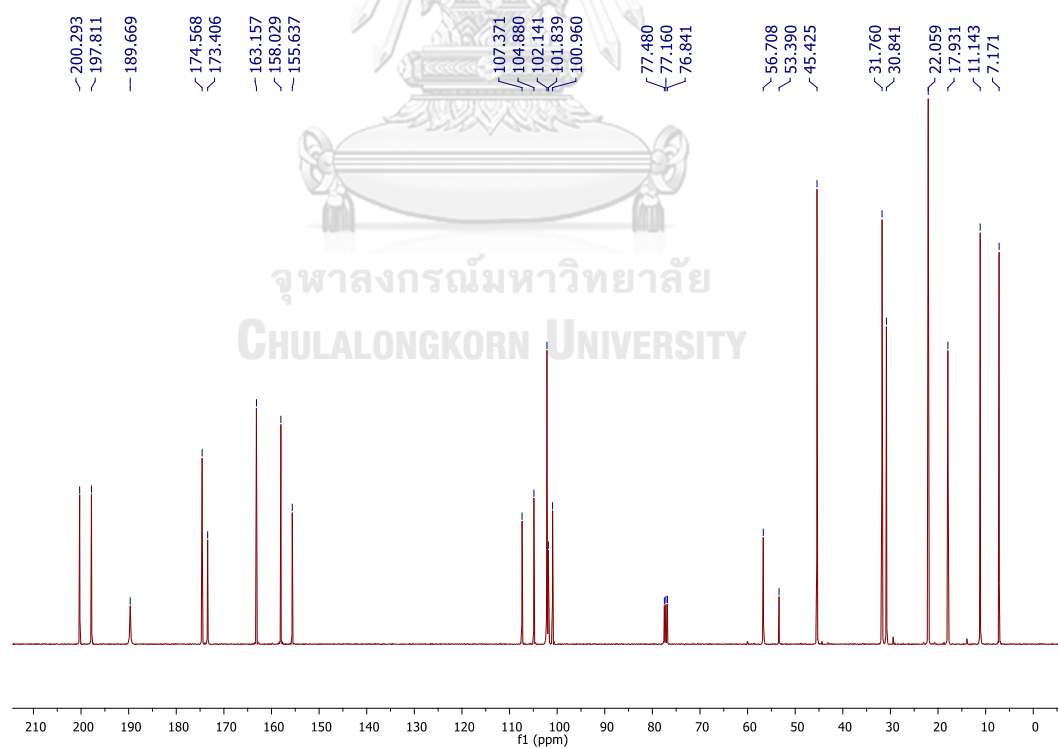
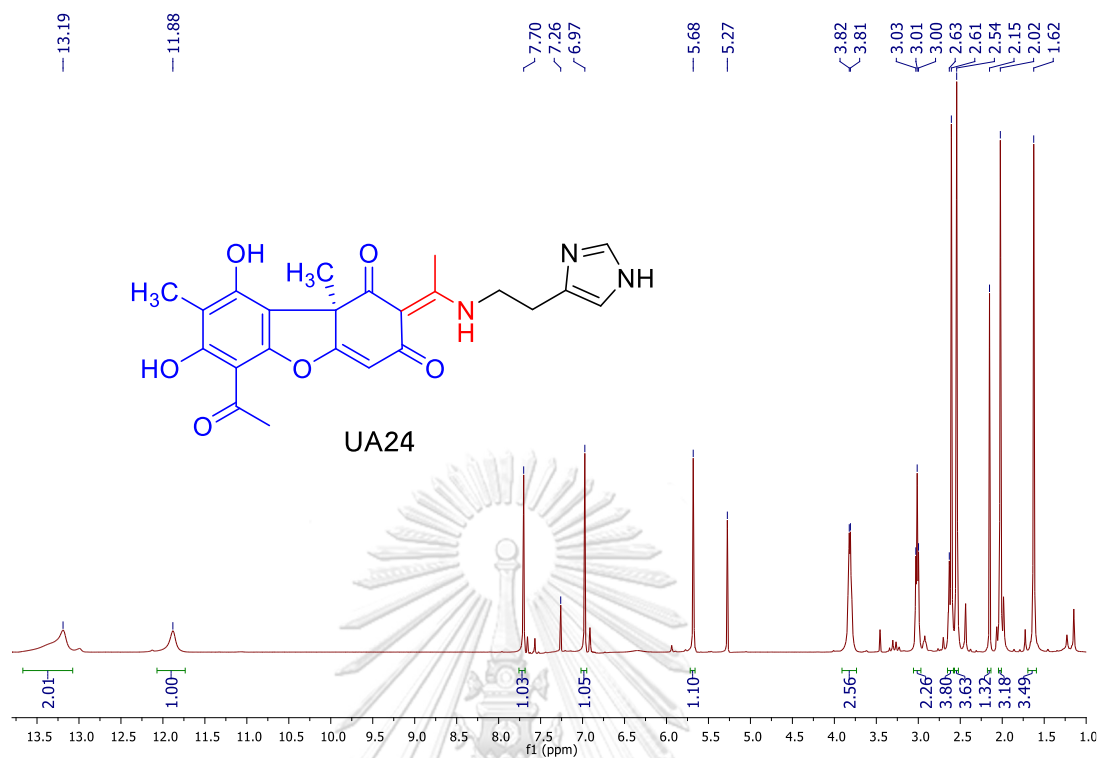
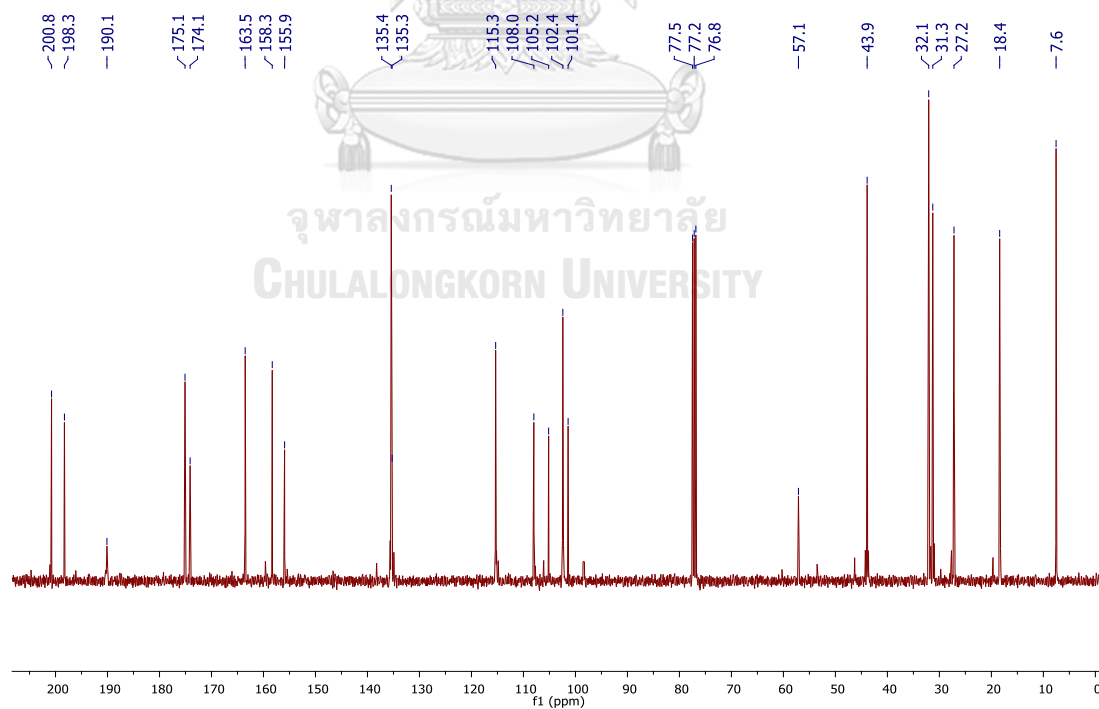


Figure A88. HRESIMS spectrum of UA17

Fig. A89.  $^1\text{H}$  NMR spectrum of UA20 in  $\text{CDCl}_3$ Fig. 90  $^{13}\text{C}$  NMR spectrum of UA20 in  $\text{CDCl}_3$



Fig. A91. <sup>1</sup>H NMR spectrum of UA24 in CDCl<sub>3</sub>Fig. 92 <sup>13</sup>C NMR spectrum of UA24 in CDCl<sub>3</sub>

## Generic Display Report

## Analysis Info

Analysis Name D:\Data\Data Service\181112pos\_TT-UA006\_2.d  
Method NV\_pos\_0.3min\_profile\_1segment\_lowNubulizerDrygas.m  
Sample Name 181112pos\_TT-UA006\_2  
Comment

Acquisition Date 11/12/2018 5:13:23 PM

Operator CU.  
Instrument micrOTOF-Q II

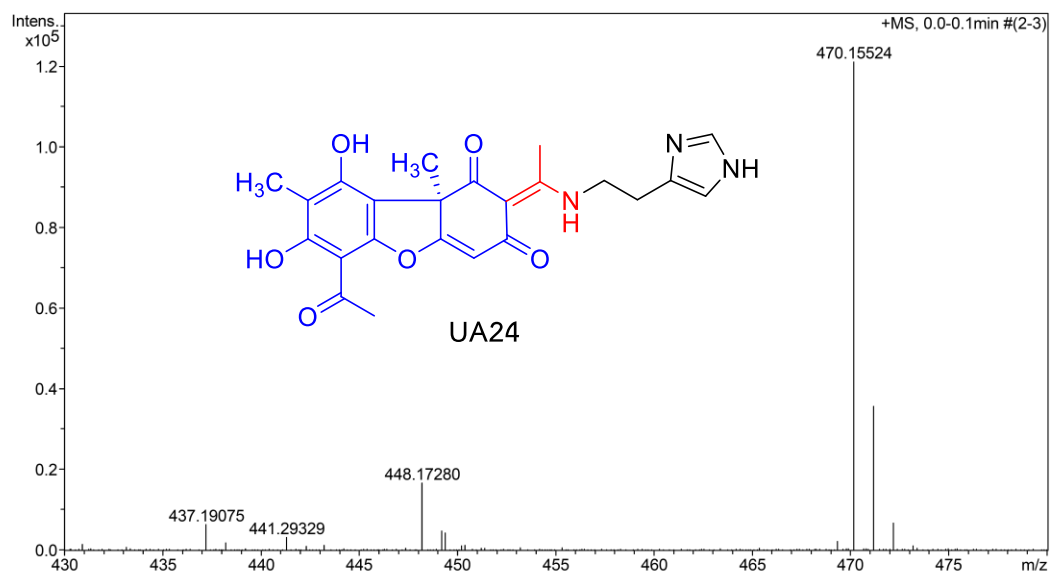
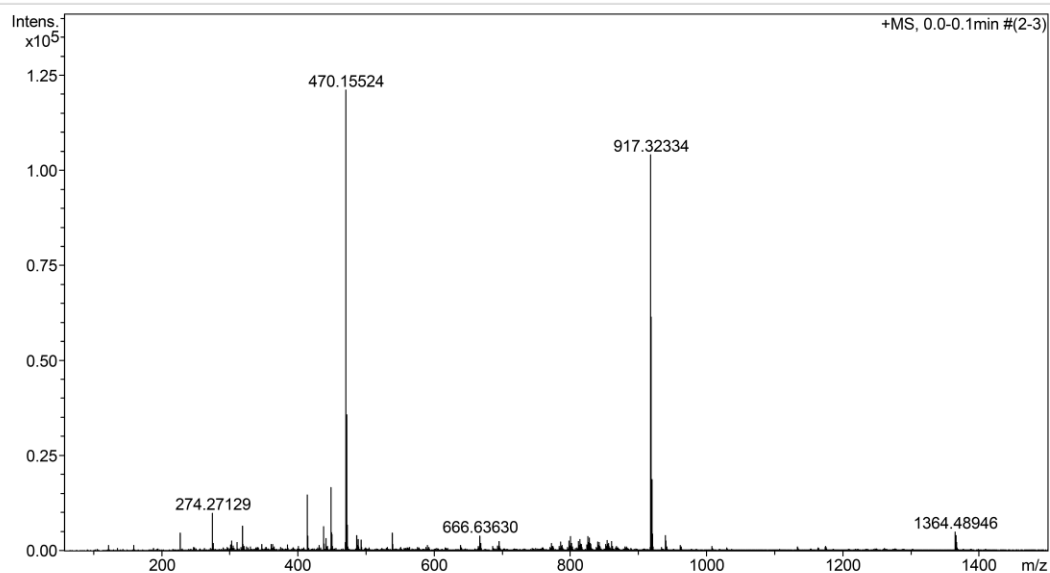
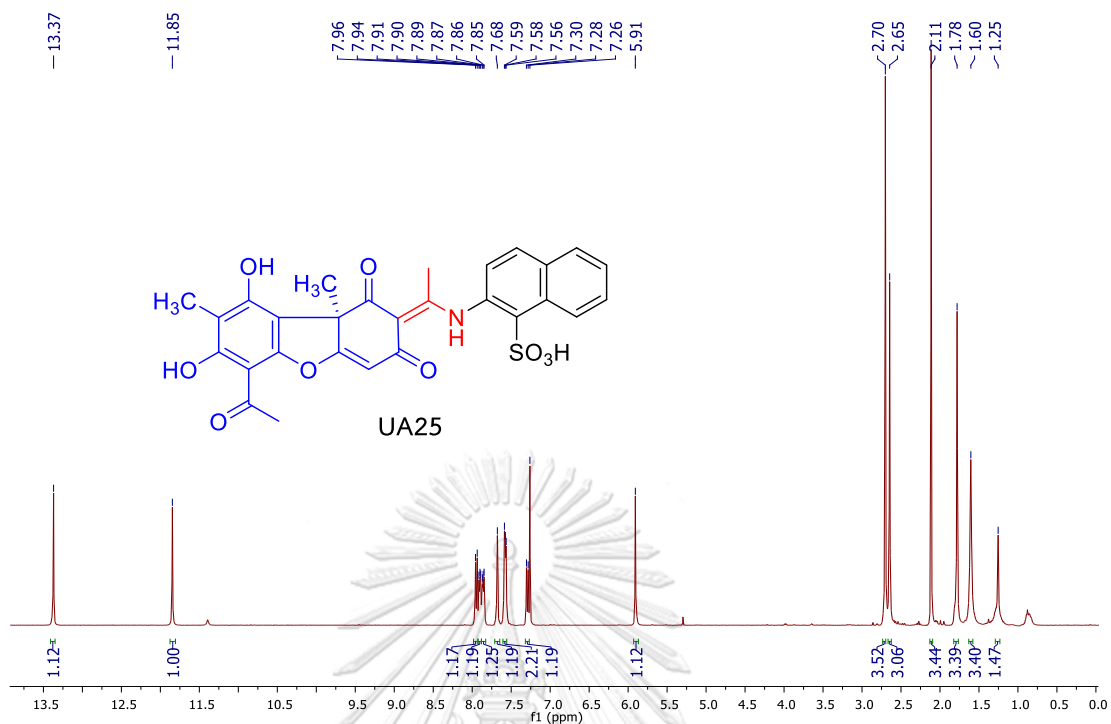
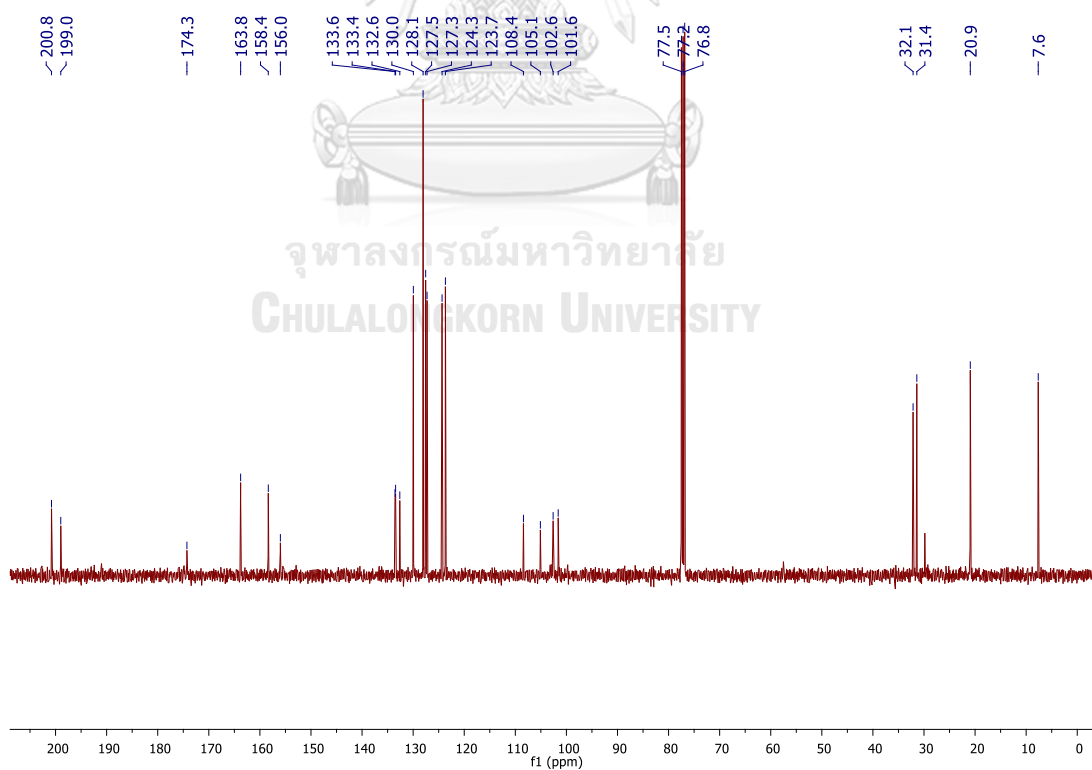


Figure A93. HRESIMS spectrum of UA24

Fig. 94. <sup>1</sup>H NMR spectrum of UA25 in CDCl<sub>3</sub>Fig. A95. <sup>13</sup>C NMR spectrum of UA25 in CDCl<sub>3</sub>

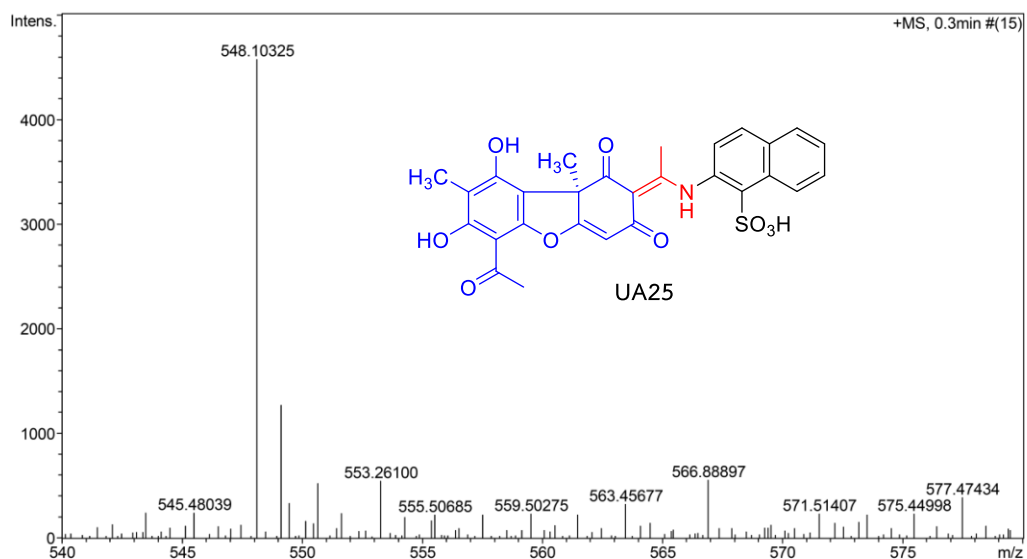
## Generic Display Report

## Analysis Info

Analysis Name D:\Data\Data Service\181112pos\_TT-UA011\_3.d  
Method NV\_pos\_0.3min\_profile\_1segment\_lowNubulizerDrygas.m  
Sample Name 181112pos\_TT-UA011\_2  
Comment

Acquisition Date 11/12/2018 2:13:50 PM

Operator CU.  
Instrument micrOTOF-Q II

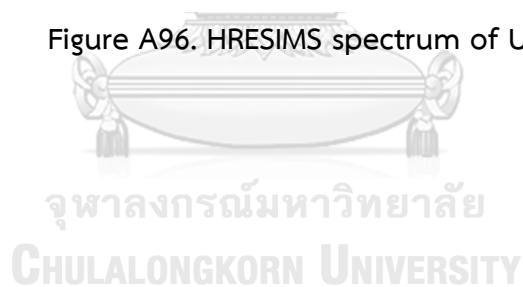


Bruker Compass DataAnalysis 4.0

printed: 11/12/2018 3:52:13 PM

Page 1 of 1

Figure A96. HRESIMS spectrum of UA25



## REFERENCES

1. Newman, D.J., G.M. Cragg, and K.M. Snader, *Natural products as sources of new drugs over the period 1981– 2002*. *Journal of natural products*, 2003. **66**(7): p. 1022-1037.
2. Samuelsson, G. and L. Bohlin, *Drugs of natural origin: a treatise of pharmacognosy*. 2017: CRC Press Inc.
3. Salim, A.A., Y.-W. Chin, and A.D. Kinghorn, *Drug discovery from plants, in Bioactive molecules and medicinal plants*. 2008, Springer. p. 1-24.
4. Kinghorn, A.D., et al., *The relevance of higher plants in lead compound discovery programs*. *Journal of natural products*, 2011. **74**(6): p. 1539-1555.
5. Atanasov, A.G., et al., *Discovery and resupply of pharmacologically active plant-derived natural products: A review*. *Biotechnology advances*, 2015. **33**(8): p. 1582-1614.
6. Torre, L.A., et al., *Global cancer statistics, 2012*. *CA: a cancer journal for clinicians*, 2015. **65**(2): p. 87-108.
7. Harvey, A.L., R. Edrada-Ebel, and R.J. Quinn, *The re-emergence of natural products for drug discovery in the genomics era*. *Nature reviews drug discovery*, 2015. **14**(2): p. 111-129.
8. Newman, D.J. and G.M. Cragg, *Natural products as sources of new drugs from 1981 to 2014*. *Journal of natural products*, 2016. **79**(3): p. 629-661.
9. Li, J.W.-H. and J.C. Vederas, *Drug discovery and natural products: end of an era or an endless frontier?* *Science*, 2009. **325**(5937): p. 161-165.
10. Butler, M.S., A.A. Robertson, and M.A. Cooper, *Natural product and natural product derived drugs in clinical trials*. *Natural product reports*, 2014. **31**(11): p. 1612-1661.
11. Pye, C.R., et al., *Retrospective analysis of natural products provides insights for future discovery trends*. *Proceedings of the National Academy of Sciences*, 2017. **114**(22): p. 5601-5606.
12. Hawksworth, D.L., *Lichen Secondary Metabolites: Bioactive Properties and*

- Pharmaceutical Potential*. Edited by Branislav Ranković. 2015. Cham, Switzerland: Springer International Publishing. Pp. v+ 202, tables, figures (some colour). Page size 235x 155 mm. ISBN 978-3-319-13373-7 (hardcover), price£ 126; ISBN 978-3-319-13374-4 (e-book), price£ 110.50. *The Lichenologist*, 2015. **47**(4): p. 277-278.
13. Nash, T.H., *Lichen biology*. 1996: Cambridge University Press.
  14. Richardson, D., *Pollution monitoring with lichens. Naturalists' handbook 19*. 1992, Richmond Press, Slough.
  15. Malhotra, S., *Lichens-role in Traditional Medicine and Drug Discovery S. Malhotraa, R. Subban b, AP Singhc*.
  16. Sak, K., K. Juerisoo, and A. Raal, *Estonian folk traditional experiences on natural anticancer remedies: From past to the future*. *Pharmaceutical biology*, 2014. **52**(7): p. 855-866.
  17. Sõukand, R. and R. Kalle, *Where does the border lie: locally grown plants used for making tea for recreation and/or healing, 1970s–1990s Estonia*. *Journal of Ethnopharmacology*, 2013. **150**(1): p. 162-174.
  18. Kiringe, J.W., *A survey of traditional health remedies used by the Maasai of Southern Kaijiado District, Kenya*. *Ethnobotany Research and Applications*, 2006. **4**: p. 061-074.
  19. Molares, S. and A. Ladio, *Medicinal plants in the cultural landscape of a Mapuche-Tehuelche community in arid Argentine Patagonia: an eco-sensorial approach*. *Journal of ethnobiology and ethnomedicine*, 2014. **10**(1): p. 61.
  20. Huneck, S. and I. Yoshimura, *Identification of lichen substances, in Identification of lichen substances*. 1996, Springer. p. 11-123.
  21. Seifert, P. and C. Bertram, *Usnic acid: natural preservation from lichens: Cosmetics: Wirkstoffe in Pharmazie und Kosmetik*. SÖFW. Seifen, Öle, Fette, Wachse, 1995. **121**(7): p. 480-485.
  22. BeGora, M.D. and D. Fahselt, *Usnic acid and atranorin concentrations in lichens in relation to bands of UV irradiance*. *The Bryologist*, 2001. **104**(1): p. 134-140.
  23. Fernández, E., et al., *Lichen metabolites as UVB filters: Lichen metabolites show photoprotector capacity*. *Cosmetics and toiletries*, 1996. **111**(12): p. 69-74.

24. Proksa, B., et al., (-)-Usnic acid and its derivatives. Their inhibition of fungal growth and enzyme activity. *Pharmazie*, 1996. **51**(3): p. 195-196.
25. Kinoshita, K., et al., *New phenolics from Protousnea species*. Hattori Shokubutsu Kenkyujo Hokoku, 1994. **75**: p. 359-364.
26. Kinoshita, K., *Topics in the chemistry of lichen compounds (Proceedings of the Symposia on Bryology and Lichenology at the 15 International Botanical Congress)--(Lichen Substances)*. Journal of the Hattori Botanical Laboratory, 1994(76): p. p227-233.
27. Kinoshita, K., et al., *Monoamine oxidase inhibitory effects of some lichen compounds and their synthetic analogues*. The Journal of the Hattori Botanical Laboratory, 2002. **92**: p. 277-284.
28. Behera, B., B. Adawadkar, and U. Makhija, *Capacity of some Graphidaceous lichens to scavenge superoxide and inhibition of tyrosinase and xanthine oxidase activities*. *Current Science*, 2004: p. 83-87.
29. Ari, F., et al., *Parmelia sulcata Taylor and Usnea filipendula Stirt induce apoptosis-like cell death and DNA damage in cancer cells*. *Cell proliferation*, 2014. **47**(5): p. 457-464.
30. Luo, H., et al., *Lecanoric acid, a secondary lichen substance with antioxidant properties from Umbilicaria antarctica in maritime Antarctica (King George Island)*. *Polar Biology*, 2009. **32**(7): p. 1033-1040.
31. Guo, L., et al., *Review of usnic acid and Usnea barbata toxicity*. *Journal of Environmental Science and Health, Part C*, 2008. **26**(4): p. 317-338.
32. Vijayan, P., et al., *Antiviral activity of medicinal plants of Nilgiris*. *Indian Journal of medical research*, 2004. **120**: p. 24-29.
33. Kim, M.-S. and H.-B. Cho, *Melanogenesis inhibitory effects of methanolic extracts of Umbilicaria esculenta and Usnea longissima*. *Journal of Microbiology (Seoul, Korea)*, 2007. **45**(6): p. 578-582.
34. Araújo, A., et al., *Review of the biological properties and toxicity of usnic acid*. *Natural product research*, 2015. **29**(23): p. 2167-2180.
35. YAMAMOTO, Y., et al., *Screening of tissue cultures and thalli of lichens and*

- some of their active constituents for inhibition of tumor promoter-induced Epstein-Barr virus activation. *Chemical and Pharmaceutical Bulletin*, 1995. **43**(8): p. 1388-1390.
36. Atalay, F., et al., *Antioxidant phenolics from Lobaria pulmonaria (L.) Hoffm. and Usnea longissima Ach. lichen species*. *Turkish Journal of chemistry*, 2011. **35**(4): p. 647-661.
37. Lee, K.A. and M.S. Kim, *Antiplatelet and antithrombotic activities of methanol extract of Usnea longissima*. *Phytotherapy Research: An International Journal Devoted to Pharmacological and Toxicological Evaluation of Natural Product Derivatives*, 2005. **19**(12): p. 1061-1064.
38. Correché, E.R., et al., *Cytotoxic and apoptotic effects on hepatocytes of secondary metabolites obtained from lichens*. *Alternatives to Laboratory Animals*, 2004. **32**(6): p. 605-615.
39. Verma, N., B. Behera, and U. Makhija, *Antioxidant and hepatoprotective activity of a lichen Usnea ghattensis in vitro*. *Applied biochemistry and biotechnology*, 2008. **151**(2-3): p. 167-181.
40. Koçer, S., et al., *The synthesis, characterization, antimicrobial and antimutagenic activities of hydroxyphenylimino ligands and their metal complexes of usnic acid isolated from Usnea longissima*. *Dalton Transactions*, 2014. **43**(16): p. 6148-6164.
41. Brandão, L.F.G., et al., *Cytotoxic evaluation of phenolic compounds from lichens against melanoma cells*. *Chemical and Pharmaceutical Bulletin*, 2012: p. c12-00739.
42. Paranagama, P.A., et al., *Heptaketides from Corynespora sp. inhabiting the cavern beard lichen, Usnea cavernosa: first report of metabolites of an endolichenic fungus*. *Journal of natural products*, 2007. **70**(11): p. 1700-1705.
43. Cahyana, A.H., W.P. Suwarso, and M. Nurdin, *Isolation and structure elucidation of eumitrin A1 from lichen Usnea blepharea Motyka and its cytotoxic activity*. *International journal of pharmtech research*, 2015. **8**(4): p. 782-789.
44. Choudhary, M.I. and S. Jalil, *Bioactive phenolic compounds from a medicinal lichen, Usnea longissima*. *Phytochemistry*, 2005. **66**(19): p. 2346-2350.



45. Sultana, N. and A.J. Afolayan, *A new depsidone and antibacterial activities of compounds from Usnea undulata Stirton*. Journal of Asian natural products research, 2011. **13**(12): p. 1158-1164.
46. Odabasoglu, F., et al., *Diffraactaic acid, a novel proapoptotic agent, induces with olive oil both apoptosis and antioxidative systems in Ti-implanted rabbits*. European journal of pharmacology, 2012. **674**(2-3): p. 171-178.
47. Leandro, L.F., et al., *Assessment of the genotoxicity and antigenotoxicity of (+)-usnic acid in V79 cells and Swiss mice by the micronucleus and comet assays*. Mutation Research/Genetic Toxicology and Environmental Mutagenesis, 2013. **753**(2): p. 101-106.
48. Karagoz, I.D., et al., *Hepatoprotective effect of diffractaic acid on carbon tetrachloride-induced liver damage in rats*. Biotechnology & Biotechnological Equipment, 2015. **29**(5): p. 1011-1016.
49. Okuyama, E., et al., *Usnic acid and diffractaic acid as analgesic and antipyretic components of Usnea diffracta*. Planta Medica, 1995. **61**(02): p. 113-115.
50. Ghione, M., D. Parrello, and L. Grasso, *Usnic acid revisited, its activity on oral flora*. Chemioterapia: international journal of the Mediterranean Society of Chemotherapy, 1988. **7**(5): p. 302-305.
51. Lauterwein, M., et al., *In vitro activities of the lichen secondary metabolites vulpinic acid, (+)-usnic acid, and (-)-usnic acid against aerobic and anaerobic microorganisms*. Antimicrobial agents and chemotherapy, 1995. **39**(11): p. 2541-2543.
52. Conover, M.A., et al., *Usnic acid amide, a phytotoxin and antifungal agent from Cercosporidium henningsii*. Phytochemistry, 1992. **31**(9): p. 2999-3001.
53. Fournet, A., et al., *Activity of compounds isolated from Chilean lichens against experimental cutaneous leishmaniasis*. Comparative Biochemistry and Physiology Part C: Pharmacology, Toxicology and Endocrinology, 1997. **116**(1): p. 51-54.
54. Lawrey, J.D., *Lichen secondary compounds: evidence for a correspondence between antiherbivore and antimicrobial function*. Bryologist, 1989: p. 326-328.
55. Ingólfssdóttir, K.n., et al., *Antimycobacterial activity of lichen metabolites in*

- vitro*. European Journal of Pharmaceutical Sciences, 1998. **6**(2): p. 141-144.
56. Ingolfsdottir, K., et al., *In vitro* susceptibility of *Helicobacter pylori* to protolichesterinic acid from the lichen *Cetraria islandica*. Antimicrobial agents and Chemotherapy, 1997. **41**(1): p. 215-217.
  57. Fujikawa, F., et al., *Studies on antiseptics for foodstuff. LXXI. Studies on orsellinic acid ester, beta-orcinolcarboxylic acid ester and olivetonide as a preservative for sake*. Yakugaku zasshi: Journal of the Pharmaceutical Society of Japan, 1970. **90**(12): p. 1517.
  58. Ingolfsdottir, K., S. Bloomfield, and P. Hylands, *In vitro* evaluation of the antimicrobial activity of lichen metabolites as potential preservatives. Antimicrobial agents and chemotherapy, 1985. **28**(2): p. 289-292.
  59. Raghava Raju, K. and P. Rao, *Chemistry of lichen products: part V—Synthesis and antimicrobial activity of some new 1, 4–benzimidazones from pulvinic acid dilactone*. Indian Journal of Chemistry, 1986. **25**: p. 94-96.
  60. Anke, H., I. Kolthoum, and H. Laatsch, *Metabolic products of microorganisms. 192. The anthraquinones of the Aspergillus glaucus group. II. Biological activity*. Archives of Microbiology, 1980. **126**(3): p. 231-236.
  61. Gollapudi, S.R., et al., *Alectosarmentin, a new antimicrobial dibenzofuranoid lactol from the lichen, Alectoria sarmentosa*. Journal of natural products, 1994. **57**(7): p. 934-938.
  62. Neamati, N., et al., *Depsidines and depsidones as inhibitors of HIV-1 integrase: discovery of novel inhibitors through 3D database searching*. Journal of medicinal chemistry, 1997. **40**(6): p. 942-951.
  63. Pengsuparp, T., et al., *Mechanistic evaluation of new plant-derived compounds that inhibit HIV-1 reverse transcriptase*. Journal of natural products, 1995. **58**(7): p. 1024-1031.
  64. Wood, S., et al., *Antiviral activity of naturally occurring anthraquinones and anthraquinone derivatives*. Planta Medica, 1990. **56**(06): p. 651-652.
  65. Lavie, G., et al., *Studies of the mechanisms of action of the antiretroviral agents hypericin and pseudohypericin*. Proceedings of the National Academy of Sciences, 1989. **86**(15): p. 5963-5967.

66. Cohen, P., J. Hudson, and G. Towers, *Antiviral activities of anthraquinones, bianthrone and hypericin derivatives from lichens*. *Experientia*, 1996. **52**(2): p. 180-183.
67. Kupchan, S.M. and H.L. Kopperman, *L-Usnic acid: tumor inhibitor isolated from lichens*. *Experientia*, 1975. **31**(6): p. 625-625.
68. Takai, M., Y. Uehara, and J.A. Beisler, *Usnic acid derivatives as potential antineoplastic agents*. *Journal of medicinal chemistry*, 1979. **22**(11): p. 1380-1384.
69. Bézivin, C., et al., *Cytotoxic activity of compounds from the lichen: Cladonia convoluta*. *Planta medica*, 2004. **70**(09): p. 874-877.
70. Hirayama, T., et al., *Anti-tumor activities of some lichen products and their degradation products (author's transl)*. *Yakugaku zasshi: Journal of the Pharmaceutical Society of Japan*, 1980. **100**(7): p. 755-759.
71. Correche, E., et al., *Cytotoxic screening activity of secondary lichen metabolites*. *Acta Farmaceutica Bonaerense*, 2002. **21**(4): p. 273-278.
72. Müller, K., et al., *Simple analogues of anthralin: unusual specificity of structure and antiproliferative activity*. *Journal of medicinal chemistry*, 1997. **40**(23): p. 3773-3780.
73. Chai, C.L., et al., *Scabrosin esters and derivatives: chemical derivatization studies and biological evaluation*. *Bioorganic & medicinal chemistry*, 2004. **12**(22): p. 5991-5995.
74. Koyama, M., et al., *Intercalating agents with covalent bond forming capability. A novel type of potential anticancer agents. 2. Derivatives of chrysophanol and emodin*. *Journal of medicinal chemistry*, 1989. **32**(7): p. 1594-1599.
75. Ohmura, Y., I. Skirina, and F. Skirin, *Contribution to the knowledge of the genus Usnea (Parmeliaceae, Ascomycota) in southern Far East Russia*. *Bull. Natl. Mus. Nat. Sci. Ser. B*, 2017. **43**: p. 1-10.
76. Randlane, T., et al., *Key to European Usnea species*. *Bibliotheca lichenologica*, 2009. **100**: p. 419-462.
77. Hawksworth, D.L., et al., *Ainsworth & Bisby's dictionary of the fungi*. *Revista Do Instituto De Medicina Tropical De Sao Paulo*, 1996. **38**(4): p. 272-272.

78. Qi, H.Y., Y.P. Jin, and Y.P. Shi, *A new depsidone from Usnea diffracta*. Chinese Chemical Letters, 2009. **20**(2): p. 187-189.
79. Safe, S., L.M. Safe, and W.S. Maass, *Sterols of three lichen species: Lobaria pulmonaria, Lobaria scrobiculata and Usnea longissima*. Phytochemistry, 1975. **14**(8): p. 1821-1823.
80. Keeton, J. and M. Keogh, *Caperatic acid from Usnea alata*. Phytochemistry, 1973.
81. Keogh, M.F. and M.E. Zurita,  *$\alpha$ -(15-Hydroxyhexadecyl) itaconic acid from Usnea aliphatica*. Phytochemistry, 1977. **16**(1): p. 134-135.
82. Mendiondo, M. and J. Coussio, *Usnic, norstictic and salazinic acids from Usnea densirostra and Usnea angulata*. Phytochemistry, 1972.
83. Lohézic-Le Dévéhat, F., et al., *Stictic acid derivatives from the lichen Usnea articulata and their antioxidant activities*. Journal of natural products, 2007. **70**(7): p. 1218-1220.
84. Yang, D.-M., et al., *The structures of eumitrins A1, A2 and B: The yellow pigments of the lichen, Usnea bayleyi (Stirt.) Zahlbr.* Tetrahedron, 1973. **29**(3): p. 519-528.
85. Din, L.B., et al., *Chemical profile of compounds from lichens of Bukit Larut, Peninsular Malaysia*. Sains Malaysiana, 2010. **39**(6): p. 901-908.
86. Van Nguyen, K., et al., *Chemical constituents of the lichen Usnea bayleyi (Stirt.) Zahlbr.* Tetrahedron Letters, 2018. **59**(14): p. 1348-1351.
87. Keogh, M.F. and I. Duran, *A new fatty acid from Usnea meridensis*. Phytochemistry, 1977. **16**(10): p. 1605-1606.
88. Truong, T.L., et al., *A new depside from Usnea aciculifera growing in Vietnam*. Natural product communications, 2014. **9**(8): p. 1934578X1400900831.
89. Karuppiyah, P. and M. Mustafa, *Antibacterial and antioxidant activities of Musa sp. leaf extracts against multidrug resistant clinical pathogens causing nosocomial infection*. Asian Pacific journal of tropical biomedicine, 2013. **3**(9): p. 737-742.
90. Suroengrit, A., et al., *Halogenated Chrysin inhibit Dengue and Zika virus*

- infectivity*. Scientific reports, 2017. **7**(1): p. 13696.
91. FUJITA, M., et al., *O-Methylation effect on the carbon-13 nuclear magnetic resonance signals of ortho-disubstituted phenols and its application to structure determination of new phthalides from Aspergillus silvaticus*. Chemical and Pharmaceutical Bulletin, 1984. **32**(7): p. 2622-2627.
  92. Verma, N., B. Behera, and B.O. Sharma, *Glucosidase inhibitory and radical scavenging properties of lichen metabolites salazinic acid, sekikaic acid and usnic acid*. Hacettepe J Biol Chem, 2012. **40**(1): p. 7-21.
  93. Van Dyck, S.M., et al., *Synthesis of 4-O-methylcedrusin. Selective protection of catechols with diphenyl carbonate*. Molecules, 2000. **5**(2): p. 153-161.
  94. Narui, T., et al., *NMR assignments of depsides and tridepsides of the lichen family Umbilicariaceae*. Phytochemistry, 1998. **48**(5): p. 815-822.
  95. Sakurai, A. and Y. Goto, *Chemical studies on the Lichen. I. The structure of isolecanoric acid, a new ortho-depside isolated from Parmelia tinctorum despr.* Bulletin of the Chemical Society of Japan, 1987. **60**(5): p. 1917-1918.
  96. Papadopoulou, P., et al.,  *$\beta$ -Orcinol Metabolites from the Lichen Hypotrachyna revoluta*. Molecules, 2007. **12**(5): p. 997-1005.
  97. Pejtin, B., et al., *Stictic acid inhibits cell growth of human colon adenocarcinoma HT-29 cells*. Arabian Journal of Chemistry, 2017. **10**: p. S1240-S1242.
  98. Elix, J.A. and J.H. Wardlaw, *The structure of chalybaezanic acid and quaesitic acid, two new lichen depsidones related to salazinic acid*. Australian journal of chemistry, 1999. **52**(7): p. 713-716.
  99. Nguyen, D.M., et al., *Phenolic compounds from the lichen Lobaria orientalis*. Journal of natural products, 2017. **80**(2): p. 261-268.
  100. König, G.M. and A.D. Wright,  *$^1H$  and  $^{13}C$ -NMR and biological activity investigations of four lichen-derived compounds*. Phytochemical Analysis, 1999. **10**(5): p. 279-284.
  101. Melgarejo, M., et al., *More investigations in potent activity and relationship structure of the lichen antibiotic (+)-usnic acid and its derivate dibenzoylusnic acid*. Revista Boliviana de Quimica, 2008. **25**(1): p. 24-29.

102. Riaz, T., M. Abbasi, and M. Ajaib, *Isolation, structure elucidation and antioxidant screening of some natural products from Colebrookia oppositifolia*. Bioscience Research, 2012. **9**(2): p. 68-76.
103. Elix, J., A. Whitton, and A. Jones, *Triterpenes from the lichen genus Physcia*. Australian Journal of Chemistry, 1982. **35**(3): p. 641-647.
104. Takaishi, Y., et al., *Investigation of the constituents of Inonotus mikadoi*. 1987.
105. Li, T.-X., et al., *Unusual dimeric tetrahydroxanthone derivatives from Aspergillus lentulus and the determination of their axial chiralities*. Scientific reports, 2016. **6**: p. 38958.
106. Rönnsberg, D., et al., *Pro-apoptotic and immunostimulatory tetrahydroxanthone dimers from the endophytic fungus Phomopsis longicolla*. The Journal of organic chemistry, 2013. **78**(24): p. 12409-12425.
107. Wu, G., et al., *Versixanthonones A–F, cytotoxic xanthone–chromanone dimers from the marine-derived fungus Aspergillus versicolor HDN1009*. Journal of natural products, 2015. **78**(11): p. 2691-2698.
108. Neubig, R.R., et al., *International Union of Pharmacology Committee on Receptor Nomenclature and Drug Classification. XXXVIII. Update on terms and symbols in quantitative pharmacology*. Pharmacological reviews, 2003. **55**(4): p. 597-606.
109. Abid, N.B.S., et al., *Assessment of the cytotoxic effect and in vitro evaluation of the anti-enteroviral activities of plants rich in flavonoids*. Journal of Applied Pharmaceutical Science, 2012. **2**(5): p. 74.
110. Qin, T., et al., *Atropselective syntheses of (-) and (+) rugulotrosin A utilizing point-to-axial chirality transfer*. Nature chemistry, 2015. **7**(3): p. 234.
111. Riss, T.L., et al., *Cell viability assays*, in *Assay Guidance Manual [Internet]*. 2016, Eli Lilly & Company and the National Center for Advancing Translational Sciences.
112. Reyim, M., *Adiljan; Abdulla, A*. China Brewing, 2010. **11**: p. 122-124.
113. Ingoldsdottir, K., *Usnic acid*. Phytochemistry, 2002. **61**(7): p. 729-736.
114. Neff, G.W., et al., *Severe hepatotoxicity associated with the use of weight loss*

- diet supplements containing ma huang or usnic acid.* Journal of hepatology, 2004. **41**(6): p. 1062-1064.
115. Favreau, J.T., et al., *Severe hepatotoxicity associated with the dietary supplement LipoKinetix.* Annals of internal medicine, 2002. **136**(8): p. 590-595.
116. Ribeiro-Costa, R.M., et al., *In vitro and in vivo properties of usnic acid encapsulated into PLGA-microspheres.* Journal of Microencapsulation, 2004. **21**(4): p. 371-384.
117. da Silva Santos, N.P., et al., *Nanoencapsulation of usnic acid: an attempt to improve antitumour activity and reduce hepatotoxicity.* European Journal of Pharmaceutics and Biopharmaceutics, 2006. **64**(2): p. 154-160.
118. Bruno, M., et al., *(+)-Usnic acid enamines with remarkable cicatrizing properties.* Bioorganic & medicinal chemistry, 2013. **21**(7): p. 1834-1843.
119. Bazin, M.-A., et al., *Synthesis and cytotoxic activities of usnic acid derivatives.* Bioorganic & medicinal chemistry, 2008. **16**(14): p. 6860-6866.
120. Tazetdinova, A., et al., *Amino-derivatives of usnic acid.* Chemistry of natural compounds, 2009. **45**(6): p. 800-804.
121. Luzina, O., et al., *Chemical modification of usnic acid 2. Reactions of (+)-usnic acid with amino acids.* Russian Chemical Bulletin, 2007. **56**(6): p. 1249-1251.
122. Seo, C., et al., *Usimines A- C, Bioactive Usnic Acid Derivatives from the Antarctic Lichen Stereocaulon alpinum.* Journal of natural products, 2008. **71**(4): p. 710-712.
123. Millot, M., et al., *Usnic acid derivatives from Leprocaulon microscopicum.* Phytochemistry Letters, 2013. **6**(1): p. 31-35.
124. Yu, X., et al., *Usnic acid derivatives with cytotoxic and antifungal activities from the lichen Usnea longissima.* Journal of natural products, 2016. **79**(5): p. 1373-1380.
125. Natić, M., et al., *Synthesis and biological activity of Pd (II) and Cu (II) complexes with acylhydrazones of usnic acid.* Synthesis and Reactivity in Inorganic and Metal-Organic Chemistry, 2004. **34**(1): p. 101-113.
126. Rakhmanova, M., et al., *Synthesis and cytotoxic activity of usnic acid cyanoethyl derivatives.* Russian Chemical Bulletin, 2016. **65**(2): p. 566-569.

127. Luzina, O. and N. Salakhutdinov, *Biological activity of usnic acid and its derivatives: part 2. Effects on higher organisms. Molecular and physicochemical aspects*. Russian Journal of Bioorganic Chemistry, 2016. **42**(3): p. 249-268.
128. Vanga, N.R., et al., *Synthesis and anti-inflammatory activity of novel triazole hybrids of (+)-usnic acid, the major dibenzofuran metabolite of the lichen *Usnea longissima**. Molecular diversity, 2017. **21**(2): p. 273-282.
129. Luzina, O., et al., *Synthesis and biological activity of usnic acid enamine derivatives*. Chemistry of natural compounds, 2015. **51**(4): p. 646-651.
130. Zakharenko, A., et al., *Tyrosyl-DNA phosphodiesterase 1 inhibitors: usnic acid enamines enhance the cytotoxic effect of camptothecin*. Journal of natural products, 2016. **79**(11): p. 2961-2967.
131. Bruno, M., et al., *Synthesis of a potent antimalarial agent through natural products conjugation*. ChemMedChem, 2013. **8**(2): p. 221-225.
132. Thadhani, V.M. and V. Karunaratne, *Potential of lichen compounds as antidiabetic agents with antioxidative properties: A review*. Oxidative medicine and cellular longevity, 2017. **2017**.
133. Bangalore, P.K., et al., *Usnic Acid Enaminone-Coupled 1, 2, 3-Triazoles as Antibacterial and Antitubercular Agents*. Journal of Natural Products, 2019.
134. Ramadhan, R. and P. Phuwapraisirisan, *New arylalkanones from *Horsfieldia macrobotrys*, effective antidiabetic agents concomitantly inhibiting  $\alpha$ -glucosidase and free radicals*. Bioorganic & medicinal chemistry letters, 2015. **25**(20): p. 4529-4533.



## VITA

**NAME** Truong Tuong Lam

**DATE OF BIRTH** 02 September 1986

**PLACE OF BIRTH** Nghe An Province, Vietnam

**INSTITUTIONS ATTENDED** -Department of Organic Chemistr, Faculty of Chemistry, Ho Chi Minh City Universtiy of Science, Vietnam  
-Department of Chemistry, Faculty of Science, Chulalongkorn University

**HOME ADDRESS** Ho Chi Minh City, Vietnam

**PUBLICATION** Truong, T.L., Thammarat, A., Lien, D.T.M., Phung, K.P.N., Piyanuch, W., Warinthorn, C. Dimeric tetrahydroxanthones from the Lichen *Usnea aciculifera*, *Fitoterapia*. 2019, 137, 104194-104201.

**AWARD RECEIVED** - The Graduate Scholarship Program for ASEAN Countries, Office of Academic Affair  
- The 90th Anniversary Chulalongkorn University Fund (Ratchadaphiseksomphot Endowment Fund).